ISSN 0042-8469
e-ISSN 2217-4753
УДК 623 + 355/359

Вол. 70, бр. 2
2022

ВТГ

70 ГОДИНА ОД 1953.

НАУЧНИ ЧАСОПИС МИНИСТАРСТВА ОДБРАНЕ И ВОЈСКЕ СРБИЈЕ

ВОЈНОТЕХНИЧКИ ГЛАСНИК

2 2022 ВОЈНОТЕХНИЧКИ ГЛАСНИК

ВТГ.МО.УПР.СРБ

www.vtg.mod.gov.rs

ISSN 0042-8469
e-ISSN 2217-4753
УДК 623 + 355/359

Том 70, № 2
2022

ВТГ

70 С 1953 г. ЛЕТ

НАУЧНЫЙ ЖУРНАЛ МИНИСТЕРСТВА ОБОРОНЫ
И ВООРУЖЕННЫХ СИЛ РЕСПУБЛИКИ СЕРБИЯ

ВОЕННО-ТЕХНИЧЕСКИЙ ВЕСТНИК

ВОЕННО-ТЕХНИЧЕСКИЙ ВЕСТНИК

2 2022

ВТГ.МО.УПР.СРБ

www.vtg.mod.gov.rs

ISSN 0042-8469
e-ISSN 2217-4753
UDC 623 + 355/359

Vol. 70, Issue 2
2022

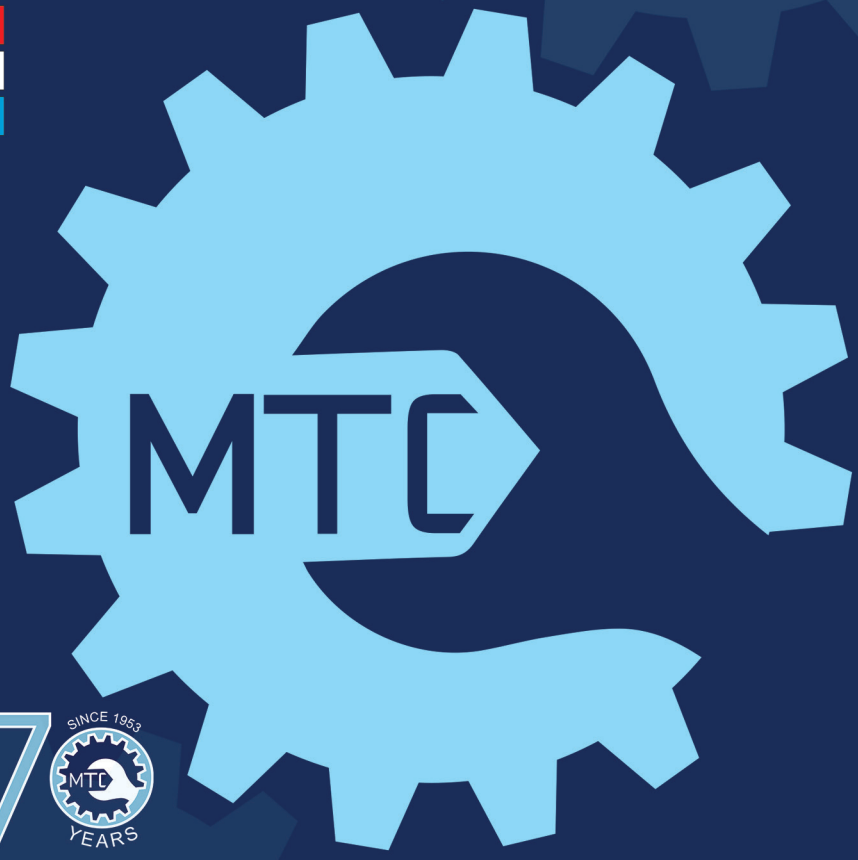

SCIENTIFIC JOURNAL OF THE MINISTRY OF DEFENCE AND THE SERBIAN ARMED FORCES

MILITARY TECHNICAL COURIER

MILITARY TECHNICAL COURIER

2 2022

ВТГ.МО.УПР.СРБ

www.vtg.mod.gov.rs

ISSN 0042-8469
e-ISSN 2217-4753
UDC 623 + 355/359

НАУЧНИ ЧАСОПИС МИНИСТАРСТВА ОДБРАНЕ И ВОЈСКЕ СРБИЈЕ

ВОЈНОТЕХНИЧКИ ГЛАСНИК

ВОЛУМЕН 70 • БРОЈ 2 • АПРИЛ–ЈУН 2022.

NAUČNI ČASOPIS MINISTARSTVA ODBRANE I VOJSKE SRBIJE

VOJNOTEHNIČKI GLASNIK

VOLUMEN 70 • BROJ 2 • APRIL–JUN 2022.

втг.мо.упр.срб
www.vtg.mod.gov.rs
COBISS.SR-ID: 4423938
COBISS.SR-ID: 181287436
DOI: 10.5937/VojnotehnickiGlasnik

ISSN 0042-8469
e-ISSN 2217-4753
UDC 623 + 355/359

НАУЧНЫЙ ЖУРНАЛ МИНИСТЕРСТВА ОБОРОНЫ И ВООРУЖЁННЫХ СИЛ РЕСПУБЛИКИ СЕРБИЯ

ВОЕННО-ТЕХНИЧЕСКИЙ ВЕСТНИК

ТОМ 70 • НОМЕР ВЫПУСКА 2 • АПРЕЛЬ-ИЮНЬ 2022.

SCIENTIFIC JOURNAL OF THE MINISTRY OF DEFENCE AND SERBIAN ARMED FORCES

MILITARY TECHNICAL COURIER

VOLUME 70 • ISSUE 2 • APRIL-JUNE 2022

втг.мо.упр.срб
www.vtg.mod.gov.rs
COBISS.SR-ID: 4423938
COBISS.SR-ID: 181287436
DOI: 10.5937/VojnotehnickiGlasnik

ВЛАСНИЦИ:
Министарство одбране и Војска Србије

ИЗДАВАЧ:
Универзитет одбране у Београду, Војна академија

СОБСТВЕННИКИ: Министерство обороны и Вооружённые силы Республики Сербия

ИЗДАТЕЛЬСТВО: Университет обороны в г. Белград, Военная академия

OWNERS:
Ministry of Defence and Serbian Armed Forces

PUBLISHER:
University of Defence in Belgrade, Military Academy

С А Д Р Ж А Ј

С О Д Е Р Ж А Н И Е

C O N T E N T S

ОРИГИНАЛНИ НАУЧНИ РАДОВИ
ОРИГИНАЛЬНЫЕ НАУЧНЫЕ СТАТЬИ
ORIGINAL SCIENTIFIC PAPERS

A STUDY ON INTEGRAL TRANSFORMS OF THE GENERALIZED LOMMEL-WRIGHT FUNCTION

Mohammad Saeed Khan[a], *Sirazul* Haq[b], *Moharram Ali* Khan[c], *Nicola* Fabiano[d]

[a] Sefako Makgatho Health Sciences University, Department of Mathematics and Applied Mathematics, Ga-Rankuwa, Republic of South Africa, e-mail: drsaeed9@gmail.com, ORCID iD: https://orcid.org/0000-0003-0216-241X

[b] J. S. University, Department of Applied Science, Shikohabad, Ferozabad, U.P., Republic of India, e-mail: sirajulhaq007@gmail.com, ORCID iD: https://orcid.org/0000-0001-9297-2445

[c] Umaru Musa Yaradua University, Department of Mathematics and Statistics, Katsina, Federal Republic of Nigeria, e-mail: mkhan91@gmail.com, ORCID iD: https://orcid.org/0000-0002-5563-4743

[d] University of Belgrade, "Vinča" Institute of Nuclear Sciences - Institute of National Importance for the Republic of Serbia, Belgrade, Republic of Serbia, e-mail: nicola.fabiano@gmail.com, **corresponding author**, ORCID iD: https://orcid.org/0000-0003-1645-2071

DOI: 10.5937/vojtehg70-36402;https://doi.org/10.5937/vojtehg70-36402

FIELD: Mathematics
ARTICLE TYPE: Original scientific paper

Abstract:

Introduction/purpose: The aim of this article is to establish integral transforms of the generalized Lommel-Wright function.

Methods: These transforms are expressed in terms of the Wright Hypergeometric function.

Results: Integrals involving the trigonometric, generalized Bessel function and the Struve functions are obtained.

Conclusions: Various interesting transforms as the consequence of this method are obtained.

Key words: Generalized Lommel-Wright functions $J(z)$, Hankel transform, K-transform, Wright function, Whittaker function.

Introduction

The transform defined by the following integral equation

$$R_\nu\{f(x);p\} = g(p,\nu) = \int_0^{+\infty} (px)^{1/2} K_\nu(px) f(x)dx \tag{1}$$

is called the k transform with p as a complex parameter and $K_\nu(px)$ is called the Modified Bessel function of the third kind or the Macdonald function, see (Mathai et al, 2010, p.53). The Hankel transform of a function $f(x)$, denoted by $g(p,\nu)$ is defined as

$$g(p,\nu) = \int_0^{+\infty} (px)^{1/2} J_\nu(px) f(x)dx, \;\; p>0 \tag{2}$$

where $J_\nu(px)$ is called the Bessel-Maitland function or the Maitland-Bessel function (Mathai et al, 2010, p.22 and p.56).

The Wright hypergeometric function defined by the series (Srivastava & Manocha, 1984):

$${}_p\psi_q\left[\begin{array}{c}(\alpha_1,A_1),\,..,(\alpha_p,A_p);\\ \\ (\beta_1,B_1)...,(\beta_q,B_q)\end{array} z\right] = \sum_{k=0}^{+\infty} \frac{\prod_{j=1}^{p}\Gamma(\alpha_j+A_jk)z^k}{\prod_{j=1}^{q}\Gamma(\beta_j+B_jk)k!}, \tag{3}$$

where the coefficients $A_1,....A_p$ and $B_1,....B_q$ are positive real numbers such that

$$1+\sum_{j=1}^{q} B_j - \sum_{j=1}^{p} A_j \geq 0, \tag{4}$$

can be slightly generalized (3) as given below.

$${}_p\psi_q\left[\begin{array}{c}(\alpha_1,1),\,..,(\alpha_p,1);\\ \\ (\beta_1,1)...,(\beta_q,1)\end{array} z\right] = \frac{\prod_{j=1}^{p}\Gamma(\alpha_j)}{\prod_{j=1}^{q}\Gamma(\beta_j)} {}_pF_q\left[\begin{array}{c}\alpha_1,..,\alpha_p;\\ \\ \beta_1,...,\beta_q\end{array} z\right], \tag{5}$$

where ${}_pF_q$ is the generalized hypergeometric function defined by (Srivastava & Manocha, 1984; Rainville, 1960)

$$ {}_pF_q\left[\begin{array}{c} \alpha_1,..,\alpha_p; \\ \\ \beta_1,...,\beta_q \end{array} z\right] = \sum_{k=0}^{+\infty} \frac{(\alpha_1)_n,....,(\alpha_p)_n z^n}{(\beta_1)_n,....,(\beta_q)_n n!} = $$
$$ {}_pF_q(\alpha_1,...,\alpha_p;\beta_1,....,\beta_q;z), \tag{6} $$

where $(\lambda)_n$ is the well known Pochhammer symbol (Srivastava & Manocha, 1984).

The series representation of the generalized Lommel Wright function as (Kachhia & Prajapati, 2016);

$$ J_{\nu,\lambda}^{\mu,m}(z) = \sum_{k=0}^{+\infty} \frac{(-1)^k \Gamma(k+1)(\frac{z}{2})^{2k+\nu+2\lambda}}{\Gamma(\lambda+k+1)^m \Gamma(\nu+k\mu+\lambda+1)k!}, $$
$$ (z \in \mathbb{C}/(-\infty,0],\ m \in \mathbb{N},\ \nu,\lambda \in \mathbb{C}, \mu > 0). \tag{7} $$

Also, we have the following relations of the generalized Lommel Wright functions with trigonometric functions and the generalized Bessel function $\mathbb{J}_{\nu,\lambda}^{\mu}(z)$ and the Struve function as follows:

$$ J_{1/2,0}^{1,1}(z) = \sqrt{\frac{2}{\pi z}}\sin(z) \tag{8} $$

$$ J_{-1/2,0}^{1,1}(z) = \sqrt{\frac{2}{\pi z}}\cos(z) \tag{9} $$

$$ J_{\nu,\lambda}^{\mu,1}(z) = \mathbb{J}_{\nu,\lambda}^{\mu}(z) \tag{10} $$

$$ J_{\nu,1/2}^{1,1}(z) = H_\nu(z). \tag{11} $$

The following known results of Mathai and Saxena (Mathai & Saxena, 1973):

$$ \int_0^{+\infty} x^{\delta-1} J_\eta(ax)dx = \frac{2^{\delta-1}a^{-\delta}\Gamma(\frac{\delta+\eta}{2})}{\Gamma(1+\frac{\eta-\delta}{2})}, \quad \Re(\eta) < \Re(\delta) < 3/2, \quad a > 0 \tag{12} $$

$$\int_0^{+\infty} x^{\delta-1} K_\eta(ax)dx = 2^{\delta-2}a^{-\delta}\Gamma(\delta \pm \eta)/2, \tag{13}$$

$$\int_0^{+\infty} x^{\delta-1} \exp(-at) K_\eta(ax)dx = \frac{\Gamma(\delta \pm \eta)/2}{(2a)^{\delta-1}\Gamma(\delta + 1/2)}, \tag{14}$$

$$\int_0^{+\infty} x^{\delta-1} \exp(1/2\ x) W_{(\eta,\alpha)}(x)dx = \frac{\Gamma(1/2 \pm \alpha + \delta)\Gamma(-\eta - \delta)}{\Gamma(1/2 \pm \alpha - \eta)}, \tag{15}$$

$$\int_0^{+\infty} x^{\delta-1} \exp(-1/2\ x) M_{(\eta,m)}(x)dx = \frac{\Gamma(2m+1)\Gamma(m+\delta+1/2)\Gamma(\eta-\delta)}{\Gamma(m-\delta+1/2)\Gamma(m+\eta+1/2)}, \tag{16}$$

$$\int_0^{+\infty} x^{\delta-1} W_{(\eta,\alpha)}(x) W_{(-\eta,\alpha)}(x)dx = \frac{\Gamma((\delta+1)/2 \pm \alpha)\Gamma(\delta+1)}{2\Gamma(1+\delta/2 \pm \eta)}. \tag{17}$$

Various generalizations and cases of the Lommel-Wright function have been investigated. For details, see (Paneva-Konovska, 2007; Menaria et al, 2016; Mondal & Nisar, 2017; Srivastava & Daoust, 1969; Kiryakova, 2000).

Integral formulas involving the Lommel-Wright functions have been developed by many authors. See e.g., (Choi & Agarwal, 2013; Choi et al, 2014; Jain et al, 2016; Chaurasia & Pandey, 2010). In this sequel, here, we aim at establishing a certain new generalized integral formula involving the generalized Lommel-Wright function $J_{\nu,\lambda}^{\mu,m}(z)$ interesting integral formulas which are derived as special cases.

Main results

This section deals with the evaluation of integrals formulas involving the Lommel-Wright function defined in (7) and the integrals involving the product of the Bessel function of first kind, the Kelvin‘s function and Whittaker function (Whittaker & Watson, 2013) with the generalized Lommel-Wright function.

THEOREM 1. *Let* $z \in \mathbb{C}/(-\infty,0],\ m \in \mathbb{N},\ \nu,\lambda \in \mathbb{C}, \mu > 0$. *Then the Hankel transform of the generalized Lommel-Wright function defined in (7) is given by*

$$\int_0^{+\infty} z^{\rho-1} J_\eta(az) J_{\nu,\lambda}^{\mu,m}(b\, z^w)dz = \frac{1}{2}\left(\frac{b}{2}\right)^{\nu+2\lambda}\left(\frac{2}{a}\right)^{\rho+w(\nu+2\lambda)} \times$$
$$2\psi_{m+2}\left[\begin{matrix}(1,1),(\frac{\eta+\rho+w\nu+2w\lambda}{2},w);\\ (\lambda+1,1),...,(\lambda+1,1),(\nu+\lambda+1,\mu),((\frac{2+\eta-(\rho+w\nu+2w\lambda)}{2}),-w);\end{matrix}\left(\frac{-b^2}{4}\right)\left(\frac{4}{a^2}\right)^w\right]. \tag{18}$$

Proof. On using (7) in the integrand of (1) which is verified by uniform convergence of the involved series under the given conditions, we get

$$\int_0^{+\infty} z^{\rho-1} J_\eta(az) J_{\nu,\lambda}^{\mu,m}(bz^w)dz =$$
$$\sum_{n=0}^{+\infty} \frac{(-1)^n \Gamma(n+1)(b/2)^{2n+\nu+2\lambda}}{\Gamma(\lambda+n+1)^m \Gamma(\nu+\lambda+n\mu+1)n!} \int_0^{+\infty} z^{\rho+w(2n+\nu+2\lambda)-1} J_\eta(az)dz.$$

Now using (12) in the above equation we get

$$\int_0^{+\infty} z^{\rho-1} J_\eta(az) J_{\nu,\lambda}^{\mu,m}(bz^w)dz = \left(1/2\right)\left(b/2\right)^{\nu+2\lambda}\left(2/a\right)^{\rho+w(\nu+2\lambda)} \times$$
$$\sum_{n=0}^{+\infty} \frac{\Gamma(n+1)\Gamma(\eta+\rho+w\nu+2w\lambda+2wn)/2\left(-b^2/4\right)^n\left(4/a^2\right)^{wn}}{\Gamma(\lambda+n+1)^m\Gamma(\nu+\lambda+n\mu+1)\Gamma(2+\eta-\rho-w\nu-2w\lambda-2wn)/2\ n!}$$
$$= \frac{1}{2}\left(\frac{b}{2}\right)^{\nu+2\lambda}\left(\frac{2}{a}\right)^{\rho+w(\nu+2\lambda)} \times$$
$$2\psi_{m+2}\left[\begin{matrix}(1,1),\left(\frac{\eta+\rho+w\nu+2w\lambda}{2},w\right);\\ (\lambda+1,1),...,(\lambda+1,1),(\nu+\lambda+1,\mu),\left(\left(\frac{2+\eta-(\rho+w\nu+2w\lambda)}{2}\right),-w\right);\end{matrix}\left(\frac{-b^2}{4}\right)\left(\frac{4}{a^2}\right)^w\right]. \tag{19}$$

□

THEOREM 2. *Let* $z \in \mathbb{C}/(-\infty,0],\ m \in \mathbb{N},\ \nu,\lambda \in \mathbb{C}, \mu > 0$. *Then the K-Transform of the generalized Lommel-Wright function defined in (7) is given*

by

$$\int_0^{+\infty} z^{\rho-1}K_\eta(az)J_{\nu,\lambda}^{\mu,m}(b\,z^w)dz = \frac{1}{4}\left(\frac{b}{2}\right)^{\nu+2\lambda}\left(\frac{2}{a}\right)^{\rho+w(\nu+2\lambda)}\times$$
$$_2\psi_{m+1}\left[\begin{matrix}(1,1),(\frac{\rho+w\nu+2w\lambda\pm\eta}{2},w);\\(\lambda+1,1),...,(\lambda+1,1),(\nu+\lambda+1,\mu);\end{matrix}\left(\frac{-b^2}{4}\right)\left(\frac{4}{a^2}\right)^w\right]. \quad (20)$$

Proof. On using (7) in the integrand of (2) which is verified by uniform convergence of the involved series under the given conditions, we get

$$\int_0^{+\infty} z^{\rho-1}K_\eta(az)J_{\nu,\lambda}^{\mu,m}(bz^w)dz =$$
$$\sum_{n=0}^{+\infty}\frac{(-1)^n\Gamma(n+1)(b/2)^{2n+\nu+2\lambda}}{\Gamma(\lambda+n+1)^m\Gamma(\nu+\lambda+n\mu+1)n!}\int_0^{+\infty} z^{\rho+w(2n+\nu+2\lambda)-1}K_\eta(az)dz.$$

Now using (13) in the above equation we get

$$\int_0^{+\infty} z^{\rho-1}K_\eta(az)J_{\nu,\lambda}^{\mu,m}(bz^w)dz = \left(1/4\right)\left(b/2\right)^{\nu+2\lambda}\left(2/a\right)^{\rho+w(\nu+2\lambda)}\times$$
$$\sum_{n=0}^{+\infty}\frac{\Gamma(n+1)\Gamma(\rho+w\nu+2w\lambda\pm\eta+2wn)/2\left(-b^2/4\right)^n\left(4/a^2\right)^{nw}}{\Gamma(\lambda+n+1)^m\Gamma(\nu+\lambda+n\mu+1)n!}$$
$$= \frac{1}{4}\left(\frac{b}{2}\right)^{\nu+2\lambda}\left(\frac{2}{a}\right)^{\rho+w(\nu+2\lambda)}$$
$$_2\psi_{m+1}\left[\begin{matrix}(1,1),(\frac{\rho+w\nu+2w\lambda\pm\eta}{2},w);\\(\lambda+1,1),...,(\lambda+1,1),(\nu+\lambda+1,\mu);\end{matrix}\left(\frac{-b^2}{4}\right)\left(\frac{4}{a^2}\right)^w\right]. \quad (21)$$

□

THEOREM 3. *Let* $z \in \mathbb{C}/(-\infty,0]$, $m \in \mathbb{N}$, $\nu,\lambda \in \mathbb{C},\mu > 0$. *Then the K-Transform of the generalized Lommel-Wright function defined in (7) is given by*

$$\int_0^{+\infty} z^{\rho-1}\exp(-az)K_\eta(az)J_{\nu,\lambda}^{\mu,m}(b\,z^w)dz = \frac{2a\sqrt{\pi}\left(b/2\right)^{\nu+2\lambda}}{(2a)^{\rho+w(\nu+2\lambda)}}\times$$
$$_2\psi_{m+2}\left[\begin{matrix}(1,1),(\rho+w\nu+2w\lambda\pm\eta,2w);\\(\lambda+1,1),...,(\lambda+1,1),(\nu+\lambda+1,\mu),(\rho+w\nu+2w\lambda+1/2,2w);\end{matrix}\right.$$

$$\left(\frac{-b^2}{4(4a^2)^w}\right)\Bigg]. \tag{22}$$

Proof. On using (7) in the integrand of (3) which is verified by uniform convergence of the involved series under the given conditions, we get

$$\int_0^{+\infty} z^{\rho-1}\exp(-az)K_\eta(az)J_{\nu,\lambda}^{\mu,m}(bz^w)dz = \sum_{n=0}^{+\infty}\frac{(-1)^n\Gamma(n+1)(b/2)^{2n+\nu+2\lambda}}{\Gamma(\lambda+n+1)^m\Gamma(\nu+\lambda+n\mu+1)n!}\times \int_0^{+\infty} z^{\rho+w(2n+\nu+2\lambda)-1}\exp(-az)K_\eta(az)dz. \tag{23}$$

Now using (14) in the above equation we get

$$\int_0^{+\infty} z^{\rho-1}\exp(-az)K_\eta(az)J_{\nu,\lambda}^{\mu,m}(bz^w)dz = \frac{2a\sqrt{\pi}\left(b/2\right)^{\nu+2\lambda}}{(2a)^{\rho+w(\nu+2\lambda)}}\times \sum_{n=0}^{+\infty}\frac{\Gamma(n+1)\Gamma(\rho+w\nu+2w\lambda\pm\eta+2wn)(\frac{-b^2}{4(4a)^w})^n}{\Gamma(\lambda+n+1)^m\Gamma(\nu+\lambda+n\mu+1)(\rho+w\nu+2w\lambda+1/2,2w)n!}$$
$$= \frac{2a\sqrt{\pi}(b/2)^{\nu+2\lambda}}{(2a)^{\rho+w(\nu+2\lambda)}}\times {}_2\psi_{m+2}\left[\begin{matrix}(1,1),(\rho+w\nu+2w\lambda\pm\eta,2w);\\ (\lambda+1,1),...,(\lambda+1,1),(\nu+\lambda+1,\mu),(\rho+w\nu+2w\lambda+1/2,2w);\end{matrix}\left(\frac{-b^2}{4(4a^2)^w}\right)\right]. \tag{24}$$

□

THEOREM 4. *Let $z\in\mathbb{C}/(-\infty,0]$, $m\in\mathbb{N}$, $\nu,\lambda\in\mathbb{C},\mu>0$. Then the product of the Whittaker function and the generalized Lommel-Wright function defined in (7) is given by*

$$\int_0^{+\infty} z^{\rho-1}\exp(az/2)W_{\eta,\alpha}(az)J_{\nu,\lambda}^{\mu,m}(w\,z^\theta)dz = \frac{\left(w/2\right)^{\nu+2\lambda}}{(a)^{\rho+\theta(\nu+2\lambda)}\Gamma(1/2\pm\alpha-\eta)}$$
$${}_3\psi_{m+1}\left[\begin{matrix}(1,1),(1/2\pm\alpha+\rho+\nu\theta+2\lambda\theta,2\theta),(-\eta-\rho-\nu\theta-2\theta\lambda,-2\theta);\\ (\lambda+1,1),...,(\lambda+1,1),(\nu+\lambda+1,\mu);\end{matrix}\right.$$

$$\left(\frac{-w^2}{4(a^2)^\theta}\right)\Bigg]. \tag{25}$$

Proof. Putting $az = x, adz = dx$ as $z \to 0, x \to 0$ and $z \to +\infty, x \to +\infty$ and using (7) in the integrand of (4) which is verified by uniform convergence of the involved series under the given conditions, we get

$$\int_0^{+\infty} z^{\rho-1}\exp(az/2)W_{\eta,\alpha}(az)J^{\mu,m}_{\nu,\lambda}(wz^\theta)dz =$$
$$\frac{\left(w/2\right)^{\nu+2\lambda}}{(a)^{\rho+\theta(\nu+2\lambda)}}\sum_{n=0}^{+\infty}\frac{\Gamma(n+1)\left(\frac{-w^2}{4(a^2)^\theta}\right)^n}{\Gamma(\lambda+n+1)^m\Gamma(\nu+\lambda+n\mu+1)n!}\times$$
$$\int_0^{+\infty} x^{\rho+\theta(2n+\nu+2\lambda)-1}\exp(x/2)W_{\eta,\alpha}(x)dx.$$

Now using (15) in the above equation we get

$$\int_0^{+\infty} z^{\rho-1}\exp(az/2)W_{\eta,\alpha}(az)J^{\mu,m}_{\nu,\lambda}(wz^\theta)dz = \frac{(w/2)^{\nu+2\lambda}}{(a)^{\rho+\theta(\nu+2\lambda)}\Gamma(1/2\pm\alpha-\eta)}\times$$
$$\sum_{n=0}^{+\infty}\Bigg[\frac{\Gamma(n+1)\Gamma(1/2\pm\alpha+\rho+\theta\nu+2\theta\lambda+2\theta\ n)\Gamma(-\eta-\rho-\theta\nu-2\theta\lambda-2\theta\ n)}{\Gamma(\lambda+n+1)^m\Gamma(\nu+\lambda+n\mu+1)n!}$$
$$\times\left(\frac{-w^2}{4(a^2)^\theta}\right)^n\Bigg] = \frac{\left(w/2\right)^{\nu+2\lambda}}{(a)^{\rho+\theta(\nu+2\lambda)}\Gamma(1/2\pm\alpha-\eta)}\times$$
$${}_3\psi_{m+1}\Bigg[\begin{matrix}(1,1),(1/2\pm\alpha+\rho+\theta\nu+2\theta\lambda,2\theta),(-\eta-\rho-\nu\theta-2\theta\lambda,-2\theta);\\(\lambda+1,1),...,(\lambda+1,1),(\nu+\lambda+1,\mu);\end{matrix}$$
$$\left(\frac{-w^2}{4(a^2)^\theta}\right)\Bigg]. \tag{26}$$

□

THEOREM 5. *Let* $z \in \mathbb{C}/(-\infty,0]$, $m \in \mathbb{N}$, $\nu,\lambda \in \mathbb{C}, \mu > 0$. *Then the product of the Whittaker function and the generalized Lommel-Wright function defined in (7) is given by*

$$\int_0^{+\infty} z^{\rho-1}\exp(-az/2)M_{\eta,\alpha}(az)J^{\mu,m}_{\nu,\lambda}(w\ z^\theta)dz =$$

$$\frac{\left(w/2\right)^{\nu+2\lambda}(1/a)^{\theta(\nu+2\lambda)}\Gamma(2\alpha+1)}{(a)^{\rho}\Gamma(\alpha+\eta+1/2)}\times$$

$${}_3\psi_{m+2}\left[\begin{array}{c}(1,1),(\alpha+\rho+1/2+\nu\theta+2\lambda\theta,2\theta),(\eta-\rho-\nu\theta-2\theta\lambda,-2\theta);\\(\lambda+1,1),...,(\lambda+1,1),(\nu+\lambda+1,\mu),(\alpha-\rho-\theta\nu-2\theta\lambda+1/2,-2\theta);\end{array}\left(\frac{-w^2}{4(a^2)^{\theta}}\right)\right]. \tag{27}$$

Proof. Putting $az=x, adz=dx$ as $z\to 0, x\to 0$ and $z\to+\infty, x\to+\infty$ and using (7) in the integrand of (5) which is verified by uniform convergence of the involved series under the given conditions, we get

$$\int_0^{+\infty} z^{\rho-1}\exp(-az/2)M_{\eta,\alpha}(az)J^{\mu,m}_{\nu,\lambda}(wz^{\theta})dz=\frac{\left(w/2\right)^{\nu+2\lambda}(1/a)^{\theta(\nu+2\lambda)}}{(a)^{\rho}}\times$$

$$\sum_{n=0}^{+\infty}\frac{\Gamma(n+1)\left(\frac{-w^2}{4(a^2)^{\theta}}\right)^n}{\Gamma(\lambda+n+1)^m\Gamma(\nu+\lambda+n\mu+1)n!}\times$$

$$\int_0^{+\infty} x^{\rho+\theta(2n+\nu+2\lambda)-1}\exp(-x/2)M_{\eta,\alpha}(x)dx.$$

Now using (16) in the above equation we get

$$\int_0^{+\infty} z^{\rho-1}\exp(-az/2)M_{\eta,\alpha}(az)J^{\mu,m}_{\nu,\lambda}(wz^{\theta})dz=$$

$$\frac{(w/2)^{\nu+2\lambda}(1/a)^{\theta(\nu+2\lambda)}\Gamma(2\alpha+1)}{(a)^{\rho}\Gamma(\alpha+\eta+1/2)}\times$$

$$\sum_{n=0}^{+\infty}\left[\frac{\Gamma(n+1)\Gamma(\alpha+\rho+\theta\nu+2\theta\lambda+1/2+2\theta\ n)\Gamma(\eta-\rho-\theta\nu-2\theta\lambda-2\theta\ n)}{\Gamma(\lambda+n+1)^m\Gamma(\nu+\lambda+n\mu+1)\Gamma(\alpha-\rho-\theta\nu-2\theta\lambda-2n\theta+1/2)n!}\times\right.$$

$$\left.\left(\frac{-w^2}{4(a^2)^{\theta}}\right)^n\right]=\frac{\left(w/2\right)^{\nu+2\lambda}(1/a)^{\theta(\nu+2\lambda)}\Gamma(2\alpha+1)}{(a)^{\rho}\Gamma(\alpha+\eta+1/2)}\times$$

$${}_3\psi_{m+2}\left[\begin{array}{c}(1,1),(\alpha+\rho+1/2+\nu\theta+2\lambda\theta,2\theta),(\eta-\rho-\nu\theta-2\theta\lambda,-2\theta);\\(\lambda+1,1),...,(\lambda+1,1),(\nu+\lambda+1,\mu),(\alpha-\rho-\theta\nu-2\theta\lambda+1/2,-2\theta);\end{array}\left(\frac{-w^2}{4(a^2)^{\theta}}\right)\right]. \tag{28}$$

□

THEOREM 6. *Let* $z \in \mathbb{C}/(-\infty,0],\ m \in \mathbb{N},\ \nu,\lambda \in \mathbb{C}, \mu > 0$. *Then the product of the Whittaker function and the generalized Lommel-Wright function defined in (7) is given by*

$$\int_0^{+\infty} z^{\rho-1} W_{\eta,\alpha}(az) W_{-\eta,\alpha}(az) J_{\nu,\lambda}^{\mu,m}(w\ z^{\theta}) dz = \frac{\left(w/2\right)^{\nu+2\lambda} (1/a)^{\theta(\nu+2\lambda)}}{(a)^{\rho}}$$
$$ {}_3\psi_{m+2}\left[\begin{matrix} (1,1), (\frac{\rho+\theta(\nu+2\lambda)+1}{2} \pm \alpha, \theta), (\rho+\theta(\nu+2\lambda)+1, 2\theta); \\ (\lambda+1,1), ..., (\lambda+1,1), (\nu+\lambda+1,\mu), 2(1+\frac{\rho+\theta(\nu+2\lambda)}{2} \pm \eta, \theta); \end{matrix} \left(\frac{-w^2}{4(a^2)^{\theta}}\right)\right]. \tag{29}$$

Proof. Putting $az = x, adz = dx$ as $z \to 0, x \to 0$ and $z \to +\infty, x \to +\infty$ and using (7) in the integrand of (6) which is verified by uniform convergence of the involved series under the given conditions, we get

$$\int_0^{+\infty} z^{\rho-1} W_{-\eta,\alpha}(az) W_{\eta,\alpha}(az) J_{\nu,\lambda}^{\mu,m}(wz^{\theta}) dz = \frac{\left(w/2\right)^{\nu+2\lambda} (1/a)^{\theta(\nu+2\lambda)}}{(a)^{\rho}} \times$$
$$\sum_{n=0}^{+\infty} \frac{\Gamma(n+1)\left(\frac{-w^2}{4(a^2)^{\theta}}\right)^n}{\Gamma(\lambda+n+1)^m \Gamma(\nu+\lambda+n\mu+1) n!} \times$$
$$\int_0^{+\infty} x^{\rho+\theta(2n+\nu+2\lambda)-1} W_{-\eta,\alpha}(x) W_{\eta,\alpha}(x) dx.$$

Now using (17) in the above equation we get

$$\int_0^{+\infty} z^{\rho-1} W_{-\eta,\alpha}(az) W_{\eta,\alpha}(az) J_{\nu,\lambda}^{\mu,m}(wz^{\theta}) dz = \frac{(w/2)^{\nu+2\lambda} (1/a)^{\theta(\nu+2\lambda)}}{(a)^{\rho}} \times$$
$$\sum_{n=0}^{+\infty} \frac{\Gamma(n+1)\Gamma(\frac{\rho+\theta(\nu+2\lambda+2n+1)}{2} \pm \alpha)\Gamma(\rho+\theta\nu+2\theta\lambda+2\theta\ n)(\frac{-w^2}{4(a^2)^{\theta}})^n}{\Gamma(\lambda+n+1)^m \Gamma(\nu+\lambda+n\mu+1) 2\Gamma(1+\frac{\rho+\theta(\nu+2\lambda+2n)}{2} \pm \eta) n!}$$
$$= \frac{\left(w/2\right)^{\nu+2\lambda} (1/a)^{\theta(\nu+2\lambda)}}{(a)^{\rho}} \times$$

$$ {}_3\psi_{m+2}\left[\begin{array}{c} (1,1),(\frac{\rho+\theta(\nu+2\lambda)+1}{2}\pm\alpha,\theta),(\rho+\theta(\nu+2\lambda)+1,2\theta); \\ (\lambda+1,1),...,(\lambda+1,1),(\nu+\lambda+1,\mu),2(1+\frac{\rho+\theta(\nu+2\lambda)}{2}\pm\eta,\theta); \\ \left(\frac{-w^2}{4(a^2)^\theta}\right)\end{array}\right]. \tag{30} $$

□

Special cases

In this section, we get some integral formulas involving a trigonometric function and the generalized Lommel-Wright function as follows:

COROLLARY 1. *If we take* $m=1,\mu=1,\lambda=0$ *and* $\nu=1/2$ *in* (1) *and then by using* (8)*, we derive the following integral formula:*

$$ \int_0^{+\infty} z^{\rho-w/2-1}J_\eta(az)\sin(b\,z^w)dz=\left(b/4\right)\sqrt{\pi}\left(\frac{2}{a}\right)^{\rho+w/2}\times $$
$$ {}_1\psi_2\left[\begin{array}{c} (\frac{\eta+\rho+w/2}{2},w); \\ (3/2,1),((\frac{2+\eta-(\rho+w/2)}{2}),-w);\end{array}\left(\frac{-b^2}{4}\right)\left(\frac{4}{a^2}\right)^w\right]. \tag{31} $$

COROLLARY 2. *If we take* $m=1,\mu=1,\lambda=0$ *and* $\nu=1/2$ *in* (2) *and then by using* (8)*, we obtain:*

$$ \int_0^{+\infty} z^{\rho-w/2-1}K_\eta(az)\sin(b\,z^w)dz=\left(b/8\right)\sqrt{\pi}\left(\frac{2}{a}\right)^{\rho+w/2}\times $$
$$ {}_1\psi_1\left[\begin{array}{c} (\frac{\rho+w/2\pm\eta}{2},w); \\ (3/2,1);\end{array}\left(\frac{-b^2}{4}\right)\left(\frac{4}{a^2}\right)^w\right]. \tag{32} $$

COROLLARY 3. *If we take* $m=1,\mu=1,\lambda=0$ *and* $\nu=1/2$ *in* (3) *and then by using* (8)*, we obtain:*

$$ \int_0^{+\infty} z^{\rho-w/2-1}\exp(-az)K_\eta(az)\sin(b\,z^w)dz=\left(\frac{\pi\,ab}{(2a)^{\rho+w/2}}\right)\times $$
$$ {}_1\psi_2\left[\begin{array}{c} (\rho+w/2\pm\eta,2w); \\ (3/2,1),(\rho+w/2+1/2,2w);\end{array}\left(\frac{-b^2}{4(4a^2)^w}\right)\right]. \tag{33} $$

COROLLARY 4. *If we take* $m=1,\mu=1,\lambda=0$ *and* $\nu=1/2$ *in* (4) *and then by using* (8)*, we obtain:*

$$\int_0^{+\infty} z^{\rho-\theta/2-1}\exp(az/2)W_{\eta,\alpha}(az)\sin(w\ z^{\theta})dz = \left(\frac{w/2\sqrt{\pi}}{(a)^{\rho+w/2}(\Gamma(1/2\pm\alpha-\eta))}\right)\times {}_2\psi_1\left[\begin{matrix}(1/2\pm\alpha+\rho+\theta/2,2\theta),(\eta-\rho-\theta/2,-2\theta);\\(3/2,1);\end{matrix}\ \left(\frac{-w^2}{4(a^2)^{\theta}}\right)\right]. \quad (34)$$

COROLLARY 5. *If we take* $m=1,\mu=1,\lambda=0$ *and* $\nu=1/2$ *in* (5) *and then by using* (8)*, we obtain:*

$$\int_0^{+\infty} z^{\rho-\theta/2-1}\exp(-az/2)M_{\eta,\alpha}(az)\sin(w\ z^{\theta})dz = \left(\frac{w/2\sqrt{\pi}(1/a)^{\theta/2}\Gamma(2\alpha+1)}{(a)^{\rho}(\Gamma(\alpha+\eta+1/2))}\right)\times {}_2\psi_2\left[\begin{matrix}(\alpha+\rho+\theta/2,2\theta),(\eta-\rho-\theta/2,-2\theta);\\(3/2,1),(\alpha-\theta+1/2,-2\theta);\end{matrix}\ \left(\frac{-w^2}{4(a^2)^{\theta}}\right)\right]. \quad (35)$$

COROLLARY 6. *If we take* $m=1,\mu=1,\lambda=0$ *and* $\nu=1/2$ *in* (6) *and then by using* (8)*, we obtain:*

$$\int_0^{+\infty} z^{\rho-\theta/2-1}W_{\eta,\alpha}(az)W_{-\eta,\alpha}(az)\sin(w\ z^{\theta})dz = \left(\frac{w/2\sqrt{\pi}(1/a)^{\theta/2}}{(a)^{\rho}}\right) {}_2\psi_2\left[\begin{matrix}(\frac{\rho+\theta/2+1}{2}\pm\alpha,\theta),(\rho+\theta/2+1,2\theta);\times\\(3/2,1),2(1+\frac{\rho+\theta/2}{2}\pm\eta,\theta);\end{matrix}\ \left(\frac{-w^2}{4(a^2)^{\theta}}\right)\right]. \quad (36)$$

COROLLARY 7. *If we take* $m=1,\mu=1,\lambda=0$ *and* $\nu=-1/2$ *in* (1) *and then by using* (9)*, we derive the following integral formula:*

$$\int_0^{+\infty} z^{\rho-w/2-1}J_{\eta}(az)\cos(z)dz = \sqrt{\left(\frac{\pi}{4}\right)}\left(2/a\right)^{\rho-w/2}\times {}_1\psi_2\left[\begin{matrix}(\frac{\eta+\rho-w/2}{2},w);\\(1/2,1),((\frac{2+\eta-(\rho-w/2)}{2}),-w);\end{matrix}\ \left(\frac{-b^2}{4}\right)\left(\frac{4}{a^2}\right)^{w}\right]. \quad (37)$$

COROLLARY 8. *If we take* $m = 1, \mu = 1, \lambda = 0$ *and* $\nu = -1/2$ *in* (2) *and then by using* (9)*, we obtain:*

$$\int_0^{+\infty} z^{\rho-w/2-1} K_\eta(az)\cos(z)dz = 1/4\sqrt{\pi}\left(\frac{2}{a}\right)^{\rho-w/2} \times {}_1\psi_1\left[\begin{matrix}(\frac{\rho-w/2\pm\eta}{2}, w);\\ (1/2,1);\end{matrix}\ \left(\frac{-b^2}{4}\right)\left(\frac{4}{a^2}\right)^w\right]. \tag{38}$$

COROLLARY 9. *If we take* $m = 1, \mu = 1, \lambda = 0$ *and* $\nu = -1/2$ *in* (3) *and then by using* (9)*, we obtain:*

$$\int_0^{+\infty} z^{\rho-w/2-1}\exp(-az)K_\eta(az)\cos(b\ z^w)dz = \left(\frac{2a\pi}{(2a)^{\rho-w/2}}\right) \times {}_1\psi_2\left[\begin{matrix}(\rho-w/2\pm\eta, 2w);\\ (1/2,1),(\rho-w/2+1/2,2w);\end{matrix}\ \left(\frac{-b^2}{4(4a^2)^w}\right)\right]. \tag{39}$$

COROLLARY 10. *If we take* $m = 1, \mu = 1, \lambda = 0$ *and* $\nu = -1/2$ *in* (4) *and then by using* (9)*, we obtain:*

$$\int_0^{+\infty} z^{\rho-\theta/2-1}\exp(az/2)W_{\eta,\alpha}(az)\cos(w\ z^\theta)dz = \left(\frac{\sqrt{\pi}}{(a)^{\rho-\theta/2}(\Gamma(1/2\pm\alpha-\eta))}\right)\times {}_2\psi_1\left[\begin{matrix}(1/2\pm\alpha+\rho-\theta/2,2\theta),(\eta-\rho+\theta/2,-2\theta);\\ (1/2,1);\end{matrix}\ \left(\frac{-w^2}{4(a^2)^\theta}\right)\right]. \tag{40}$$

COROLLARY 11. *If we take* $m = 1, \mu = 1, \lambda = 0$ *and* $\nu = -1/2$ *in* (5) *and then by using* (9)*, we obtain:*

$$\int_0^{+\infty} z^{\rho-\theta/2-1}\exp(-az/2)M_{\eta,\alpha}(az)\cos(w\ z^\theta)dz = \left(\frac{\sqrt{\pi}(1/a)^{-\theta/2}\Gamma(2\alpha+1)}{(a)^\rho(\Gamma(\alpha+\eta+1/2))}\right)\times {}_2\psi_2\left[\begin{matrix}(\alpha+\rho-\theta/2+1/2,2\theta),(\eta-\rho+\theta/2,-2\theta);\\ (1/2,1),(\alpha-\rho+\theta+1/2,-2\theta);\end{matrix}\ \left(\frac{-w^2}{4(a^2)^\theta}\right)\right]. \tag{41}$$

COROLLARY 12. *If we take* $m=1,\mu=1,\lambda=0$ *and* $\nu=-1/2$ *in* (6) *and then by using* (9)*, we obtain:*

$$\int_0^{+\infty} z^{\rho-\theta/2-1}W_{\eta,\alpha}(az)W_{-\eta,\alpha}(az)\cos(w\ z^{\theta})dz=\left(\frac{\sqrt{\pi}(1/a)^{-\theta/2}}{(a)^{\rho}}\right)\times$$
$$_2\psi_2\left[\begin{matrix}(\frac{\rho-\theta/2+1}{2}\pm\alpha,\theta),(\rho-\theta/2+1,2\theta);\\(1/2,1),2(1+\frac{\rho-\theta/2}{2}\pm\eta,\theta);\end{matrix}\ \left(\frac{-w^2}{4(a^2)^{\theta}}\right)\right]. \tag{42}$$

COROLLARY 13. *If we take* $m=1$ *in* (1) *and then by using* (10)*, we derive the following integral formula:*

$$\int_0^{+\infty} z^{\rho-1}J_{\eta}(az)J_{\nu,\lambda}^{\mu,1}(b\ z^{w})dz=\left(1/2\right)\left(b/2\right)^{\nu+2\lambda}\left(2/a\right)^{\rho+w(\nu+2\lambda)}\times$$
$$_2\psi_3\left[\begin{matrix}(1,1)(\frac{\eta+\rho+w\nu+2w\lambda}{2},w);\\(\lambda+1,1),(\nu+\lambda+1,\mu),((\frac{2+\eta-(\rho+w\nu+2w\lambda)}{2}),-w);\end{matrix}\ \left(\frac{-b^2}{4}\right)\left(\frac{4}{a^2}\right)^{w}\right]. \tag{43}$$

COROLLARY 14. *If we take* $m=1$ *in* (2) *and then by using* (10)*, we obtain:*

$$\int_0^{+\infty} z^{\rho-1}K_{\eta}(az)J_{\nu,\lambda}^{\mu,1}(b\ z^{w})dz=\left(1/4\right)\left(b/2\right)^{\nu+2\lambda}\left(2/a\right)^{\rho+w(\nu+2\lambda)}\times$$
$$_2\psi_2\left[\begin{matrix}(1,1),(\frac{\rho+w\nu+2w\lambda\pm\eta}{2},w);\\(\lambda+1,1),(\nu+\lambda+1,\mu);\end{matrix}\ \left(\frac{-b^2}{4}\right)\left(\frac{4}{a^2}\right)^{w}\right]. \tag{44}$$

COROLLARY 15. *If we take* $m=1$ *in* (3) *and then by using* (10)*, we obtain:*

$$\int_0^{+\infty} z^{\rho-1}\exp(-az)K_{\eta}(az)J_{\nu,\lambda}^{\mu,1}(b\ z^{w})dz=\left(\frac{2a\sqrt{\pi}(b/2)^{\nu+2\lambda}}{(2a)^{\rho+w(\nu+2\lambda)}}\right)\times$$
$$_2\psi_3\left[\begin{matrix}(1,1),(\rho+w\nu+2w\lambda\pm\eta,2w);\\(\lambda+1,1),(\nu+\lambda+1,\mu),(\rho+w(\nu+2\lambda)+1/2,2w);\end{matrix}\ \left(\frac{-b^2}{4(4a^2)^{w}}\right)\right]. \tag{45}$$

COROLLARY 16. *If we take* $m=1$ *in* (4) *and then by using* (10)*, we obtain:*

$$\int_0^{+\infty} z^{\rho-1}\exp(az/2)W_{\eta,\alpha}(az)J_{\nu,\lambda}^{\mu,1}(w\ z^{\theta})dz=$$

$$\left(\frac{(w/2)^{\nu+2\lambda}}{(a)^{\rho+\theta(\nu+2\lambda)}(\Gamma(1/2\pm\alpha-\eta))}\right)\times$$
$${}_3\psi_2\left[\begin{array}{c}(1,1)(1/2\pm\alpha+\rho+\theta\nu+2\theta\lambda,2\theta),(\eta-\rho-\theta\nu-2\theta\lambda,-2\theta);\\(\lambda+1,1),(\nu+\lambda+1,\mu);\end{array}\left(\frac{-w^2}{4(a^2)^\theta}\right)\right]. \quad (46)$$

COROLLARY 17. *If we take* $m=1$ *in* (5) *and then by using* (10)*, we obtain:*

$$\int_0^{+\infty} z^{\rho-1}\exp(-az/2)M_{\eta,\alpha}(az)J^{\mu,1}_{\nu,\lambda}(w\ z^\theta)dz=$$
$$\left(\frac{(w/1)^{\nu+2\lambda}(1/a)^{\theta(\nu+2\lambda)}\Gamma(2\alpha+1)}{(a)^\rho(\Gamma(\alpha+\eta+1/2))}\right)\times$$
$${}_3\psi_3\left[\begin{array}{c}(1,1),(\alpha+\rho+\theta\nu+2\theta\lambda+1/2,2\theta),(\eta-\rho-\theta\nu-2\theta\lambda,-2\theta);\\(\lambda+1,1),(\nu+\lambda+1,\mu),(\alpha-\rho-\theta\nu-2\theta\lambda+1/2,-2\theta);\end{array}\left(\frac{-w^2}{4(a^2)^\theta}\right)\right]. \quad (47)$$

COROLLARY 18. *If we take* $m=1$ *in* (6) *and then by using* (10)*, we obtain:*

$$\int_0^{+\infty} z^{\rho-1}W_{\eta,\alpha}(az)W_{-\eta,\alpha}(az)J^{\mu,1}_{\nu,\lambda}(w\ z^\theta)dz=\left(\frac{(w/2)^{\nu+2\lambda}(1/a)^{\theta(\nu+2\lambda)}}{(a)^\rho}\right)\times$$
$${}_3\psi_3\left[\begin{array}{c}(1,1),(\frac{\rho+\theta(\nu+2\lambda)+1}{2}\pm\alpha,\theta),(\rho+\theta(\nu+2\lambda)+1,2\theta);\\(\lambda+1,1),(\nu+\lambda+1,\mu),2(1+\frac{\rho+\theta(\nu+2\lambda)}{2}\pm\eta,\theta);\end{array}\left(\frac{-w^2}{4(a^2)^\theta}\right)\right]. \quad (48)$$

COROLLARY 19. *If we take* $m=1,\mu=1$ *and* $\lambda=1/2$ *in* (1) *and then by using* (11)*, we derive the following integral formula:*

$$\int_0^{+\infty} z^{\rho-1}J_\eta(az)H_\nu(b\ z^w)dz=\left(1/2\right)\left(b/2\right)^{\nu+1}\left(2/a\right)^{\rho+w(\nu+1)}\times$$
$${}_2\psi_3\left[\begin{array}{c}(1,1)(\frac{\eta+\rho+w\nu+w}{2},w);\\(3/2,1),(\nu+3/2,1),((\frac{2+\eta-(\rho+w\nu+w)}{2}),-w);\end{array}\left(\frac{-b^2}{4}\right)\left(\frac{4}{a^2}\right)^w\right]. \quad (49)$$

COROLLARY 20. *If we take* $m=1,\mu=1$ *and* $\lambda=1/2$ *in* (2) *and then by using* (11)*, we obtain:*

$$\int_0^{+\infty} z^{\rho-1}K_\eta(az)H_\nu(b\ z^w)dz=\left(1/4\right)\left(b/2\right)^{\nu+1}\left(2/a\right)^{\rho+w(\nu+1)}\times$$

$$ {}_2\psi_2\left[\begin{array}{c}(1,1),(\frac{\rho+w\nu+w\pm\eta}{2},w);\\(3/2,1),(\nu+3/2,\mu);\end{array}\left(\frac{-b^2}{4}\right)\left(\frac{4}{a^2}\right)^w\right]. \quad (50) $$

COROLLARY 21. *If we take* $m=1,\mu=1$ *and* $\lambda=1/2$ *in* (3) *and then by using* (11)*, we obtain:*

$$ \int_0^{+\infty} z^{\rho-1}\exp(-az)K_\eta(az)H_\nu(b\,z^w)dz=\left(\frac{2a\sqrt{\pi}(b/2)^{\nu+1}}{(2a)^{\rho+w(\nu+1)}}\right)\times $$
$$ {}_2\psi_3\left[\begin{array}{c}(1,1),(\rho+w\nu+w\pm\eta,2w);\\(3/2,1),(\nu+3/2,1),(\rho+w(\nu+1)+1/2,2w);\end{array}\left(\frac{-b^2}{4(4a^2)^w}\right)\right]. \quad (51) $$

COROLLARY 22. *If we take* $m=1,\mu=1$ *and* $\lambda=1/2$ *in* (4) *and then by using* (11)*, we obtain:*

$$ \int_0^{+\infty} z^{\rho-1}\exp(az/2)W_{\eta,\alpha}(az)H_\nu(w\,z^\theta)dz=\left(\frac{(w/2)^{\nu+1}}{(a)^{\rho+\theta(\nu+1)}(\Gamma(1/2\pm\alpha-\eta))}\right) $$
$$ {}_3\psi_2\left[\begin{array}{c}(1,1)(1/2\pm\alpha+\rho+\theta\nu+\theta,2\theta),(\eta-\rho-\theta\nu-\theta,-2\theta);\\(3/2,1),(\nu+3/2,1);\\\left(\frac{-w^2}{4(a^2)^\theta}\right)\end{array}\right]. \quad (52) $$

COROLLARY 23. *If we take* $m=1,\mu=1$ *and* $\lambda=1/2$ *in* (5) *and then by using* (11)*, we obtain:*

$$ \int_1^{+\infty} z^{\rho-1}\exp(-az/2)M_{\eta,\alpha}(az)H_\nu(w\,z^\theta)dz= $$
$$ \left(\frac{(w/2)^{\nu+1}(1/a)^{\theta(\nu+1)}\Gamma(2\alpha+1)}{(a)^\rho(\Gamma(\alpha+\eta+1/2))}\right)\times $$
$$ {}_3\psi_3\left[\begin{array}{c}(1,1),(\alpha+\rho+\theta\nu+\theta+1/2,2\theta),(\eta-\rho-\theta\nu-\theta,-2\theta);\\(3/2,1),(\nu+3/2,1),(\alpha-\rho-\theta\nu-\theta+1/2,-2\theta);\\\left(\frac{-w^2}{4(a^2)^\theta}\right)\end{array}\right]. \quad (53) $$

COROLLARY 24. *If we take* $m=1,\mu=1$ *and* $\lambda=1/2$ *in* (6) *and then by using* (11)*, we obtain:*

$$ \int_0^{+\infty} z^{\rho-1}W_{\eta,\alpha}(az)W_{-\eta,\alpha}(az)H_\nu(w\,z^\theta)dz=\left(\frac{(w/2)^{\nu+1}(1/a)^{\theta(\nu+1)}}{(a)^\rho}\right)\times $$

$$ {}_3\psi_3\left[\begin{array}{c}(1,1),(\frac{\rho+\theta(\nu+1)+1}{2}\pm\alpha,\theta),(\rho+\theta(\nu+1)+1,2\theta);\\(3/2,1),(\nu+3/2,1),2(1+\frac{\rho+\theta(\nu+1)}{2}\pm\eta,\theta);\end{array}\left(\frac{-w^2}{4(a^2)^\theta}\right)\right]. \quad (54) $$

References

Chaurasia, V.B.L. & Pandey, S.C. 2010. On the fractional calculus of generalized Mittag-Leffler function. *SCIENTIA Series A: Mathematical Sciences*, 20, pp.113-122 [online]. Available at: https://citeseerx.ist.psu.edu/viewdoc/download?doi=10.1.1.399.5089&rep=rep1&type=pdf [Accessed: 9 February 2022].

Choi, J. & Agarwal, P. 2013. Certain unified integrals associated with Bessel functions. *Boundary Value Problems*, art.number:95. Available at: https://doi.org/10.1186/1687-2770-2013-95.

Choi, J., Mathur, S. & Purohit, S.D. 2014. Certain new integral formulas involving the generalized Bessel functions. *Bulletin of the Korean Mathematical Society*, 51(4), pp.995-1003. Available at: https://doi.org/10.4134/BKMS.2014.51.4.995.

Jain, S., Choi, J., Agarwal, P. & Nisar, K.S. 2016. Integrals involving Laguerre type plynomials and Bessel functions. *Far East Journal of Mathematical Sciences (FJMS)*, 100(6), pp.965-976. Available at: https://doi.org/10.17654/MS100060965.

Kachhia, K.B. & Prajapati, J.C. 2016. On generalized fractional kinetic equations involving generalized Lommel-Wright functions. *Alexandria Engineering Journal*, 55(3), pp.2953-2957. Available at: https://doi.org/10.1016/j.aej.2016.04.038.

Kiryakova, V.S. 2000. Multiple(multiindex) Mittag-Leffler functions and relations to generalized fractional calculus. *Journal of Computational and Applied Mathematics*, 118(1-2), pp.241-259. Available at: https://doi.org/10.1016/S0377-0427(00)00292-2.

Mathai, A.M., Saxena, R.K. & Haubold, H.J. 2010. *The H-function: Theory and Applications*. New York, NY: Springer. Available at: https://doi.org/10.1007/978-1-4419-0916-9.

Mathai, A.M. & Saxena, R.K. 1973. *Generalized Hypergeometric Functions with Applications in Statistics and Physical Sciences*. Berlin Heidelberg: Springer-Verlag. Available at: https://doi.org/10.1007/BFb0060468.

Menaria, N., Nisar, K.S. & Purohit, S.D. 2016. On a new class of integrals involving product of generalized Bessel function of the first kind and general class of polynomials. *Acta Universitatis Apulensis*, 46, pp.97-105 [online]. Available at: https://www.emis.de/journals/AUA/pdf/74_1366_aua_2841701.pdf [Accessed: 9 February 2022].

Mondal, S.R. & Nisar, K.S. 2017. Certain unified integral formulas involving the generalized modified k-Bessel function of first kind. *Communications of the Korean Mathematical Society*, 32(1), pp.47-53. Available at: https://doi.org/10.4134/CKMS.c160017.

Paneva-Konovska, J. 2007. Theorems on the convergence of series in generalized Lommel-Wright functions. *Fractional Calculus and Applied Analysis*, 10(1), pp.59-74 [online]. Available at: http://eudml.org/doc/11298 [Accessed: 9 February 2022].

Rainville, E.D. 1960. *Special Functions*. New York: The Macmillan Company.

Srivastava, H.M. & Daoust, M.C. 1969. Certain generalized Neumann expansions associated with Kampe-de-Feriet function. *Proceedings of the Koninklijke Nederlandse Akademie van Wetenschappen Series A-Mathematical Sciences*, 72(5), pp.449-457.

Srivastava, H.M. & Manocha, H.L. 1984. *A treatise on generating functions*. Chichester, West Sussex, England: E. Horwood & New York: Halsted Press. ISBN: 9780853125082.

Whittaker, E.T. & Watson, G.N. 2013. *A Course of Modern Analysis, reprint of the fourth* (1927) edition. Cambridge University Press, Cambridge Mathematical Library. Available at: https://doi.org/10.1017/CBO9780511608759.

ИССЛЕДОВАНИЕ ИНТЕГРАЛЬНЫХ ПРЕОБРАЗОВАНИЙ ОБОБЩЕННЫХ ФУНКЦИЙ ЛОММЕЛЯ-РАЙТА

Мохаммад Саид Кхан[а], *Сиразул* Хак[б], *Мохаррам Али* Кхан[в], *Никола* Фабиано[г]

[а] Университет медицинских наук Сефако Макгато, кафедра математики и прикладной математики, г. Га-Ранкува, Южно-Африканская Республика

[б] Дж. С. Университет, департамент прикладных наук, г. Шикохабад, Фирозабад, штат Уттар-Прадеш, Республика Индия

[в] Университет Умару Мусы Яр' Адуа, Кафедра математики и статистики, г. Катсина, Федеративная Республика Нигерия

[г] Белградский университет, Институт ядерных исследований «Винча» − Институт государственного значения для Республики Сербия, г. Белград, Республика Сербия, **корреспондент**

РУБРИКА ГРНТИ: 27.23.21 Интегральные преобразования. Операционное исчисление,
27.23.25 Специальные функции,
27.27.19 Функции многих комплексных переменных

ВИД СТАТЬИ: оригинальная научная статья

Резюме:

Введение/цель: Целью данной статьи является установление интегральных преобразований обобщенной функции Ломмеля-Райта.

Методы: Эти преобразования выражаются в терминах гипергеометрической функции Райта.

Результаты: В результате получены интегралы с тригонометрическими, обобщенными функциями Бесселя и Струве.

Выводы: Вследствие применения данного метода получаются различные интересные преобразования.

Ключевые слова: обобщенные функции Ломмеля-Райта J(z), преобразование Ханкеля, K-преобразование, функция Райта, функция Уиттекера.

СТУДИЈА О ИНТЕГРАЛНИМ ТРАНСФОРМАЦИЈАМА ГЕНЕРАЛИЗОВАНЕ ФУНКЦИЈЕ ЛОМЕЛА И РАЈТА

Мохамед Саид Кан[а], *Сиразул* Хак[б],
Мохарам Али Кан[в], *Никола* Фабиано[г]

[а] Универзитет здравствених наука Сефако Макгато, Департман за математику и примењену математику, Га-Ранкува, Република Јужна Африка

[б] Универзитет J. C., Одељење за примењене науке, Шикохабад, Фирозабад, Утар Прадеш, Република Индија

[в] Универзитет Умару Муса Иарадуа, Департман за математику и статистику, Катсина, Савезна Република Нигерија

[г] Универзитет у Београду, Институт за нуклеарне науке "Винча"- Институт од националног значаја за Републику Србију, Београд, Република Србија, **аутор за преписку**

ОБЛАСТ: математика
ВРСТА ЧЛАНКА: оригинални научни рад

Сажетак:

Увод/циљ: Циљ овог рада јесте успостављање интегралних трансформација генерализоване функције Ломела и Рајта.

Методе: Интегралне трансформације изражене су помоћу Рајтове хипергеометријске функције.

Резултати: Добијени су интеграли који укључују тригонометријске, генерализоване Беселове и Струвеове функције.

Закључак: Као последице ове методе добијају се разне занимљиве трансформације.

Кључне речи: генерализоване функције Ломела и Рајта J(z), Ханкелова трансформација, K-трансформација, Рајтова функција, Витакерова функција.

Paper received on / Дата получения работы / Датум пријема чланка: 10.02.2022.
Manuscript corrections submitted on / Дата получения исправленной версии работы / Датум достављања исправки рукописа: 14.03.2022.
Paper accepted for publishing on / Дата окончательного согласования работы / Датум коначног прихватања чланка за објављивање: 16.03.2022.

AN APPROACH OF PROBABILITY-BASED MULTI–OBJECTIVE OPTIMIZATION CONSIDERING ROBUSTNESS FOR MATERIAL ENGINEERING

Maosheng Zheng[a], *Haipeng* Teng[b], *Yi* Wang[c]

Northwest University, School of Chemical Engineering,
Xi'an, People's Republic of China

[a] e-mail: mszhengok@aliyun.com, **corresponding author**,
ORCID iD: https://orcid.org/0000-0003-3361-4060

[b] e-mail: tenghp@nwu.edu.cn,
ORCID iD: https://orcid.org/0000-0003-2987-7415

[c] e-mail: wangyi11@nwu.edu.cn,
ORCID iD: https://orcid.org/0000-0001-6711-0026

DOI: 10.5937/vojtehg70-35795; https://doi.org/10.5937/vojtehg70-35795

FIELD: Materials, Mathematics
ARTICLE TYPE: Original scientific paper

Abstract:

Introduction/purpose: The newly developed probability-based multi – objective optimization (MOO) has introduced a novel concept of preferable probability to represent a preferability degree of a candidate in optimization in order to overcome the inherent shortcomings of subjective and "additive" factors in the previous MOO methods. In this paper, the new method is extended to include robust optimization for material engineering. Furthermore, energy consumption in a melting process with orthogonal array design and the robust optimization of four different process schemes in machining an electric globe valve body are taken as examples.

Methods: The arithmetic mean value of each performance utility indicator of the candidate contributes to one part of the partial preferable probability, while the deviation of each performance utility indicator from its arithmetic mean value of the candidate contributes to the other part of the partial preferable probability quantitatively. Furthermore, following the procedures of the newly developed probability-based multi–objective optimization (PMOO), the total preferable probability of a candidate is obtained, which thus transfers a multi–objective optimization problem into a single–objective optimization problem.

Results: The optimal control factors of lower electric energy consumption with robustness are bundled steel, loose steel, and uncleaned steel of

12.5%, 50% and 37.5% by weight, respectively, in this steel melting process. This case is closely followed by the scenario of 50 wt% bundled steel, 50 wt% loose steel, and 0 wt% uncleaned steel. The robust optimization of four different process schemes for machining an electric globe valve body is scheme No. 1.

Conclusion: The extension of probability-based multi-objective optimization while considering robustness is successful, which can be easily used to deal with the optimal problem with dispersion of data to get objectively an optimal result with robustness in material engineering. The extension of probability-based multi-objective optimization while considering robustness will be beneficial to relevant research and process optimization.

Key words: multi-objective optimization, probability theory, preferable probability, material engineering, robustness.

Introduction

Recently, the probability-based multi–objective optimization (PMOO) method was developed (Zheng et al, 2021) in an attempt to solve the inherent problems of personal and subjective factors in previous multi–objective optimizations (MOOs). The new concept of preferable probability was introduced to represent a preferable degree of a candidate in optimization. In PMOO, all performance utility indicators of candidates are divided into two types, i.e., beneficial or unbeneficial types according to their functions in the selection; each performance utility indicator of the candidate makes its contribution to a partial preferable probability quantitatively, and furthermore, the product of all partial preferable probabilities makes the total preferable probability of a candidate in the viewpoint of probability theory, which is the unique decisive index in the selection process and thus transfers the multi – objective optimization problem into single–objective optimization. PMOO was also extended to the application of the multi-objective orthogonal test design method (OTDM) and the uniform design method (UDM) as well, where appropriate achievements have been obtained (Zheng et al, 2021; Zheng, 2022).

In general, quality improvement of products and optimization of processes are continuously demanded by manufacturers. In 1980s, Taguchi once contributed a discipline and structure to the design and assessment of experiments so as to raise the quality of products by means of design optimization with efficient cost (Roy, 2010). In Taguchi's method, a formal way is incorporated to include noise factors in the experiment layout, which aims to make products and processes

insensitive to the influence of uncontrollable (noise) factors. He created an orthogonal experiment design to study the effects of noise factors with smaller size of experiments, which results in a favorable performance with the mean close to the target and reduced variation around the mean (Roy, 2010). The main point is to focus on the prechosen target for the output response with great extent and less variability. The controllable factors are called control factors. It is assumed that the majority of variability around the target is due to the existence of a second set of factors called noise factors or variables. Noise factors are uncontrollable in the product design or process operation (Myers et al, 2016). As a result, the term robust parameter design entails designing the system so as to get robustness (insensitivity) to inevitable changes in the noise variables. Taguchi suggested using a factor called “signal - to - noise ratio” (SNR) to characterize robustness. Taguchi suggested some primary SNRs. The three specific commonly used goals are: 1). the smaller the better; 2). the larger the better; 3). the target is the best.

Taguchi suggested a SNR for cases in which the response standard deviation is related to the mean linearly. For this case, Taguchi’s SNR for “the target is the best” condition is given by

$$SNR = -10\log(\bar{y}^2 / s^2) \quad (1)$$

where the SNR is to be maximized; $\bar{y}$ is the mean value of the test points, and s is the standard error.

In fact, for a set of actual experiments or processes, the mean value of the test points $\bar{y}$ and the standard error s are independent factors in general.

While, in Eq. (1), the SNR condenses the two factors into one factor, the optimization of the maximum of the SNR is not equivalent to the optimizations of the both minima of s and $\bar{y}$ closing to the target at the same time. What is worse is that in the cases of “the smaller the better” and “the larger the better’, the expressions of SNRs suggested by Taguchi even excluded the factor of the standard error. This point was criticized by many statisticians (Box, 1988; Box & & Meyer, 1986; Welch et al, 1990, 1992; Nair et al, 1992) though the essence of the SNR in Taguchi’s approach to robust parameter design is to propose an easy-to-use performance criterion which takes the process mean and variance into consideration. Statisticians further suggested taking both response mean and variance into account by using separate models. Therefore, for robust optimization, the optimization of the both minima of s and $\bar{y}$

closing to the target should be conducted with individual models at the same time.

In this paper, the new PMOO method is extended to include robust optimization of dispersion of data in material engineering due to the advantage of impersonality of the PMOO method, where both the response mean $\bar{y}$ and the variance s are taken into account by using separate models. Furthermore, energy consumption in the melting process with orthogonal array design and robust optimization of four different process schemes in the machining process of the electric globe valve body are studied as examples.

Extension of the probability-based multi–objective optimization method to include robustness

In PMOO, all performance utility indicators of candidates are divided into beneficial or unbeneficial types according to their functions in the selection where each performance utility indicator of the candidate makes its contribution to a partial preferable probability quantitatively, and furthermore, the product of all partial preferable probabilities makes the total preferable probability of a candidate in the viewpoint of the probability theory, which is the unique decisive index in the selection process and transfers the multi–objective optimization problem into a single–objective optimization problem (Zheng et al, 2021; Zheng, 2022).

In traditional MOO, the performance indexes of candidates are assumed to be well determined without any uncertainty. However, this is not always the case; for example, if we perform one experiment for ten times, we could get ten experimental data in general and both the arithmetic mean value of the ten data and the mean deviation can be taken as representatives for these experiments; In some other cases, the performance indexes and attributes are often vague, which results in un-exact numerical values instead of well determined data. In order to assess such problems containing uncertain elements, a proper approach is still needed. Taguchi created a formal way to include noise factors (Roy, 2010), but it is puzzling. Here we propose an extension for the newly developed PMOO to include the dispersion of data so as to establish probability-based multi–objective robust optimization.

In general, an uncertain element X_{ij} has the form of Eq. (2),

$$X_{ij} = \overline{X}_{ij} \pm \delta X_{ij} \tag{2}$$

In Eq. (2), $\overline{X}_{ij}$ represents the arithmetic mean value of the uncertain element X_{ij}, and δX_{ij} is the mean deviation of the performance index X_{ij}.

The arithmetic mean value $\overline{X}_{ij}$ represents the main function of the performance of a candidate, which quantitatively contributes one part of partial preferable probability according to its type of being either beneficial or unbeneficial relating to their functions in the selection.

For the beneficial type of performance, it contributes one part of partial preferable probability linearly in a positive manner; as to the unbeneficial type of performance, it contributes one part of partial preferable probability linearly in a negative manner (Zheng et al, 2021; Zheng, 2022).

Under condition of the uncertain element X_{ij}, the beneficial type of the arithmetic mean value $\overline{X}_{ij}$ of the uncertain element X_{ij} makes one part of the performance index according to

$$P_{ij1} = \alpha_{j1}\overline{X}_{ij}\text{ , } i = 1,2,\ldots, n;\ j = 1, 2, \ldots, m. \quad (3)$$

In Eq. (3), P_{ij1} represents one part of the partial preferable probability of the beneficial utility index $\overline{X}_{ij}$; n is the total number of candidates in the candidate group involved; m is the total number of the performance utility indices of each candidate in the group; α_{ij1} is the normalized factor of the j-th utility index of the candidate performance indicator, $\alpha_{ij1} = 1/(n\bar{\bar{X}}_j)$, $\bar{\bar{X}}_j$ is the arithmetic mean value of the utility index of the performance indicator in the candidate group involved,

$$\bar{\bar{X}}_j = \frac{1}{n}\sum_{i=1}^{n}\overline{X}_{ij}\text{ .} \quad (4)$$

For the unbeneficial type of performance, $\overline{X}_{ij}$ makes one part of its partial preferable probability of the performance according to

$$P_{ij1} = \beta_{j1}(\overline{X}_{j\max} + \overline{X}_{j\min} - \overline{X}_{ij})\text{ , } i = 1,2,\ldots, n;\ j = 1, 2, \ldots, m. \quad (5)$$

In Eq. (5), $\bar{X}_{jmax}$ and $\bar{X}_{jmin}$ represent the maximum and minimum values of the performance utility indices $\bar{X}_{ij}$ of the candidate performance indicator in the group, respectively, and β_{j1} is the normalized factor of the j-th utility indices of the candidate performance indicator, $\beta_{j1} = 1/[n(\overline{X}_{j\min} + \overline{X}_{j\max}) - n\bar{\bar{X}}_j]$.

The mean deviation δX_{ij} is the unbeneficial type of the performance index in assessment in general, which has the characteristic of "the lower the better". The mean deviation δX_{ij} contributes the other part of the uncertain element X_{ij}, P_{ij2}, which is assessed according to Eq. (6),

$$P_{ij2} = \beta_{j2}(\delta X_{j\max} + \delta X_{j\min} - \delta X_{ij}) \text{ , } i = 1,2,\ldots, n;\ j = 1, 2, \ldots, m. \quad (6)$$

In Eq. (6), δX_{jmax} and δX_{jmin} represent the maximum and minimum values of the performance utility indices δX_{ij} of the candidate performance indicator in the group, respectively, and β_{j2} is the normalized factor of the j-th utility indices of candidate performance indicator, $\beta_{j2} = 1/[n(\delta X_{j\min} + \delta X_{j\max}) - n\overline{\delta X}_j]$.

The entire partial preferable probability of the uncertain element X_{ij} is the arithmetic mean of both parts, or square root of their product, i.e.,

$$P_{ij} = (P_{ij1} + P_{ij2})/2, \text{ or } P_{ij} = (P_{ij1} \times P_{ij2})^{0.5}. \quad (7)$$

The entire partial preferable probability P_{ij} includes all information of the uncertain element X_{ij} comprehensively, which is the overall representative of the uncertain element X_{ij} in the selection process competitively.

Moreover, the total / comprehensive preferable probability of the i^{th} candidate in a multi-objective optimization problem is the product of its partial preferable probability P_{ij} of each utility index of the candidate performance indicator in the overall selection due to the "simultaneous optimization" of multiple objectives in the viewpoint of probability theory (Zheng et al, 2021), i.e.,

$$P_i = P_{i1} \cdot P_{i2} \cdots P_{im} = \prod_{j=1}^{m} P_{ij} \text{ .} \quad (8)$$

The total preferable probability of a candidate is the uniquely decisive index in the overall selection process competitively, which transfers a multi–objective optimization problem (MOOP) into a single – objective optimization one. The main characteristic of the new probability-based multi–objective optimization is that the treatment for both beneficial utility index and unbeneficial utility index is equivalent and conformable, which is without any artificial or subjective scaling factors involved in the process.

Application of the extended PMOO to assess an optimal problem with dispersion of data in material engineering

In the following study, the entire partial preferable probability of the uncertain element X_{ij} takes the arithmetic mean of both parts of Eq. (7).

1) Robust optimization for saving electric energy consumption of a foundry

Electric furnaces are generally used in foundries widely, including cupola furnaces, rotary furnaces, and induction furnaces. The induction furnace is usually utilized to melt a massive amount of steel. The electricity consumed for melting 1 ton of metal is in the range of 600–680 kWh/ton (Deshmukh & Hiremath, 2020). Deshmukh et al reported an orthogonal array experiment for the optimization of the process parameters in the melting process in the foundry with a “Signal to Noise Ratio” effect (Deshmukh & Hiremath, 2020). The study was focused on varying the process parameters so as to reduce consumption of electrical energy and get an optimization robust property (Deshmukh & Hiremath, 2020). An L9 orthogonal array was used to conduct the design experiment for control factors: bundled steel, loose steel and uncleaned steel in wt %, see Table 1.

Nine experiments were performed five times to reflect the variations that might be caused by noise factors. Table 2 shows the tested data of electric energy consumption from these designed experiments.

Table 1 –Control factors in experiment design
Таблица 1 – Контрольные факторы при проектировании эксперимента
Табела 1 – Контролни фактори при пројектовању експеримента

Scheme	Bundled steel (% by weight)	Loose steel (% by weight)	Uncleaned steel (% by weight)
1	12.5	37.5	50
2	33	33	33
3	37.5	12.5	50
4	50	0	50
5	12.5	50	37.5
6	50	12.5	37.5
7	50	50	0
8	33	33	33
9	37.5	50	12.5

Table 2 – Test data of electric energy consumption from these experiments

Таблица 2 – Данные о потреблении электроэнергии в результате экспериментов

Табела 2 – Подаци о утрошку електричне енергије из наведених експеримената

	Test data (kWh)					Representative data	
Scheme	1	2	3	4	5	Mean	Deviation
1	110	112	131	108	104	113	9.3808
2	109	111	120	121	114	115	4.7749
3	112	120	115	118	110	115	3.6878
4	98	102	106	112	104	104.4	4.6303
5	117	112	109	113	108	111.8	3.1875
6	121	116	109	107	113	113.2	4.9960
7	114	118	108	110	112	112.4	3.4409
8	116	112	110	104	109	110.2	3.9192
9	110	118	112	109	107	111.2	3.7630

Since the optimization of this problem is intended for saving electric energy consumption, the mean value of the electric energy consumption in Table 2 belongs to an unbeneficial performance index, thus Eq. (5) is employed to assess its portial preferable probability. Besides, Eq. (6) is used to assess the deviation contribution to the partial preferable probability. Finally, the entire partial preferable probability of each scheme is assessed by Eq. (7). Table 3 shows the results of the assessments. P_{mean}, and $P_{deviation}$ in Table 3 indicate one part of partial preferable probability of the mean value and the deviation value of electric energy consumption, respectively; P_{entire} is the entire partial preferable probability of electric energy consumption, which determines the ranking of each scheme in Table 3.

From Table 3, it can be seen that scheme 5 is the optimal one, since it consumes lower electric energy with less deviation, i.e., it is robust. The optimal control factors of bundled steel, loose steel and uncleaned steel are 12.5%, 50%and 37.5% by weight in this steel melting process, respectively; scheme 7 is No. 2, being close to scheme 5 with the control factors of bundled steel, loose steel and uncleaned steel at 50%, 50% and 0 % by weight, respectively.

Table 3 – Results of the assessments for the preferable probability of all schemes and their ranking

Таблица 3 – Результаты оценивания предпочтительной вероятности всех схем и их ранжирования

Табела 3 – Резултати оцењивања пожељних вероватноћа свих схема и њихово рангирање

Scheme	P_{mean}	$P_{deviation}$	P_{entire}	Rank
1	0.1099	0.0447	0.0773	9
2	0.1078	0.1093	0.1085	7
3	0.1078	0.1245	0.1161	5
4	0.1188	0.1113	0.1150	6
5	0.1111	0.1315	0.1213	1
6	0.1097	0.1062	0.1079	8
7	0.1105	0.1280	0.1192	2
8	0.1128	0.1212	0.1170	4
9	0.1117	0.1234	0.1176	3

2) Robust optimization for multi-objective decision making of mechanical processing plans based on the interval number

Han et al conducted multi-objective robust decision making of a mechanical processing plan based on the interval number (Han et al, 2020); four different process schemes for machining process of the electric globe valve body are comparetively studied, which is taken as an example here as well.

Table 4 shows the technical parameters of the four schemes. In this optimization process, only the rate of the qualified product is the beneficial type of the performance index, others belong to the unbeneficial type. Table 5 lists the partial preferable probability and the total preferable probability of each plan, as well as the overall ranking comparatively.

Table 4 – Technical parameters of the four plans
Таблица 4 – Технические параметры четырех планов
Табела 4 – Технички параметри четири плана

Plan	Time for product A (min)	Rate of qualified products B (%)	Total cost C (RMB Yuan)	Material consump. D (yuan)	Electric energy consump. E (°)	Solid waste F (kg)	Waste liquid discharge G (L)
1	[40, 51]	[96, 98]	[238, 285]	[82.6, 114.5]	[18.6, 21.5]	[0.86, 0.97]	[2.8, 3.1]
2	[48, 59]	[91, 95]	[254, 303]	[92.4, 123.3]	[19.8, 23.2]	[0.95, 1.22]	[2.9, 3.5]
3	[50, 62]	[89, 92]	[258, 310]	[94.2, 126.1]	[20.3, 25.2]	[1.07, 1.28]	[3.1, 3.9]
4	[42, 56]	[92, 96]	[245, 292]	[86.8, 116.9]	[19.1, 22.3]	[0.92, 1.15]	[2.9, 3.3]

Table 5 – Partial preferable probability and the total preferable probability of each plan, as well as their ranking.
Таблица 5 – Частичная предпочтительная вероятность и общая предпочтительная вероятность каждого плана, а также их ранжирование
Табела 5 – Делимичне пожељне вероватноће и укупна пожељна вероватноћа сваког плана и њихово рангирање

	Partial preferable probability							Total	
Plan	A	B	C	D	E	F	G	$P_t \times 10^4$	Rank
1	0.2732	0.3113	0.2597	0.2544	0.2778	0.3344	0.3080	1.6082	1
2	0.2534	0.2151	0.2469	0.2473	0.2545	0.1997	0.2332	0.3944	3
3	0.2376	0.2572	0.2369	0.2405	0.2026	0.2317	0.1782	0.2913	4
4	0.2357	0.2164	0.2565	0.2578	0.2651	0.2343	0.2805	0.5875	2

Table 5 shows that scheme No. 1 is the optimal one with a robust property.

Conclusion

The extension of the probability-based multi-objective optimization considering robustness is successful, which can be easily used to deal with an optimization problem with dispersion of data to get objectively an optimal result with robustness in material engineering.

Robust optimization design is a very important technology to improve quality of products and optimize processes for manufacturers. The extension of the probability-based multi-objective optimization considering robustness will be beneficial to relevant research and process optimization.

References

Box, G. 1988. Signal-to-Noise Ratios, Performance Criteria, and Transformations. *Technometrics*, 30(1), pp.1-17. Available at: https://doi.org/10.2307/1270311.

Box, G.E.P. & Meyer, R.D. 1986. Dispersion Effects from Fractional Designs. *Technometrics*, 28(1), pp.19-27. Available at: https://doi.org/10.1080/00401706.1986.10488094.

Deshmukh, R. & Hiremath, R. 2020. Societal application of Taguchi method for optimization of process parameters in the Melting Process in the Foundry. In: *Pawar, P., Ronge, B., Balasubramaniam, R., Vibhute, A. & Apte, S. (Eds.) Techno-Societal 2018*, pp.215-221. Springer, Cham. Available at: https://doi.org/10.1007/978-3-030-16962-6_22.

Han, Z., Shan, W. & He, T. 2020. Multi-objective Robust Decision-Making of Machining Process Scheme Based on Interval Number. *Modern Manufacturing Engineering*, 5, pp.98-101. Available at: https://doi.org/10.16731/j.cnki.1671-3133.2020.05.015.

Myers, R.H., Montgomery, D.C. & Anderson-Cook, C.M. 2016. *Response Surface Methodology: Process and Product Optimization Using Designed Experiments, 4th Edition*. Hoboken, NJ, USA: John Wiley & Sons, Inc. ISBN: 978-1-118-91601-8.

Nair, V.N., Abraham, B., MacKay, J., Box, G., Kacker, R.N., Lorenzen, T.J., Lucas, J.M., Myers, R.H., Vining, G.G., Nelder, J.A., Phadke, M.S., Sacks, J., Welch, W.J., Shoemaker, A.C., Tsui, K.L., Taguchi, S. & Jeff Wu, C.F. 1992. Taguchi's Parameter Design: A Panel Discussion. *Technometrics*, 34(2), pp.127-161. Available at: https://doi.org/10.2307/1269231.

Roy, R.K. 2010. *A Primer on the Taguchi Method, 2nd edition*. Dearborn, MI, USA: Society of Manufacturing Engineers. ISBN-13: 978-0872638648.

Welch, W.J., Yu, T-K., Kang, S.M. & Sacks, J. 1990. Computer experiments for quality control by parameter design. *Journal of Quality Technology*, 22(1), pp.15-22. Available at: https://doi.org/10.1080/00224065.1990.11979201.

Welch, W.J., Buck, R.J., Sacks, J., Wynn, H.P., Mitchell, T.J. & Morris, M.D. 1992. Screening, Predicting, and Computer Experiments. *Technometrics*, 34(1), pp.15-25 [online]. Available at: https://www.tandfonline.com/doi/abs/10.1080/00401706.1992.10485229 [Accessed: 5 January 2022].

Zheng, M. 2022. Application of probability-based multi–objective optimization in material engineering. *Vojnotehnički glasnik/Military Technical Courier*, 70(1), pp.1-12. Available at: https://doi.org/10.5937/vojtehg70-35366.

Zheng, M., Wang, Y. & Teng, H. 2021. A new "intersection" method for multi-objective optimization in material selection. *Tehnički glasnik*, 15(4), pp.562-568. Available at: https://doi.org/10.31803/tg-20210901142449.

ПРИМЕНЯЕМЫЙ В МАТЕРИАЛОВЕДЕНИИ ПОДХОД МНОГОКРИТЕРИАЛЬНОЙ ОПТИМИЗАЦИИ, ОСНОВАННОЙ НА ВЕРОЯТНОСТИ С УЧЕТОМ РОБАСТНОСТИ

Маошенг Чжэн, **корреспондент**, *Хайпэн* Тенг, *Йи* Вонг
Северо-западный политехнический университет,
факультет химической инженерии,
г. Сиань, Народная Республика Китай

РУБРИКА ГРНТИ: 27.00.00 МАТЕМАТИКА:
27.47.00 Математическая кибернетика;
27.47.19 Исследование операций
81.00.00 ОБЩИЕ И КОМПЛЕКСНЫЕ ПРОБЛЕМЫ ТЕХНИЧЕСКИХ И ПРИКЛАДНЫХ НАУК И ОТРАСЛЕЙ НАРОДНОГО ХОЗЯЙСТВА:
81.09.00 Материаловедение
45.00.00 ЭЛЕКТРОТЕХНИКА:
45.09.00 Электротехнические материалы
ВИД СТАТЬИ: оригинальная научная статья

Резюме:

Введение/цель: Недавно разработанный подход многокритериальной оптимизации, основанной на вероятности (МОО) ввел новую концепцию предпочтительной вероятности для представления степени предпочтительности кандидатов в оптимизации, с целью преодоления существующих в предыдущих методах МОО недостатков, касающихся субъективных и "аддитивных" факторов. В данной статье представлен новый расширенный метод, включающий робастную оптимизацию применяемую в области материаловедения. Кроме того, приведены примеры энергопотребления в процессе плавки с ортогональной конструкцией решетки и робастной оптимизации четырех различных схем при машинном изготовлении корпуса электрического шарового крана.

Методы: Среднее арифметическое показателя эффективности кандидата способствует одной стороне частичной предпочтительной вероятности, в то время как отклонения показателя эффективности каждого кандидата от среднего арифметического количественно способствует другой стороне частичной предпочтительной вероятности. Также следует отметить, что при применении новоразработанной многокритериальной оптимизации, основанной на вероятности (МОО) вычисляется суммарная предпочтительная вероятность кандидата, что переводит задачу многокритериальной оптимизации в задачу однокритериальной оптимизации.

Результаты: Оптимальными контрольными факторами снижения потребления электроэнергии за счет робастности являются: импортная сталь, свободная сталь и сталь с примесями 12,5, 50 и 37,5 весовых процентов в соответствии с данным процессом плавки стали. Затем следует сценарий 50, 50 и 0 весовых процентов. Из четырех схем различных процессов машинного изготовления корпуса электрического шарового крана робастная оптимизация является схемой номер один.

Выводы: Многокритериальная оптимизация, основанная на вероятности, дополненная фактором робастности, оказалась более успешной, следовательно ее безусловно можно использовать при решении задач оптимальности с дисперсией данных для получения объективно оптимального результата с робастностью в области материаловедения. Расширение многокритериальной оптимизации, основанной на вероятности, учитывая робастность существенно поможет в релевантных исследованиях и оптимизации процессов.

Ключевые слова: многокритериальная оптимизация, теория вероятности, предпочтительная вероятность, материаловедение, робастность.

ПРИСТУП ВИШЕКРИТЕРИЈУМСКЕ ОПТИМИЗАЦИЈЕ ЗАСНОВАНЕ НА ВЕРОВАТНОЋИ, КОЈИ УЗИМА У ОБЗИР РОБУСТНОСТ, ПРИМЕЊЕН У ТЕХНОЛОГИЈИ МАТЕРИЈАЛА

Маошенг Џенг, **аутор за преписку**, *Хајпен* Тенг, *Ји* Вонг
Универзитет Северозапад, Факултет хемијског инжењерства,
Сијан, Народна Република Кина

ОБЛАСТ: математика, материјали
ВРСТА ЧЛАНКА: оригинални научни рад

Сажетак:

Увод/циљ: Новоразвијени метод вишекритеријумске оптимизације заснован на вероватноћи (МОО) увео је концепт пожељне вероватноће да представи степен пожељности кандидата при оптимизацији као покушај да се превазиђу инхерентни недостаци субјективних и адитивних фактора у претходним методама МОО. У овом раду нова метода се проширује и укључује робустну оптимизацију приликом примене у области технологије материјала. Наведени су примери утрошка електричне енергије у процесу топљења са дизајном ортогоналног низа, као и робустне оптимизације четири различите шеме процеса машинске израде тела електричног лоптастог вентила.

Zheng, M. et al, An approach of probability-based multi–objective optimization considering robustness for material engineering, pp.283-296

Методе: Аритметичка средња вредност показатеља перформанси корисности кандидата доприноси једној страни делимичне пожељне вероватноће, док девијација сваког показатеља перформанси корисности кандидата од аритметичке средње вредности доприноси квантитативно другој страни делимичне пожељне вероватноће. Такође, применом поступка новоразвијене вишекритеријумске оптимизације, засноване на вароватноћи (МОО), добија се укупна пожељна вероватноћа кандидата, чиме се проблем вишекритеријумске оптимизације преводи у проблем једнокритеријумске оптимизације.

Резултати: Оптимални контролни фактори смањене потрошње електричне енергије помоћу робустности јесу увезани челик, слободни челик и челик с нечистоћама од 12,5, 50 и 37,5 тежинских процената, респективно, у овом процесу топљења челика. Одмах затим следи сценарио од 50, 50 и 0 тежинских процената, респективно. Од схема четири ратличита процеса машинске израде тела електричног лоптастог вентила, робустна оптимизација је схема број један.

Закључак:. Вишекритеријумска оптимизација заснована на вероватноћи проширена је помоћу робустности, што се показало успешним, тако да се може лако користити при решавању проблема оптималности са дисперзијом података како би се добио објективно оптимални резултат са робустношћу у технологији материјала. Проширивање вишекритеријумске оптимизације засноване на вероватноћи узимајући у обзир робустност биће од користи за релевантна истраживања и оптимизације процеса.

Кључне речи: вишекритеријумска оптимизација, теорија вероватноће, пожељна вероватноћа. технологија материјала, робустност.

Paper received on / Дата получения работы / Датум пријема чланка: 10.01.2022.
Manuscript corrections submitted on / Дата получения исправленной версии работы / Датум достављања исправки рукописа: 14.03.2022.
Paper accepted for publishing on / Дата окончательного согласования работы / Датум коначног прихватања чланка за објављивање: 16.03.2022.

FUZZY-BASED SMART SYSTEM FOR CONTROLLING ROAD LIGHTS

Ihab Abdulrahman Satam
Northern Technical University, Electronics Techniques Department, Mosul, Nineveh, Republic of Iraq;
Obuda University, School of Safety and Security Sciences, Budapest, Hungary,
e-mail: Ihab.satam@uni-obuda.hu,
ORCID iD: https://orcid.org/0000-0002-9749-0944

DOI: 10.5937/vojtehg70-36670; https://doi.org/10.5937/vojtehg70-36670

FIELD: Mathematics, Computer science
ARTICLE TYPE: Original scientific paper

Abstract:

Introduction: The energy consumed for street lighting is a major expenditure in urban environments. According to the World Bank, it constitutes up to 65% of cities' electricity costs and 10% of their overall budgets. The demand for lighting is growing significantly due to rapid urbanization, thus eating up even more energy and money - unless smarter solutions are deployed to reduce costs.

Method: In this paper, a model for street lighting was established, consisting of several lamp posts on both sides of the street. The model was the exact replica of the street lighing system inside the city of Kirkuk, Iraq. The number of objects passing along the street was monitored, both during and out of rush hours.This all was taken into account in the energy consumption calculation. The controller used for this model is Arduino UNO. The Arduino receives signals from 3 IR sensors, processes these signals, and then sends the action to the lamp posts. Fuzzy logic was applied in two cases: the first one is during the daylight, the second one is during the sunrise and the sunset, to control the intensity of the light of the lamp posts.

Results: Both cases showed significant results regarding the reliability, efficiency, and countability of the system in decreasing the level of energy consumption.

Conclusion: The system can be applicable for smart city projects. It is efficient, cost effective and shows reliable results in saving energy.

Keywords: fuzzy logic, arduino, smart street lighting, energy consumption, road lights.

Introduction

City authorities see street lights as one of the largest portions of energy costs. Overlit streets waste energy and generate a high level of

CO_2 emissions and costs. There are some major challenges in street lights that need to be resolved. Sometimes road lamp posts remain ON during the daylight. To manage and reduce that cost, they have to be like hubs of smart technology while helping provide the community with significant energy savings and a safer environment. Some previous studies dealt with smart systems for lights. Several studies regarding smart systems have been implemented. E.M. Diaconu (2021) implemented a basic design for an electronic circuit to a smart system. The system is controlled using an android application and the communication is maintained using the Bluetooth HC-05 module. Kumar et al (2021) came up with an idea to use a PIR sensor to detect motion and an LDR sensor to reduce unnecessary waste of power during the daytime. The idea was good; however, it is only restricted to turning the light ON and OFF. Chenwei et al also designed a system to control lighting using an android application that communicates with the system using the Bluetooth Technique (Feng et al, 1976). The design was easy, efficient and of low cost. Dankan et al used the SLS (Smart Lighting System) based on the IoT technique in order to fully control the system. The main idea of the system is to save more dissipated energy (Gowda et al, 2021). The energy saved reached up to 40 %. A smart system of calibrating energy consumption inside the building was presented by Yerbol et al (Aussat et al, 2022). This system measures illuminance and occupancy from sensors located at each workstation inside the building. The system compares between the illuminance and the dimming level inside the workstation and depending on that the control system will specify the desired illuminance of the bulb. Leo et al used the PIR sensor to detect the occupancy of a room so the system can determine whether the lights are ON or OFF for the purpose of saving energy inside the house or a building (Botler & Sadok, 2016). Arun et al presented a work of full setup for the hardware required for a lighting system inside the room. His idea deals with a system capable of varying light intensities using an Android App which provides better visual comfort for the user (Kumar et al, 2019). Amit et al (Sikder et al, 2018) presented an overview of IoT-based systems for smart lighting for energy-saving enhancement. They review different IoT-enabled communication protocols that can be used in the SLS; the result was the IoT-enabled SLS in both indoor and outdoor settings which can reduce power consumption percent up to 33%. The interesting work of Bozanic et al (2021) in the fuzzy system presents neuro-fuzzy as a method of decision making to support the selection of construction machines. Precup et al (2020) poposed a network control problem solution using fuzzy logic. Some studies regarding the smart lighting system SSL have been established. Francis et al (Montalbo &

Enriquez, 2020) used a PIR sensor and NodeMCU V3 with Wi-Fi to detect the occupancy of a classroom, so that the lights will be turned ON and OFF to save more energy. Nursyazwani and his team (Adnan et al, 2019) used IoT technology to control the light in illumination-based human activity. The system measures the intensity of ambient light and controls artificial lights for the comfort of the eye. However, the system controls illumination manually. Another study was conducted by Bevek et al (Subba et al, 2020). The system used Both LDR and PIR sensors to detect the presence of people inside the room and as result, they control the light bulb ON and OFF.

The communication between the sensors and the controllers was achieved using the ZigBee transmitter and the receiver. The system was a traditional one that does not involve fuzzy logic. A description of a smart street lighting system (SSL) as an approach of massive function for smart cities was presented by Vasja Roblek (Subrahmanian & Shastri, 2018). With the use of Temp, Dampness, and Lights of the ambient conditions, K. Pargash et al controlled lamp posts ON and OFF (Poongothai et al, 2018). LoRa (Long Range) Technology can be used in SSL, and that is what Ezgi and his team (Bingöl et al, 2019) established in their work (A LoRa-based Smart Streetlighting System for Smart Cities) - the idea is to control and monitor the road remotely so that the ON-OFF function of road lights is executed. Zhang et al (2022) combined the Narrow Band Internet of Things (NB-IoT) with the LoRa communication technology to demonstrate the design of a smart street lighting system. By adopting an optimized street lamp control algorithm, the system can realize the automatic control of street lights according to the real-time traffic flow information.

This paper will focus on enhancing the control of a street light system by applying a fuzzy logic algorithm in order to control the ON-OFF status and the intensity level of the light itself in order to save more energy. The idea of using fuzzy logic is based on its easiness in use, program, and uploading to the system with very good results.

The overall view of the system

The intelligent street lighting system introduced in this paper consists of a model for a street with lamp posts on each side. The control system ensures efficient control of the light and is energy saving. Figure 1 shows the basic overview of the model.

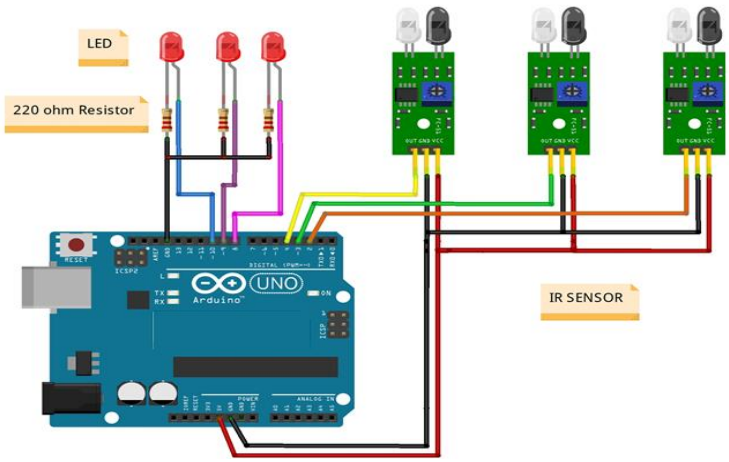

Figure 1 –Design of a street lighting system
Рис. 1 – Проект уличного освещения
Слика 1 – Пројекат система уличног осветљења

System structure

The system was constructed using several parts shown in Table 1 below.

Table 1 – System components
Таблица 1 – Компоненты системы
Табела 1 – Компоненте система

	Part	Description
1	Arduino	An open-source controller, easy to install, connect and control
2	IR Sensor	An electronic device using Infrared to sense the surrounding
3	LED	A semiconductor that produces light when a current flows through it
4	LDR	A cell that decreases resistance when receiving light on the component sensitive surface
5	PIR	An electronic device that senses the radiation of the ambient environment
6	Extra Parts	Wires, Batteries, Breadboard.

Fuzzy logic and its application to the problem of saving electricity

Using fuzzy logic inside the control system enables controling the intensity of road lights with respect to the intensity of daylight in the sunrise and sunset periods of the day. Fuzzy logic is one of the strongest tools in complex problem solving since this approach to computing is based on “Degrees of Truth” rather than on the usual “true or false” Boolean logic on which modern computers are based. Figure 2 shows the basic difference between Boolean and fuzzy logics (Ghosh & Haldar, 2014; Yusuf et al, 2020; Htwe et al, 2020). Power Saving System Using LDR And PIR Sensor.

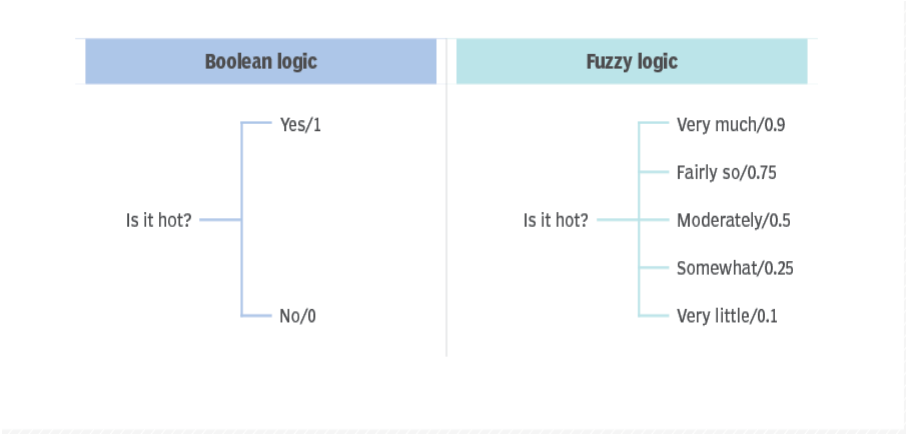

Figure 2 – Boolean logic Vs fuzzy logic
Рис. 2 – Булева логика против нечеткой логики
Слика 2 – Болеанова логика и фази логика

The idea was first introduced by Lotfi Zadeh in 1960 (AL-Forati & Rashid, 2020; Saputra et al, 2020; Hameed et al, 2021; Madrigal et al, 2019). Zadeh was working on the problem of computer understanding of natural language. Natural language -- like most other activities in life and indeed the universe -- is not easily translated into the absolute terms of 0 and 1. Whether everything is ultimately describable in binary terms is a philosophical question worth pursuing, but in practice, much data is required to feed a computer is in some state in between and so, frequently, are the results of computing. It may help to see fuzzy logic as the way reasoning really works and binary, or Boolean, logic is simply a special case of it (Huangwei et al, 2021; AL-Forati & Rashid, 2020; Saputra et al, 2020; Hameed et al, 2021; Madrigal et al, 2019).

The architecture of fuzzy logic is shown in Figure 3 below.

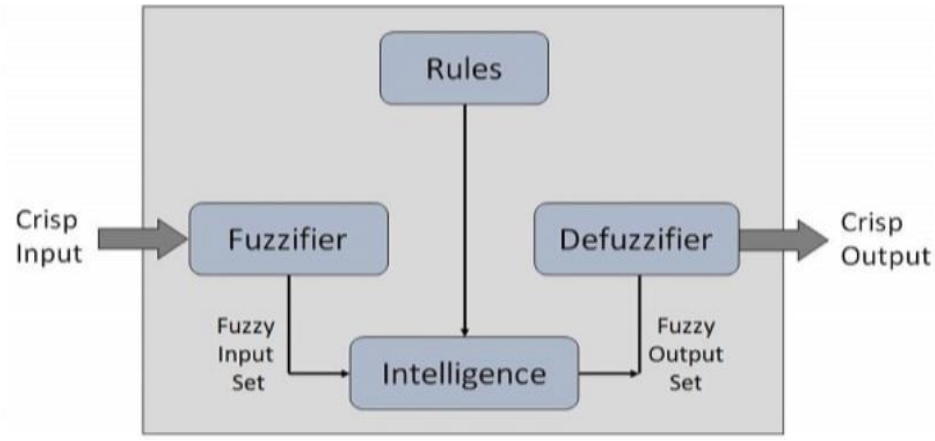

Figure 3 – Fuzzy logic
Рис. 3 – Нечеткая логика
Слика 3 – Фази логика

From Figure 3, there are four main parts of fuzzy logic which will be explained in this section.

Fuzzification

It is the method of transforming a crisp quantity into a fuzzy quantity. This can be achieved by identifying various known crisp and deterministic quantities as completely nondeterministic and quite uncertain in nature. This uncertainty may have emerged because of vagueness and imprecision which then lead the variables to be represented by a membership function as they can be fuzzy in nature (Sofian & Rambely, 2020; Lah & Arbaiy, 2020; Abdul-Adheem, 2020).

For example, if the temperature to be said is 45° Celsius, the viewer converts the crisp input value into a linguistic variable like favorable temperature for the human body, hot or cold.

Rule base

It contains all the rules and the **IF-THEN** conditions offered by experts to control the decision-making system. The recent updates in the fuzzy theory provide various methods for the design and tuning of fuzzy controllers. These updates significantly reduce the number of the fuzzy sets of rules**.**

Inference engine

It helps to determine the degree of match between a fuzzy input and the rules. Based on the % match, it determines which rules need implementing in accordance with the given input field. After this, the applied rules are combined to develop the control actions.

Defuzzification

It is the inversion of fuzzification where mapping is done to convert crisp results into fuzzy results while in defuzzification mapping is done to convert fuzzy results into crisp results.

This process can generate a nonfuzzy control action which illustrates the possibility distribution of an inferred fuzzy control action.

The defuzzification process can also be treated as the rounding off process, where a fuzzy set having a group of membership values on the unit interval is reduced to a single scalar quantity.

Applying fuzzy to the system

The system model shown in Figure 4 is the actual system experimented with within this work. It consists of several lampposts on both sides of the road; IR sensors are mounted between them to detect the motion of objects. Besides, the road lights are switched on and off. In addition, light intensity changes during the sunrise and the sunset. The intensity of daylight changes due to the sun's movement; in these periods, the road light's intensity does not have to be on to the fullest. This is useful for saving energy. In order to achieve that, fuzzy logic is applied since fuzzy logic is based on the "degree of truth" as mentioned before. The sunlight intensity is counted as levels of lighting. These levels are explained in Tables 2 and 3.

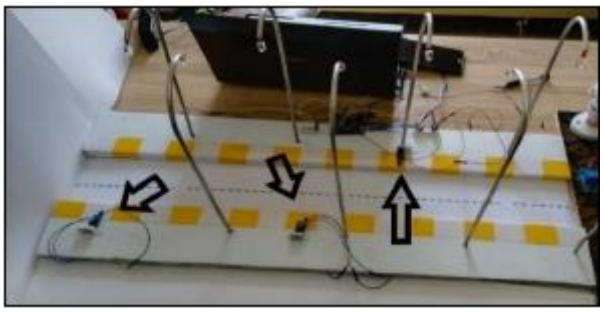

Figure 4 – Smart lighting system
Рис. 4 – Умная система освещения
Слика 4 – Паметни систем осветљења

Table 2 represents the inputs (Sun Light SL and Cars or Object C) and the output (LEDs light) linguistic variables for the system.

Table 2 – Input and output parameters
Таблица 2 – Входные и выходные параметры
Табела 2 – Улазни и излазни параметри

Parameter	Linguistic variable	Symbol	Fuzzy set
Input	Sun Light	SL	V Low
			Low
			Medium
			High
			V High
	Car or Object	C	Pass
			Not Pass
Output	LEDs Light	L	High
			Medium
			Low

The output indicated in the table above as High, Medium, and Low means the percent of light intensity. The Low output value is 25 %, the Medium value is 50% and the High value is a full 100%.

Table 3 represents the fuzzy rule base.

Table 3 – Fuzzy rules
Таблица 3 – Фаззи правила
Табела 3 – Фази правила

No	Rule								
1	**IF**	**SL**	**V Low**	**AND**	**C**	**Pass**	**THEN**	**L**	**High**
2			**Low**						**Medium**
3			**Medium**						**Low**
4			**High**						**Low**
5			**V High**						**Low**
6			**V Low**			**Not Pass**			**Low**
7			**Low**						**Low**
8			**Medium**						**Low**
9			**High**						**Low**
10			**V High**						**Low**

The inputs for the system are shown in Figure 5.

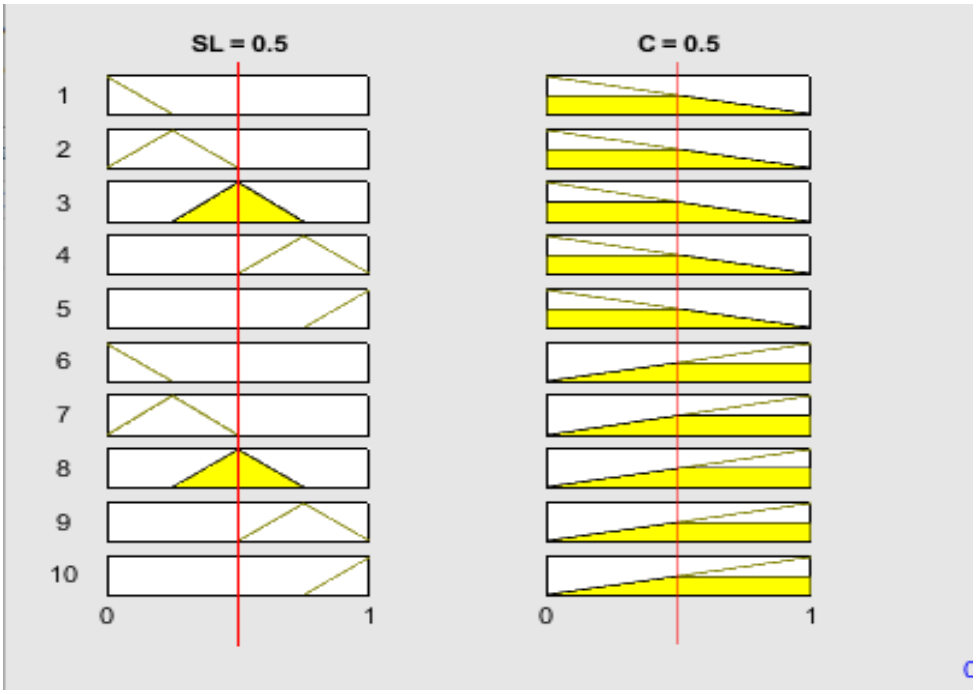

Figure 5 – Input variables for the system

Рис. 5 – Входные переменные системы

Слика 5 – Улазне варијабле за систем

Research results and discussion

The results of the system are shown in Figures 6, 7 and 8. Figures 6 and 7 show the output of the fuzzy system, while Figure 8 shows the comparison of the energy consumption between the system with and without using fuzzy logic.

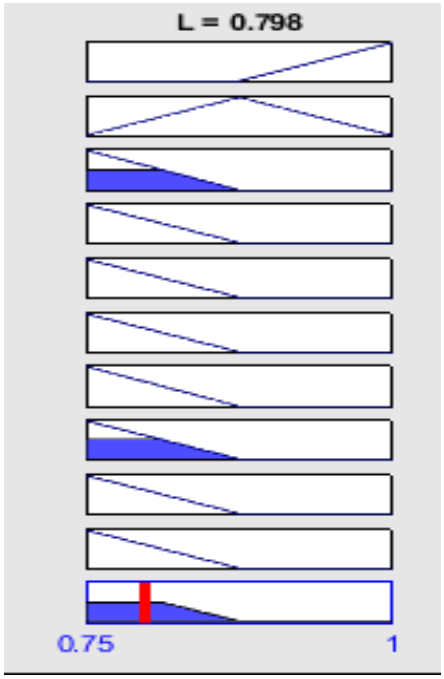

Figure 6 – Fuzzy output of smart street lighting
Рис. 6 – Нечеткий вывод умного уличного освещения
Слика 6 – Фазни излаз паметног уличног осветљења

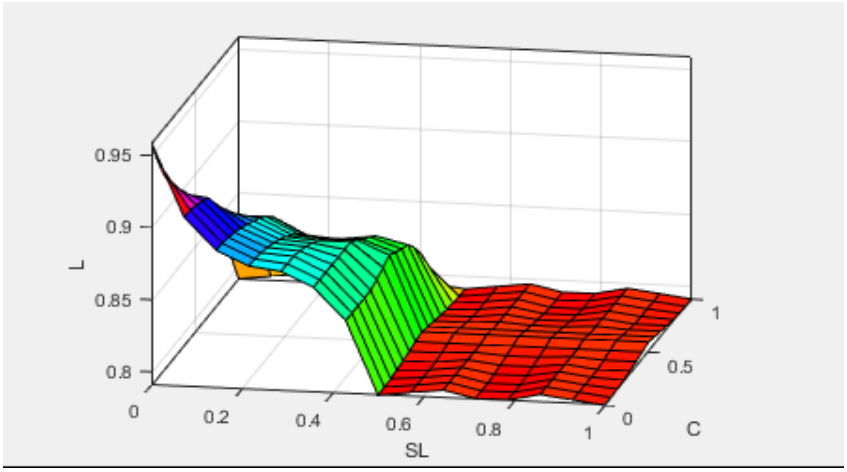

Figure 7 – 3D Plot of the fuzzy output of smart street lighting
Рис. 7 –3Д-график нечеткого вывода умного уличного освещения
Слика 7 – 3Д приказ фазног излаза паметног уличног осветљења

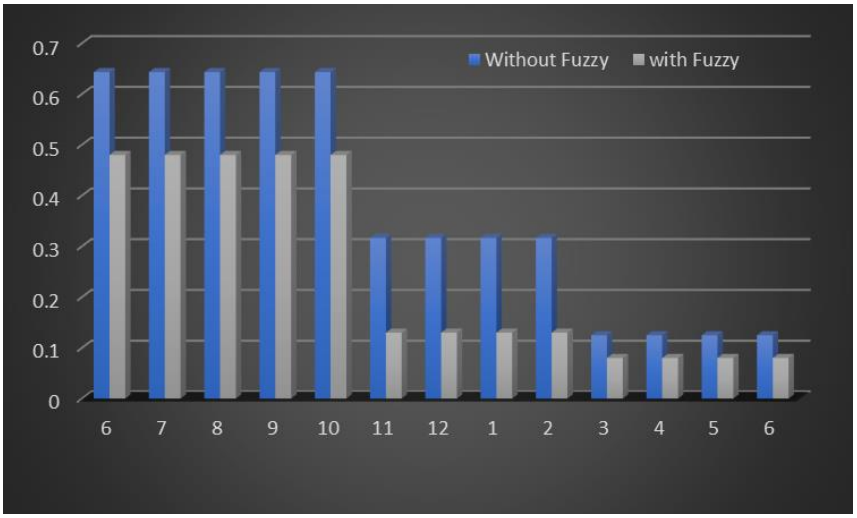

Figure 8 – Difference of SSL energy consumption with and without applying fuzzy logic
Рис. 8 – Разница в энергопотреблении умной системы уличного освещения с применением нечеткой логики и без нее
Слика 8 – Разлика у потрошњи енергије паметног система уличног осветљења са применом фази логике и без њене примене

As it can be seen in the figure above, the system shows good results in energy consumption since the system takes into account the two important factors, the object (Pass or not Pass) and the intensity level of sunlight. With comparison to the result established by (Gagliardi et al, 2020), the work calculates the daily consumption of energy. The saved energy percent for 10 lamps was about 42 %. The model used in this paper was the exact replica of an actual street with the same number of lamps and the average number of cars that passed in the street during three days of observation. The energy percent saved in this work was 44% for 6 lamps.

Conclusion

The objective of this work has been accomplished. Depending on both types of IR sensors and the application of fuzzy logic which is less used in the research of smart lighting, the problem of energy consumption was solved. The saved energy can be used for lighting other streets or for any other application requiring power supply. From the economic angle, dissipated energy costs a lot - more energy requires more oil for power plants which then leads to more money paid by citizens. The most

important advantage of this idea is that lights can be controlled at two levels: level one is the ON-OFF control based on passing objects and level two is the control during the sunrise and sunset hours when there is no need for the full intensity of light bulbs. In third world countries, electric power is consumed randomly due to a lack of understanding of power distribution from the station as well as lack of awareness among people to save energy. That is why a smart system is the most valuable option. In the future, the system can be updated by adding more sensors such as cameras and by using image processing in order to monitor the flow of objects inside the street.

References

Abdul-Adheem, W.R. 2020. Design and simulation of a normalized fuzzy logic controller for the quadruple-tank process. *Indonesian Journal of Electrical Engineering and Computer Science,* 18(1), pp.227-234, 2019. Available at: https://doi.org/10.11591/ijeecs.v18.i1.pp227-234.

Adnan, N., Kamal N. & Chellappan, K. 2019. An IoT Based Smart Lighting System Based on Human Activity. In: *IEEE 14th Malaysia International Conference on Communication (MICC)*, Selangor, Malaysia, pp.65-68, December 2-4. Available at: https://doi.org/10.1109/MICC48337.2019.9037601.

AL-Forati, I.S.A. & Rashid, A. 2020. Multi-Robot Localization System using an Array of LEDs and LDR Sensors. *International Journal of Computer Applications*, 176(10), pp.9-12. Available at: https://doi.org/10.5120/ijca2020920001.

Aussat, Y., Rosmanis, A. & Keshav, S. 2022. A Power-Efficient Self-Calibrating Smart Lighting System. *Energy and Buildings*, 259(art.ID:111874). Available at: https://doi.org/10.1016/j.enbuild.2022.111874.

Bingöl, E., Kuzlu, M. & Pipattanasompom, M. 2019. A LoRa-based Smart Streetlighting System for Smart Cities. In: *7th International Istanbul Smart Grids and Cities Congress and Fair (ICSG)*, Istanbul, Turkey, pp.66-70, April 25-26. Available at: https://doi.org/10.1109/SGCF.2019.8782413.

Botler, L.H. & Sadok, D.H. 2016. A presence sensor for smart lighting systems. In: *IECON 2016 - 42nd Annual Conference of the IEEE Industrial Electronics Society*, Florence, Italy, pp.6001-6006, October 23-26. Available at: https://doi.org/10.1109/IECON.2016.7793173.

Bozanic, D., Tešić, D., Marinković, D. & Milić, A. 2021. Modeling of neuro-fuzzy system as a support in decision-making processes. *Reports in Mechanical Engineering*, 2(1), pp.222-234. Available at: https://doi.org/10.31181/rme2001021222b.

Diaconu, E.M. 2021. Smart Lighting System. *The Scientific Bulletin of Electrical Engineering Faculty*, 21(1), pp.6-9. Available at: https://doi.org/10.2478/sbeef-2021-0002.

Feng, C., Wang, X., Li, Z., Lin, W., Ji, H. & Shen, S. 1976. Smart lighting system based on Bluetooth. *Journal of Physics: Conference Series*, 1976(art.ID:012028). Available at: https://doi.org/10.1088/1742-6596/1976/1/012028.

Gagliardi, G., Lupia, M., Cario, G., Tedesco, F., Gaccio, F.C., Scudo, F.L. & Casavola, A. 2020. Advanced Adaptive Street Lighting Systems for Smart Cities. *Smart Cities*, 3(4), pp.1495-1512. Available at: https://doi.org/10.3390/smartcities3040071.

Ghosh, S. & Haldar, N. 2014. Solar tracking system using AT89C51 microcontroller and LDR. *International Journal of Emerging Technology and Advanced Engineering*, 4(12), pp.403-407.

Gowda, D.V., Annepu, A., Ramesha, M., Kumar, K.P. & Singh, P. 2021. IoT Enabled Smart Lighting System for Smart Cities. *Journal of Physics: Conference Series*, 2089(art.ID:012037). Available at: https://doi.org/10.1088/1742-6596/2089/1/012037.

Hameed, M.S., Mukhtar, S., Khan, H.N., Ali, S., Mateen, M.H. & Gulzar, M. 2021. Pythagorean Fuzzy N -Soft Groups. *Indonesian Journal of Electrical Engineering and Computer Science*, 21(2), pp.1030-1038. Available at: http://doi.org/10.11591/ijeecs.v21.i2.pp1030-1038.

Htwe, T.Z., Tun, A.T. & Aung, C.S. 2020. Power Saving System Using LDR And PIR Sensor. *Iconic Research and Engineering Journals*, 4(2), pp.51-55.

Huangwei, C., Rongjian, T., Fuan, N., Jihua, Z., Bin, S., Zhongyong, L., Can, C. & Liming, C. 2021. A New PCR/LDR-Based Multiplex Functional Molecular Marker for Marker-Assisted Breeding in Rice. *Rice Science*, 28(1), pp.6-10. Available at: https://doi.org/10.1016/j.rsci.2020.11.002.

Kumar, A., Shareef, A., Harn, K.T., Kar, P. & Panda, S.K. 2019. A Complete Hardware Setup for Smart Lighting System. In: *IEEE International Conference on Sustainable Energy Technologies and Systems (ICSETS)*, Bhubaneswar, India, pp.297-301, February 26 - March 1. Available at: https://doi.org/10.1109/ICSETS.2019.8744873.

Kumar, V., Sharma, P. & Kamaldeep, K. 2021. Smart Lighting System Using Arduino. In: *IEEE 8th Uttar Pradesh Section International Conference on Electrical, Electronics and Computer Engineering (UPCON)*, Dehradun, India, pp.1-5, November 11-13. Available at: https://doi.org/10.1109/upcon52273.2021.9667610.

Lah, M.S.C. & Arbaiy, N. 2020. A simulation study of first-order autoregressive to evaluate the performance of measurement error based symmetry triangular fuzzy number. *Indonesian Journal of Electrical Engineering and Computer Science*, 18(3), pp.1559-1567. Available at: https://doi.org/10.11591/ijeecs.v18.i3.pp1559-1567.

Madrigal, G.A., Cuevas, K.G., Hora, V., Jimenez, K.M., Manato, J.N., Porlaje, M.J. & Fortaleza, B. 2019. Fuzzy logic-based maximum power point tracking solar battery charge controller with backup stand-by AC generator. *Indonesian Journal of Electrical Engineering and Computer Science*, 16(1), pp.136-146. Available at: https://doi.org/10.11591/ijeecs.v16.i1.pp136-146.

Montalbo, F.J. & Enriquez, E. 2020. An IoT Smart Lighting System for University Classrooms. In: *International Symposium on Educational Technology (ISET)*, Bangkok, Thailand, pp.3-7, August 24-27. Available at: https://doi.org/10.1109/ISET49818.2020.00011.

Poongothai, M., Subramanian, P. M. & Rajeswari, A. 2018. Design and implementation of IoT based smart laboratory. In: *5th International Conference on Industrial Engineering and Applications (ICIEA)*, Singapore, pp.169-173, April 26-28. Available at: https://doi.org/10.1109/IEA.2018.8387090.

Precup, R-E., Preitl , S., Petriu, E., Bojan-Dragos , C-A., Szedlak-Stinean, A-I., Roman, R-C. & Hedrea, E-L. 2020. Model-Based Fuzzy Control Results for Networked Control Systems. *Reports in Mechanical Engineering*, 1(1), pp.10-25. Available at: https://doi.org/10.31181/rme200101010p.

Saputra, M.M., Yudhawati, D. & Aminda, R.S. 2020. Pengaruh loan to deposit ratio (LDR) dan non performing loan (NPL) terhadap return on asset (ROA). *Manager: Jurnal Ilmu Manajemen*, 3(1), pp.85-93, 2020. Available at: https://doi.org/10.32832/manager.v3i1.3836.

Sikder, A.K., Acar, A., Aksu, H., Uluagac, A.S., Akkaya, K. & Conti, M. 2018. IoT-enabled smart lighting systems for smart cities. In: *IEEE 8th Annual Computing and Communication Workshop and Conference (CCWC)*, Las Vegas, NV, USA, pp.639-645, February 27. Available at: https://doi.org/10.1109/CCWC.2018.8301744.

Sofian, S.S. & Rambely, A.S. 2020. Measuring perceptions of students toward game and recreational activity using fuzzy conjoint analysis. *Indonesian Journal of Electrical Engineering and Computer Science*, 20(1), pp.395-404. Available at: https://doi.org/10.11591/ijeecs.v20.i1.pp395-404.

Subba, B., Wangchuk, C., Ghalley, S., Jigmi, L.J. & Chedup, S. 2020. Design and Simulation of IoT and Zigbee based Smart Lighting System. *IARJSET - International Advanced Research Journal in Science, Engineering and Technology*, 7(9), pp.31-37. Available at: https://doi.org/10.17148/iarjset.2020.7908.

Subrahmanian, R.R. & Shastri, A. 2018. Sustainable development of a historic town: preserving the past to sustain the future. In: *AMPS Proceedings Series 15.2*, *Tangible – Intangible Heritage(s),* pp.168-179 [online]. Available at: http://architecturemps.com/wp-content/uploads/2021/07/Amps-Proceedings-Series-15.2.pdf [Accessed: 20 February 2022].

Yusuf, S.D., Nmezi, S.N., Loko, A.Z. & Lumbi, W.L. 2020. Design and construction of an automatic streetlight controller using microcontroller and LDR. *International Journal of Academic Research and Development*, 5(3), pp.50-56 [online]. Available at: https://www.academicjournal.in/archives/2020/vol5/issue3 [Accessed: 20 February 2022].

Zhang, J-j., Zeng, W-h., a, Hou, S-l., Chen, Y-q., Guo, L-y. & Li, Y-x. 2022. A low-power and low cost smart streetlight system based on Internet of Things technology. *Telecommunication Systems*, 79, pp.83-93, 2022. Available at: https://doi.org/10.1007/s11235-021-00847-1.

УМНАЯ СИСТЕМА УПРАВЛЕНИЯ УЛИЧНЫМ ОСВЕЩЕНИЕМ, ОСНОВАННАЯ НА НЕЧЕТКОЙ ЛОГИКЕ

Ихаб Абдулрахман Сатам
Северный технический университет, кафедра электронной техники, г. Мосул, Ниневия, Республика Ирак;
Обудский университет, факультет машиноведения и безопасности, г. Будапешт, Венгрия

РУБРИКА ГРНТИ: 27.47.00 Математическая кибернетика;
27.47.19 Исследование операций
ВИД СТАТЬИ: оригинальная научная статья

Резюме:

Введение/цель: Потребление электроэнергии для уличного освещения является основным расходом в городской среде. По данным Всемирного банка, потребление электроэнергии на уличное освещение составляет 65% от общего потребления электроэнергии в городах и 10% от общего городского бюджета. Потребность в освещении значительно возрастает из-за стремительной урбанизации, которая требует все больше и больше электроэнергии, а соответственно и финансовых средств. В данной связи необходимо разработать разумные решения по сокращению расходов.

Методы: В данной статье представлена разработанная модель уличного освещения, состоящая из нескольких фонарных столбов, размещенных по обе стороны улицы. Модель является точной копией системы уличного освещения в городе Киркук в Ираке. При расчете потребления электроэнергии учитывалось количество объектов, проходящих по улице, как в часы пик, так и в другое время. В качестве контроллера для данной модели использовался Arduino UNO. Arduino получает сигналы от 3 ИК-датчиков, обрабатывает их, а затем отправляет их светильникам уличного освещения. Нечеткая логика применялась в двух случаях: первый − при дневном освещении, второй – во время восхода и заката солнца, с целью управления интенсивностью света уличного освещения.

Результаты: Оба случая показали значительные результаты в отношении надежности, эффективности и снижении уровня энергопотребления.

Выводы: Система может быть применима в осуществлении проектов "умные города". Она эффективна, надежна и выгодна, а также способствует электросбережению.

Ключевые слова: нечеткая логика, arduino, умное уличное освещение, энергопотребление, освещения автомобильных дорог.

ПАМЕТНИ СИСТЕМ ЗА УПРАВЉАЊЕ УЛИЧНИМ ОСВЕТЉЕЊЕМ ЗАСНОВАН НА ФАЗИ ЛОГИЦИ

Ихаб Абдулрахман Сатам
Северни технички универзитет, Одсек за електронске технике,
Мосул, Нинива, Република Ирак;
Универзитет Обуда, Факултет безбедносних студија,
Будимпешта, Мађарска

ОБЛАСТ: математика, рачунарске науке
ВРСТА ЧЛАНКА: оригинални научни рад

Сажетак

Увод/циљ: Потрошња електричне енергије за осветљавање улица представља знатан трошак у урбаним срединама. Према Светској банци, та потрошња чини 65% свеукупне потрошње електричне енергије у градовима и 10% њиховог укупног буџета. Потреба за осветљавањем у знатном је порасту услед брзе урбанизације, што изискује све више енергије и финансијских средстава – осим ако се не примене паметна решења за смањивање трошкова.

Методе: Представљен је модел уличног осветљења који се састоји од неколико уличних лампи постављених с обе стране улице. Модел представља верну реплику система уличног осветљења у граду Киркуку у Ираку. При израчунавању потрошње електричне енергије узет је у обзир и број објеката који су пролазили улицом у шпицу и ван њега. Контролер за овај модел је Arduino UNO који прима сигнале из три ИЦ сензора, процесира их и шаље до уличних светиљки. Фази логика је примењена у два случаја: у време дневног светла и током изласка и заласка сунца како би се контролисала јачина светлости уличних светиљки.

Резултати: Оба случаја су показала значајне резултате када је реч о поузданости, ефикасности и сигурности система да смањи ниво потрошње електричне енергије.

Закључак: Систем може бити примењен у пројектима паметних градова. Ефикасан је, исплатив и сигурно штеди енергију.

Кључне речи: фази логика, Arduino, паметно улично осветљење, потрошња енергије, путна светла.

Paper received on / Дата получения работы / Датум пријема чланка: 26.02.2022.
Manuscript corrections submitted on / Дата получения исправленной версии работы / Датум достављања исправки рукописа: 18.03.2022.
Paper accepted for publishing on / Дата окончательного согласования работы / Датум коначног прихватања чланка за објављивање: 20.03.2022.

DIBR – FUZZY MARCOS MODEL FOR SELECTING A LOCATION FOR A HEAVY MECHANIZED BRIDGE

Duško Z. Tešić[a], *Darko* I. Božanić[b], *Dragan* S. Pamučar[c], *Jamalud* Din[d]

[a] University of Defence in Belgrade, Military Academy, Dean Office, Belgrade, Republic of Serbia, e-mail: tesic.dusko@yahoo.com, **corresponding author**, ORCID iD: https://orcid.org/0000-0002-5277-3270

[b] University of Defence in Belgrade, Military Academy, Department of Army Weapons and Equipment of the Land Forces, Belgrade, Republic of Serbia, e-mail: dbozanic@yahoo.com, ORCID iD: https://orcid.org/0000-0002-9657-0889

[c] University of Defence in Belgrade, Military Academy, Department of Logistics, Belgrade, Republic of Serbia, e-mail: dragan.pamucar@va.mod.gov.rs, ORCID iD: https://orcid.org/0000-0001-8522-1942

[d] Quaid-I-Azam University, Department of Mathematics, Islamabad, Islamic Republic of Pakistan, e-mail: jd@math.qau.edu.pk, ORCID iD: https://orcid.org/0000-0002-2276-8550

DOI: 10.5937/vojtehg70-35944; https://doi.org/10.5937/vojtehg70-35944

FIELD: Applied mathematics, Military sciences
ARTICLE TYPE: Original scientific paper

Abstract:

Introduction/purpose: The paper presents the DIBR-FMARCOS model of multi-criteria decision-making for defining a location for placing a bridge over an obstacle using a heavy mechanized bridge (TMM-3). After the application of the proposed model, the sensitivity analysis of the output results was performed and it was concluded that the model is stable, i.e. that the model gives consistent results and that its application is possible in real situations.

Methods: The DIBR method was used to determine the weight coefficients of the criteria, while the ranking of alternatives was performed by the FuzzyMARCOS method.

Results: The application of this model has led to the selection of the location for placing a bridge from the TMM-3 set, based on the defined criteria. After applying the proposed model, the sensitivity analysis of the output results was performed and the consistency of the output results of the method was proven.

Conclusion: Finally, it was concluded that the proposed model can be applied in practice, because it gives stable output results. It was also concluded that the DIBR method facilitates the process of obtaining the weight coefficients of the criteria, and the FMARCOS method copes well with unclear and inaccurate input data and has good stability. This model can be further improved by more detailed operationalization of the criteria, as well as by the use of other different methods for determining the weights of the criteria and ranking.

Key words: location, bridge, MCDM, DIBR, Fuzzy, MARCOS.

Introduction

Ensuring the attack pace during offensive operations is an imperative of every army in the world. During their deployment, military units often encounter obstacles, both artificial and natural, which can have a direct impact on the possibility of continuing the ongoing operation, and ultimately on the final outcome of the entire operation. In order to deal with this problem, military units employ bridge systems to overcome obstacles fast and efficiently thus creating conditions for further deployment of their own troops. The Serbian Army has TMM-3 sets of heavy mechanized bridges in its engineering units as one option for surmounting obstacles.

The TMM-3 heavy mechanized bridge is intended for the construction of bridges over natural and artificial obstacles up to 40 m wide and up to 3 m deep for enabling the crossing of tracked vehicles weighing up to 60 tons and wheeled vehicles with the axle pressure up to 11 tons.

The TMM-3 set consists of four bridge-builders (KRAZ-255B vehicle) with four track-type bridge blocks, and all operations during the assembly or disassembly of the bridge are performed by the crew of this vehicle. The length of each bridge block is 10.5 m, while the width of the road is 3.8 m (SSNO,1973; Weaponsystem.net, 2021).

In order to set up a bridge from the TMM-3 set, it is necessary that a chosen location on an obstacle meet certain conditions. These conditions depend on the characteristics of the obstacle itself and on the specifications and constructional features of the bridge block and the bridge-builder.

In order to define the optimal location for erecting a bridge over an obstacle, a choice must be made among several different locations on the obstacle that meet the minimum requirements for the use of this system, for which the application of multicriteria decision-making methods is suitable.

Since the characteristics of obstacles are diverse, and do not always represent quantitative properties, i.e. the input data are very often of a qualitative type, it is desirable to use one of the ways of defining uncertainty to describe certain properties, such as the fuzzy set theory.

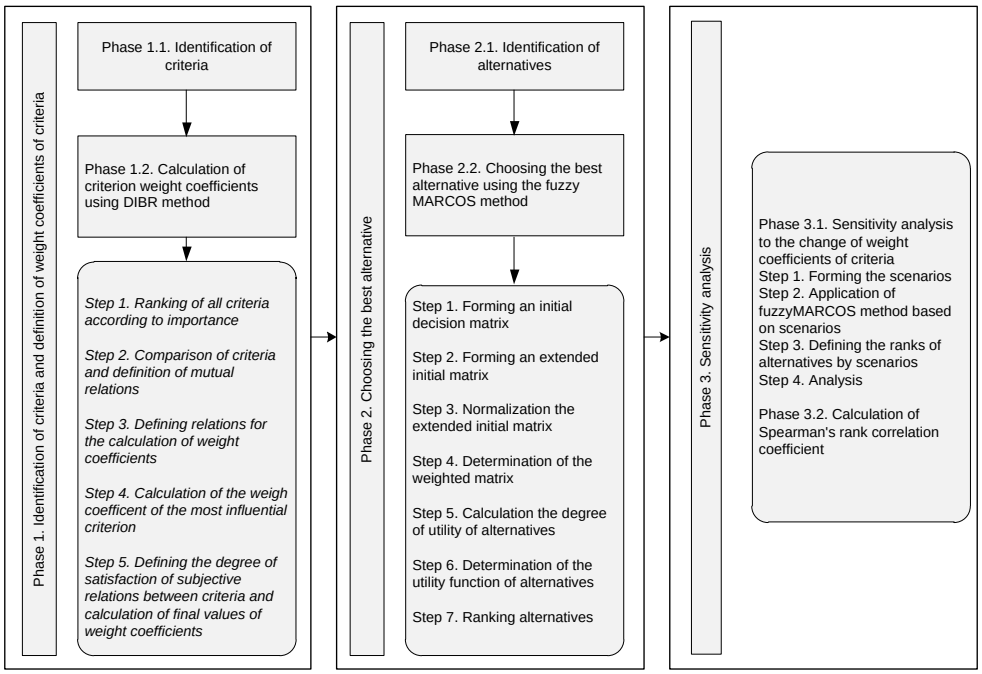

Figure 1 – Phases and steps for the application of the proposed MCDM methodology
Рис. 1 – Этапы и шаги применения многокритериальной методологии принятия решений
Слика 1 – Фазе и кораци за примену методологије вишекритеријумског одлучивања

The application of this theory, in combination with some of the methods of multi-criteria decision-making which treat different problems, has been presented in many papers: for selecting the most efficient procedure for rectification of the optical sight of the long-range rifle in the MCDM model with the AHP and VIKOR methods (Radovanovic et al, 2020), for supplier selection in combination with the PIPERCIA and SAW methods (Đalić et al, 2020), for evaluating websites with the WASPAS method (Stanujkić & Karabašević, 2018), as an auxiliary tool in optimizing the procurement process in order to achieve additional savings by developing stronger cooperation with the optimal supplier,

applying the AHP and TOPSIS methods (Chatterjee & Stević, 2019), to select a supplier using the ELECTRE method (Milovanović et al, 2021), for choosing directions of action of the Group for additional hindering with the AHP and ANP methods (Pamučar et al, 2012), to select a construction machine in the neuro-fuzzy model (Božanić et al, 2021), for risk assessment of natural disasters (Pamučar et al, 2016), to resolve the problems of inadequate, indistinct, and discrepant information (Zulqarnain et al, 2021), for a third party reverse logistic provider (3PRLP) optimization problem (Riaz et al, 2021), etc.

This paper presents the application of the MCDM model for determining the best location for bridge construction over an obstacle using the TMM-3, in which the DIBR methods and the MARCOS method, modified by triangular fuzzy numbers, were applied. The overview of the applied methodology is given in Figure 1.

Literature review

Different methods are used to solve different problems of multicriteria decision making. This part of the paper gives an overview of the literature focusing on the location choice as well as on the DIBR and MARCOS methods.

The problem of location selection has been elaborated in many papers in which multicriteria decision-making methods are applied. Yücenur and Ipekçi select the location for an offshore power plant using the SWARA and WASPAS methods (Yücenur & Ipekçi, 2021), Mihajlović et al (2019) evaluate the locations for the logistics and distribution center in the southern and eastern region of Serbia using the AHP and WASPAS methods, while Kaya (2021) consider the problem of choosing a location for a small hotel in a case study of Cappadocia in Turkey, using the PIPRECIA and ARAS methods. Many authors deal with the problem of choosing the location for a warehouse: applying the integrated gray GPSI (gray preference selection index) model, GPIV (gray proximity indexed value) and comparing with the TOPSIS, WASPAS and COPRAS methods in the sensitivity analysis (Ulutaş et al, 2021), using the UTASTAR method (Ehsanifar et al, 2021), for selecting a location for a warehouse for a humanitarian supply chain, with the AHP and TOPSIS methods (Ak & Acar, 2021), by applying a hierarchical fuzzy model of multicriteria decision making (Arif et al, 2021), using the fuzzy AHP method (Singh et al, 2018), etc. The study of the problem of site selection in the field of military application is presented in the following papers: to select a firing position for mortar units using the LBWA and

FMABAC model (Jokić et al, 2021), to solve the problem of a location for a unmanned border and coastal anti-aircraft gun using the improved genetic algorithm (IGA) (Xu et al, 2021), to select the location for a brigade command post using the FUCOM - Z-number - MABAC model (Bozanic et al, 2020a), for selecting a location for deep wading as a technique of crossing the river by tanks (Bozanic et al, 2018), for the selection of a location for the construction of a single-span Bailey bridge using the FUCOM - Fuzzy MABAC model (Bozanic et al, 2019), to select the location for tanks to drive across the ice using the FAHP and TOPSIS methods (Tešić et al, 2018), etc.

The DIBR method is a new method developed in 2021 (Pamucar et al, 2021a) and so far no paper has been published that solves the problems of determining the weights of criteria by this method, except for the paper in which it was presented.

The MARCOS method has been processed in a large number of papers that deal with and solve various problems: selecting a location for offshore wind farms using interval rough numbers with the Best-Worst method (Deveci et al, 2021); choosing sustainable suppliers using the fuzzy theory (Puška et al, 2021); assessing the quality of e-services in the aviation industry together with the application of the fuzzy theory and the AHP method (Bakır & Atalık, 2021); selecting a location for a landfill for medical waste in urban areas with the BWM method and the gray theory (Torkayesh et al, 2021); regional evaluation of renewable energy sources in Turkey with the AHP method (Karaaslan et al, 2021); inventory classification, together with the SWARA method (Miškić et al, 2021); assessing vehicles on alternative fuels for sustainable road transport in the USA with the FUCOM method and the fuzzy theory (Pamucar et al, 2021b); determining the impact of insurance companies in connection with the COVID-19 pandemic on health services in a fuzzy environment (Ecer & Pamucar, 2021); South African traffic safety evaluation model with the CRITIC and DEA methods (Stević et al, 2021), etc.

Description of methods

DIBR method

The DIBR method is based on defining the relationship between ranked criteria, i.e. it considers the relationship between adjacent criteria, and this method consists of five steps presented below (Pamucar et al, 2021a):

Step 1. Ranking of criteria according to significance.

On a defined set of n criteria $C=\{C_1,C_2,...,C_n\}$ the criteria are ranked according to their significance as $C_1 > C_2 > C_3 > ... > C_n$.

Step 2. Comparison of criteria and definition of mutual relations.

When comparing the criteria, the values $\lambda_{12},\lambda_{13},...,\lambda_{n-1,n}$ and λ_{1n} are obtained; for example, when comparing the criteria C_1 with C_2, a value λ_{12} is optained, etc., and all comparison values must satisfy the condition $\lambda_{n-1,n},\lambda_{1n} \in [0,1]$. Based on the defined conditions and relationships, the following relationships between the criteria are reached:

$$w_1 : w_2 = (1-\lambda_{12}) : \lambda_{12} \quad (1)$$

$$w_2 : w_3 = (1-\lambda_{23}) : \lambda_{23} \quad (2)$$

...

$$w_{n-1} : w_n = (1-\lambda_{n-1,n}) : \lambda_{n-1,n} \quad (3)$$

$$w_1 : w_n = (1-\lambda_{1,n}) : \lambda_{1,n} \quad (4)$$

Relationships (1) - (4) and the value $\lambda_{n-1,n}$ can be viewed as relationships by which the decision maker divides the total significance interval of the 100% criterion into two observed criteria.

Step 3. Defining equations for the calculation of weight coefficients.

Based on the relationship from step 2, the expressions for determining the weight coefficients of the criteria $w_2, w_3, ..., w_n$ are derived:

$$w_2 = \frac{\lambda_{12}}{(1-\lambda_{12})} w_1 \quad (5)$$

$$w_3 = \frac{\lambda_{23}}{(1-\lambda_{23})} w_2 = \frac{\lambda_{12}\lambda_{23}}{(1-\lambda_{12})(1-\lambda_{23})} w_1 \quad (6)$$

...

$$w_n = \frac{\lambda_{n-1,n}}{(1-\lambda_{n-1,n})} w_{n-1} = \frac{\lambda_{12}\lambda_{23}\cdot ... \cdot \lambda_{n-1,n}}{(1-\lambda_{12})(1-\lambda_{23})\cdot ... \cdot (1-\lambda_{n-1,n})} w_1 = \frac{\prod_{i=1}^{n-1} \lambda_{i,i+1}}{\prod_{i=1}^{n-1} (1-\lambda_{i,i+1})} w_1 \quad (7)$$

Step 4. Calculation of the weight coefficient of the most influential criterion

Based on expressions (5) - (7) and the condition that it is $\sum_{j=1}^{n} w_j = 1$, the following mathematical relation is defined

$$w_1\left(1+\frac{\lambda_{12}}{(1-\lambda_{12})}+\frac{\lambda_{12}\lambda_{23}}{(1-\lambda_{12})(1-\lambda_{23})}+...+\frac{\prod_{i=1}^{n-1}\lambda_{i,i+1}}{\prod_{i=1}^{n-1}(1-\lambda_{i,i+1})}\right)=1 \quad (8)$$

From expression (8), the final expression for defining the weighting coefficient of the most influential criterion derives:

$$w_1=\frac{1}{1+\frac{\lambda_{12}}{(1-\lambda_{12})}+\frac{\lambda_{12}\lambda_{23}}{(1-\lambda_{12})(1-\lambda_{23})}+...+\frac{\prod_{i=1}^{n-1}\lambda_{i,i+1}}{\prod_{i=1}^{n-1}(1-\lambda_{i,i+1})}} \quad (9)$$

Based on the obtained value w_1, and using the defined expressions (5) - (7), the weight coefficients of other criteria $w_2, w_3, ..., w_n$ are obtained.

Step 5. Defining the degree of satisfying subjective relationships between the criteria.

Based on expression (4), the value of the weight coefficient of the criterion w_n is defined:

$$w_n=\frac{\lambda_{1n}}{(1-\lambda_{1n})}w_1 \quad (10)$$

Expression (4) is a relation for controlling expression (7), which is intended to check the satisfaction of the decision maker's preference, and from which the value $\lambda'_{1,n}$ is defined, expression (11):

$$\lambda'_{1,n}=\frac{w_n}{w_1+w_n} \quad (11)$$

If the values λ_{1n} and $\lambda'_{1,n}$ are approximately equal, then it can be concluded that the preference of the DM decision is satisfied. If they differ, it is necessary to first check the relationship for λ_{1n}. If the decision maker considers that the relationship λ_{1n} is well defined, the relationship between the criteria should be redefined and the weighting of the criteria should be recalculated. If this is not the case, it is necessary to redefine

the relationship λ_{1n}. It is necessary that the deviation of the value λ_{1n} and $\lambda_{1,n}^{'}$ be up to a maximum of 10%. If this is not the case, it is necessary to redefine the relationships between the criteria in order to achieve this condition.

Fuzzy MARCOS method

The MARCOS method was first presented in the article (Stević et al, 2020) and consists of the following 7 steps:

Step 1. Forming the initial decision matrix.

Multicriteria models involve defining a set of n criteria and m alternatives.

For the fuzzyfication of elements of the initial decision matrix, triangular fuzzy numbers were used (Figure 2). Triangular fuzzy numbers have a form $\tilde{M}$ *=(m_1,m_2,m_3).*

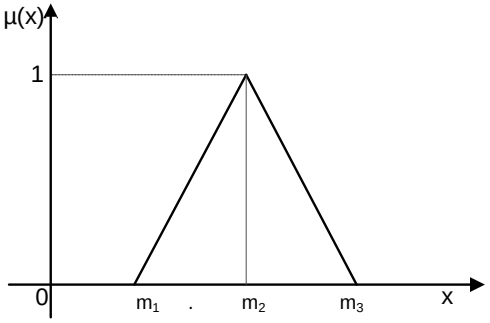

Figure 2 – Triangular fuzzy number $\tilde{M}$

Рис. 2 – Треугольное фаззи-число $\tilde{M}$

Слика 2 – Троугласти fuzzy број $\tilde{M}$

The fuzzy number $\tilde{M}$ membership function is defined by the following expressions:

$$\mu_{\tilde{M}}(x)=\begin{cases}0, & x<m_1\\ \dfrac{x-m_1}{m_2-m_1}, & m_1\le x\le m_2\\ 1, & x=m_2\\ \dfrac{m_3-x}{m_3-m_2}, & m_2\le x\le m_3\\ 0, & x>m_3\end{cases} \tag{12}$$

Since all criteria are subject to subjective assessment by the decision maker and the influence of various factors on the value of the criteria, the degree of confidence is introduced in the process of fuzzification (Božanić et al, 2015) and the distributions of the fuzzy number change according to the expression:

$$\tilde{M} = (m_1, m_2, m_3) = \begin{cases} m_1 = \gamma m_2, & m_1 \le m_2 \\ m_2 = m_2 & \\ m_3 = (2-\gamma) m_2, & m_3 \le m_2 \end{cases} \tag{13}$$

The fuzzy number $\tilde{M} = (m_1, m_2, m_3) = (x\gamma, x, (2-\gamma)x)$, $x \in [1, \infty]$ is defined by the expressions (Božanić et al, 2015):

$$m_1 = x\gamma = \begin{cases} x\gamma, & \forall\ 1 \le x\gamma \le x \\ 1, & \forall\ x\gamma < 1 \end{cases} \tag{14}$$

$$m_2 = x, \ \forall\ x \in [1, \infty]$$

$$m_3 = (2-\gamma)x, \forall x \in [1, \infty]$$

By implementing the degree of confidence in the given statement, the fuzzification of all values of the criteria for all alternatives is performed, thus obtaining a fictionalized initial decision matrix.

Step 2. Forming an extended initial matrix.

Expansion of the initial decision matrix is done by defining the anti-ideal (AAI) and ideal (AI) solutions.

$$X = \begin{array}{c} \\ AAI \\ A_1 \\ A_2 \\ \dots \\ A_m \\ AI \end{array} \begin{array}{c} \begin{array}{cccc} C_1 & C_2 & \dots & C_n \end{array} \\ \begin{bmatrix} x_{aa1} & x_{aa2} & \dots & x_{aan} \\ x_{11} & x_{12} & \dots & x_{1n} \\ x_{21} & x_{22} & \dots & x_{2n} \\ \dots & \dots & \dots & \dots \\ x_{m1} & x_{22} & \dots & x_{mn} \\ x_{ai1} & x_{ai2} & \dots & x_{ain} \end{bmatrix} \end{array} \tag{15}$$

The anti-ideal solution (AAI) represents the worst alternative while the ideal solution (AI) represents the alternative with the best feature, and they are obtained by applying expressions (16) and (17):

$$AAI = \min_j \tilde{x}_{ij} \quad if\ \ j \in B \quad and \quad \max_j \tilde{x}_{ij} \quad if\ \ j \in C \tag{16}$$

$$AI = \max_j \tilde{x}_{ij} \quad if \ \ j \in B \quad and \quad \min_j \tilde{x}_{ij} \quad if \ \ j \in C \tag{17}$$

where B refers to the benefit criteria and C represents the cost criteria.

Step 3. Normalization of the extended initial matrix ($\tilde{X}$).

The normalized matrix $\tilde{N} = \left[\tilde{n}_{ij} \right]_{m \times n}$, i.e. its elements are obtained by applying expressions (18) and (19):

$$n_{ij} = \frac{x_{ai}}{x_{ij}} \quad if \ \ j \in C \tag{18}$$

$$n_{ij} = \frac{x_{ij}}{x_{ai}} \quad if \ \ j \in B \tag{19}$$

where $\tilde{x}_{ij}$ and $\tilde{x}_{ai}$ represent the elements of the matrix $\tilde{X}$.

Step 4. Determination of the weighted matrix $\tilde{V} = \left[\tilde{v}_{ij} \right]_{m \times n}$.

The weithted matrix $\tilde{V}$ is obtained on the basis of expression (20).

$$\tilde{v}_{ij} = \tilde{n}_{ij} \times \tilde{w}_j \tag{20}$$

Using expressions (21) and (22), the degrees of utility of the alternative in relation to the anti-ideal and ideal solutions are obtained.

$$\tilde{K}_i^{-} = \frac{\tilde{S}_i}{\tilde{S}_{aai}} \tag{21}$$

$$\tilde{K}_i^{+} = \frac{\tilde{S}_i}{\tilde{S}_{ai}} \tag{22}$$

Step 5. Calculation of the degree of utility of alternatives $\tilde{K}_i$.

The degree of utility of alternatives represents the sum of the elements of the matrix $\tilde{V}$, expression (23)

$$\tilde{S}_i = \sum_{i=1}^{n} \tilde{v}_{ij} \tag{23}$$

where $\tilde{S}_i \in (i = 1, 2, .., m)$

Step 6. Determination of the utility function of alternatives $f\left(K_i\right)$.

The utility function of alternatives is obtained by applying expression (24)

$$f\left(K_i\right)=\frac{K_i^+ + K_i^-}{1+\frac{1-f\left(K_i^+\right)}{f\left(K_i^+\right)}+\frac{1-f\left(K_i^-\right)}{f\left(K_i^-\right)}}; \quad (24)$$

where $f\left(K_i^-\right)$ represents the defuzzification value of the utility function in relation to the anti-ideal solution while $f\left(K_i^+\right)$ represents the defuzzification value of the utility function in relation to the ideal solution, and they are obtained by expressions (25) and (26).

$$f\left(K_i^-\right)=\frac{K_i^+}{K_i^+ + K_i^-} \quad (25)$$

$$f\left(K_i^+\right)=\frac{K_i^-}{K_i^+ + K_i^-} \quad (26)$$

where all values are defuzzificated using one of the following expressions (Seiford, 1996; Liou & Wang, 1992):

$$M=((m_3-m_1)+(m_2-m_1))/3+m_1 \quad (27)$$

$$M=\left[\lambda m_3+m_2+(1-\lambda)m_1\right]/2 \quad (28)$$

where λ represents an index of optimism $\lambda\in[0,1]$ (Bozbura et al, 2007).

Step 7. Ranking alternatives.

Ranking is done by ranking the values of utility functions (higher value, better ranking).

Application of the DIBR-FMARCOS model

Respecting the phases of the formed MCDM model (Figure 1), the first step is to define the criteria and calculate their weighting coefficients.

Defining the criteria and the weighting coefficients of the criteria

After the analysis of the literature related to the problem (SSNO,1973; Weaponsystem.net, 2021), seven criteria have been identified, as follows:

Criterion 1 (C_1) – The width of the obstacle (Cost) – It represents the distance from one shore to the other and cannot be longer than 40 m,

since the obstacle is overcome with one set of TMM-3. The value of the criterion is expressed in meters (m).

Criterion 2 (C_2) – The depth of the obstacle at the places where the supports are placed (Cost) – means the place on the obstacle where the supports of the bridge block are placed and cannot be deeper than 3 m. The value of the criterion is expressed in meters (m).

Criterion 3 (C_3) – The slope of the shore at the place of placing the bridge (Cost) – is the angle measured in degrees in relation to the horizontal plane. The slopes of the shores must not be higher than: longitudinal up to 10°, transverse up to 6°. Otherwise, it is necessary to perform certain engineering works that require additional resources and time in order to adjust the slopes of the coast to the allowed limits. The value of the criterion is expressed in degrees (°).

Criterion 4 (C_4) – The slope of the bottom of the obstacle at the places where the supports are placed (Cost) – means the angle measured in degrees in relation to the horizontal plane at the bottom of the obstacle where the bridge block support is placed and must meet the following limits: the axis along the bridge up to 30° and the axis perpendicular to the bridge up to 20°. The value of the criterion is expressed in degrees (°).

Criterion 5 (C_5) – Access roads (Benefit) – This criterion represents the roads leading to and from the obstacle to be overcome, and considers the following characteristics: quality, transverse slope of the access road (cannot exceed 20°), longitudinal slope of the access road (cannot exceed 30°), and the possibility of concealed access. The value of the criterion is expressed on a five-point scale: 1 – insufficient, 2 - sufficient, 3 - good, 4 - very good, and 5 - excellent.

Criterion 6 (C_6) – Load-bearing capacity of the ground on the banks of obstacles (Benefit) – It represents the stability of the banks depending on the soil category. The value of the criteria is expressed on a five-point scale: 1 - insufficient (1st and 2nd category soil), 2 - sufficient (3rd category soil), 3 - good (4^{th} category soil), 4 - very good (5^{th} category soil), and 5 - excellent (6^{th} and 7^{th} category soil) (Mijatović, 2008, p.17).

Criterion 7 (C_7) – Maneuver space (Benefit) – represents the necessary space on the bank for maneuvering (approach, turning and work) bridge-builders. The value of the criteria is expressed on a five-point scale: 1 - insufficient, 2 - sufficient, 3 - good, 4 - very good, and 5 - excellent.

Based on the above, a set of seven criteria was determined $C_1, C_2, ..., C_7$, which are ranked in order of importance as $C_1 > C_2 > C_3 > C_4 > C_5 > C_6 > C_7$. Based on the rank of the criteria, the

values $\lambda_{12}, \lambda_{13}, ..., \lambda_{67}$ and λ_{17} are defined, as follows: $\lambda_{12} = 0.45$, $\lambda_{23} = 0.44$, $\lambda_{34} = 0.47$, $\lambda_{45} = 0.46$, $\lambda_{56} = 0.49$, $\lambda_{67} = 0.45$ and $\lambda_{17} = 0.27$, after which the following relations were defined:

$$w_1 : w_2 = 0.55 : 0.45$$
$$w_2 : w_3 = 0.56 : 0.44$$
$$w_3 : w_4 = 0.53 : 0.47$$
$$w_4 : w_5 = 0.54 : 0.46$$
$$w_5 : w_6 = 0.51 : 0.49$$
$$w_6 : w_7 = 0.55 : 0.45$$
$$w_1 : w_7 = 0.73 : 0.27$$

Based on the previous relations, expressions (5) - (7) are used for defining the expressions for the values of the weight coefficients of the criteria:

$w_2 = 0.818 w_1$; $w_3 = 0.786 w_2 = 0.643 w_1$; $w_4 = 0.873 w_3 = 0.561 w_1$; $w_5 = 0.839 w_4 = 0.471 w_1$; $w_6 = 0.961 w_5 = 0.452 w_1$ and $w_7 = 0.818 w_6 = 0.370 w_1$.

Based on the condition $\sum_{j=1}^{7} w_j = 1$ and expression (9), it follows that it is

$$w_1 = \frac{1}{1 + 0.818 + 0.643 + 0.561 + 0.471 + 0.452 + 0.370} = 0.2318$$

Expressions (5) - (7) are used for calculating the weight coefficients of the remaining criteria $w_2 = 0.1896$; $w_3 = 0.1490$; $w_4 = 0.1300$; $w_5 = 0.1091$; $w_6 = 0.1048$ and $w_7 = 0.0858$.

With expression (11), the control value $\lambda'_{1,7}$ is calculated.

$$\lambda'_{1,7} = \frac{w_7}{w_1 + w_7} = \frac{0.0858}{0.2318 + 0.0858} = 0.2701$$

Since $\lambda_{17} \approx \lambda'_{1,7}$, ie $\lambda'_{1,7} = 0.2701$ and $\lambda_{17} = 0.27$, it is concluded that expert preferences are well defined, i.e. that the transitive relations that define the significance of the criteria are met.

The previously explained steps of the DIBR method are applied in order to obtain the following weight coefficients of the criteria:

Table 1 – Values of the weight coefficients of the criteria
Таблица 1 – Значения весовых коэффициентов критериев
Табела 1 – Вредности тежинских коефицијената критеријума

Criterion	Weight coefficient of the criterion
K-1	0.2318
K-2	0.1896
K-3	0.1490
K-4	0.1300
K-5	0.1091
K-6	0.1048
K-7	0.0858

Ranking alternatives

Based on the defined criteria and four alternatives on the obstacle on which it is necessary to build a bridge from the TMM-3 set and based on the opinion of experts, the following decision matrix was defined, which is the first step in applying the MARCOS method:

$$X = \begin{array}{c} \\ A_1 \\ A_2 \\ A_3 \\ A_4 \end{array} \begin{array}{c} \begin{array}{ccccccc} C_1 & C_2 & C_3 & C_4 & C_5 & C_6 & C_7 \end{array} \\ \begin{bmatrix} (35,90) & (1.9,90) & (4,100) & (5,80) & (4,80) & (4,60) & (5,100) \\ (37,80) & (2,100) & (3,90) & (4,90) & (5,70) & (5,80) & (4,80) \\ (32,100) & (2.8,90) & (4,80) & (3,90) & (4,80) & (4,100) & (4,80) \\ (39,80) & (2.6,90) & (4,90) & (4,100) & (4,80) & (5,90) & (5,90) \end{bmatrix} \end{array}$$

where the element of the set X, for example (35,90), represents the following: 35 is the value of the criterion C_1 for the alternative A_1 defined by the decision maker (the width of the obstacle of 35 meters), and 90 is the degree of confidence (the decision maker is 90% sure that the value of the criterion C_1 for the alternative A_1 (35) is correct).

By implementing the degree of confidence and applying expression (14), a fuzzy initial decision matrix is obtained:

$$X = \begin{array}{c} \\ A_1 \\ A_2 \\ A_3 \\ A_4 \end{array} \begin{array}{c} \begin{array}{ccccccc} C_1 & C_2 & C_3 & C_4 & C_5 & C_6 & C_7 \end{array} \\ \begin{bmatrix} (31.5,35,38.5) & (1.71,1.9,2.09) & (4,4,4) & (4,5,6) & (3.2,4,4.8) & (2.4,4,5.6) & (5,5,5) \\ (29.6,37,44.4) & (2,2,2) & (2.7,3,3.3) & (3.6,4,4.4) & (3.5,5,6.5) & (4,5,6) & (3.2,4,4.8) \\ (32,32,32) & (2.52,2.8,3.08) & (3.2,4,4.8) & (2.7,3,3.3) & (3.2,4,4.8) & (4,4,4) & (3.2,4,4.8) \\ (31.2,39,46.8) & (2.34,2.6,2.86) & (3.6,4,4.4) & (4,4,4) & (3.2,4,4.8) & (4.5,5,5.5) & (4.5,5,5.5) \end{bmatrix} \end{array}$$

Step 2. Forming an extended initial matrix.

By applying expressions (16) and (17), an extended initial decision matrix was obtained.

$$X = \begin{array}{c} \\ AII \\ A_1 \\ A_2 \\ A_3 \\ A_4 \\ AI \end{array} \begin{array}{c} C_1 \\ \begin{bmatrix} (32,39,46.8) \\ (31.5,35,38.5) \\ (29.6,37,44.4) \\ (32,32,32) \\ (31.2,39,46.8) \\ (29.6,32,32) \end{bmatrix} \end{array} \begin{array}{c} C_2 \\ \begin{bmatrix} (2.52,2.8,3.08) \\ (1.71,1.9,2.09) \\ (2,2,2) \\ (2.52,2.8,3.08) \\ (2.34,2.6,2.86) \\ (1.71,1.9,2) \end{bmatrix} \end{array} \begin{array}{c} C_3 \\ \begin{bmatrix} (4,4,4.8) \\ (4,4,4) \\ (2.7,3,3.3) \\ (3.2,4,4.8) \\ (3.6,4,4.4) \\ (2.7,3,3.3) \end{bmatrix} \end{array} \begin{array}{c} C_4 \\ \begin{bmatrix} (4,5,6) \\ (4,5,6) \\ (3.6,4,4.4) \\ (2.7,3,3.3) \\ (4,4,4) \\ (2.7,3,3.3) \end{bmatrix} \end{array} \begin{array}{c} C_5 \\ \begin{bmatrix} (3.2,4,4.8) \\ (3.2,4,4.8) \\ (3.5,5,6.5) \\ (3.2,4,4.8) \\ (3.2,4,4.8) \\ (3.5,5,6.5) \end{bmatrix} \end{array} \begin{array}{c} C_6 \\ \begin{bmatrix} (2.4,4,4) \\ (2.4,4,5.6) \\ (4,5,6) \\ (4,4,4) \\ (4.5,5,5.5) \\ (4.5,5,6) \end{bmatrix} \end{array} \begin{array}{c} C_7 \\ \begin{bmatrix} (3.2,4,4.8) \\ (5,5,5) \\ (3.2,4,4.8) \\ (3.2,4,4.8) \\ (4.5,5,5.5) \\ (5,5,5.5) \end{bmatrix} \end{array}$$

Step 3. Normalization of the extended initial matrix (X)

The normalized values for the cost criteria were calculated with expression (18) and the normalized values for the benefit criteria were calculated with expression (19).

$$X = \begin{array}{c} \\ AII \\ A_1 \\ A_2 \\ A_3 \\ A_4 \\ AI \end{array} \begin{array}{c} C_1 \\ \begin{bmatrix} (0.632,0.759,0.632) \\ (0.769,0.846,0.94) \\ (0.667,0.8,1) \\ (0.925,0.925,0.925) \\ (0.632,0.759,0.949) \\ (0.925,0.925,1) \end{bmatrix} \end{array} \begin{array}{c} C_2 \\ \begin{bmatrix} (0.555,0.611,0.555) \\ (0.818,0.9,1) \\ (0.855,0.855,0.855) \\ (0.555,0.611,0.679) \\ (0.598,0.658,0.731) \\ (0.855,0.9,1) \end{bmatrix} \end{array} \begin{array}{c} C_3 \\ \begin{bmatrix} (0.563,0.675,0.563) \\ (0.675,0.675,0.675) \\ (0.818,0.9,1) \\ (0.563,0.675,0.844) \\ (0.614,0.675,0.75) \\ (0.818,0.9,1) \end{bmatrix} \end{array} \begin{array}{c} C_4 - C_6 \\ \begin{bmatrix} \\ \\ . \\ \\ \\ \end{bmatrix} \end{array} \begin{array}{c} C_7 \\ \begin{bmatrix} (0.582,0.727,0.873) \\ (0.909,0.909,0.909) \\ (0.582,0.727,0.873) \\ (0.582,0.727,0.873) \\ (0.818,0.909,1) \\ (0.909,0.909,1) \end{bmatrix} \end{array}$$

Step 4. Determination of the weighted matrix $V = \left[v_{ij} \right]_{m \times n}$

This step represents the determination of the weighted normalized matrix using expression (20) by multiplying all the values of the normalized matrix by the values of the criteria:

$$X = \begin{array}{c} \\ AII \\ A_1 \\ A_2 \\ A_3 \\ A_4 \\ AI \end{array} \begin{array}{c} C_1 \\ \begin{bmatrix} (0.147,0.176,0.147) \\ (0.178,0.196,0.218) \\ (0.155,0.185,0.232) \\ (0.214,0.214,0.214) \\ (0.147,0.176,0.22) \\ (0.214,0.214,0.232) \end{bmatrix} \end{array} \begin{array}{c} C_2 \\ \begin{bmatrix} (0.105,0.116,0.105) \\ (0.155,0.171,0.19) \\ (0.162,0.162,0.162) \\ (0.105,0.116,0.129) \\ (0.113,0.125,0.139) \\ (0.162,0.171,0.19) \end{bmatrix} \end{array} \begin{array}{c} C_3 \\ \begin{bmatrix} (0.084,0.101,0.084) \\ (0.101,0.101,0.101) \\ (0.122,0.134,0.149) \\ (0.084,0.101,0.126) \\ (0.091,0.101,0.112) \\ (0.122,0.134,0.149) \end{bmatrix} \end{array} \begin{array}{c} C_4 - C_6 \\ \begin{bmatrix} \\ \\ . \\ \\ \\ \end{bmatrix} \end{array} \begin{array}{c} C_7 \\ \begin{bmatrix} (0.05,0.062,0.075) \\ (0.078,0.078,0.078) \\ (0.05,0.062,0.075) \\ (0.05,0.062,0.075) \\ (0.07,0.078,0.086) \\ (0.078,0.078,0.086) \end{bmatrix} \end{array}$$

Step 5. Calculating the degree of utility of alternatives K_i *.*

Expressions (21) - (23) are used for calculating the degrees of utility of alternatives in relation to the antideal and ideal solutions.

Table 2 – Values of the utility degree of the alternatives
Таблица 2 – Значения степеней полезности альтернатив
Табела 2 – Вредности степена корисности алтернатива

	S_i			K_i^-			K_i^+		
Antiideal	0.498	0.592	0.550	0.906	1.000	1.104	0.498	0.669	0.670
A1	0.666	0.752	0.852	1.212	1.271	1.712	0.666	0.850	1.039
A2	0.697	0.803	0.929	1.268	1.356	1.867	0.697	0.907	1.133
A3	0.683	0.747	0.824	1.243	1.262	1.655	0.683	0.844	1.005
A4	0.642	0.721	0.820	1.167	1.219	1.648	0.642	0.815	1.000
Ideal	0.820	0.885	1.000	1.492	1.496	2.009	0.820	1.000	1.219

Step 6. Determination of the utility function of alternatives $f\left(K_i\right)$.

The utility function of alternatives is defined by applying expressions (24) - (26), and their defuzzification is performed by applying expression (28), where the optimism index (λ) is taken to be 0.5.

Table 3 – Values of the utility function of the alternatives
Таблица 3 – Значения функции полезности альтернатив
Табела 3 – Вредности функције корисности алтернатива

	$F(K_i^-)$			$F(K_i^+)$			$f(K_i)$
A1	0.404	0.424	0.571	0.222	0.283	0.346	0.470
A2	0.423	0.452	0.622	0.232	0.302	0.378	0.546
A3	0.415	0.421	0.552	0.228	0.281	0.335	0.461
A4	0.389	0.406	0.549	0.214	0.272	0.333	0.430

Step 7. Ranking alternatives.

The ranking of the alternatives is done based on the final values of the utility functions.

Table 4 – Rank of the alternatives
Таблица 4 – Ранг альтернатив
Табела 4 – Ранг алтернатива

f(Ki)	Rank
0.470	2
0.546	1
0.461	3
0.430	4

Sensitivity analysis

The sensitivity analysis is a logical step in model validation and has been presented in a large number of papers (Božanić et al, 2021; Božanić et al, 2020b; Muhammad et al, 2021; Durmić et al, 2020; Božanić et al, 2015). The paper analyzes the sensitivity of the model output results to the changes in the weight coefficients (Pamučar et al, 2017), through the following 18 scenarios (Table 5):

Table 5 – Scenarios of changes in the weight coefficients of the criteria
Таблица 5 – Сценарии изменения весовых коэффициентов критериев
Табела 5 – Сценарији промене тежинских коефицијената критеријума

	K1	K2	K3	K4	K5	K6	K7
S1	0.143	0.143	0.143	0.143	0.143	0.143	0.143
S2	0.218	0.192	0.151	0.132	0.111	0.107	0.088
S3	0.204	0.194	0.154	0.135	0.114	0.109	0.090
S4	0.190	0.197	0.156	0.137	0.116	0.112	0.093
S5	0.176	0.199	0.158	0.139	0.118	0.114	0.095
S6	0.162	0.201	0.161	0.142	0.121	0.116	0.097
S7	0.148	0.204	0.163	0.144	0.123	0.119	0.100
S8	0.134	0.206	0.165	0.146	0.125	0.121	0.102
S9	0.121	0.208	0.168	0.149	0.128	0.123	0.104
S10	0.107	0.210	0.170	0.151	0.130	0.126	0.107
S11	0.093	0.213	0.172	0.153	0.132	0.128	0.109
S12	0.079	0.215	0.174	0.156	0.135	0.130	0.111
S13	0.065	0.217	0.177	0.158	0.137	0.133	0.114
S14	0.051	0.220	0.179	0.160	0.139	0.135	0.116
S15	0.037	0.222	0.181	0.162	0.142	0.137	0.118
S16	0.023	0.224	0.184	0.165	0.144	0.140	0.121
S17	0.009	0.227	0.186	0.167	0.146	0.142	0.123
S18	0.002	0.228	0.187	0.168	0.147	0.143	0.124

After applying the weight coefficients of the criteria given in Table 5, the Spearman's rank correlation coefficient (S) is calculated (Srđević et al, 2009) with the use of the following expression:

$$S = 1 - \frac{6\sum_{i=1}^{n} D_i^2}{n(n^2 - 1)} \tag{29}$$

where:

D_i – is the difference between the rank of a given element in the vector w and the rank of the corresponding element in the reference vector, and

n – is the number of ranked elements.

The identical ranks of the elements define the value of Spearman's coefficient 1 ("ideal positive correlation"). The value of Spearman's coefficient -1 means that the ranks are absolutely opposite ("ideal negative correlation"), and when the value of Spearman's coefficient is 0, the ranks are uncorrelated.

By applying the above scenarios in the proposed model, the correlation of ranks is obtained, i.e.. the relationship between the initial rank and the ranks obtained by applying the given scenarios, presented in Figure 3:

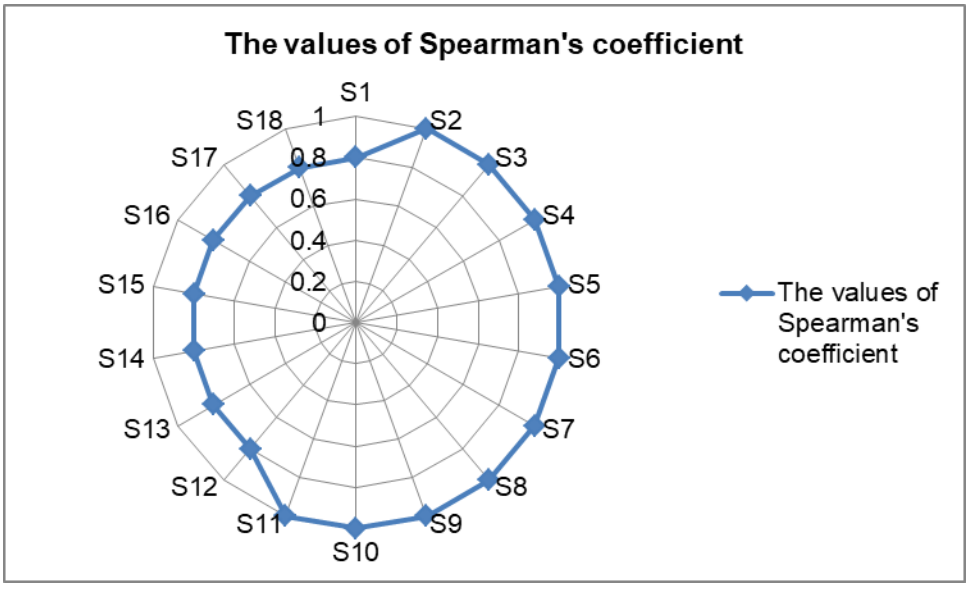

Figure 3 – The values of Spearman's rank correlation coefficient
Рис. 3 – Значение коэффициента ранговой корреляции Спирмена
Слика 3 – Вредности Спирманового коефицијента корелације рангова

Based on the rank correlation values from Figure 3, we can conclude that the ranks are well correlated, i.e. that the output values of the applied model are consistent and stable.

Conclusion

Overcoming obstacles during deployment of military units is one of the most difficult combat operations and the selection of locations for overcoming them requires extensive knowledge and experience of commanding officers. Given a large number of segments that need to be considered in the decision-making process about the location of the bridge, multi-criteria decision-making methods can significantly help decision-makers.

The paper presents a multi-criteria model DIBR-FMARCOS to support decision-making in overcoming obstacles using a TMM-3 set of heavy mechanized bridge. The model have given stable results in the analysis of sensitivity to changes in weights and can find its application in real situations.

The DIBR method gives consistent results regardless of the number of evaluation criteria and eliminates the shortcomings of the nine-point scale used in the BWM and AHP methods while its application facilitates the process of calculating the weights of the criteria when their number is large.

The FMARCOS method improves the area of multi-criteria decision-making by implementing the analysis of the relationship between alternatives and reference points, i.e. between the values of alternatives and the ideal and anti-ideal values. The MARCOS method has shown better stability compared to many other methods, especially when changing the weight coefficients of the criteria.

This model can be further upgraded by more detailed operationalization of the criteria as well as by the application of other, different methods for determining weighting coefficients and ranking alternatives.

References

Ak, M.F. & Acar, D. 2021. Selection of Humanitarian Supply Chain Warehouse Location: A Case Study Based on the MCDM Methodology. *European Journal of Science and Technology,* 22, pp.400-409 [online]. Available at: https://dergipark.org.tr/en/pub/ejosat/issue/59649/849896 [Accessed: 15 January 2022].

Arif, M., Wirjodirdjo, B., Astika, I. & Rivai, A. 2021. Analysis of selection of arsenal warehouse locations to support KRI operations in the koarmada ii area analysis of arsenal storage location selection to support the operations of Indonesian navy warship (KRI) in the 2nd naval fleet territory. *Journal ASRO*, 12(01), pp.40-45. Available at: https://doi.org/10.37875/asro.v12i01.379.

Bakır, M. & Atalık, Ö. 2021. Application of Fuzzy AHP and Fuzzy MARCOS Approach for the Evaluation of E-Service Quality in the Airline Industry. *Decision Making: Applications in Management and Engineering*, 4(1), pp.127-152. Available at: https://doi.org/10.31181/dmame2104127b.

Bozbura, F.T, Beskese, A. & Kahraman, C. 2007. Prioritization of human capital measurement indicators using fuzzy AHP. *Expert Systems with Applications*, 32, pp.1100–1112. Available at: https://doi.org/10.1016/j.eswa.2006.02.006.

Božanić, D., Karović, S. & Pamučar, D. 2015. Fazifikacija Saaty-jeve skale primenom trouglastog fuzzy broja sa promenljivim intervalom poverenja (in Serbian). In: *Proceedings of XLII International Symposium on Operational Research SYM-OP-IS 2015,* Srebrno jezero, Serbia, pp.420-424, September 15-18 [online]. Available at: http://symopis2015.matf.bg.ac.rs/ZbornikN.pdf [Accessed: 15 January 2022].

Božanić, D., Milić, A., Tešić, D., Sałabun, W. & Pamučar, D. 2021. D numbers – FUCOM – fuzzy RAFSI model for selecting the group of construction machines for enabling mobility. *Facta Universitatis, Series: Mechanical Engineering*, 19(3), pp.447-471. Available at: https://doi.org/10.22190/FUME210318047B.

Božanić, D., Ranđelović, A., Radovanović, M. & Tešić, D. 2020b. A hybrid LBWA-IR-MAIRCA multi-criteria decision-making model for determination of constructive elements of weapons. *Facta Universitatis, Series: Mechanical Engineering*, 18(3), pp.399-418. Available at: https://doi.org/10.22190/FUME200528033B.

Božanić, D., Tešić, D. & Kočić, J. 2019. Multi-criteria FUCOM – Fuzzy MABAC model for the selection of location for construction of single-span bailey bridge. *Decision Making: Applications in Management and Engineering*, 2(1), pp.132-146 [online]. Available at: https://dmame.rabek.org/index.php/dmame/article/view/32 [Accessed: 15 January 2022].

Božanić, D., Tešić, D. & Milić, A. 2020a. Multicriteria decision making model with Z-numbers based on FUCOM and MABAC model. *Decision Making: Applications in Management and Engineering*, 3(2), pp.19-36 [online]. Available at: https://dmame.rabek.org/index.php/dmame/article/view/72 [Accessed: 15 January 2022].

Božanić, D., Tešić, D. & Milićević, J. 2018. A hybrid fuzzy AHP-MABAC model: Application in the Serbian Army – The selection of the location for deep wading as a technique of crossing the river by tanks. *Decision Making: Applications in Management and Engineering*, 1(1), pp.143-164 [online].

Available at: https://dmame.rabek.org/index.php/dmame/article/view/2 [Accessed: 15 January 2022].

Chatterjee, P. & Stević, Ž. 2019. A two-phase fuzzy AHP - fuzzy TOPSIS model for supplier evaluation in manufacturing environment. *Operational Research in Engineering Sciences: Theory and Applications*, 2(1), pp.72-90 [online]. Available at: https://www.oresta.rabek.org/index.php/oresta/article/view/19 [Accessed: 15 January 2022].

Deveci, M., Özcan, E., John, R., Pamucar, D. & Karaman, H. 2021. Offshore wind farm site selection using interval rough numbers based Best Worst Method and MARCOS. *Applied Soft Computing*, 109, 107532. Available at: https://doi.org/10.1016/j.asoc.2021.107532.

Durmić, E., Stević, Ž., Chatterjee, P., Vasiljević, M. & Tomašević , M. 2020. Sustainable supplier selection using combined FUCOM – Rough SAW model. *Reports in Mechanical Engineering*, 1(1), pp.34-43 [online]. Available at: https://www.frontpres.rabek.org/index.php/asd/article/view/4 [Accessed: 15 January 2022].

Đalić, I., Stević, Ž., Karamasa, C. & Puška, A. 2020. A novel integrated fuzzy PIPRECIA – interval rough SAW model: green supplier selection. *Decision Making: Applications in Management and Engineering*, 3(1), pp.126-145 [online]. Available at: https://dmame.rabek.org/index.php/dmame/article/view/60 [Accessed: 15 January 2022].

Ecer, F. & Pamucar D. 2021. Marcos Technique Under Intuitionistic Fuzzy Environment for Determining the Covid-19 Pandemic Performance of Insurance Companies in Terms of Healthcare Services. *Applied Soft Computing*, 104, art.ID:107199. Available at: https://doi.org/10.1016/j.asoc.2021.107199.

Ehsanifar, M., Wood, D.A. & Babaie, A. 2021. UTASTAR method and its application in multi-criteria warehouse location selection. *Operations Management Research*, 14, pp.202–215. Available at: https://doi.org/10.1007/s12063-020-00169-6.

Jokić, Ž., Božanić, D. & Pamučar, D. 2021. Selection of fire position of mortar units using LBWA and Fuzzy MABAC model. *Operational Research in Engineering Sciences: Theory and Applications*, 4(1), pp.115-135 [online]. Available at: https://oresta.rabek.org/index.php/oresta/article/view/89 [Accessed: 15 January 2022].

Karaaslan, A., Adar, T. & Delice, E.K. 2021. Regional evaluation of renewable energy sources in Turkey by new integrated AHP-MARCOS methodology: a real application. *International Journal of Sustainable Energy*, pp.1-23. Available at: https://doi.org/10.1080/14786451.2021.1897126.

Kaya, T. 2021. Small Hotel Location Selection Problem: The Case of Cappadocia. *Advances in Hospitality and Tourism Research (AHTR)*, 9(2), pp.368-389. Available at: https://doi.org/10.30519/ahtr.899626.

Liou, T-S. & Wang, M-J.J. 1992. Ranking Fuzzy Numbers With Integral Value. *Fuzzy Sets and Systems*, 50(3), pp.247-255. Available at: https://doi.org/10.1016/0165-0114(92)90223-Q.

Mihajlović, J., Rajković, P., Petrović, G. & Ćirić, D. 2019. The Selection of the Logistics Distribution Center Location Based on MCDM Methodology in Southern and Eastern Region in Serbia. *Operational Research in Engineering Sciences: Theory and Applications*, 2(2), pp.72-85 [online]. Available at: https://oresta.rabek.org/index.php/oresta/article/view/28 [Accessed: 15 January 2022].

Mijatović, R. 2008. *Normativi i standardi rada u građevinarstvu - Niskogradnja 6* (in Serbian). Belgrade: Građevinska knjiga & Novi Sad: Stylos. ISBN: 978-86-395-0564-6

Milovanović, V.R., Aleksić, A.V., Sokolović, V.S. & Milenkov, M.A. 2021. Uncertainty modeling using intuitionistic fuzzy numbers. *Vojnotehnički glasnik/Military Technical Courier*, 69(4), pp.905-929. Available at: https://doi.org/10.5937/vojtehg69-33301.

Miškić, S, Stević, Ž. & Tanackov, I. 2021. A novel integrated SWARA-MARCOS model for inventory classification. *International Journal of Industrial Engineering & Production Research*; 32 (4), pp.1-17. Available at: https://doi.org/10.22068/ijiepr.32.4.6.

Muhammad, L.J., Badi, I., Haruna, A.A. & Mohammed, I.A. 2021. Selecting the Best Municipal Solid Waste Management Techniques in Nigeria Using Multi Criteria Decision Making Techniques. *Reports in Mechanical Engineering*, 2(1), pp.180-189. Available at: https://doi.org/10.31181/rme2001021801b.

Pamucar, D., Deveci, M., Gokasar, I., Işık, M. & Zizovic, M. 2021a. Circular economy concepts in urban mobility alternatives using integrated DIBR method and fuzzy Dombi CoCoSo model. *Journal of Cleaner Production*, 323, art.ID:129096. Available at: https://doi.org/10.1016/j.jclepro.2021.129096.

Pamucar, D., Ecer, F. & Deveci, M. 2021b. Assessment of alternative fuel vehicles for sustainable road transportation of United States using integrated fuzzy FUCOM and neutrosophic fuzzy MARCOS methodology. *Science of The Total Environment*, 788, art.ID:147763. Available at: https://doi.org/10.1016/j.scitotenv.2021.147763.

Pamučar, D., Božanić, D. & Komazec, N. 2016. Risk Assessment of Natural Disasters Using Fuzzy Logic System of Type 2. *Management - Journal for Theory and Practice Management*, 21(80), pp.23-34. Available at: https://doi.org/10.7595/management.fon.2016.0016.

Pamučar, D., Božanić, D. & Randjelovic, A. 2017. Multi-criteria decision making: An example of sensitivity analysis. *Serbian Journal of Management*, 12(1), pp.1-27. Available at: https://doi.org/10.5937/sjm12-9464.

Pamučar, D., Đorović, B., Božanić, D. & Ćirović, G. 2012. Modification of the dynamic scale of marks in analytic hierarchy process (AHP) and analytic network approach (ANP) through application of fuzzy approach. *Scientific Research and Essays,* 7(1), pp.24-37 [online]. Available at: https://academicjournals.org/journal/SRE/article-full-text-pdf/7CF489125747/ [Accessed: 15 January 2022].

Puška, A., Stević, Ž. & Stojanović, I. 2021. Selection of Sustainable Suppliers Using the Fuzzy MARCOS Method. *Current Chinese Science,* 1(2),

pp.218-229. Available at: https://doi.org/10.2174/2210298101999201109214028.

Radovanovic, M., Ranđelović, A. & Jokić, Ž. 2020. Application of hybrid model fuzzy AHP - VIKOR in selection of the most efficient procedure for rectification of the optical sight of the long-range rifle. *Decision Making: Applications in Management and Engineering*, 3(2), pp.131-148 [online]. Available at: https://dmame.rabek.org/index.php/dmame/article/view/149 [Accessed: 15 January 2022].

Riaz M., Farid H.M.A., Aslam M., Pamucar D. & Bozanić D. 2021. Novel Approach for Third-Party Reverse Logistic Provider Selection Process under Linear Diophantine Fuzzy Prioritized Aggregation Operators. *Symmetry,* 13(7), art.ID:1152. Available at: https://doi.org/10.3390/sym13071152.

Seiford, L.M. 1996. Data envelopment analysis: The evolution of the state of the art (1978–1995). *Journal of Productivity Analysis*, 7, pp.99-137. Available at: https://doi.org/10.1007/BF00157037.

Singh, R.K., Chaudhary, N. & Saxena, N. 2018. Selection of warehouse location for a global supply chain: A case study. *IIMB Management Review*, 30(4), pp.343-356. Available at: https://doi.org/10.1016/j.iimb.2018.08.009.

Srđević, B., Srđević, Z. & Suvočarev, K. 2009. Analitički hijerarhijski proces – individualna i grupna konzistentnost donosilaca odluka. *Vodoprivreda*, 41(1-3), pp.13-21 [online]. Available at: https://www.vodoprivreda.net/analiticki-hijerarhijski-proces-individualna-i-grupna-konzistentnost-donosilaca-odluka/ (in Serbian) [Accessed: 15 January 2022].

-SSNO. 1973. *Teški lansirni most TMM-3 na automobilu KRAZ-255B, knjiga 1 (opis, rukovanje i održavanje)* (in Serbian). Belgrade: SSNO, Tehnička uprava.

Stanujkić, D. & Karabašević, D. 2018. An extension of the WASPAS method for decision-making problems with intuitionistic fuzzy numbers: a case of website evaluation. *Operational Research in Engineering Sciences: Theory and Applications*, 1(1), pp.29-39 [online]. Available at: https://www.oresta.rabek.org/index.php/oresta/article/view/4 [Accessed: 15 January 2022].

Stević, Z., Pamučar, D., Puška, A. & Chaterjee, P. 2020. Sustainable supplier selection in healthcare industries using a new MCDM method: Measurement of Alternatives and Ranking according to COmpromise Solution (MARCOS). *Computeras and Industrial Engineering*, 140, art.ID:106231. Available at: https://doi.org/10.1016/j.cie.2019.106231.

Stević, Ž., Das, D.K. & Kopić, M. 2021. A Novel Multiphase Model for Traffic Safety Evaluation: A Case Study of South Africa. *Mathematical Problems in Engineering*, 2021, art.ID:5584599. Available at: https://doi.org/10.1155/2021/5584599.

Tešić, D. & Božanić, D. 2018. Application of the MAIRCA method in the selection of the location for crossing tanks under water. *Tehnika*, 73(6), pp.860-867. Available at: https://doi.org/10.5937/tehnika1806860T.

Torkayesh, A.E., Hashemkhani Zolfani, S., Kahvand, M. & Khazaelpour, P. 2021. Landfill location selection for healthcare waste of urban areas using hybrid BWM-grey MARCOS model based on GIS. *Sustainable Cities and Society*, 67, art.ID:102712. Available at: https://doi.org/10.1016/j.scs.2021.102712.

Ulutaş, A., Balo, F., Sua, L., Demir, E., Topal, A. & Jakovljević, V. 2021. A new integrated grey MCDM model: case of warehouse location selection. *Facta Universitatis, Series: Mechanical Engineering*, 19(3), pp.515-535. Available at: https://doi.org/10.22190/FUME210424060U.

-Weaponsystem.net. 2021. *TMM, Tyazhelyy Mekhanizirovannyy Most* [online]. Available at: https://development.weaponsystems.net/system/1276-CC06%20-%20TMM [Accessed: 20.12.2021].

Xu, Y., Li, H. & Lyu, M. 2021. Research on the location problem of unmanned border and coastal air defense anti-aircraft gun. In: *2021 IEEE 5th Advanced Information Technology, Electronic and Automation Control Conference (IAEAC)*, Chongqing, China, pp.339-343, March 12-14. Available at: https://doi.org/10.1109/IAEAC50856.2021.9390701.

Yücenur, G.N. & Ipekçi, A. 2021. SWARA/WASPAS Methods for a Marine Current Energy Plant Location Selection Problem. *Renewable Energy*, 163, pp.1287-1298. Available at: https://doi.org/10.1016/j.renene.2020.08.131.

Zulqarnain, R.M., Siddique, I., Ali, R., Pamučar, D., Marinković, D. & Bozanic, D. 2021. Robust Aggregation Operators for Intuitionistic Fuzzy Hypersoft Set with Their Application to Solve MCDM Problem. *Entropy*, 23(6), art.ID:688. Available at: https://doi.org/10.3390/e23060688.

МОДЕЛЬ DIBR – FUZZY MARCOS ПРИ ВЫБОРЕ МЕСТОПОЛОЖЕНИЯ ДЛЯ УСТАНОВКИ ТЯЖЕЛОГО МЕХАНИЗИРОВАННОГО МОСТА

Душко З. Тешич[а], *Дарко* И. Божанич[б], *Драган* С. Памучар[в], *Ямалуд* Дин[г]

[а] Университет обороны в г. Белград, Военная академия, деканат, г. Белград, Республика Сербия, **корреспондент**

[б] Университет обороны в г. Белград, Военная академия, департамент вооружения и техники сухопутных войск, г. Белград, Республика Сербия

[в] Университет обороны в г. Белград, Военная академия, департамент логистики, г. Белград, Республика Сербия

[г] Университет Куэйд-и-Азам, департамент математики, г. Исламабад, Исламская Республика Пакистан

РУБРИКА ГРНТИ: 27.47.00 Математическая кибернетика;
27.47.19 Исследование операций,
78.25.00 Вооружение и военная техника,
ВИД СТАТЬИ: оригинальная научная статья

Резюме:

Введение/цель: В данной статье представлена модель многокритериального принятия решений DIBR-FMARCOS для определения места установки моста на препятствии с использованием тяжелого механизированного моста (ТММ-3). После применения предложенной модели был проведен анализ чувствительности выходных результатов, который подтвердил стабильность модели и согласованность ее результатов, следовательно данная модель пригодна для применения в реальных ситуациях.

Методы: Для определения весовых коэффициентов критериев использовался метод DIBR, а ранжирование альтернатив выполнялось методом FuzzyMARCOS.

Результаты: Применение данной модели способствовало выбору места установки моста из комплекта ТММ-3 с учетом определенных критериев. После применения предложенной модели был проведен анализ чувствительности выходных результатов и доказана согласованность выходных результатов примененного метода.

Выводы: В итоге был сделан вывод, что предложенную модель можно применять на практике, так как она дает стабильные выходные результаты. Также выявлено, что метод DIBR облегчает процедуру получения весовых коэффициентов критериев, а метод FMARCOS благоприятен для обработки нечетких и неточных входных данных, поскольку обладает соответствующей стабильностью. Данная модель может быть дополнительно улучшена за счет более детальной операционализации критериев, а также применения иных методов определения весов и ранжирования.

Ключевые слова: местоположение, мост, многокритериальное принятие решений, DIBR, фаззи, MARCOS.

МОДЕЛ DIBR – FUZZY MARCOS ЗА ИЗБОР ЛОКАЦИЈЕ ЗА ПОСТАВЉАЊЕ ТЕШКОГ МЕХАНИЗОВАНОГ МОСТА

Душко З. Тешић[а], *Дарко* И. Божанић[б],
Драган С. Памучар[в], *Јамалуд* Дин[г]

[а] Универзитет одбране у Београду, Војна академија, Деканат, Београд, Република Србија, **аутор за преписку**

[б] Универзитет одбране у Београду, Војна академија, Катедра наоружања и опреме копнене војске, Београд, Република Србија

[в] Универзитет одбране у Београду, Војна академија, Катедра логистике, Београд, Република Србија

[г] Универзитет Quaid-I-Azam, Департман математике, Исламабад, Исламска Република Пакистан

ОБЛАСТ: математика, операциона истраживања, војне науке
ВРСТА ЧЛАНКА: оригинални научни рад

Сажетак:

Увод/циљ: У раду је представљен модел вишекритеријумског одлучивања DIBR-FMARCOS за дефинисање локације за постављање моста на препреци применом тешког механизованог моста (ТММ-3). Након примене предложеног модела извршена је анализа осетљивости излазних резултата. Закључено је да је модел стабилан, односно да даје конзистентне резултате и да је његова примена могућа у реалним ситуацијама.

Методе: За одређивање тежинских коефицијената критеријума коришћена је метода DIBR, док је рангирање алтернатива извршено методом Fuzzy MARCOS.

Резултати: Применом овог модела дошло се до избора места за постављање моста од комплета ТММ-3, на основу дефинисаних критеријума. Након примене предложеног модела извршена је анализа осетљивости излазних резултата и доказана конзистентност излазних резултата методе.

Закључак: Предложени модел може се применити у пракси, јер даје стабилне излазне резултате. Такође, метода DIBR олакшава поступак добијања тежинских коефицијената критеријума, а метода FMARCOS добро подноси нејасне и непрецизне улазне податке и има добру стабилност. Овај модел може се додатно унапредити детаљнијом операционализацијом критеријума, као и употребом других и различитих метода за одређивање тежинских коефицијената критеријума и рангирања.

Кључне речи: локација, мост, вишекритеријумско одлучивање, DIBR, Fuzzy, MARCOS.

Paper received on / Дата получения работы / Датум пријема чланка: 18.01.2022.
Manuscript corrections submitted on / Дата получения исправленной версии работы / Датум достављања исправки рукописа: 10.03.2022.
Paper accepted for publishing on / Дата окончательного согласования работы / Датум коначног прихватања чланка за објављивање: 12.03.2022.

AN EFFICIENT APPROACH FOR CALCULATING A DEFINITE INTEGRAL WITH ABOUT A DOZEN OF SAMPLING POINTS

Jie Yu[a], *Maosheng* Zheng[b], *Haipeng* Teng[c], *Yi* Wang[d]

[a] Northwest University, School of Life Science,
Xi'an, People's Republic of China,
e-mail: yujie@nwu.edu.cn,
ORCID iD: https://orcid.org/0000-0001-6606-5462

[b] Northwest University, School of Chemical Engineering,
Xi'an, People's Republic of China,
e-mail: mszhengok@aliyun.com, **corresponding author**,
ORCID iD: https://orcid.org/0000-0003-3361-4060

[c] Northwest University, School of Chemical Engineering,
Xi'an, People's Republic of China,
e-mail: tenghp@nwu.edu.cn,
ORCID iD: https://orcid.org/0000-0003-2987-7415

[d] Northwest University, School of Chemical Engineering,
Xi'an, People's Republic of China,
e-mail: wangyi11@nwu.edu.cn,
ORCID iD: https://orcid.org/0000-0001-6711-0026

DOI: 10.5937/vojtehg70-36029; https://doi.org/10.5937/vojtehg70-36029

FIELD: Mathematics, Materials
ARTICLE TYPE: Original scientific paper

Abstract:

Introduction/purpose: An approximate approach to definite integral calculation has been an attractive problem continuously since the creation of integration due to practical needs in scientific and engineering areas. In most practical cases, the integrand is complex, which leads to a difficulty of obtaining an exact value of integration, so an approximate value of the definite integral with certain accuracy is satisfactory for practical applications. In this paper, an efficient approach for calculating a definite integral with a small number of sampling points is proposed based on the uniform design method from the viewpoint of practical application.

Methods: The distribution of sampling points in its single peak domain is deterministic and uniform, which follows the rule of the uniform design method and good lattice points.

ACKNOWLEDGMENT: This work was supported by the Project Shaanxi Provincial Key Research and Development Program (No.2019SF-056).

Results: The efficient evaluation of a definite integral for a periodical function in its single peak domain can be obtained by using 11 sampling points in one dimension, 17 sampling points in two dimensions, and 19 sampling points in three dimensions.

Conclusion: The efficient approach for a definite integral developed here on the basis of the uniform test design method is promised from the viewpoint of practical application; the sampling points are deterministically and uniformly distributed according to the rule of the uniform design method and "good lattice points". The efficient approach developed in this article will be beneficial to relevant research and application.

Key words: uniform design method, good lattice point, definite integral, single peak domain, finite sampling points.

Introduction

An approximate approach to definite integral calculation has been an attractive problem continuously since the creation of integration due to practical needs from science and engineering, information processing, and theoretical analysis, etc. In most practical cases, the integrand is complex, which leads to the difficulty of gaining an exact value of integration, thus an approximate result of a definite integral with certain accuracy is satisfactory. Therefore, it is of considerable importance to seek appropriate approximation for a definite integral in practical applications.

In the one-dimensional case, many classical quadrature rules are available, such as the rectangle rule (midpoint rule), the trapezoidal rule, Simpson's rule, or the Gauss rule, which have the following form (Leobacher & Pillichshammer, 2014),

$$T_m(f) = \sum_{n=0}^{m} q_n f(x_n), \tag{1}$$

with the quadrature points x_0, x_1, x_2, …, x_n, …, x_m from [0, 1], and with the weights q_0, q_1, q_2, …, q_n, …, q_m. In the case of the trapezoidal rule, $q_0 = q_m = 1/(2m)$, for other weights, $q_n = 1/m$ with $n = 1, 2, \ldots, m-1$. If $f \in C^2([0; 1])$, the error of the trapezoidal rule is of the order $O(m^{-2})$.

Furthermore, under the condition of s dimensions, it results in the following form

$$T_m(f) = \sum_{n=0}^{m} w_n f(x_n), \tag{2}$$

with the set of s-fold quadrature points $\{\boldsymbol{x_0}, \boldsymbol{x_1}, \boldsymbol{x_2}, \ldots, \boldsymbol{x_n}, \ldots, \boldsymbol{x_m}\}$ in the $[0, 1]^s$ domain. Hence the total number of nodes is $N = (m+1)^s$, which

grows dramatically with the dimension *s*. But in terms of the actual number N = m + 1 of integration nodes, this error is of the order $O(N^{-2/s})$.

For large dimensions, which might be in the hundreds for practical problems, such an error convergence is less than satisfying (Leobacher & Pillichshammer, 2014). This phenomenon is often called the *curse of dimensionality* (Leobacher & Pillichshammer, 2014).

The Monte Carlo method was proposed as a calculation approach with stochastic sampling in mid-1940s. However, this method needs a large number of random numbers (sampling points) for simulation calculation (Fang et al, 1994, 2018) and with a rather slow convergence speed.

The idea of a uniformly distributed point set was proposed by Korobov in 1959, followed by the development of the good lattice point (GLP) method with low discrepancy by Hua and Wang (1981). According to the GLP, the convergence speed of integration is much higher than the Monte Carlo method. In 1980s, Fang and Wang established a uniform design method on the basis of the "good lattice point". In the uniform design method (Fang et al, 1994, 2018), the distribution of the sampling points in the space is well deterministic, rather than random. Such kinds of algorithms belong to the “quasi - Monte Carlo method” (QMC) thereafter (Tezuka, 1998, 2002; Paskov & Traub, 1995; Paskov, 1996; Sloan & Woiniakowski, 1998).

Consequently, the so-called “curse of dimensionality” problem puzzled the application of QMC method for many years as well (Tezuka, 1998, 2002; Paskov & Traub, 1995; Paskov, 1996; Sloan & Woiniakowski, 1998). However, the situation changed dramatically in 1990s when Paskov and Traub used Halton sequences and Sobol sequences for accounting a ten-tranche CMO (Collateralized Mortgage Obligation) in high dimensions even reaching to 360 dimensions and found that QMC methods performed very well as compared to simple MC methods, as well as to antithetic MC methods (Tezuka, 1998, 2002; Paskov & Traub, 1995; Paskov, 1996; Sloan & Woiniakowski, 1998). Afterwards, a lot of analogical phenomena were found in different pricing problems by using different types of low-discrepancy sequences (Tezuka, 1998). All these results are really counter-intuitive, so it was difficult to understand that the point distribution from low discrepancy sequences is with so much singular convergence speed compared to that of the distribution of random numbers. Sloan and Wozniakowski proposed an idea of a so-called "weighted" discrepancy to explain this conundrum (Sloan & Woiniakowski, 1998), while Caflisch et al proposed a concept of effective dimensions to demonstrate the miracle (Caflisch et al, 1997). These

achievements indicate the effectiveness of QMC methods though the reason is unclear. Here we do not focus our attention on it in more detail, but develop an efficient approach for the calculation of a definite integral in the viewpoint of practical application instead.

Actually, the integrand in an integral has a certain form and with a clear physical meaning. Therefore, the value of the integrand varies according to a certain rule as the point in space changes from one position to the next, so it is more appropriate to conduct the numerical integration according to a point set which pursues a certain rule and possesses a regular distribution in space in principle.

Here in this article, we try to use a certain number of sampling points with regular distribution to perform approximate assessment for a definite integral. It aims to develop an efficient approach with certain accuracy for a definite integral. The characteristic analysis of a periodical function within its one period is conducted first. The result shows that 11 sampling points of the circumference could supply an effective approximation to the peak value with a relative error not greater than 4%, which enlightens us on exploring to use the 11 sampling points to carry out an efficient approach for the definite integral of a function within its monotonic peak domain. Thereafter, an analogical analysis for two and three dimensional problems is performed as well. Afterwards, some typical examples of the definite integral of physical problems is studied to check the validity of the approach.

Characteristic analysis of the periodical function within one periodical domain

1) One dimensional problem

Generally, the value of a function in a domain varies from point to point. Take a one dimensional monotonic peak function in a domain as an example, represented as,

$$y = A\cdot[1+Sin(2\pi x/\lambda)]. \quad (3)$$

In Eq. (3), A indicates the amplitude coefficient, λ is the period (wave length) of the periodical function, and x is the coordinate value in one dimension.

Clearly, the function y takes its peak value at $x = x_0 = \lambda/4$, i.e., y takes $2A$. While at $x_1 = x_0 + \Delta x/2$, $\Delta x/2$ is the deviation from x_0, the value of the function y decreases, $y_1 = A\cdot[1+Sin(2\pi x_1/\lambda)] = A\cdot\{1+Sin[2\pi(x_0 + \Delta x/2)/\lambda]\} = A\cdot[1+Sin(\pi/2 + \Delta x\pi/\lambda)]$.

While, as $\Delta x\pi/\lambda = 0.2856$ radian, the function y takes the value $y_1 = 1.92A$, which leads to a relative error not greater than 4% for the y value with respect to its peak value of $2A$.

The above analysis indicates that if one attempts to give an approximation value of the periodical function y with a relative error not greater than 4% with respect to its peak value by subdividing the period, the partition number n of the subdivision in the period range (wave length) λ of this periodical function within one period is,

$$n = \lambda/\Delta x = \pi/0.2856 \cong 11. \quad (4)$$

Simultaneously, the distance between the nearest sampling points is $\Delta x = \lambda/11$.

Eq. (4) indicates that the 11 sampling points of the one periodical range (wave length) could provide an efficient approximation to the peak value with a relative error not greater than 4% to its peak value for the function in one dimension.

2) Two dimensional case

Under the condition of two dimensions, it is a problem on a plane where a rectangular coordinate system could be set up, consisting of two orthogonal coordinate axes, let us say the X and Y axes.

First, if we only use the preliminary condition of the uniform design method (Fang et al, 1994, 2018), i.e., the projections of any two sample points on each coordinate axis will not coincide, perhaps we obtain the worst case, which is the status of all the sampling points being distributed along the diagonal line of the square. Even in this case, the distance between the nearest sampling points will be enlarged by $\sqrt{1^2+1^2}=\sqrt{2}$ times as that of the distance between the nearest sampling points of one dimension. Therefore, if one attempts to provide an appropriate approximation with a relative error around 4% as similar to that of the one dimensional problem for the function, the subdivision should be refined by about $1/\sqrt{2}$ times, let us take 1/1.5, which leads to the number of sampling points n' to the period (wave length) λ range of this periodical function within one period to be

$$n' = 1.5n = 1.5 \times 11 = 16.5 \cong 17. \quad (5)$$

Eq. (5) indicates that 17 sampling points for two dimensions in one periodical range (wave length) could provide an appropriate approximation for the peak value of the sine function with a relative error around 4% to its peak value.

Second, one could use the next requirement of uniform design that the sampling points must satisfy both projection properties and spatial filling or spatial uniformity. Then one could rearrange the spatial distributions of the sampling points so that their distributions meet the demand of spatial uniformity at the same time (Fang et al, 1994, 2018).

Ripley (1981) pointed out that, in the problem of spatial sampling, the expected value of the mean square error of the sample decreases with the spatial correlation of the samples, which leads to the situation that the number of sampling will decrease with the spatial correlation of the samples. This might be related to the counter-intuitive phenomena of using QMC in high dimensions mentioned in the previous section.

3) Three dimensional case

Analogically, in the three dimensional case, i.e., cube, a rectangular coordinate system is set up, consisting of three orthogonal coordinate axes, in general *X, Y* and *Z* axes. Again, let us consider the worst case first. When all the sampling points are distributed along the diagonal line of the cube, the distance between the nearest sampling points will be enlarged by $\sqrt{1^2+1^2+1^2}=\sqrt{3}$ times as that of the distance between the nearest sampling points of one dimension. So, if one attempts to provide an appropriate approximation for the peak value of the function with a relative error around 4% as similar to that of the one dimensional problem for the function once more, the subdivision should be refined by about 1/1.7 times, which results in the number of sampling points *n"* to the period (wave length) λ range of this periodical function within one period

$$n" = 1.7n = 1.7 \times 11 = 18.7 \cong 19. \quad (6)$$

Eq. (6) indicates that the 19 sampling points of the one periodical range (wave length) could provide an accurate estimation for the peak value of the sine function with a relative error around 4% to its peak value in three dimensions.

Then one could rearrange the spatial distributions of the sampling points according to the procedure of the uniform design method (Fang et al, 1994, 2018).

The above discussion shows that if one attempts to provide an appropriate approximation for a periodical function within one single peak domain, 11 sampling points (in one dimension), 17 sampling points (in two dimensions), or 19 sampling points (in three dimensions) are needed for the calculation of a definite integral, respectively, while the sampling

points are deterministically distributed according to the rule of the uniform design method and GLP. In the following sections, we will check the applicability of the above descriptions.

Efficient approach for numerical integration on the basis of the uniform test design method and GLD for a single peak function

According to Hua and Wang, a set of good lattice points (GLP) could give an efficient value for a definite integral with low-discrepancy (Hua & Wang, 1981; Fang et al, 1994, 2018), and the discrepancy of the sum approximation of its function values in the discretized GLPs with respect to its precise value of integration in one dimension is not greater than $V(f)\cdot D(n)$, where $V(f)$ is the variation of the function $f(x)$ in its domain by the n uniformly distributed sampling points, $D(n)$ is the discrepancy of the point set with the n uniformly distributed sampling points, and $D(n) = O(n^{-1})$ (Hua & Wang, 1981; Fang et al, 1994, 2018).

The previous sections indicate that 11 uniformly distributed sampling points of the circumference in the one dimensional case could provide an appropriate approximation for the peak value of the function with a relative error not greater than 4% to its peak value. So, the relative error of the summation of the sinusoidal function in the discretized GLPs with respect to its precise value of integration is expected to be around $4\% \times O(n^{-1}) = 4\% \times O(11^{-1}) \approx 0.4\%$ in one dimension.

Similarly, the consequences in the last sections present that 17 and 19 uniformly distributed sampling points in one periodical range could provide an appropriate approximation with a relative error of around 0.4% as compared to its precise value of integration for the sinusoidal function in 2 and 3 dimensions, respectively.

In addition, other functions can be expanded as sine or cosine functions generally.

Hence, here in this section, let us conduct some typical definite integrals to show the rationality of the approach. The sampling points are with the characteristics of GLP so as to give low-discrepancy (Hua & Wang, 1981; Fang et al, 1994, 2018).

1) One dimensional problems

A1) Approximation for the probability integral

Our first example is the probability integral (Navidi, 2020),

$$\int_0^{\infty} \exp(-x^2) \cdot dx = \frac{\sqrt{\pi}}{2} \approx 0.886227 \ , \tag{7}$$

i.e.,

$$\int_0^{\infty} \exp(-x^2) \cdot dx = \int_0^{\infty} f(x) \cdot dx \approx 0.886227 \ . \tag{8}$$

In Eq. (8), $f(x) = exp(-x^2)$ is the integrand function. As to $exp(-x^2)$, at $x_u = 4$ its value is $f(x_u) = 1.125 \times 10^{-7}$, therefore the upper limit of the integral could be set as $x_u = 4$.

According to the uniform design method (Fang et al, 1994, 2018), the distribution of the sampling points in the integral domain [0, 4] is shown in Table 1, and the integration Eq. (8) is thus discretized as

$$I_0 = \int_0^4 f(x) \cdot dx \approx \frac{4}{11} \sum_{i=1}^{11} f(x_i) \, . \tag{9}$$

The positions of the distribution of the sampling points in the domain [0, 4] are obtained according to the following formula (Hua & Wang, 1981; Fang et al, 1994, 2018),

$$x_j = 4 \times (2j - 1)/(2 \times 11), \ j \in 1, 2, 3, \ldots, 11. \tag{10}$$

Table 1 – The positions of the distribution of the sampling points in the integral domain [0, 4]
Таблица 1 – Позиции распределения точек выборки в интегральной области [0, 4]
Табела 1 – Позиције расподеле тачака узорковања у домену интеграције [0, 4]

Point No.	1	2	3	4	5	5	7	8	9	10	11
Location	0.182	0.545	0.909	1.273	1.636	2.0	2.364	2.727	3.091	3.455	3.818

The summation of the right-hand side of Eq. (9) indicates a value of 0.886227, which equals to the probability integral of 0.886227 fortunately, which is with a higher accuracy (Navidi, 2020).

A2) Approximation of the elliptic integral calculus for the magnetic induction intensity of an elliptical current-carrying ring

Take an elliptical current-carrying ring as an example, which is with the major axis *a*, the minor axis *b*, the distance between the focal point *F* and the center *O* is *c*; the distance from a point *M* on the ellipse to the center *O* is *r*, see Fig.1. The problem is to find the magnetic induction intensity at the center of the ellipse.

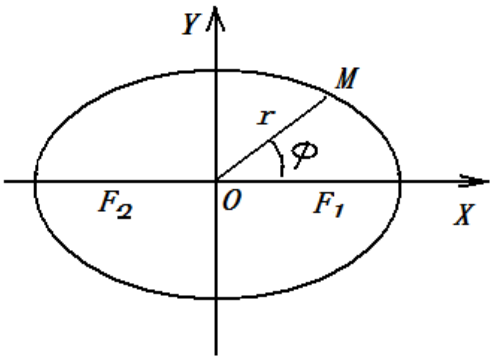

Fig. 1 – Polar coordinate of the elliptical current-carrying ring
Рис. 1 – Полярные координаты эллиптического скользящего кольца
Слика 1 – Поларне координате елиптичног клизног прстена

The solution:

In the polar coordinate system, the elliptic equation with the center *0* is

$$r = \sqrt{a^2\cos^2\varphi + b^2\sin^2\varphi} = a\sqrt{1-k^2\sin^2\varphi}\,, \tag{11}$$

in Eq. (11), $k \equiv c/a = (a^2 - b^2)^{0.5}/a$.

Thus, the expression of the magnetic induction at the center of the current-carrying ellipse can be written as (Ju et al, 2005),

$$B = \frac{\mu_0 I}{4\pi a}\int_0^{2\pi}\frac{d\varphi}{\sqrt{1-k^2\sin^2\varphi}} = \frac{\mu_0 I}{\pi a}\int_0^{\pi/2}\frac{d\varphi}{\sqrt{1-k^2\sin^2\varphi}}\,. \tag{12}$$

In Eq. (12), *I* and μ_0 represent the intensity of the electric current and the permeability of vacuum, respectively.

Let us mark the integration part in Eq. (12) as *Q*, i.e., $Q = \int_0^{\pi/2}\frac{d\varphi}{\sqrt{1-k^2\sin^2\varphi}} = \int_0^{\pi/2} q(\varphi)\cdot d\varphi$, then Eq. (12) can be rewritten as

$$B = \frac{\mu_0 I}{\pi a}Q\,. \tag{13}$$

Under the condition of $k = 0.3$, one could try to evaluate the value of *Q* by our approximate approach.

Again, according to the uniform experimental design method (Fang et al, 1994, 2018), the distribution of the sampling points in the integral

domain [0, π/2] is shown in Table 2, and thus the integration Eq. (13) is discretized as

$$Q = \int_0^{\pi/2} q(\varphi) \cdot d\varphi \approx \frac{\pi/2}{11} \sum_{i=1}^{11} f(\varphi_i) . \quad (14)$$

Table 2 – Distribution of the sampling points in the integral domain [0, π/2]
Таблица 2 – Распределение точек выборки в интегральной области [0, π/2]
Табела 2 – Расподела тачака узорковања у домену интеграције [0, π/2]

Point No.	1	2	3	4	5	5	7	8	9	10	11
Loca-tion	0.0714	0.2142	0.3570	0.4998	0.6426	0.7854	0.9282	1.0710	1.2138	1.3566	1.4994

The approximate result of the right-hand side of Eq. (14) gets a value of 1.608049, which equals to the exact value of the elliptic integral of 1.608049 luckily (Ju et al, 2005; Byrd & Friedman, 1971), implying a much higher accuracy of the approximate approach.

2) Two dimensional case

Under the condition of two or three dimensions, Fang and Wang developed a series of uniform design tables and their utility tables according to GLP and number – theoretic methods (Fang et al, 1994, 2018), which are specific for uniform design. Here the uniform design table $U^*_{17}(17^5)$ is the proper selection for our usage, which contains 17 sampling points.

Here, let us take the integration of $J = \int_{x_1=1.4}^{2.0} dx_1 \int_{x_2=1.0}^{1.5} \ln(x_1 + 2x_2) \cdot dx_2$ as an example.

The integration of $J = \int_{x_1=1.4}^{2.0} dx_1 \int_{x_2=1.0}^{1.5} \ln(x_1 + 2x_2) \cdot dx_2 = \int_{x_1=1.4}^{2.0} dx_1 \int_{x_2=1.0}^{1.5} J(x_1, x_2) \cdot dx_2$ is with the precise value of 0.429560 (Song & Chen, 2004).

The distribution of the sampling points in the integral domain [1.4, 2.0] × [1.0, 1.5] is shown in Table 3, in which x_{10} and x_{20} indicate the original positions from the uniform design table $U^*_{17}(17^5)$ for [1, 17] × [1, 17] domain (Fang et al, 1994, 2018).

Table 3 – Distribution of the sampling points in the integral domain [1.4, 2.0] × [1.0, 1.5]
Таблица 3 – Распределение точек выборки в интегральной области [1.4, 2.0] × [1.0, 1.5]
Табела 3 – Расподела тачака узорковања у домену интеграције [1.4, 2.0] × [1.0, 1.5]

No.	x_{10}	x_{20}	x_1	x_2
1	1	7	1.4176	1.1912
2	2	14	1.4529	1.3971
3	3	3	1.4882	1.0735
4	4	10	1.5235	1.2794
5	5	17	1.5588	1.4853
6	6	6	1.5941	1.1618
7	7	13	1.6294	1.3676
8	8	2	1.6647	1.0441
9	9	9	1.7	1.25
10	10	16	1.7353	1.4559
11	11	5	1.7706	1.1324
12	12	12	1.8059	1.3382
13	13	1	1.8412	1.0147
14	14	8	1.8765	1.2206
15	15	15	1.9118	1.4265
16	16	4	1.9471	1.1029
17	17	11	1.9824	1.3088

According to the uniform design method (Fang et al, 1994, 2018), the integration J in the domain [1.4, 2.0] × [1.0, 1.5] is discretized as

$$J \approx \frac{0.6\times 0.5}{17}\sum_{j=1}^{17} J(x_{1j}, x_{2j})\,. \tag{15}$$

The summation result of the right-hand side of Eq. (15) indicates a value of 0.429609, which gives a relative error of 1.14×10^{-4}% with respect to its precise value of 0.429560 (Song & Chen, 2004).

3) Three dimensional problem

Chen et al (2010) took the integration $S=\int_{x_1=0}^{1}dx_1\int_{x_2=0}^{1}dx_2\int_{x_3=0}^{1}(x_1^3+x_1\cdot x_2^3\cdot x_3^2+x_3)\,dx_3$ as an example to study the validity of the integration of multivariate functions by orthogonal arrays (Chen et al, 2010). Let us reanalyze it by using our newly developed approximate

approach for a definite integral on the basis of the uniform test design method and the “good lattice point” (GLP) method here.

The integration of $S = \int_{x_1=0}^{1} dx_1 \int_{x_2=0}^{1} dx_2 \int_{x_3=0}^{1} (x_1^{\,3} + x_1 \cdot x_2^{\,3} \cdot x_3^{\,2} + x_3) \cdot dx_3$ $= \int_{x_1=0}^{1} dx_1 \int_{x_2=0}^{1} dx_2 \int_{x_3=0}^{1} S(x_1, x_2, x_3) \cdot dx_3$ is with the precise value of 19/24 = 0.791667 (Chen et al, 2010). The uniform design table $U^*_{19}(19^7)$ is a proper selection for our usage, which contains 19 partition points. The distribution of the sampling points in the integral domain [0, 1] × [0, 1] × [0, 1] is presented in Table 4 (Fang et al, 1994, 2018), in which x_{10}, x_{20} and x_{30} indicate the original positions from the uniform design table $U^*_{19}(19^7)$ for the [1, 19] × [1, 19] × [1, 19] domain (Fang et al, 1994, 2018).

Table 4 – Distribution of the sampling points in the integral domain [0, 1] × [0, 1] × [0, 1]
Таблица 4 – Распределение точек выборки в интегральной области [0, 1] × [0, 1] × [0, 1]
Табела 4 – Расподела тачака узорковања у домену интеграције [0, 1] × [0, 1] × [0, 1]

No.	x_{10}	x_{20}	x_{30}	x_1	x_2	x_3
1	1	11	13	0.0263	0.5526	0.6579
2	2	2	6	0.0789	0.0789	0.2895
3	3	13	19	0.1316	0.6579	0.9737
4	4	4	12	0.1842	0.1842	0.6053
5	5	15	5	0.2368	0.7636	0.2368
6	6	6	18	0.2895	0.2895	0.9211
7	7	17	11	0.3421	0.8684	0.5526
8	8	8	4	0.3947	0.3947	0.1842
9	9	19	17	0.4474	0.9737	0.8684
10	10	10	10	0.5	0.5	0.5
11	11	1	3	0.5526	0.0263	0.1316
12	12	12	16	0.6053	0.6053	0.8158
13	13	3	9	0.6579	0.1316	0.4474
14	14	14	2	0.7105	0.7105	0.0789
15	15	5	15	0.7632	0.2368	0.7632
16	16	16	8	0.8158	0.8158	0.3947
17	17	7	1	0.8684	0.3421	0.0263
18	18	18	14	0.9211	0.9211	0.7105
19	19	9	7	0.9737	0.4474	0.3421

According to the uniform design method (Fang et al, 1994, 2018), the integration *S* in the integral domain [0, 1] × [0, 1] × [0, 1] is discretized as

$$S \approx \frac{1}{19}\sum_{j=1}^{19} S(x_{1j}, x_{2j}, x_{3j}). \tag{16}$$

The summation result of the right-hand side of Eq. (16) results in a value of 0.801534, which gives a relative error of 1.25% with respect to its precise value of 0.791667, while Chen et al gave a relative error of 0.04% by simulation calculation with 100 tests in $L_{100}(2^{99})$ orthogonal arrays (Chen et al, 2010). Obviously, their amount of simulation calculation is really huge.

Discussion

The above studies including the analysis and example calculations indicate that the efficient result for a definite integral of a function with an accuracy of around 0.4% within its single peak domain could be obtained by using the new approach with 11 sampling points for one dimension, 17 sampling points for two dimensions, and 19 sampling points for three dimensions. This result is much better than those of classic methods on the one hand; besides, the approach is even better than the MC simulation in the sense of workload of calculation. The novelty and contribution of this study is to use a small number of sampling points to obtain an efficient result for a definite integral with a certain accuracy. As to this target, the aim is fulfilled. Of course, more sampling points could further improve the accuracy provided the distribution of sampling points follows the rules of uniform design and good lattice points at this stage.

Exploration of much better distributions of sampling points might be one of future directions for a more efficient assessment of a definite integral. Applications of the present approach might be another orientation for future studies.

Conclusion

The efficient approach to a definite integral developed here on the basis of the uniform test design method is promising from the viewpoint of practical application. An efficient result for a definite integral of a function could be obtained by using this approach with 11 sampling points for one dimension, 17 sampling points for two dimensions, and 19 sampling points for three dimensions within its single peak domain. The sampling points are deterministically and uniformly distributed according to the rule of the uniform design method and “good lattice points”. The

efficient approach developed in this article will be beneficial to relevant research and application.

References

Byrd, P.F. & Friedman, M.D. 1971. *Hand Book of Elliptic Integrals for Engineers and Scientists, 2nd Ed.* Berlin, Heidelberg: Springer-Verlag. Available at: https://doi.org/10.1007/978-3-642-65138-0.

Caflisch, R.E., Morokoff, W. & Owen, A. 1997. Valuation of mortgage-backed securities using Brownian bridges to reduce effective dimension. *Journal of Computational Finance*, 1(1), pp.27-46. Available at: https://doi.org/10.21314/JCF.1997.005.

Chen, Z., Zheng, X., Luo, C., Zhang, Y. & Chen, X. 2010. Integration of Multivariate Functions by Orthogonal Arrays. *Journal of Shanghai Institute of Technology (Natural Science), 2*, pp.119-123 [online]. In Chinese. Available at: http://caod.oriprobe.com/articles/25690087/Integration_of_Multivariate_Functions_by_Orthogonal_Arrays.htm [Accessed: 20 January 2022].

Fang, K-T., Liu, M-Q., Qin, H. & Zhou, Y-D. 2018. *Theory and Application of Uniform Experimental Designs*. Beijing: Science Press & Singapore: Springer Nature. Available at: https://doi.org/10.1007/978-981-13-2041-5.

Fang, K-T. & Wang, Y. 1994. *Number-theoretic Methods in Statistics*. London, UK: Chapman & Hall. ISBN: 0-412-46520-5.

Hua, L-K. & Wang, Y. 1981. *Applications of Number Theory to Numerical Analysis*. Berlin; New York: Springer-Verlag & Beijing: Science Press. ISBN: 9783540103820.

Ju, S., Yang, X. & Liu, G. 2005. Application of elliptic integral calculus in computing magnetic induction intensity. *Journal of Changchun Institute of Technology (Natural Science Edition),* 6, pp.70-72 [online]. Available at: https://kns.cnki.net/kcms/detail/detail.aspx?dbcode=CJFD&dbname=CJFD2005&filename=CGCZ200504024&uniplatform=NZKPT&v=ryxpXwQqLAxChu6YS1miYma1Skh6baZ6482KF04E5VURFrx0iFF1b9u19uS2b7G2 (in Chinese) [Accessed: 15 January 2022].

Leobacher, G. & Pillichshammer, F. 2014. *Introduction to Quasi-Monte Carlo Integration and Applications.* Springer International Publishing Switzerland. Available at: https://doi.org/10.1007/978-3-319-03425-6.

Navidi, W. 2020. *Statistics for Engineers and Scientists, 5th* edition. New York: McGraw-Hill Education. ISBN: 9781260431025.

Paskov, S.H. 1996. New methodologies for valuing derivatives. In: Pliska, S. & Dempster, M. & (Eds.) *Mathematics of Derivative Securities,* pp.545-582*.* Cambridge: Isaac Newton Institute & Cambridge University Press. Available at: https://doi.org/10.7916/D8TB1FRJ.

Paskov, S.H. & Traub, J.F. 1995. Faster valuation of financial derivatives. *Journal of Portfolio Management* 22(1), pp.113-120. Available at: https://doi.org/10.3905/jpm.1995.409541.

Ripley, B.D. 1981. *Spatial Statistics.* Hoboken, NJ: John Wiley & Sons. ISBN: 0-47169116-X.

Sloan, I.H. & Woiniakowski, H. 1998. When Are Quasi-Monte Carlo Algorithms Efficient for High Dimensional Integrals?. *Journal of Complexity*, 14(1), pp.1-33. Available at: https://doi.org/10.1006/jcom.1997.0463.

Song, S. & Chen, S. 2004. Two Effective Quadrature Schemes for Calculating Double Integration. *Journal of Zhengzhou University*, 36, pp.16-19 [online]. Available at: https://kns.cnki.net/kcms/detail/detail.aspx?dbcode=CJFD&dbnam e=CJFD2004&filename=ZZDZ200401003&uniplatform=NZKPT & v=kCi42ClkKjv8yV3dacrXPRtdvn0JHnYAx3nBIo6p2qVlawH9fBMWaaiKoulEFMmf (in Chinese) [Accessed: 15 January 2022].

Tezuka, S. 1998. Financial applications of Monte Carlo and Quasi-Monte Carlo methods. In: Hellekalek, P. & Larcher, G.(Eds.) *Random and Quasi-Random Point Sets. Lecture Notes in Statistics,* 138*,* pp.303-332, New York: Springer. Available at: https://doi.org/10.1007/978-1-4612-1702-2_7.

Tezuka, S. 2002. Quasi-Monte Carlo - Discrepancy between theory and practice. In: Fang, K.T., Niederreiter, H. & Hickernell, F.J. (Eds.) *Monte Carlo and Quasi-Monte Carlo Methods 2000*, pp.124-140. Heidelberg: Springer-Verlag. Available at: https://doi.org/10.1007/978-3-642-56046-0_8.

ЭФФЕКТИВНЫЙ ПОДХОД К ВЫЧИСЛЕНИЮ ОПРЕДЕЛЕННОГО ИНТЕГРАЛА С ПРИМЕРНО ДЕСЯТЬЮ ТОЧКАМИ ВЫБОРКИ

Джи Йю[а], *Маошенг* Чжэн[б], **корреспондент**, Хайпэн Тен[б], *Йи* Вон[б]

Северо-западный политехнический университет,
г. Сиань, Народная Республика Китай

[а] факультет естественных наук

[б] факультет химической инженерии

РУБРИКА ГРНТИ: 27.47.00 Математическая кибернетика,
27.47.19 Исследование операций,
81.09.00 Материаловедение,
45.09.00 Электротехнические материалы

ВИД СТАТЬИ: оригинальная научная статья

Резюме:

Введение/цель: Приближенный подход к вычислению определенного интеграла всегда был привлекательной задачей с самого зарождения интегрального исчисления из-за практических потребностей в научных и инженерных областях. На практике в большинстве случаев подынтегральная функция бывает сложной, что затрудняет получение точного значения интегрирования, поэтому для практических целей достаточно найти приближенное значение определенного интеграла с некоторой точностью. В данной статье предлагается эффективный подход к вычислению определенного интеграла

при небольшом числе точек дискретизации, основанный на методе единого проектирования с точки зрения практического применения.

Методы: Распределение точек дискретизации в области изолированного пика является детерминированным и равномерным, что следует из правил методов единого проектирования и точек идеальной решетки.

Результаты: Эффективная оценка определенного интеграла периодической функции в области ее изолированного пика может быть получена при использовании 11 точек выборки в одном измерении, 17 точек выборки в двух измерениях и 19 точек выборки в трех измерениях.

Выводы: Разработанный эффективный подход к определенному интервалу на основе единых методов проектирования перспективен с точки зрения практического применения. Точки выборки детерминировано и равномерно распределены в соответствии с правилами методов единого проектирования и точек идеальной решетки. Эффективный подход, разработанный в данной статье, окажется полезным в соответствующих исследованиях и применении на практике.

Ключевые слова: единый метод проектирования, точки идеальной решетки, определенный интеграл, область с изолированным пиком, конечные точки выборки.

ЕФИКАСАН ПРИСТУП ИЗРАЧУНАВАЊУ ОДРЕЂЕНОГ ИНТЕГРАЛА СА ОКО ДЕСЕТАК ТАЧАКА УЗОРКОВАЊА

Ђе Ју[а], *Маошенг* Ценг[б], **аутор за преписку**, *Хаипенг* Тенг[б], *Ји Ванг*[б]

Универзитет Северозапад, Сијан, Народна Република Кина

[а] Факултет природних наука

[б] Факултет хемијског инжењерства

ОБЛАСТ: математика, материјали
ВРСТА ЧЛАНКА: оригинални научни рад

Сажетак:

Увод/циљ: Приближни приступ израчунавању одређеног интеграла представљао је проблем још од почетака интегралног рачуна због потреба у областима науке и инжењерства. У већини случајева у пракси, интегранд је сложен, што отежава добијање тачне вредности интеграције, тако да је, за практичне потребе, довољно наћи приближну вредност одређеног интеграла са извесном тачношћу. У овом раду предлаже се ефикасан приступ

Yu, J. et al, An efficient approach for calculating a definite integral with about a dozen of sampling points, pp.340-356

израчунавању одређеног интеграла с малим бројем тачака узорковања, заснован на методу униформног пројектовања са становишта практичне примене.

Методе: Дистрибуција тачака узорковања у подручју издвојеног врха је детерминистичка и униформна, што следи из правила метода униформног пројектовања и тачака добре решетке.

Резултати: Ефикасна процена одређеног интеграла за периодичну функцију у њеном подручју издвојеног врха може се добити помоћу 11 тачака узорковања у једној димензији, 17 тачака узорковања у две димензије и 19 тачака узорковања у три димензије.

Закључак: Ефикасан приступ одређеном интервалу, који је у раду развијен на основу метода униформног пројектовања, перспективан је са становишта практичне примене. Тачке узорковања су детерминистички и униформно распоређене у складу с правилима метода униформног пројектовања и тачака добре мреже. Ефикасан приступ биће од користи за релевантна истраживања и практичне примене.

Кључне речи: метод униформног пројектовања, тачке добре мреже, одређени интеграл, подручје издвојеног врха, тачке коначног узорковања.

Paper received on / Дата получения работы / Датум пријема чланка: 23.01.2022.
Manuscript corrections submitted on / Дата получения исправленной версии работы / Датум достављања исправки рукописа: 16.03.2022.
Paper accepted for publishing on / Дата окончательного согласования работы / Датум коначног прихватања чланка за објављивање: 18.03.2022.

HIGH SPEED TARGET TRACKING RADAR SYSTEM BASED ON THE USE OF BPSK SIGNAL AND DIGITAL DOPPLER SHIFT COMPENSATION

Zoran T. Golubičić[a], *Slobodan* M. Simić[b], *Aleksa* J. Zejak[c], *Boro* M. Reljić[d], *Svetislav* Marić[e]

[a] Peripolis elektronika, Belgrade, Republic of Serbia,
e-mail: golubicic.zoran@gmail.com,
ORCID iD: https://orcid.org/0000-0003-1698-7017

[b] University of Defence in Belgrade, Military Academy,
Department for MilitaryElectronic Systems,
Belgrade, Republic of Serbia,
e-mail: slobodan.simic@va.mod.gov.rs**, corresponding author**,
ORCID iD: https://orcid.org/0000-0002-6846-4886

[c] R&D Institute, RT-RK Computer based systems,
Novi Sad, Republic of Serbia,
e-mail: aleksa.zejak@rt-rk.com,
ORCID iD: https://orcid.org/0000-0001-5114-2867

[d] R&D Institute, RT-RK Computer based systems,
Novi Sad, Republic of Serbia,
e-mail: boro.reljic@gmail.com,
ORCID iD: https://orcid.org/0000-0002-7660-9854

[e] University of California San Diego, Division of Extended Studies,
La Jolla, CA, USA,
e-mail: smaric@ucsd.edu,
ORCID iD: https://orcid.org/0000-0001-5705-9124

DOI: 10.5937/vojtehg70-36589; https://doi.org/10.5937/vojtehg70-36589

FIELD: Electronics, Telecommunications, Radar technology
ARTICLE TYPE: Original scientific paper

Abstract:

Introduction/purpose: This paper presents a model of a high speed target radar tracking system that is much simpler than the existing ones. The Doppler shift is compensated before signal compression, simultaneously with the modification of the clock signal in the compression filter. This is possible thanks to the development of FPGA technology. The most important for this application are very fast clock control units which enable operation with different frequency references up to 1 GHz with an accuracy far below 1 Hz.

Methods: In this paper, the methodology of mathematical modeling and simulation is used.

Results:The results of the analysis of the most important effects in radars caused by high-speed targets are presented and discussed - target migration through resolution cells and compression filter response distortion due to high target acceleration.

Conclusion: Thanks to flexible RF and signal processing hardware, complex radar processing procedures are not required. The sensitivity of the BPSK signal to the Doppler shift (which is usually considered a disadvantage) can be used to reject targets at a slightly different rate. This system can be used in space debris tracking, airspace target tracking, car driving, etc.

Key words: target migration, FPGA, DDS.

Introduction

High speed target detection and tracking present a serious problem for classical radar systems. A high speed target generates a high Doppler frequency shift in the receiving signal. High Doppler frequency can generate significant losses in the radar compression filter even if the signal with reduced sensitivity to the Doppler shift is applied. A well-known problem is “stop and go”, when a target passes a few range resolution cells during the pulse time. This problem is frequently analyzed in the synthetic-aperture radar (SAR) processing (Tang et al, 2019). The problem is typical for radars operating with very long pulses such as space debris radars (NASA-Handbook 8719.14, 2008). Even if a radar system operates with high radio frequency (RF) power and short pulses, there is a problem with target migration from one pulse to another. These problems are usually resolved by complex radar processing employing banks of matching filters and alignment algorithms (Addabbo et al, 2019; Yang et al, 2017). Complexity in the detection process could be increased by significant target acceleration. It increases the required number of filters in the filter bank and increases the complexity of iterative algorithms. In the case of surveillance radars, such a complex procedure is unavoidable. But, in the case of the tracking radar, the processing method could be adjusted according to the tracked target type. Usually, targets with high velocity have no high acceleration and vice versa. This is the consequence of the target inertial limitations. For example, space targets have high velocity but low acceleration, and drones can have low velocity but high radial acceleration. It means that signal processing in tracking radars could be significantly simplified by adjusting a processing method to a particular target. In this paper, a simple processing method for high speed target tracking is highlighted. In order to obtain enough signal-to-noise ratio (SNR) with limited RF power, a target has to be illuminated long time which

causes high target migration during the dwell period. Examples related to space debris radars will support the method applicability (Klinkrad, 2006; Losacco & Schirru, 2019).

The application of matching filter banks or complex iterative algorithms is suitable for off line signal processing. Otherwise, extremely high power numeric processing machines are required. The proposed simplification is applicable not only for space control radars (which are a representative example in this paper) but also for other radars utilizing long pulses. The examples are high resolution radars for autonomous vehicle guidance (when two close vehicles have to be separated by different speed) or military purpose (when a plane has to be separated from a lunched missile). All these systems require real time signal processing with reasonable hardware resources. Sometimes, problems with high Doppler frequency do not have origin only in high speed but in high frequency (millimeter wave radar for autonomous navigation) and wide bandwidth (required high resolution in the slant range). Independently of the origin, high Doppler frequency and wide bandwidth cause the received signal compression and target migration problems that should be resolved in real time.

A common tracking radar employs linear frequency modulated (LFM) signals. An LFM signal is known as a Doppler resistive signal. But, this signal is also sensitive to “stop and go” effects and a compression filter should be based on the bank of matching filters. However, the binary phase shift keying (BPSK) modulation is known as the Doppler sensitive modulation and requires a high number of matching filters inside the filter bank. In the case of the tracking radar, the velocity of the target is known (with some uncertainty) and the advantage of the LFM modulation is not significant. On the other hand, the BPSK matching filter structures intended for wideband signals are significantly simpler (than the LFM matching filter) because they do not need hardware multipliers. In the case of the tracking radar, the BPSK Doppler sensitivity should be exploited for non-tracked target rejection. In the next section, a fast target tracking method based on the BPSK radar signal is presented. Critical Doppler uncertainty is simply resolved by using target speed measurement and appropriate signal processing techniques avoiding requirements for the filter bank.

Proposed radar configuration

A simplified block schematic of the proposed tracking radar is presented in Fig. 1. A radar signal is digitally generated at the low intermediate frequency (IF) frequency and up-converted by two fixed local oscillators(LO) to the output frequency. The input signal is down-converted

by the same LO to the low IF frequency that is similar to the frequency of the digitally generated Tx signal. The difference is in the Doppler shift.

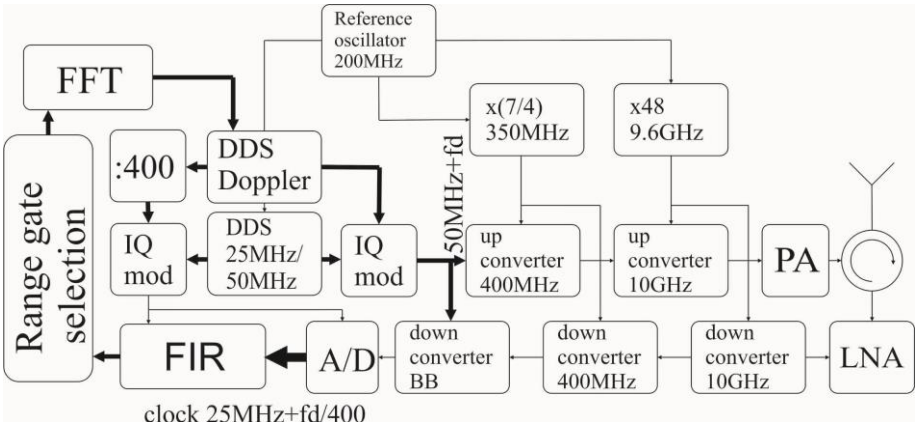

Figure 1 – Simplified block schematic of the tracking radar
Рис. 1 – Упрощенная блок-схема РЛС слежения
Слика 1 – Упрошћена блок-шема радара за праћење

This signal is down-converted to baseband (BB) by the LO signal generated by the direct digital synthesis (DDS). The frequency of this signal corresponds to the IF frequency of the receiving signals i.e. the baseband signal has no Doppler component. The baseband signal without a Doppler component is compressed by the standard finite impulse response (FIR) filter. Because the complete signal spectrum suffers from the high Doppler shifting, the bit rate in the BPSK signal is changed. For that reason, the FIR filter clock has to be modified. In the Rx mode, the DDS has to generate a new clock with the offset respectively to the Tx signal bit rate:

$$f_{clk}^{offset} = f_{doppler} * \left(\frac{f_{clktx}}{f_o}\right) \quad (1)$$

where $f_{doppler}$ is the measured Doppler frequency, f_o is the output central frequency, and f_{clktx} is the generated chip rate. This offset has to compensate for pulse stretching or extension caused by the Doppler effects.

Knowing the Doppler shift at the central frequency, the target velocity could be estimated with high accuracy. Knowing the target velocity, a prediction of the target migration could be performed. This prediction enables a right selection of the pulses participating in the coherent signal

integration. So, the key parameter that has to be measured is the target radial velocity.

Although this architecture seems simple, there are a few reasons why it is not widely applied in practice. The digital generation of wideband radar signals at IF frequency was limited by the FPGA (Field programmable Gate Array) maximum clock and the FPGA numeric capacity. The DDS were usually realized as separate devices with limitation in the configuration speed. It was limited by the accumulator word length and the frequency resolution. The FPGA clocks were limited by the one clock manager circuit. New FPGA circuits operate with clocks up to 1GHz permitting different references to difference clock manager, simultaneously achieving an accuracy that is far below 1 Hz. Doppler shifts can be compensated before signal compression, simultaneously with compression filter clock modifications. In this way, methods utilizing filter banks and signal oversampling (few tenths of time) are avoided.

Signal processing is divided in two consecutive phases. The first phase is velocity determination. After that, the down converter and the filter matched to the Rx sequence will be configured in real time and target migration from pulse to pulse will be determined. In accordance with the calculated values, a coherent or non-coherent integration process could be performed.

Velocity (Doppler) measurement

The first phase in the tracking process has to be target velocity measurement (this measurement should be performed simultaneously with angular measurement and tracking). For this measurement, the radar should transmit and receive non modulated pulses. The received signal should be sampled and the FFT (Fast Fourier Transform) of the received signal should be performed. Because the pulse is long in time, the main part of energy should be concentrated around the Doppler frequency. A component from the pulse modulation will be present, but the energy of these components should be below the carrier component. A simple frequency analysis can highlight the carrier (Doppler) frequency. The dwell time has the main influence on the precision of the frequency measurement.

The resolution of the Doppler frequency Δf can be determined as:

$$\Delta f = \frac{1}{\tau_{ill}} \Rightarrow \Delta v = \frac{c*\Delta f}{2f_0} = \frac{c}{2f_0\tau_{ill}} = \frac{\lambda_0}{2\tau_{ill}} \quad (2)$$

where τ_{ill}presents the target illumination time (dwell time), Δv is the velocity resolution, c is the speed of the light and λ_0 is the transmission signal wavelength. If the number of pulses during the dwell time is N, the maximum uncertainty in the target position should be:

$$\Delta l = N * PRI * \Delta v = N * PRI * \frac{\lambda_0}{2\tau_{ill}} \quad (3)$$

where PRI is the pulse repetition interval. If Δr is the range resolution, then:

$$\Delta l \ll \Delta r \quad (4)$$

As an example, a space debris radar with 10ms long pulse and 6m range resolution cell integrates 32 pulses with the PRI of 25ms (duty factor 40%). It means that the dwell time is 0.8s. The frequency resolution is 1.25Hz. The velocity uncertainty for a 10GHz radar should be 0.019m/s. The uncertainty in the target position for the dwell time should be 15cm. Since the received signal is a pulse amplitude modulation (PAM) signal, the obtained spectrum will have components at both sides of the carrier signal. The carrier peak presents the received Doppler frequency and the frequency of the other component depends on the PRI and the pulse time. An example of the spectrum of the 400kHz Doppler shift is presented in Fig. 2 (left).

The diagram in Fig. 2 (right) presents a zoomed part of the full span when components at 40Hz (25ms PRI) exist. The highest component presents the carrier (Doppler) frequency. The presented spectrums are without noise. In practice, the noise floor minimum 20dB below the maximum components is desirable.

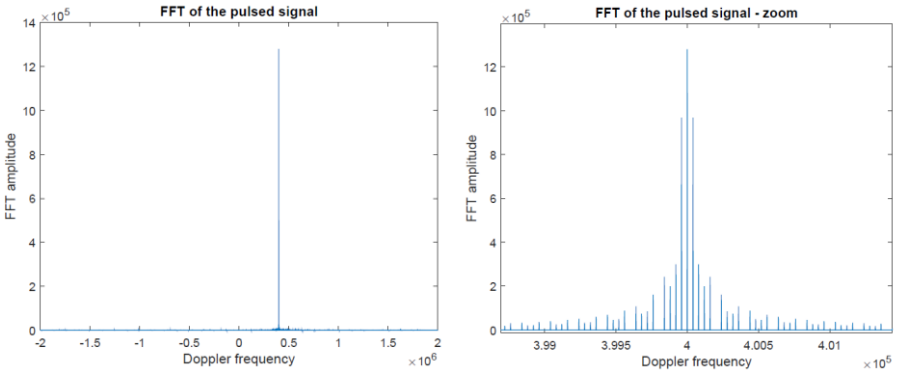

Figure 2 – Spectrum of the pulsed signal modulated with the Doppler frequency
Рис. 2 – Спектр импульсного сигнала, модулированного доплеровской частотой
Слика 2 – Спектар импулсног сигнала модулисаног Доплеровом фреквенцијом

Matching filter configuration

Knowing the target speed, the LO frequency and the compression FIR filter clock should be adjusted in accordance with the Doppler shift. The DDS generating the measured Doppler frequency can modulate (shift) the LO carrier. The chip frequency is always generated as a fraction of the LO carrier frequency i.e. this frequency will be shifted for the carrier frequency shift divided by a constant fraction. Knowing the Doppler frequency f_d, and knowing the ratio between the carrier frequency and the chip frequency, a new chip frequency (the FIR filter clock) can be calculated as:

$$f'_{chip} = \frac{f_0 + f_d}{\frac{f_0}{f_{chip}}} \quad T'_{chip} = \frac{1}{f'_{chip}} \tag{5}$$

where f_{chip} is the frequency of the PN chip clock in the Tx signal and f'_{chip} is the frequency of the PN chip clock in the Rx signal. It means that the FIR filter has to change the clock frequency in accordance with the relation given above. For example, if the carrier frequency is 10GHz, and the symbol frequency is 25MHz, the symbol frequency presents the 1/400th part of the carrier frequency i.e. the symbol frequency is generated by the carrier frequency divider 1:400. If the carrier shift is 400kHz, the symbol rate is changed 1 kHz. It means that if the LO frequency of the DDS is shifted from 50MHz to 5040kHz, the symbol frequency will be shifted from 25000kHz to 25001kHz. A new symbol frequency is the frequency fed to AD converters and FIR filters. Other processing parts of the matching filter are the simplified FIR filters (Golubičić et al, 2013; Simić et al, 2013) easily incorporated in the low-cost FPGA circuits. A simplified schematic is presented in Fig. 3. It is clear that the filter has a simple structure without hardware multipliers. During 10ms, 250000 chips of 40ns will be compressed by the FIR filter.

Fig. 4 (left) presents the FIR filter response when the filter is perfectly matched to the receiving signal Doppler frequency. Fig. 4 (right) shows how the filter response drops when it is non-matched to the Doppler shift. According to the diagrams, the filter has to be matched to the Doppler frequency with the range of ±10Hz.

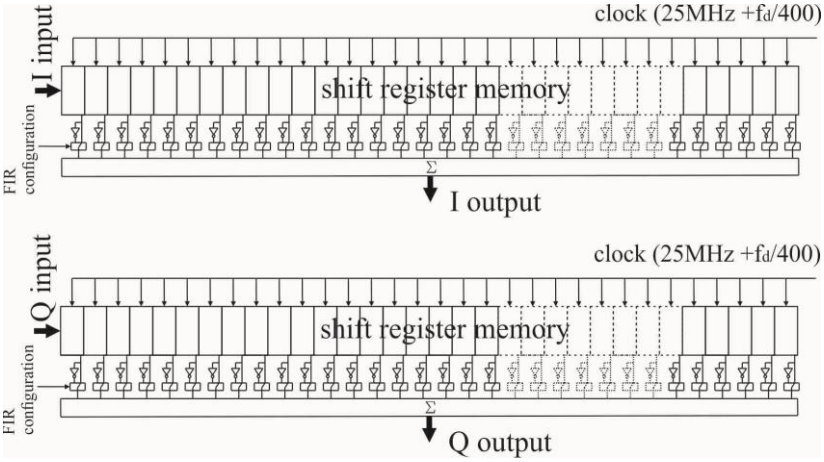

Figure 3 – Simplified schematic of the BPSK compression filter
Рис. 3 – Упрощенная схема фильтра сжатия BPSK
Слика 3 – Упрошћена шема BPSK компресионог филтера

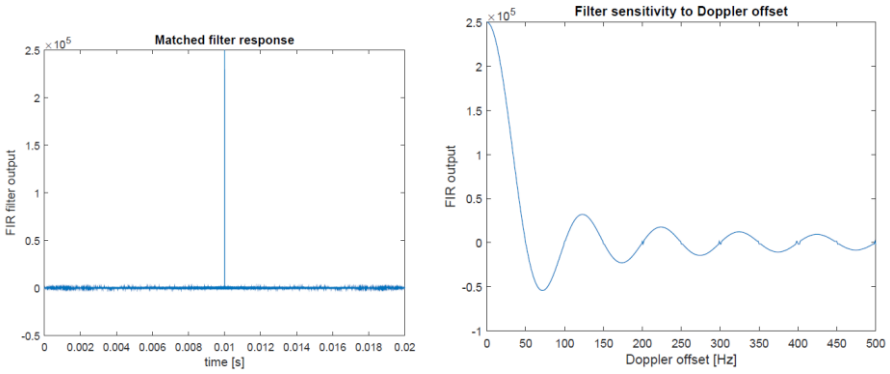

Figure 4 – Matching filter characteristics
Рис. 4 – Характеристики согласованного фильтра
Слика 4 – Карактеристике прилагођеног филтера

Main effects of high speed targets on the radar tracking system

Due to high target speed, the range between the radar and a target varies during the coherent processing interval (CPI). Because of that variation in the range, not all the echo signals from the target appear in the same range cell. This is called target migration through range cells. Equally, a high acceleration of the target causes that the Doppler frequency is also spread over multiple cells and this is called the Doppler cell migration.

Effect of target migration

The problem of target migration is presented in Fig. 5. Because the velocity of the target is high, the distance between the target and the radar should be different from one pulse to another. In that case, the pulses from the same range gates could not be used in the integration process. The solutions for this problem were usually analyzed for the LFM radars operation (Li et al, 2009).

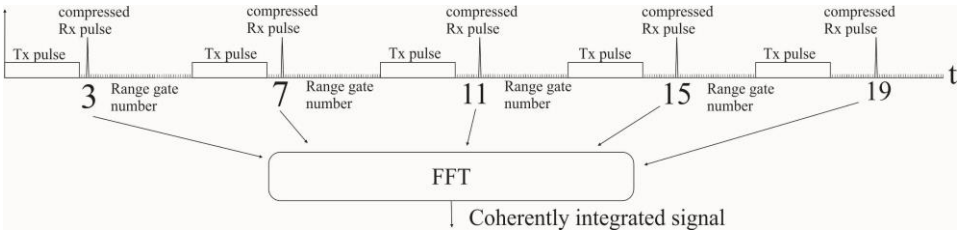

Figure 5 – Target migration between pulses
Рис. 5 – Миграция цели между импульсами
Слика 5 – Миграција циља између импулса

This radar has a problem with the range gate coupling and cannot exploit velocity knowledge. In the proposed method, this is not the case. The range gate of the returned signal (from one target) will be changed from one pulse to another. As a consequence, signals from different range cells have to be included in the integration process. The selection of the range gates that participate in one integration process is determined by the target velocity. When the target velocity is known, the migration of the target from one pulse to another could be predicted.

$$\Delta_{lp} = v * PRI \qquad \Delta_{lp}^2 = \Delta_v * PRI \tag{6}$$

where *v* is the target speed, Δ_{lp} is the difference in the distance between the radar and the target in successive pulse repetition intervals, $\Delta_v$is the uncertainty of the target speed, and Δ_{lp}^2 is the uncertainty of the target position. For example, the target migration between pulses with the target speed of up to 8000m/s and the PRI of 25ms could be between 0m and 200m i.e. between 0 and 34 range gates. The uncertainty in the position between two pulses (if Δv is 0.019m/s) could be 0.5mm. It means that a prediction of the target migration could be very accurate. The uncertainty in the target position during the dwell time of 0.8s is 15cm. Since the uncertainty of the velocity, compared with the range resolution cell, is low, a prediction of the range gate migration should be simple. Theoretically, there is a possibility that the migration distance coincide with the integer

number of the range cell distance. In that case, it is not clear which range cell contains the target. But, because this point is predictable, two series of range cells can be formed. The sum or the FFT should be performed over both pulse series.

The number of the range cells that has to participate in the FFT calculation should be found as

$$N = floor\left(v * PRI * \frac{n}{\Delta r}\right) \tag{7}$$

where *n* is the number of the Tx pulses and *Δr* is the range resolution. Taking into account the maximum and minimum velocity, different *N* vectors could be established, providing all possible range cell combinations. Fig. 6 illustrates target migrations through the range cells, starting from the first two range cells. The linear lines present possible target velocities. It is clear that, for the second range cell, there is ambiguity at the 8th Tx pulse, and it is necessary to integrate this pulse with two different sets.

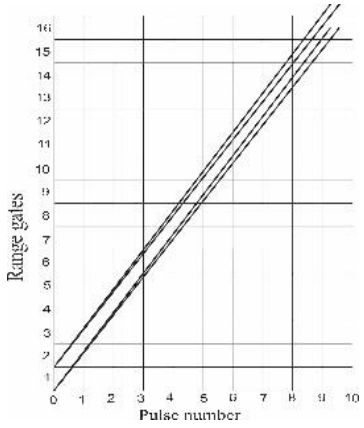

Figure 6– Target migrations through the range cells
Рис. 6 – Миграция цели по ячейкам диапазона
Слика 6 – Миграција циља кроз резолуционе ћелије

Acceleration effect

In theory, target velocity is not always constant. Because of that, a compression filter is not always matched to target velocity. But, in practice, the correlation function is not sensitive to real acceleration values, as it is shown in Fig. 7 that presents the correlation function for the (non-matched) Doppler velocity up to ±200Hz and the acceleration of ±200Hz/s^2. For the 10GHz radar, it corresponds to the realistic velocity of ±5m/s and the acceleration of ±5m/s^2 when a 10ms pulse is applied (Murray et al, 2019).

But, at very high accelerations, significant distortion in the response of the compression filter is evident. Fig. 8 presents the FIR filter outputs for target accelerations up to 500m/s^2 (±360Hz/s^2). In that case, the matching filter has to include acceleration (even the third order phase function) (Jin et al, 2019; Chen et al, 2019).

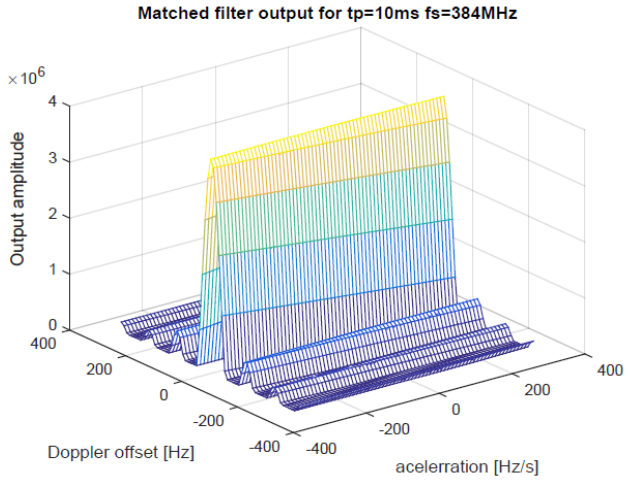

Figure 7– FIR filter outputs for different velocities and accelerations
Рис. 7 – Выход КИХ-фильтра при различных скоростях и ускорении
Слика 7 – Излаз из FIR филтера при различитим брзинама и убрзањима

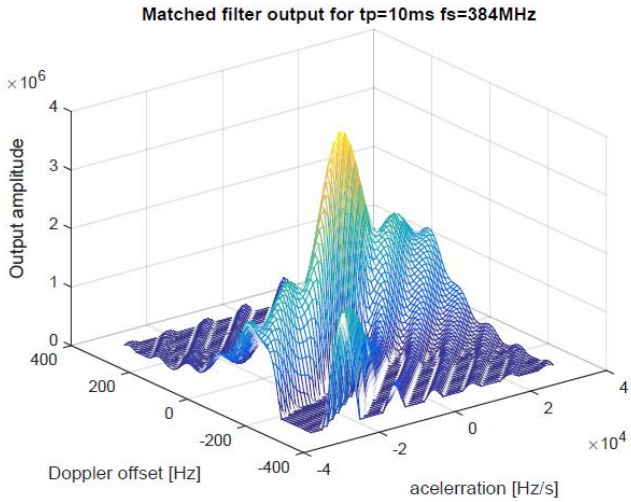

Figure 8– FIR filter outputs for different velocities and high accelerations
Рис. 8 – Выход КИХ-фильтра при различных скоростях и сильном ускорении
Слика 8 – Излаз из FIR филтера при различитим брзинама и великим убрзањима

Conclusion

Thanks to the flexible RF and processing hardware, the tracking radar does not need complex processing procedures with unknown target positions and velocities. Radars operating with long pulses (in order to compress high energy) can measure target speeds and positions alternatively employing the obtained data from one measurement to facilitate the other. The sensitivity of the BPSK signals to the Doppler shift (usually mentioned as a disadvantage) could be used for the rejection of targets with slightly different velocity. This system can find application in space debris tracking, aerial target tracking, automotive car driving, etc.

References

Addabbo, P., Orlando, D. & Ricci, G. 2019. Adaptive Radar Detection of Dim Moving Targets in Presence of Range Migration. *IEEE Signal Processing Letters*, 26(10), pp.1461-1465. Available at: https://doi.org/10.1109/LSP.2019.2936650.

Chen, J., Jin, K., Yu, S., Lai, T. & Zhao, Y. 2019. Radar Coherent Detection for Maneuvering Target Based on Product-Scaled Integrated Cubic Phase Function. *International Journal of Antennas and Propagation*, 2019(art.ID:8691903). Available at: https://doi.org/10.1155/2019/8691903.

Golubičić, Z., Simić, S. & Zejak, A.J. 2013. Design and FPGA implementation of digital pulse compression for band-pass radar signals. *Journal of Electrical Engineering*, 64(3), pp.191-195. Available at: https://doi.org/10.2478/jee-2013-0028.

Jin, K., Lai, T., Wang, Y., Li, G. & Zhao, Y. 2019. Coherent Integration for Radar High-Speed Maneuvering Target Based on Frequency-Domain Second-Order Phase Difference. *MDPI electronics*, 8(3), art.ID:287. Available at: https://doi.org/10.3390/electronics8030287.

Klinkrad, H. 2006. The Current Space Debris Environment and its Sources. In: *Space Debris. Springer Praxis Books.*Berlin, Heidelberg:Springer. Available at: https://doi.org/10.1007/3-540-37674-7_2. ISBN: 978-3-540-37674-3.

Li, J., Liu, H. & He, Z-S. 2009. A practical method for range migration compensation in chirp radar. *Progress In Electromagnetics Research M*, 7, pp.15-28. Available at: https://doi.org/10.2528/PIERM09022302.

Losacco, M. & Schirru, L. 2019. Orbit Determination of Resident Space Objects Using the P-Band Mono-Beam Receiver of the Sardinia Radio Telescope. *Applied Science*, 9(19), art.ID:4092. Available at: https://doi.org/10.3390/app9194092.

Murray, J., Miller, R., Matney, M. & Kennedy, T. 2019. Orbital Debris Radar Measurements from the Haystack Ultra-wideband Satellite Imaging Radar (HUSIR): 2014-2017. In: *International Orbital Debris Conference (IOC)*, Sugar Land, TX, Document ID:20190033902, Patent Number:IOC6133, December 9-12 [online]. Availble at: https://ntrs.nasa.gov/citations/20190033902 [Accessed: 20 February 2022].

-NASA-Handbook 8719.14. 2008. *Handbookfor limiting orbital debris*. Washington, DC: NASA-Handbook [online]. Availble at: https://explorers.larc.nasa.gov/APMIDEX2016/MO/pdf_files/NHBK871914.pdf[Accessed: 20 February 2022].

Simić, S., Zejak, A.J. & Golubičić, Z. 2013. Hardware implementation of DIRLS mismatched compressor applied to a pulse-Doppler radar system. *Microprocessors and Microsystems*, 37(4-5), pp.381-393. Available at: https://doi.org/10.1016/J.MICPRO.2013.04.001.

Tang, S., Guo, P., Zhang, L. & Lin, C. 2019. Modelling and Precise Processing for Spaceborne Transmitter/Missile-Borne Receiver SAR Signals. *Remote Sensing*, 11(3), art.ID:346. Available at: https://doi.org/10.3390/rs11030346.

Yang, S., Li, Y., Zhang, K. & Liu, J. 2017. A Signal Processing Algorithm Based on 2D Matched Filtering for SSAR. *Mathematical Problems in Engineering*, 2017(art.ID:4047983). Available at: https://doi.org/10.1155/2017/4047983.

РАДИОЛОКАЦИОННАЯ СИСТЕМА СЛЕЖЕНИЯ ЗА ВЫСОКОСКОРОСТНЫМИ ЦЕЛЯМИ, ОСНОВАННАЯ НА ИСПОЛЬЗОВАНИИ СИГНАЛА BPSK И ЦИФРОВОЙ КОМПЕНСАЦИИ ДОПЛЕРОВСКОГО СДВИГА

Зоран Т. Голубичич[а], *Слободан* М. Симич[б],
Алекса Й. Зеяк[в], *Боро* М. Реич[в], *Светислав* Марич[г]

[а] Периполис электроника, г. Белград, Республика Сербия

[б] Университет обороны в г. Белград, Военная академия, департамент военного электронного инжиниринга, г. Белград, Республика Сербия, **корреспондент**

[в] Институт РТ-РК, г. Нови-Сад, Республика Сербия

[г] Калифорнийский университет в Сан-Диего, отделение расширенных исследований, г. Ла-Хойя, Калифорния, Соединенный Штаты Америки

РУБРИКА ГРНТИ: 47.49.29 Радиолокационные системы, станции,
78.25.16 Вооружение и техника ракетных войск,
78.25.17 Вооружение и техника войск ПВО

ВИД СТАТЬИ: оригинальная научная статья

Резюме:

Введение/цель: В данной статье представлена модель радиолокационной системы слежения за высокоскоростными целями, которая намного проще существующих. Доплеровский сдвиг компенсируется перед сжатием сигнала одновременно с модификацией тактового сигнала в компрессионном фильтре. Это стало возможным благодаря развитию технологии FPGA. Важнейшими факторами в ее применении являются сверхбыстрые блоки управления тактовой частотой, которые

позволяют работать с различными опорными частотами до 1 ГГц, с точностью намного ниже 1 Гц.

Методы: В данной статье используется методология математического моделирования и ситуационного моделирования.

Результаты: В статье представлены и обсуждены результаты анализа наиболее важных радиолокационных приемов, касающихся высокоскоростных целей и миграции цели через ячейки разрешения и искажения отклика фильтра сжатия вследствие сильного ускорения цели.

Выводы: Благодаря гибкому оборудованию радиочастотной обработки и обработки сигналов нет необхдимости в сложных процедурах обработки радиолокационных данных. Чувствительность сигнала BPSK к доплеровскому сдвигу (что обычно считается недостатком) может быть использована для отклонения целей с отличающейся скоростью. Данная система может быть использована при отслеживании космического мусора, слежении за целями в воздушном пространстве, управлении транспортным средством и пр.

Ключевые слова: миграция цели, FPGA, DDS.

РАДАРСКИ СИСТЕМ ЗА ПРАЋЕЊЕ ЦИЉЕВА ВЕЛИКИХ БРЗИНА ЗАСНОВАН НА УПОТРЕБИ BPSK СИГНАЛА И ДИГИТАЛНОЈ КОМПЕНЗАЦИЈИ ДОПЛЕРОВОГ ПОМАКА

Зоран Т. Голубичић[а], *Слободан* М. Симић[б],
Алекса Ј. Зејак[в], *Боро* М. Рељић[в], *Светислав* Марић[г]

[а] Периполис електроника, Београд, Република Србија

[б] Универзитет одбране у Београду, Војна академија, Катедра војноелектронског инжењерства, Београд, Република Србија, **аутор за преписку**

[в] Институт РТ-РК, Нови Сад, Република Србија

[г] Калифорнијски универзитет у Сан Дијегу, Одсек за проширене студије, Калифорнија, Ла Хоја, Сједињене Америчке Државе

ОБЛАСТ: електроника, телекомуникације, радарска техника
ВРСТА ЧЛАНКА: оригинални научни рад

Сажетак:

Увод/циљ: У овом раду представљен је модел радарског система за праћење циља велике брзине који је знатно једноставнији од постојећих. Доплеров помак се компензује пре компресије сигнала, истовремено с модификацијом сигнала такта у компресионом

филтеру. То је могуће захваљујући развоју FPGA технологије. За ову примену најважнији су веома брзи блокови за контролу такта, који омогућују рад с различитим референцама фреквенција до 1 GHz, са тачношћу много испод 1 Hz.

Методе: Коришћена је методологија математичког моделирања и симулација.

Резултати: Представљени су и разматрани резултати анализе најважнијих ефеката у радарима које изазивају циљеви великих брзина – миграција циља кроз резолуционе ћелије и изобличење одзива компресионог филтера услед великих убрзања циља.

Закључак: Захваљујући флексибилном RF и хардверу за обраду сигнала, радару за праћење нису потребне сложене процедуре обраде. Осетљивост BPSK сигнала на Доплеров помак (обично се помиње као недостатак) може се искористити за одбацивање циљева с мало другачијом брзином. Овај систем може наћи примену у праћењу свемирског отпада, циљева у ваздушном простору, при вожњи аутомобила итд.

Кључне речи: миграција циља, FPGA, DDS.

Paper received on / Дата получения работы / Датум пријема чланка: 22.02.2022.
Manuscript corrections submitted on / Дата получения исправленной версии работы / Датум достављања исправки рукописа: 18.03.2022.
Paper accepted for publishing on / Дата окончательного согласования работы / Датум коначног прихватања чланка за објављивање: 20.03.2022.

A PILOT COMPARATIVE ANALYSIS OF THE CUCKOO AND DRAKVUF SANDBOXES: AN END-USER PERSPECTIVE

Slaviša Ž. Ilić[a], *Milan* J. Gnjatović[b], *Brankica* M. Popović[c], *Nemanja* D. Maček[d],

[a] Ministry of Defense of the Republic of Serbia, Belgrade, Republic of Serbia, e-mail: slavisa.ilic@mod.gov.rs, **corresponding author**, ORCID iD: https://orcid.org/0000-0003-3314-5794

[b] University of Criminal Investigation and Police Studies, Belgrade, Republic of Serbia, e-mail: milan.gnjatovic@kpu.edu.rs, ORCID iD: https://orcid.org/0000-0002-0343-7596

[c] University of Criminal Investigation and Police Studies, Belgrade, Republic of Serbia, e-mail: brankica.popovic@kpu.edu.rs, ORCID iD: https://orcid.org/0000-0002-8276-1481

[d] School of Electrical and Computer Engineering, Academy of Technical and Art Applied Studies, Belgrade, Republic of Serbia, e-mail: nmacek@viser.edu.rs, ORCID iD: https://orcid.org/0000-0002-3465-7524

DOI: 10.5937/vojtehg70-36196; https://doi.org/10.5937/vojtehg70-36196

FIELD: Computer sciences, IT, Cyber security
ARTICLE TYPE: Original scientific paper

Abstract:

Introduction/purpose: This paper reports on a pilot comparative analysis of the Cuckoo and Drakvuf sandboxes. These sandboxes are selected as the subjects of the analysis because of their popularity in the professional community and their complementary approaches to analyzing malware behavior.

Methods: Both sandboxes were set up with basic configurations and confronted with the same set of malware samples. The evaluation was primarily conducted with respect to the question of to what extent a sandbox is helpful to the human analyst in malware analysis. Thus, only the information available in Web console reports was considered.

Results: Drakvuf is expected to perform better when confronted with evasive malware and so-called "file-less" malware. Although still not mature in terms of integration, customization and tools, this sandbox is considered

a second generation sandbox because of its agentless design. On the other hand, the Cuckoo sandbox creates a better overall experience: it is supported through good documentation and strong professional community, better integrated with various tools, support more virtualization, operating system and sample types, and generates more informative reports. Even with a smaller capacity to prevent evasive malware, its Python 2 agent script makes it more powerful than Drakvuf.

Conclusion: To achieve the optimal open-source sandbox-based protection, it is recommended to apply both the Cuckoo and Drakvuf sandboxes. In circumstances of limited resources, applying the Cuckoo sandbox is preferable, especially if exposure to malware deploying evading techniques is not frequently expected.

Key words: Sandbox, Cuckoo, Drakvuf, Malware behavior analysis.

Introduction

The number of malware attacks has recently increased significantly (e.g., it has been doubled in the period between 2015 and 2019 (Melvin & Kathrine, 2020) and the average time needed to detect a data breach is considerable (e.g., in 2020 it took 203 days in average), (IBM, 2020). The identification of highly sophisticated, target specific and stealthy operated cyber threats is a challenging task, because of their underlying characteristics such as encrypted covert communication, sophisticated attack techniques, continuous monitoring and control of victim's resources, wiping or masking the traces, etc. (Chakkaravarthy et al, 2019)

Due to the complexity and severity of advanced cyber threats, defenders of valuable assets aim at discovering threats before they get in a defensive perimeter. In line with this aim, this paper provides a pilot comparative analysis of two open-source and the most frequently used sandbox solutions: Cuckoo and Drakvuf.

Sandboxes and the experimental environment

A cybersecurity sandbox is a physical or virtual environment used to execute suspicious file samples or run programs without interfering with a monitoring system or permanently affecting a device they are running on (Arntz, 2020; Chakkaravarthy et al, 2019). The sandboxing is used to detect potentially malicious codes and applications before serving them up to critical devices (Arntz, 2020). The detection is based on malware behavior analysis, which may be roughly described by an analogy to biometric behavioral description (Tot et al, 2021).

A sandbox usually consists of a management part and virtual machines (VMs) which represent victim hosts. VMs are typically configured similarly to virtual and physical computers in a given organization in order to mimic the production environment which is being protected from malware attacks. When suspected files are executed in these VMs, it is possible to monitor their behavior and react before they occur in a production environment.

The Cuckoo and Drakvuf sandboxes are selected as the subjects of the analysis in this study because of their popularity in the professional community and their complementary approaches to analyzing malware behavior. Cuckoo uses a Python script-shaped agent in the analysis VM, while Drakvuf applies an agentless approach. The network architecture adopted in the reported study is shown in Figure 1.

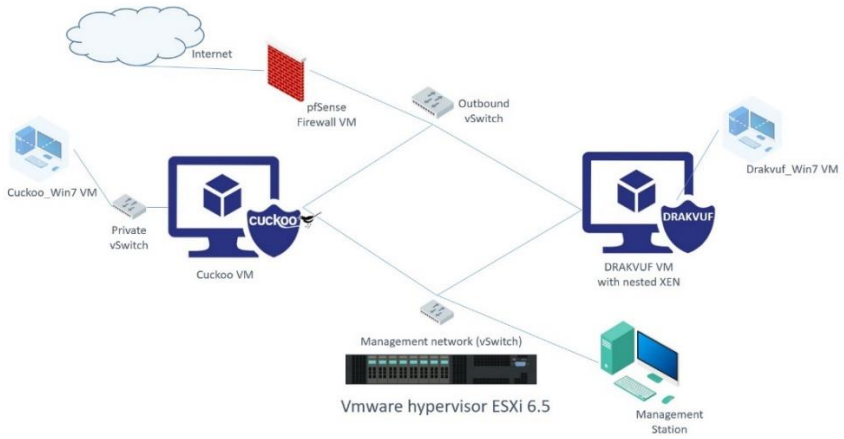

Figure 1 – ESXi network architecture with Cuckoo and Drakvuf virtual machines
Рис. 1 – Сетевая архитектура ESXi с виртуальными машинами Cuckoo и Drakvuf
Слика 1 –Мрежна архитектура ESXi са виртуелним машинама Куку и Дракеуф

Both sandbox environments can be accessed from the management network for the purposes of configuration and submission of samples for analysis through a Web interface. The characteristics of individual VMs are provided in Table1.

It is usual for Cuckoo and DRAKVUF to be installed on bare-metal (or in VM) and to have analysis VMs nested (i.e., Type 2 virtualization). In this study, we applied a different approach for Cuckoo since it supports VMware ESXi API calls. The ESXi communication with VMs allows for a more configurable environment and a more comprehensive analysis (e.g., by taking a snapshot and applying additional tools outside a sandbox

environment). In contrast, this approach is not feasible for Drakvuf, so the nested Xen virtualization is applied as the underlying hypervisor.

Table 1 – Virtual machines characteristics (operating system types, virtualization types and basic configuration)
Таблица 1 – Характеристики виртуальных машин (типы операционных систем, виды виртуализации и базовая конфигурация)
Табела 1 – Карактеристике виртуалних машина (типови оперативних система, типови виртуализације и основна конфигурација)

VM name	OS	Virt.	Basic configuration
Cuckoo	Ubuntu 18.04	ESXi	Version 2.05
Cuckoo_Win7	Windows7, 32-bit	ESXi	Office 2007, UAC and AV disabled
DRAKVUF	Ubuntu 20.04	ESXi	Version 0.18
Drakvuf_Win7	Windows7, 32-bit	Xen	Office 2007, UAC and AV disabled
pfSense	FreeBSD	ESXi	Open-source firewall

The pfSense firewall is configured in front of the whole environment in order to:

- prevent any traffic from leaving the experimental environment,
- provide additional real-time monitoring of network connections induced by the analyzed samples, and
- allow for keeping track of the sandbox-based traffic analysis across time.

A basic insight into the design of the sandboxes is provided below.

Cuckoo

The Cuckoo sandbox allows for dynamic detecting of runtime behaviors in an isolated environment, i.e. a virtual machine (including API calls, network traffic, files dropped, etc.) by the use of signatures, written as Python 2 scripts, that detect a broad range of malware, from a simple key logger to a more complicated execution of a process that has an injected code.

The malware detection is achieved via cuckoomon.dll, a dynamic link library injected into a process that allows for run-time logging of its behavior manifestations, which are then reported back to the main Cuckoo sandbox process.

Cuckoo may be integrated with local email solutions and intrusion prevention systems to identify ransomware and other potentially malicious entities, and to prevent potential breaches and data loss.

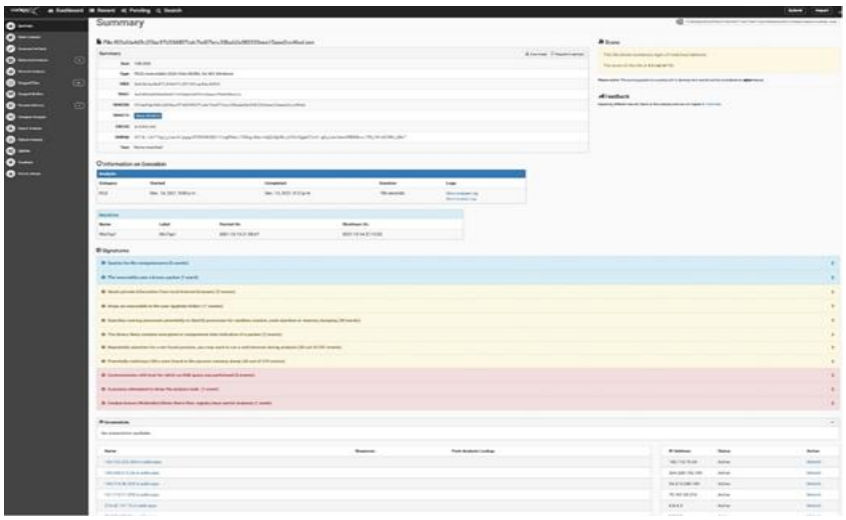

Figure 2 – Analysis results in the Cuckoo sandbox
Рис. 2 – Результаты анализа в песочнице Cuckoo
Слика 2 – Резултати анализе у софтверском окружењу Куку за изоловано извршавање програма

The analyst uses a Cuckoo host machine to manage the analysis through a command line or available Web interface. In the scope of an analysis, malware samples are submitted and reports are collected (Figure 2). Before malware execution, a VM's snapshot is reversed to the initial state which ensures that tracks of previous analyses do not interfere with the currently ongoing analysis. An in-guest Python agent serves to execute a malware sample and send a report back to the Cuckoo host.

Drakvuf

Drakvuf (Lengyel et al, 2014) is a VMI-based sandbox which has the ability to trace kernel-level and user-level malware (Melvin & Kathrine, 2020). VMI stands for Virtual Machine Introspection – external access to the virtual hardware state, which can monitor process execution, file operations, system calls and kernel function traces, all at the hypervisor level, with the ability to spot kernel rootkits and reduce the possibility for malware to use its evading techniques (Melvin & Kathrine, 2020). Instead of an in-guest agent, Drakvuf uses the breakpoint injection technique in which an instruction is written into the VM's memory at code locations of interest (Lengyel et al, 2014). By configuring a CPU to issue VMEXIT when breakpoints are executed, and configuring Xen (a virtualization hypervisor)

to forward these events to control domain, DRAKVUF is capable of trapping the execution of any code within the analysis machine. The #BP technique, previously used for the stealth debugging, is used for automatic execution tracing of the entire operating system, including also the Kernel internal functions.

Drakvuf's initial tests showed a great potential and the development of this sandbox was continued, providing a modern and powerful open-source malware analysis platform. The project is maintained and available at: https://drakvuf.com. In this study, we use the customized solution called Drakvuf sandbox (CERT of Poland) which is an actively developed project (Cert Polska, 2021, 2022), since it is easy to install and configure.

Figure 3 – Analysis results in the Drakvuf sandbox
Рис. 3 – Результаты анализа в песочнице Drakvuf
Слика 3 – Резултати анализе у софтверском окружењу Дракеуф за изоловано извршавање програма

Analysis results

Since the considered sandboxes are not of the same type, it is challenging to introduce a metric for their comparison. Instead, we decided to use a descriptive approach to evaluate different features we consider relevant. The observed features are shown in Table 1, where sign "+" is assigned to the sandbox that performs better with respect to a given feature.

Table 2 – Analysis results
Таблица 2 – Результаты анализа
Табела 2 – Резултати анализе

	Feature	Cuckoo	Drakvuf
1	Complexity of installation and setup		+
2	Scalability		+
3	Reporting	+	
4	Execution time	+	
5	Supported file types	+	
6	Evasion prevention		+
7	Variety of analysis VM versions, underlying hardware and hypervisor support	+	
8	Integration with other tools and customization	+	
9	Automated samples submission and API	+	
10	Signatures (static analysis, PE, etc.)	+	
11	Visualization		+

Complexity of installation and setup

Both sandboxes are available for free under the General Public License (GNU GPLv3) and reasonably well documented. As a more mature solution, Cuckoo is more extensively documented, which allows for comparatively easier installation and configuration. In addition, this sandbox is used by many organizations, including CERT of Poland, CERT of Estonia (publicly available at https://cuckoo.cert.ee.), Checkpoint, Avira, etc. (Estonian Information System Authority - RIA, 2017; Checkpoint Software Technologies LTD, 2019; Sick, 2014; CERT Polska, 2019), and the professional community is strong in terms of use, problem solving, customization and modifications. However, since Cuckoo is based on Python 2 (version 2.7 is used in this study), it suffers from some problems caused by dependencies on Python 3 packages. This fact prevented us from using the latest 2.07 Cuckoo version in this study, and led us to downgrade the hosting operating system from Ubuntu 20.04 to Ubuntu 18.04. The Drakvuf sandbox has good basic documentation and respectable community. The Drakvuf Sandbox (CERT of Poland edition) is enriched with a Web interface and additional plugins which create the user experience near to Cuckoo. However, with respect to the complexity of installation and setup, Drakvuf performs better, mainly due to the packet dependency problems in Cuckoo. A full rewrite of Cuckoo for Python 3 in

cooperation with the CERT of Estonia is announced and its availability for customization is expected to improve the Cuckoo's rating with respect to this feature.

Scalability

Although there are certain modifications of Cuckoo aimed at achieving the scalability for the Amazon Web Services (AWS Cloud), this sandbox is generally not easy scalable. In contrast to this, Drakvuf is easily scaled (i.e., command "draksetup scale n" accepts an input argument that represents the number of instances to be automatically configured and started for parallel samples execution).

Reporting

Table 3 provides a comparative overview of the content provided in the analysis reports of the Cuckoo and Drakvuf sandboxes.

Table 3 – Comparative overview of the content provided in the analysis reports of the Cuckoo and Drakvuf sandboxes
Таблица 3 – Сравнительный обзор содержимого, представленного в отчетах анализа песочниц Cuckoo и Drakvu
Табела 3 – Упоредни преглед садржаја извештаја добијених анализом у софтверским окружењима Куку и Драквуф за изоловано извршавање програма

Cuckoo	Drakvuf
Summary	Metadata
Information on execution	
Score (beta version functionality)	-
Yara	-
Sample download	-
Signatures (for three risk categories)	-
Screenshots	-
Network traffic information (available in a report)	Download network traffic (stored in a file)
Static analysis	-
Extracted Artifacts	-
Behavioral Analysis (more informative)	Process tree (more advanced graphical representation)
	Behavioral graph (more advanced graphical representation)
Dropped Files	-
Dropped Buffers	-
Process Memory	-
Additional operations (e.g., resubmit, reanalyze with reboot, etc.)	-

It could be observed that Drakvuf lacks many report features compared to Cuckoo, some of which could be derived from log files. The log files generated by both sandboxes are rather informative but not necessarily appropriate for human interpretation, and therefore we consider here only the information available in Web console reports.

However, the reporting functionality is primarily evaluated with respect to the question of to what extent a sandbox is helpful to the human analyst during the process of malware analysis. To assess this question, we have used 21 potential malware files, summarized in Table 4.

The samples are courtesy of the Virus total portal (Sood, 2021). The name of each sample (cf. the second column) is generated by taking the first 8 characters of its SHA-256 value.

The full 256-bit hashes are available but not provided because of possible misuse. The fourth column of Table 4 contains the numbers of antivirus engines that reported the sample as positive, while the fifth column contains the numbers of all antivirus engines that analyzed the sample. We introduce the following malware score to describe a sample (note that malware score will always be in range 0 to 1) as a division of number of positives (#P) by total number (#T).

The malware score of a sample is used as an external measure according to which the respective behavior reports obtained from the Cuckoo and Drakvuf sandboxes were evaluated. The details of this evaluation are given in Table 5.

Although Cuckoo had some difficulties analyzing malware samples that operate on a large number of files (i.e., too many files error) due to which multiple analysis restarts were required and the sandbox failed to produce reports for two samples in Table 5 (samples 002d7712 and 003add9c), the overall conclusion is that it provides more informative reports.

Table 4 – Malware samples used to compare reporting functionality of the sandboxes

Таблица 4 – Образцы вредоносных программ, используемые для сравнения функциональности отчетов в песочницах

Табела 4 – Узорци штетних програма коришћених за поређење извештаја у софтверским окружењима за изоловано извршавање програма

	Samples	File extension	#P	#T	Cuckoo score [0-10]	Cuckoo execution time (sec.)	Drakvuf default execution time (sec.)
1	000a46e1	Executables	53	67	0.6	196	600
2	898ccbcd		17	59	0	198	600
3	001a9515		50	65	0.8	197	600
4	002cca70		45	67	0.8	197	600
5	002d7712		58	68	0.6	196	600
6	003add9c		52	65	0.6	197	600
7	003afda4		50	66	4.6	196	600
8	00a67cc9	DLL files	33	57	1.2	902	600
9	00cb2289		49	56	1	307	600
10	00e02090		34	57	1	502	600
11	00f0d52f		40	56	0.6	328	600
12	9e184db7	HTML files	16	57	0	623	600
13	4db0f844	Microsoft Word documents	37	61	0	196	600
14	b56da6b0		38	60	0.4	214	600
15	e6871658		38	58	0	618	600
16	ea7db3d3	Microsoft Excel documents	29	61	0.4	196	600
17	72297378		43	59	0.4	197	600
18	6383c1aa		47	61	0.4	196	600
19	5c5d1602		18	59	0.4	196	600
20	0ecb0f42		30	55	0.4	196	600
21	0c0fe7f7		34	60	0.4	196	600

Table 5 – Details of report evaluation
Таблица 5 – Детали оценки отчетов
Табела 5 – Детаљи вредновања извештаја

Sample	Malware score	Cuckoo report	Drakvuf report
000a 46e1	0.79	Score 0.6. File operations and 2 file creation 000a46e1…exe and c:\ttdxptt.exe, various registry modifications.	More than 20 processes and files created (limited with execution time).
898c cbcd	0.29	Score 0. Yara embedded_pe Contains an embedded PE32 file, embedded_win_api. A non-Windows executable contains win32 API functions names shellcode. Matched shellcode byte patterns. No behavioral analysis.	None.
001a 9515	0.77	None.	Creation of 2 files and processes 001a9515.exe and HelpMe.exe
002c ca70	0.67	Score 3.8. Yara vmdetect - Possibly employs anti-virtualization techniques. 160 files dropped, connection to unavailable IP address for which no DNS request was made, creates modified copy of itself, etc. Various traces in static analysis.	None.
002d 7712	0.85	Could not be reported since the analysis results size is greater than supported.	Creation of 9 files (exe, dll, bcf) and 4 processes, 16 registry entries.
003a dd9c	0.80	Could not be reported since the analysis results size is greater than supported.	Creation of 16 files (dll, exe), 9 processes, around 100 registry entries.
003a fda4	0.76	Score 7.8. HTTP requests, steals private information form Internet browser, drops executables, search running process, potentially malicious URLs, communication with host without DNS query, delay attempted, enumerates services, installs itself for auto-run, creates modified copies of itself, creates worm files, registry keys and generates ICMP traffic.	Creation of 10 files and processes.
00a6 7cc9	0.58	Score 2.2. One of more buffers contain embedded PE file. Indication of a packer. Various registry accesses.	Creation of regsvr32.exe processes.

Sample	Malware score	Cuckoo report	Drakvuf report
00cb 2289	0.88	Score 1.2. Various file creation, KERNELBASE.dll.mui etc, DLL's used, process rundll32.exe. Signatures: Indication of a packer - a section with a high entropy has been found.	Creation of regsvr32.exe processes. File creation regsvr32.exe-8461dbee.pf. Process ID 2288.
00e0 2090	0.60	Score 1. Indication of a packer. Potentially malicious URLs found in process memory.	Creation of regsvr32.exe processes. File creation regsvr32.exe-8461dbee.pf. Process ID 2352.
00f0 d52f	0.71	Score 2.2. Indication of a packer. HTTP request, communication with a host for which no DNS query was performed.	Creation of regsvr32.exe processes. File creation regsvr32.exe-8461dbee.pf Process ID 2284.
9e18 4db7	0.28	Score 1.8. Potentially malicious URLs in the process memory dump. Uses Windows utilities for basic Windows functionalities. Resumes thread in a remote process (potential process injection). Two files dropped.	Creates mshta.exe process with 13 threads which makes 17 registry entries in part of Internet connection settings.
4db0 f844	0.61	Score 9.8. Creation of 18 files. Powershell sending data, 6 http requests, potentially malicious URLs, URL downloaded by powershell script, winword.exe and powershell.exe wrote an executable to disk which then attempted to execute, powershell downloaded payload, etc.	About one hundred of registry accesses.
b56d a6b0	0.63	Score 11. Creation of 18 files. Communication with host without DNS query, a script was created with unexpected parent, potential payload download by powershell.exe non safe listed process created, and ICMP traffic.	About one hundred of registry accesses.
e687 1658	0.66	Score 7.4. Various file creation (DOC, LNK, scripts). Suspicious process creation. Malicious URLs found in memory dump. Extracted script. Dropped files which are executed.	Creation of one file, about one hundred of registry accesses in networking and Microsoft Office parts.
ea7d b3d3	0.48	Score 2.2. Yara: embedded_win_api - A non-Windows executable contains win32 API functions names. Communication with host without DNS query.	Hundreds of registry accesses.

Sample	Malware score	Cuckoo report	Drakvuf report
7229 7378	0.73	Score 2.2. Http requests, changes read-write memory protection to read-execute probably to avoid detection. Potentially malicious URLs, communication with host without DNS query.	Hundreds of registry accesses.
6383 c1aa	0.77	Score 1.8. Changes read-write memory protection to read-execute probably to avoid detection, potentially malicious URLs found, communication with host without DNS query.	Hundreds of registry accesses.
5c5d 1602	0.31	Score 1.8. Changes read-write memory protection to read-execute probably to avoid detection, communication with host without DNS query.	Hundreds of registry accesses.
0ecb 0f42	0.55	Score 3.2. HTTP requests, changes read-write memory protection to read-execute probably to avoid detection. Potentially malicious URLs, communication with host without DNS query. Connects to IP address that no longer responds to requests.	Hundreds of registry accesses.
0c0f e7f7	0.57	Score 3.0. HTTP requests, creates hidden or system file, changes read-write memory protection to read-execute probably to avoid detection. Potentially malicious URLs, communication with host without DNS query. Generates some ICMP traffic.	Hundreds of registry accesses.

Execution time

From Table 3, it can be observed that Cuckoo is more efficient for the given data. However, it should be noted that Drakvuf configuration supposes a constant execution time (default is 10 minutes, but could be lowered). The Drakvuf authors probably introduced this unbalanced trade-off between the efficacy and security in order to reduce the possibility for a sample to evade the sandbox environment.

Supported file types

The file types supported by the sandboxes are shown in Figure 4. The Cuckoo sandbox has a huge advantage in terms of supported file types (including various scripts, PDF and ZIP-file type extensions) and can be

customized for generic packages by selecting applications to handle a particular sample type.

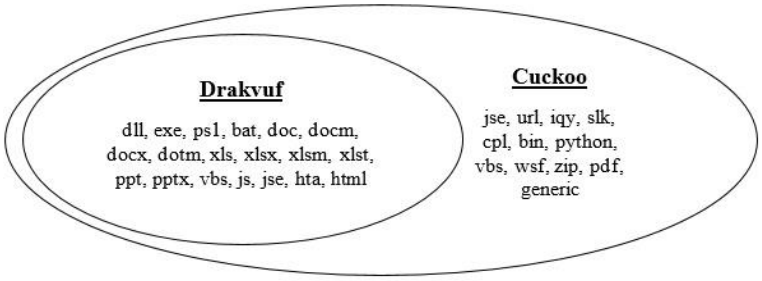

Figure 4 – Supported file types in Cuckoo and Drakvuf
Рис. 4 – Поддерживаемые типы файлов в безагентных песочницах Cuckoo и Drakvuf
Слика 4 – Подржани типови фајлова у софтверским окружењима Куку и Дракѕуф за изоловано извршавање програма

Evasion prevention

Since malware proved as evasive was not available in this study, the insight with respect to this feature is based on the sandboxes design and available research (Laing, 2017; Mills & Legg, 2021; Ferrand, 2015; Lengyel et al, 2014). It may be concluded that out-of-the-box Drakvuf performs better when confronted with evading malware, although both systems could be hardened to increase the probability of executing and reporting evasive malware.

Virtual machine, hypervisor and hardware support

Cuckoo supports Windows XP, Windows 7 64-bit and Windows 10 64-bit (not fully functional), Ubuntu 18.04 as a Linux guest operating system, and it can be configured to analyze samples in an Android environment under the Linux guest operating system. The configuration of Physical machine is also possible for the purpose of analysis. Drakvuf supports Windows 7-8, both 32-bit and 64-bit versions, 64-bit version of Windows 10 as well as 32-bit and 64-bit Linux systems running kernel 2.6.x and above, while the particular Drakvuf sandbox considered in this study is limited to Windows 7 (64-bit) and Windows 10 (64-bit) experimental.

Due to its design, Drakvuf is limited to the Intel processors, while Cuckoo can run without hardware limitations. The hypervisor support is also on the side of Cuckoo because it can communicate with analysis VMs under Xen, KVM, VMware ESXi, Oracle Virtual box, and almost on any other platform, while in the Drakvuf environment only Xen is natively

supported (KVM is in the experimental phase and VMware Workstation needs to be additionally configured). Due to its design, Drakvuf only supports nested virtualization. Thus, Cuckoo is also more advanced with respect to this feature, although Drakvuf provides enough options to work just fine in most environments.

Integration with other tools and customization

Since Cuckoo is a more mature solution, its integration possibilities are greater. Thus, it can be integrated with a range of tools for additional analysis (e.g., Cuckoo-droid, Signature updates, YARA rules, Suricata, Snort, Moloch, Volatility, Virustotal integration, etc) (Ashby, 2015; Checkpoint Software Technologies LTD, 2015). The Drakvuf sandbox allows integration with certain tools (e.g., Volatility and procmon for behavioral graph induction), but its integration possibilities are still significantly lower.

Automated samples submission and API

Cuckoo supports multiple samples submission, which in conjunction with its efficient execution allows a real-time analysis in environments with limited resources and may be applied to analyze large amounts of malware. REST API is implemented and easily accessible by the execution of a single command, enabling the automation of the analysis process. Drakvuf does support multiple samples submission but its API is still undocumented and we could not find the way to effectively use it.

Signatures

Signatures are probably the most lacking feature in Drakvuf. In contrast, Python scripts in Cuckoo are automatically updated from the repository and create signatures that recognize malicious behavior of samples. YARA rules can be defined and applied to improve this process. Signatures are also applied in the static analysis of samples.

Visualization

Cuckoo has a beta version scoring system which is visually very illustrative, but not fully informative for detailed analyses in which visually advanced reports with signatures are substantially useful. In Drakvuf, the Process tree and Behavioral graph are very useful visual tools which make Drakvuf a slightly more advanced solution with respect to the visualization functionality.

Conclusion

Table 2 shows that the Cuckoo sandbox performs better with respect to many features. However, the answer to the question of which sandbox to apply depends on the expected malware behavior.

Drakvuf is expected to perform better when confronted with evasive malware and so-called “file-less” malware (residing only in the RAM of a device). It is also suitable for capturing traces that a malware attempts to clean (i.e., deletion of temporary files), since it fetches deleted files by intercepting internal kernel calls related to the file deletion operations. On the other hand, Drakvuf has its limitations including the use of the injection mechanism to automatically start a sample (Lengyel et al, 2014) which a malware can exploit to evade an abnormal start, but research demonstrates the potential of this sandbox with respect to evading malware techniques. Although still not mature in terms of integration, customization and tools, it is considered a second generation sandbox because of its agentless design (Laing, 2017; Richards, 2021; Lengyel et al, 2014)

The Cuckoo sandbox creates a better overall experience: it is supported through good documentation and strong professional community, better integrated with various tools, supports more virtualization, operating systems and sample types. With the Python 3 rewrite, Cuckoo 3 (Hatching International B.V., 2022) is expected to perform even better. Even with a smaller capacity to prevent a malware to evade the sandbox environment, its Python 2 agent script makes it more powerful than Drakvuf. Recent research including 539 organizations and companies in Europe and USA (Spiceworks, 2019) shows that 92% of the companies apply server virtualization solutions, and predicts that the increasing number of VMs in production environments could result in lowering the frequency of evasion techniques since attackers probably would not allow to be deprived of the opportunities to target these machines.

At the given point, to achieve an adequate or optimal open-source sandbox-based protection and improve cyber security risk management practices (Ilić, 2012), it is recommendable to apply both the Cuckoo and Drakvuf sandboxes. In circumstances of limited resources, applying the Cuckoo sandbox is preferable, especially if exposure to malware deploying evading techniques is not frequently expected.

References

Arntz, P. 2020. Sandbox in security: what is it, and how it relates to malware. *Malwarebytes LABS blog*, 24 September [online]. Available at: https://blog.malwarebytes.com/awareness/2020/09/sandbox-in-security [Accessed: 30 January 2022].

Ashby, C. 2015. Extending Cuckoo Framework. *PenTest magazine*, 12 March [online]. Available at: https://pentestmag.com/cuckoo. [Accessed: 30 January 2022].

-CERT Polska. 2019. Strengthening our malware analysis capabilities. *Official web site of CERT Polska (part of NASK)*, 21 February [online]. Available at: https://cert.pl/en/posts/2019/02/strengthening-our-malware-analysis-capabilities/ [Accessed: 30 January 2022].

-CERT Polska. 2021. DRAKVUF Sandbox (v0.18.1). *Official repository of the DRAKVUF Sandbox project*, 28 October [online]. Available at: https://github.com/CERT-Polska/drakvuf-sandbox/releases/tag/v0.18.1 [Accessed: 30 January 2022].

-CERT Polska. 2022. DRAKVUF Sandbox Documentation. *DRAKVUF Sandbox documentation at Read the docs*, 10 February [online]. Available at: https://drakvuf-sandbox.readthedocs.io/_/downloads/en/latest/pdf. [Accessed: 10 February 2022].

Chakkaravarthy, S.S., Sangeetha, D. & Vaidehi, V. 2019. A Survey on malware analysis and mitigation techniques. *Computer Science Review*, 32, pp.1-23. Available at: https://doi.org/10.1016/j.cosrev.2019.01.002.

-Checkpoint Software Technologies LTD. 2015. CuckooDroid Book, Revision 13502746. *CuckooDroid at Read the docs* [online]. Available at: https://cuckoo-droid.readthedocs.io/en/latest [Accessed: 10 February 2022].

-Checkpoint Software Technologies LTD. 2019. Cuckoo SandBox on AWS. *Checkpoint research*, 11 March [online]. Available at: https://research.checkpoint.com/2019/cuckoo-system-on-aws/ [Accessed: 10 February 2022].

-Estonian Information System Authority (RIA). 2017. Annual Cyber Security Assessment 2017. *Estonian Information System Authority (RIA) official website* [online]. Available at: https://www.ria.ee/sites/default/files/content-editors/kuberturve/ria_csa_2017.pdf [Accessed: 30 January 2022].

Ferrand, O. 2015. How to detect the Cuckoo Sandbox and to Strengthen it? *Journal of Computer Virology and Hacking Techniques*, 11, pp.51-58. Available at: https://doi.org/10.1007/s11416-014-0224-9.

-Hatching International B.V., 2022. We know cuckoo. *Official web site of the Cuckoo developers* [online]. Available at: https://hatching.io/cuckoo [Accessed: 30 January 2022].

-IBM Corporation. 2020. IBM Security, report: IBM Cost of a Data Breach Report. *IBM official web site*. July [online]. Available after registration at: https://www.ibm.com/security/digital-assets/cost-data-breach-report [Accessed: 30 January 2022].

Ilić, S. 2012. CLOUD COMPUTING - Information assurance aspects in government use. In: *Proceedings of XVIII conference YU INFO*, Kopaonk, Serbia, March 01-03.

Laing, B. 2017. First-generation sandbox solutions do not beat evasive malware. *IDG Connect*. 8 February [online]. Available at: https://www.idgconnect.com/article/3581202/first-generation-sandbox-solutions-do-not-beat-evasive-malware.html [Accessed: 10 February 2022].

Lengyel, T.K., Maresca, s., Payne, B.D., Webster, G.D., Vogl, S. & Kiayias, A. 2014. Scalability, fidelity and stealth in the DRAKVUF dynamic malware analysis system. In: *ACSAC '14: Proceedings of the 30th Annual Computer Security Applications Conference*, New York, NY, USA, pp.386-395, December. Available at: https://doi.org/10.1145/2664243.2664252.

Melvin, A.A.R. & Kathrine, G.J.W. 2020. Quest for Best: A Detailed Comparison between Drakvuf - VMI-Based and Cuckoo Sandbox-Based Technique for Dynamic Malware Analysis. In: *Peter, J., Fernandes, S. & Alavi, A. (Eds.) Intelligence in Big Data Technologies - Beyond the Hype. Advances in Intelligent Systems and Computing*, 1167. Springer, Singapore. Available at: https://doi.org/10.1007/978-981-15-5285-4_27.

Mills, A. & Legg, P. 2021. Investigating Anti-Evasion Malware Triggers Using Automated Sandbox Reconfiguration Techniques. *Journal of Cybersecurity and Privacy*, 1, pp.19-39. Available at: https://doi.org/10.20944/preprints202010.0305.v1.

Richards, K. 2021. VMRay – The Hypervisor-Based Sandbox That Cannot be Detected (interview with Carsten Willems). *VpnMentor* [online]. Available at: https://www.vpnmentor.com/blog/vmray-hypervisor-based-sandbox-not-detected. [Accessed: 30 January 2022].

Sick, T. 2014. Cuckoo Sandbox vs. Reality. *Avira official web site,* 11 November [online]. Available at: https://www.avira.com/en/blog/cuckoo-sandbox-vs-reality-2 [Accessed: 10 February 2022].

Sood, G. 2021. Virustotal: R Client for the virustotal API. R package version 0.2.2. *Virus total web portal* [online]. Available at: https://www.virustotal.com [Accessed: 10 February 2022].

-Spiceworks. 2019. The 2020 State of Virtualization Technology, Survey on 539 organizations and companies in Europe and USA. *Spiceworks* [online]. Available at: https://www.spiceworks.com/marketing/reports/state-of-virtualization [Accessed: 30 January 2022].

Tot, I.A., Bajčetić, J.B., Jovanović, B.Ž., Trikoš, M.B., Bogićević, D.Lj. & Gajić, T.M. Biometric standards and methods. *Vojnotehnički glasnik/Military Technical Courier*, 69(4), pp.963-977. Available at: https://doi.org/10.5937/vojtehg69-32296.

ЭКСПЕРИМЕНТАЛЬНЫЙ СРАВНИТЕЛЬНЫЙ АНАЛИЗ ПЕСОЧНИЦ CUCKOO И DRAKVUF: ВЗГЛЯД КОНЕЧНОГО ПОЛЬЗОВАТЕЛЯ

Славиша Ж. Илич[а], *Милан* Й. Гнятович[б],
Бранкица М. Попович[б], *Неманя* Д. Мачек[в]

[а] Министерство обороны Республики Сербия,
г. Белград, Республика Сербия, **корреспондент**

[б] Университет криминалистики и полицейской подготовки,
г. Белград, Республика Сербия

[в] Школа электротехники и вычислительной техники,
Академия технических и художественных прикладных исследований,
г. Белград, Республика Сербия

РУБРИКА ГРНТИ: 20.23.25 Информационные системы с базами знаний,
81.93.29 Информационная безопасность. Защита информации

ВИД СТАТЬИ: оригинальная научная статья

Резюме:

Введение/цель: В данной статье представлен экспериментальный сравнительный анализ программных сред песочниц Cuckoo и Drakvuf. Эти системы были выбраны в качестве предмета анализа из-за их популярности в профессиональном сообществе и их взаимодополняющих подходов к анализу воздействия вредоносных программ.

Методы: Обе системы имеют базовые настройки и подвергаются воздействию одного и того же набора вредоносных программ. Анализ преимущественно проводился с целью выявления степени полезности песочниц для аналитика-человека при анализе вредоносных программ. Следовательно, учитывалась только та информация, которая была доступа в отчетах веб-интерфейсов наблюдаемых систем.

Результаты: Можно ожидать, что Drakvuf даст лучшие результаты при воздействии вредоносных программ, использующих методы обхода песочниц в виртуальных средах. Несмотря на то, что данная среда пока не достигла своей полной мощности относительно интеграции, настроек и доступных программных инструментов, ее все-таки можно считать представителем второго поколения изолированных систем программной среды, благодаря ее безагентной технологии. С другой стороны, песочница Cuckoo в целом более удобна для пользователей: она поддерживается хорошей документацией и сильным профессиональным сообществом, лучше интегрирована с различными программными

инструментами, поддерживает больше видов виртуализации, типов операционных систем и образцов, в том числе она лучше генерирует отчеты. Несмотря на то, что у этой песочницы гораздо меньше возможностей предотвращения атак вредоносных программ в виртуальной среде, применение сценария с выявлением действий вредоносных программ делает эту песочницу более эффективной.

Выводы: Для достижения оптимальной защиты на основе песочницы с открытым исходным кодом рекомендуется применять как песочницы Cuckoo, так и Drakvuf. В условиях ограниченных ресурсов предпочтительнее применять песочницу Cuckoo, особенно если не предполагается частое воздействие вредоносных программ, использующих метод уклонения от обнаружения.

Ключевые слова: изолированный запуск программы, Cuckoo, Drakvuf, динамический анализ вредоносных программ.

УПОРЕДНА ПИЛОТ-АНАЛИЗА СОФТВЕРСКИХ ОКРУЖЕЊА КУКУ И ДРАКВУФ ЗА ИЗОЛОВАНО ИЗВРШАВАЊЕ ПРОГРАМА: ПЕРСПЕКТИВА КРАЈЊЕГ КОРИСНИКА

Славиша Ж. Илић[а], *Милан* Ј. Гњатовић[б], *Бранкица* М. Поповић[б], *Немања* Д. Мачек[в]

[а] Министарство одбране Републике Србије, Београд, Република Србија, **аутор за преписку**

[б] Криминалистико-полицијски универзитет, Београд, Република Србија

[в] Висока школа електротехнике и рачунарства струковних студија, Академија техничко-уметничких струковних студија, Београд, Република Србија

ОБЛАСТ: рачунарске науке, информационе технологије, информациона безбедност
ВРСТА ЧЛАНКА: оригинални научни рад

Сажетак:

Увод/циљ: У раду се приказује упоредна пилот-анализа софтверских окружења Куку и Драквуф за изоловано извршавање програма. Ови системи одабрани су за предмет анализе због своје популарности у професионалној заједници и комплементарних приступа анализи понашања злонамерних програма.

Методе: Оба система постављена су на основна подешавања и изложена истом скупу злонамерних програма. Анализа је примарно урађена с аспекта процене степена информативности добијених извештаја о извршавању злонамерних програма за људског аналитичара. Стога су, као предмет анализе, узете у обзир само информације доступне у веб-интерфејсима посматраних система.

Резултати: Може се очекивати да ће Драквуф остварити бољи учинак када се изложи злонамерним програмима који примењују технике избегавања извршавања у виртуалним окружењима. Иако ово окружење још увек није остварило пун капацитет у смислу интегрисања, прилагођавања и доступних софтверских алата, може се сматрати представником друге генерације система за изоловано извршавање програма, због свог дизајна који искључује примену софтверског агента. С друге стране, окружење Куку ствара боље свеукупно корисничко искуство: подржано је добром документацијом и јаком професионалном заједницом, боље је интегрисано са различитим софтверским алатима, подржава више типова виртуелизације, оперативних система и типова узорака и генерише информативније извештаје. Иако поседује мањи капацитет за откривање злонамерних програма који примењују технике избегавања извршавања у виртуалним окружењима, могућност примене скрипти с дефиницијама злонамерног понашања програма чини ово окружење ефективнијим.

Закључак: Да би се постигла оптимална заштита, заснована на окружењима отвореног кода за изоловано извршавање програма, препоручује се примена оба разматрана система. У условима ограничених ресурса, примена система Куку пожељнија је, посебно ако се не очекује често излагање злонамерним програмима који примењују технике избегавања извршавања у виртуалним окружењима.

Кључне речи: изоловано извршавање програма, Cuckoo, Drakvuf, динамичка анализа злонамерних програма.

Paper received on / Дата получения работы / Датум пријема чланка: 01.02.2022.
Manuscript corrections submitted on / Дата получения исправленной версии работы / Датум достављања исправки рукописа: 16.03.2022.
Paper accepted for publishing on / Дата окончательного согласования работы / Датум коначног прихватања чланка за објављивање: 18.03.2022.

EMPLOYMENT OF PROBABILITY-BASED MULTI-RESPONSE OPTIMIZATION IN HIGH VOLTAGE THERMOFLUIDS

Joseph Chukwuka Ofodu[a], *Johnson Kehinde* Abifarin[b]

[a] University of Port Harcourt, Faculty of Engineering,
Department of Mechanical Engineering,
Choba, Rivers State, Federal Republic of Nigeria,
e-mail: rofnelenergy@yahoo.com,
ORCID iD: https://orcid.org/0000-0001-8311-7332

[b] Ahmadu Bello University, Faculty of Engineering,
Department of Mechanical Engineering,
Zaria, Federal Republic of Nigeria,
e-mail: jkabifarin@abu.edu.ng, **corresponding author,**
ORCID iD: https://orcid.org/0000-0003-4930-9132

DOI: 10.5937/vojtehg70-35764; https://doi.org/10.5937/vojtehg70-35764

FIELD: Mechanical engineering, Materials
ARTICLE TYPE: Original scientific paper

Abstract:

Introduction/purpose: Researchers of fluids for high voltage engineering application always experience problems when selecting and recommending specific fluids suitable for high voltage application. This is due to the dual functionality of fluids required for high voltage equipment.

Methods: This study introduced and employed a probability-based multi-objective optimization technique in the selection of high voltage thermofluids. Beneficial and unbeneficial preferable probability utility indexes were employed based on the desired properties of oils.

Results: It was shown that the nanofluid with 0.6 wt% Al_2O_3 is the most promising candidate for high voltage equipment compared to other produced fluids considered. It is also noteworthy to state that coconut oil exhibited better performance efficiency compared to standard oil. This study also identifies that the produced Jatropha oil was inadequate for high voltage equipment.

Conclusion: In conclusion, a preliminary study essential for final usage of 0.6 wt% Al_2O_3 nanofluids and coconut oil for high voltage equipment is recommended as well as the improvement of the performance characteristics of Jatropha oil for usage in high voltage equipment.

Keywords: preferable probability optimization, high voltage equipment, thermofluids, physicochemical properties, dielectric strength.

Introduction

High voltage engineering is an integral area of electrical and mechanical engineering. A lot of devices have been made for high voltage application - power transformers, switchgears, control equipment, communicating devices, and insulators, to mention but a few. The quality of insulating fluids used in such equipment is essential for its wellbeing and efficiency (Oparanti et al, 2020; Oparanti et al, 2022). This study comes with the motivation to apply a novel multi-objective approach in the selection of optimal processing conditions or better performance fluids for high voltage equipment.

Conventional mineral oil has been used in high voltage equipment due to its unique and multifunctional characteristics, which are efficient cooling and dielectric capacity. However, due to mineral oil non-biodegradability and other intricate production tendencies, researchers have worked on the production of alternative fluids for high voltage engineering. Abeysundara et al (2001) produced and examined the properties of coconut oil as an alternative for transformer mineral oil. Sitinjak et al (2003) examined the characteristics of palm oil and its derivative for high voltage equipment. Hosier et al (2009) studied the selection of a suitable vegetable oil for high voltage engineering. Garba et al (2013) produced and characterized Jatropha oil for transformer application. Peppas et al (2016a, 2016b) produced ultrastable natural ester-based nanofluids for high voltage engineering. Oparanti et al (2021a) developed a nanofluid from palm kernel oil for high voltage engineering. Oparanti et al (2021b), in addition to their previous work, analyzed AC breakdown of their synthesized nanofluids from palm kernel oil. In all of these studies, with the ones not mentioned, there has been a challenge in selecting a specific oil sample suitable for high voltage application, considering the dual functionality of a typical high voltage equipment oil. Hence, this study has addressed this challenge by introducing and employing a probability-based optimization technique for multiple performance characteristics of high voltage engineering oil.

Consequently, several techniques such as Ashby's method (Ashby, 2000; Ashby et al, 2004), the TOPSIS method (Deshmukh & Angira, 2019), the grey relational analysis method (Abifarin, 2021; Abifarin et al, 2021a, 2021b, 2021c; Awodi et al, 2021; Abifarin et al, 2022; Abifarin & Ofodu, 2022), and the intersection multi-objective probability method (Wang & Teng, 2021; Zheng, 2022) have been used for multiple objective optimization in several applications; probability-based multi-objective optimization has proven to be simple and more efficient (Zheng, 2022).

Hence, this study selected some data (Abeysundara et al, 2001; Garba et al, 2013; Oparanti et al, 2021a) in high voltage engineering oil development and then the new multi-objective probability optimization technique was employed for the first time to determine the most efficient oil sample among other samples in the study.

Research method

The beneficial utility index method is applied to a desired characteristic which should be as high as possible. The index characteristic indicator contributes positively to a partial preferable probability. Equation 1 is used to compute the partial positive probability index (Pij), while equation 2 is used to compute the normalized factor (α_j) of the jth utility index of the performance characteristic indicator.

$$Pij = \alpha_{ij} X_{ij},\ i = 1, 2,...,n;\ j = 1, 2,..m \quad (1)$$

$$\alpha_j = 1/(\mathrm{n}\overline{X}_J) \quad (2)$$

where X_{ij} is the jth beneficial utility index of the characteristic performance indicator of the ith number of sample, n is the total number of samples considered in the study, m is the total number of utility indices of each sample involved, and X_j is the value of the arithmetic mean of the utility index of the sample characteristic performance indicator. The performance characteristics considered for the beneficial utility index are shown in Table 1:

Table 1 – Beneficial utility high voltage characteristics
Таблица 1 – «Чем больше, тем лучше» характеристики изоляционного масла
Табела 1– Карактеристике изолационог уља типа „што више – то боље”

Performance characteristics	Beneficial utility discussion	Reference
Activation energy (eV/mol)	The higher the activation energy, the harder it becomes to reduce the viscosity of the liquid at elevated temperature. In other words, a higher activation energy of a fluid leads to a good cooling integrity of the fluid.	(Badicu et al, 2011; Liu et al, 2019; Liu et al, 2020; Oparanti et al 2021a)

Performance characteristics	Beneficial utility discussion	Reference
Breakdown voltage/Dielectric strength (kV)	Breakdown voltage or dielectric strength of an insulator is the minimum voltage that makes the portion of an insulator to experience electrical breakdown and become electrically conductive. Also the higher the breakdown voltage of a fluid, the less contaminant the oil. In other words, as high as possible breakdown voltage is required for high voltage equipment.	(Lee et al, 2012; Peppas et al, 2016a, 2016b; Abd-Elhady et al, 2018; Ghoneim et al, 2021; Oparanti et al, 2021a; Asse et al, 2022)
Flash point (°C)	Insulating fluids for high voltage equipment should exhibit a high flash point. This prevents fire outbreak, interrupted power supply and economic loss.	(Kumar et al, 2014; Oparanti et al, 2021a; Oparanti et al, 2022; Minkner & Schmid, 2022)

The unbeneficial utility index method is applied to a desired characteristic which should be as low as possible, i.e. minimization type of optimization is desired. The index characteristic indicator contributes negatively to a partial preferable probability.

Equation 3 is used to compute the partial negative probability index (Pij), while equation 4 is used to compute its normalized factor (βj) of the j^{th} utility index of the performance characteristic indicator.

$$Pij = \beta_{ij}(X_{jmax} + X_{jmin} - X_i),\ i = 1, 2,...,n;\ j = 1, 2,..m \quad (3)$$

$$\beta ij = 1/[n(X_{j\min} + X_{j\max}) - nX_j] \quad (4)$$

Table 2 – Unbeneficial utility high voltage oil characteristics
Таблица 2 – «Чем меньше, тем лучше» характеристики изоляционного масла
Табела 2 –Карактеристике изолационог уља типа „што мање – то боље”

Performance characteristics	Unbeneficial utility discussion	Reference
Cloud point	The cloud point of an insulating fluid is the temperature at which the fluid begins to condense, i.e. the smaller the cloud point of an insulating fluid, the better it is for high voltage equipment	(Garba et al, 2013; Du et al, 2013; Oyelaran et al, 2020)
Viscosity	High viscosity of a fluid usually causes poor atomization of the fluid, meaning minimization is required for high voltage equipment	(Hosier et al, 2006; Garba et al, 2013; Srinivasa & Surendra, 2019)
Specific gravity	Specific gravity is used to examine whether an object will float or sink in water. In other words, if the specific gravity of a fluid is less than one, it means that the fluid will float in water. Lower specific gravity is required to enable the dewatering of the fluid during transformer maintenance.	(Gong et al, 2018; Lin et al, 2021)
Density	Lower density of a fluid for high voltage equipment is required because it enhances mobility of the fluid. Mobility of the fluid is required for efficient equipment cooling.	(Yaacob & Alsaedi, 2015)
Moisture content	Moisture content has a negative effect on the insulating and dielectric properties of a transformer oil. No water content or as small as possible water content is desired for high voltage equipment	(Ofodu & Abifarin, 2021; Zhang et al, 2021)

Furthermore, the conclusive preferable probability of the analysis is the product of the individual partial preferable probability of a corresponding candidate sample. Afterwards, the ranking is done to show the candidate sample with the best performance characteristics.

Analysis and discussion of the results

Activation energy and breakdown voltage

Oparanti et al (2021a) developed nanofluids and examined their activation energy and breakdown voltage. However, the analysis did not reflect conclusively which oil sample is the best candidate for high voltage equipment. Table 3 shows the oil samples and their corresponding activation energies and breakdown voltages.

Table 3 – Activation energy and breakdown voltage of high voltage fluids
Таблица 3 – Энергия активации и напряжение высоковольтного пробоя жидкостей
Табела 3 – Активациона енергија и напон пуцања флуида за високонапонску опрему

Samples	Activation energy (eV/mol)	Breakdown voltage (kV)
Ester oil	0.04	21
Ester + 0.2 wt% Al_2O_3	0.09	23
Ester + 0.4 wt% Al_2O_3	0.09	27
Ester + 0.6 wt% Al_2O_3	0.09	29
Ester + 0.8 wt% Al_2O_3	0.09	29
Ester + 1 wt% Al_2O_3	0.09	27
Ester + 0.2 wt% TiO_2	0.047	26
Ester + 0.4wt% TiO_2	0.047	27
Ester + 0.6 wt% TiO_2	0.05	28
Ester + 0.8 wt% TiO_2	0.06	28
Ester + 1 wt% TiO_2	0.08	28

The data presented in Table 3 was analyzed using the beneficial utility index as the higher-the-better characteristics desired for high voltage equipment. The resulting analysis is displayed in Table 4. The multi-objective optimization shows that two oil samples exhibited the best performance - the nanofluids with 0.6 and 0.8 wt% Al_2O_3 nanoparticles. However, to save costs and to reduce agglomeration of nanoparticles in

the fluid, the nanofluid with 0.6 wt% Al_2O_3 is the most promising candidate for high voltage equipment. In addition, it is recommended to study the effect of Al_2O_3 nanoparticles using the 1wt% stepwise increase instead of the used 2wt% stepwise increase of activation energy and breakdown voltage of ester oil. This will show that perhaps 0.7 wt% has better activation energy and breakdown voltage.

Table 4 – Partial (Pij) and total preferable (Pt) probabilities of activation energy and breakdown voltage of various fluids
Таблица 4 – Частичная (Pij) и полная (Pt) предпочтительные вероятности энергии активации и напряжения пробоя различных жидкостей
Табела 4 – Делимичне (Pij) и укупне (Pt) пожељне вероватноће активационе енергије и напона пуцања разних флуида

Samples	P_{ij} of activation energy	P_{ij} of breakdown voltage (kV)	Pt*100	Rank
Ester oil	0.052	0.072	0.372	9
Ester + 0.2 wt% Al_2O_3	0.117	0.079	0.917	4
Ester + 0.4 wt% Al_2O_3	0.117	0.092	1.077	2
Ester + 0.6 wt% Al_2O_3	0.117	0.099	1.157	1
Ester + 0.8 wt% Al_2O_3	0.117	0.099	1.157	1
Ester + 1 wt% Al_2O_3	0.117	0.092	1.077	2
Ester + 0.2 wt% TiO_2	0.061	0.089	0.542	8
Ester + 0.4wt% TiO_2	0.061	0.092	0.562	7
Ester + 0.6 wt% TiO_2	0.065	0.096	0.621	6
Ester + 0.8 wt% TiO_2	0.078	0.096	0.745	5
Ester + 1 wt% TiO_2	0.104	0.096	0.993	3

Physicochemical characteristics and dielectric strength

Garba et al (2013) produced Jatropha oil, examined its properties, and compared it with diesel oil and transformer oil to see which one would perform better for transformer application. The performance characteristics of various oils are displayed in Table 5.

The flash point and dielectric strength were analyzed using the beneficial utility index (see Table 1) while the rest of the characteristics in Table 5 were analyzed using the unbeneficial utility index (see Table 2). The result showed that the developed Jatropha oil exhibited lesser performance for high voltage equipment compared to the other two

standard oils. This means that further study is essential to improve the performance characteristics of Jatropha oil for high voltage equipment. Many reports have shown that the addition of nanoparticles and the improvement of oil production can improve the performance efficiency of the oil for high voltage equipment (Jin et al, 2014; Peppas et al, 2016a, 2016b; Rafiq et al, 2016; Muangpratoom & Pattanadech, 2018; Oparanti et al, 2022).

Table 5 – Physicochemical characteristics and dielectric strength for high voltage engineering
Таблица 5 – Физико-химические характеристики и диэлектрическая прочность в области техники высоких напряжений
Табела 5 –Физичко-хемијске карактеристике и диелектрична снага у области енергетике високог напона

Oil samples	Flash point (°C)	Cloud point (°C)	Viscosity (cst)	Specific gravity	Density (g/cm^3)	Dielectric strength (kV)
Diesel	65	5	2.86	0.792	0.8162	20
Jatropha oil	150	14	8.2	0.848	0.725	22
Transformer oil	140	7	9.3	0.89	0.89	24

Table 6 – Partial (P_{ij}) and total preferable (P_t) probabilities of the physicochemical properties and dielectric strength of fluids
Таблица 6 – Частичная (Pij) и полная (Pt) предпочтительные вероятности физико-химических характеристик и диалектрической прочности жидкостей
Табела 6 – Делимичне (P_{ij}) и укупне (P_t) пожељне вероватноће физичко-хемијских карактеристика и диелектричне снаге флуида

Oil samples	(P_{ij}) of flash point	(P_{ij}) of cloud point	(P_{ij}) of viscosity	(P_{ij}) of specific gravity	(P_{ij}) of density	(P_{ij}) of dielectric strength	P_t*1000	Rank
Diesel	0.183	0.448	0.577	0.356	0.647	0.303	3.302	1
Jatropha oil	0.423	0.16	0.246	0.334	0.721	0.333	1.331	3
Transformer oil	0.395	0.384	0.177	0.317	0.587	0.364	1.817	2

Abeysundara et al (2001) produced a coconut oil, evaluated its performance characteristics and compared it with a standard oil for high voltage equipment. The properties of the two different oil types are presented in Table 7.

Table 7 – Properties of coconut oil and standard oil
Таблица 7 – Свойства кокосового масла и стандартного масел
Табела 7 – Својства кокосовог уља и стандардног уља

Oil type	Dielectric strength (kV)	Flash point (°C)	Moisture content (mg/Kg)	Viscosity (cst)	Density (Kg/dm^3)
Coconut oil	60	225	1	29	0.917
Standard oil	50	154	1.5	13	0.895

The multi-objective optimization analysis was done and presented in Table 8 based on the conditions in Table 1 and 2. It is interesting to note that the produced coconut oil exhibited a higher performance tendency for high voltage equipment compared to standard oil. This shows that it is a good candidate for high voltage engineering. Therefore, further study such as ageing, direct application of the oil in a typical high voltage equipment is recommended.

Table 8 – Partial (Pij) and total preferable (Pt) probabilities of the oil properties
Таблица 8 – Частичные (Pij) и полные (Pt) предпочтительные вероятности свойств масла
Табела 8 – Делимичне (Pij) и укупне (Pt) пожељне вероватноће својстава уља

Oil type	(Pij) of dielectric strength	(Pij) of flash point	(Pij) of moisture content	(Pij) of viscosity	(Pij) of density	Pt	Rank
Coconut oil	0.546	0.594	0.6	0.312	0.492	2.984	1
Standard oil	0.455	0.406	0.4	0.696	0.504	2.593	2

Conclusion

This study successfully introduced and employed a probability-based multi-response optimization technique in the selection of high voltage thermofluids. The results showed the possibility of the employment of the probability-based multi-objective optimization technique in the production and selection of high voltage equipment oil. It was found out that the nanofluid with 0.6 wt% Al_2O_3 is the most promising candidate for high voltage equipment compared to other produced fluids in the study of Oparanti et al (2021a). It is also noteworthy to state that coconut oil exhibited better performance efficiency compared to standard oil in the study of Abeysundara et al (2001). However, this study identifies that Jatropha oil produced by Garba et al (2013) was inadequate for high voltage equipment. Hence, preliminary study essential for the final usage

of 0.6 wt% Al_2O_3 nanofluids and coconut oil for high voltage equipment should be done while the performance characteristics of Jatropha oil for high voltage equipment should be improved. In conclusion, the multi-objective optimization technique has been successfully employed in the selection of fluids for high voltage equipment. It is clear from the study that the analysis is simple to apply. Hence, it is recommended that the probability multi-objective optimization technique be subsequently employed when selecting the most efficient fluid for high voltage equipment.

References

Abd-Elhady, A.M., Ibrahim, M.E., Taha, T.A. & Izzularab, M.A. 2018. Effect of temperature on AC breakdown voltage of nanofilled transformer oil. *IET Science, Measurement & Technology*, 12(1), pp.138-144. Available at: https://doi.org/10.1049/iet-smt.2017.0217.

Abeysundara, D.C., Weerakoon, C., Lucas, J.R., Gunatunga, K.A.I. & Obadage, K.C. 2001. Coconut oil as an alternative to transformer oil. *ResearchGate* [online]. Available at: https://www.researchgate.net/publication/268414369_Coconut_oil_as_an_alternative_to_transformer_oil [Accessed: 5 January 2022].

Abifarin, J.K. 2021. Taguchi grey relational analysis on the mechanical properties of natural hydroxyapatite: effect of sintering parameters. *The International Journal of Advanced Manufacturing Technology*, 117, pp.49-57. Available at: https://doi.org/10.1007/s00170-021-07288-9.

Abifarin, J.K., Fidelis, F.B., Abdulrahim, M.Y., Oyedeji, E.O., Nkwuo, T. & Prakash, C. 2022. Response Surface Grey Relational Analysis On The Manufacturing of High Grade Biomedical Ti-13Zr-13Nb (preprint). *The International Journal of Advanced Manufacturing Technology.* Available at: https://doi.org/10.21203/rs.3.rs-1225030/v1.

Abifarin, J.K. & Ofodu, J.C. 2022. Modeling and Grey Relational Multi-response Optimization of Chemical Additives and Engine Parameters on Performance Efficiency of Diesel Engine. *International Journal of Grey Systems,* in press. Available at: https://doi.org/10.52812/ijgs.33.

Abifarin, J.K., Olubiyi, D.O., Dauda, E.T. & Oyedeji, E.O. 2021c. Taguchi grey relational optimization of the multi-mechanical characteristics of kaolin reinforced hydroxyapatite: effect of fabrication parameters. *International Journal of Grey Systems*, 1(2), pp.20-32. Available at: https://doi.org/10.52812/ijgs.30.

Abifarin, J.K., Prakash, C. & Singh, S. 2021b. Optimization and significance of fabrication parameters on the mechanical properties of 3D printed chitosan/PLA scaffold. *Materials Today: Proceedings*. Available at: https://doi.org/10.1016/j.matpr.2021.09.386.

Abifarin, J.K., Suleiman, M.U., Abifarin, E.A., Fidelis, F.B., Oyelakin, O.K., Jacob, D.I. & Abdulrahim, M.Y. 2021a. Fabrication of mechanically enhanced hydroxyapatite scaffold with the assistance of numerical analysis. *The International Journal of Advanced Manufacturing Technology*, pp.1-14. Available at: https://doi.org/10.1007/s00170-021-08184-y.

Ashby, M.F. 2000. Multi-objective optimization in material design and selection. *Acta materialia*, 48(1), pp.359-369. Available at: https://doi.org/10.1016/S1359-6454(99)00304-3.

Ashby, M.F., Brechet, Y.J.M., Cebon, D. & Salvo, L. 2004. Selection strategies for materials and processes. *Materials & Design*, 25(1), pp.51-67. Available at: https://doi.org/10.1016/S0261-3069(03)00159-6.

Asse, J.B., Mengounou, G.M. & Imano, A.M. 2022. Impact of FeO3 on the AC breakdown voltage and acidity index of a palm kernel oil methyl ester based nanofluid. *Energy Reports*, 8, pp.275-280. Available at: https://doi.org/10.1016/j.egyr.2021.11.291.

Awodi, E., Ishiaku, U.S., Yakubu, M.K. & Abifarin, J.K. 2021. Experimentally Predicted Optimum Processing Parameters Assisted by Numerical Analysis on the Multi-physicomechanical Characteristics of Coir Fiber Reinforced Recycled High Density Polyethylene Composites (preprint). Available at: https://doi.org/10.21203/rs.3.rs-591200/v1.

Badicu, L.V., Dumitran, L.M., Notingher, P.V., Setnescu, R. & Setnescu, T. 2011. Mineral oil lifetime estimation using activation energy. In: *2011 IEEE International Conference on Dielectric Liquids*, Trondheim, Norway, pp.1-4, June 26-30. Available at: https://doi.org/10.1109/ICDL.2011.6015463.

Deshmukh, D. & Angira, M. 2019. Investigation on switching structure material selection for RF-MEMS shunt capacitive switches using Ashby, TOPSIS and VIKOR. *Transactions on Electrical and Electronic Materials*, 20(3), pp.181-188. Available at: https://doi.org/10.1007/s42341-018-00094-3.

Du, J.L., Huang, J., Hu, Y. & Wang, X.F. 2013. Determination of trace lead in beer by cloud point extraction-flame absorption spectrometry. *Science and Technology of Food Industry*, 11, pp.303-306 [online]. Available at: http://caod.oriprobe.com/articles/38800347/zhuo_dian_zuo_qu___huo_yan_yuan_zi_xi_shou_guang_pu_fa_ce_ding_pi_jiu_.htm [Accessed: 5 January 2022].

Garba, Z.N., Gimba, C.E., & Emmanuel, P. 2013. Production and characterisation of biobased transformer oil from Jatropha Curcas Seed. *Journal of Physical Science*, 24(2), p.49-61 [online]. Available at: https://jps.usm.my/jatropha-curcas-seed/ [Accessed: 5 January 2022].

Ghoneim, S.S., Dessouky, S. ., Boubakeur, A., Elfaraskoury, A.A., Abou Sharaf, A.B., Mahmoud, K., Lehtonen, M. & Darwish, M.M.F. 2021. Accurate Insulating Oil Breakdown Voltage Model Associated with Different Barrier Effects. *Processes*, 9(4), art.number:657. Available at: https://doi.org/10.3390/pr9040657.

Gong, H., Yu, B., Dai, F., Peng, Y. & Shao, J. 2018. Simulation on performance of a demulsification and dewatering device with coupling double fields: Swirl centrifugal field and high-voltage electric field. *Separation and*

Purification Technology, 207, pp.124-132. Available at: https://doi.org/10.1016/j.seppur.2018.06.049.

Hosier, I.L., Guushaa, A., Vaughan, A.S. & Swingler, S.G. 2009. Selection of a suitable vegetable oil for high voltage insulation applications. *Journal of Physics: Conference Series*, 183(1), art.ID:012014. Available at: https://doi.org//10.1088/1742-6596/183/1/012014.

Hosier, I.L., Vaughan, A.S. & Montjen, F.A. 2006. Ageing of biodegradable oils for high voltage insulation systems. In: *2006 IEEE Conference on Electrical Insulation and Dielectric Phenomena*, Kansas City, MO, USA, pp. 481-484, October 15-18. Available at: https://doi.org/10.1109/CEIDP.2006.311974.

Jin, H., Andritsch, T., Tsekmes, I.A., Kochetov, R., Morshuis, P.H. & Smit, J.J. 2014. Properties of mineral oil based silica nanofluids. *IEEE Transactions on Dielectrics and Electrical Insulation*, 21(3), pp.1100-1108. Available at: https://doi.org/10.1109/TDEI.2014.6832254

Kumar, S.S., Iruthayarajan, M.W. & Bakrutheen, M. 2014. Analysis of vegetable liquid insulating medium for applications in high voltage transformers. In: *2014 International Conference on Science Engineering and Management Research (ICSEMR)*, Chennai, India, pp.1-5, November 27-29. Available at: Available at: https://doi.org/10.1109/ICSEMR.2014.7043606.

Lee, J.C., Seo, H.S. & Kim, Y.J. 2012. The increased dielectric breakdown voltage of transformer oil-based nanofluids by an external magnetic field. *International Journal of Thermal Sciences*, 62, pp.29-33. Available at: https://doi.org/10.1016/j.ijthermalsci.2012.03.013

Lin, C.M., Herianto, S., Syu, S.M., Song, C.H., Chen, H.L. & Hou, C.Y. 2021. Applying a large-scale device using non-thermal plasma for microbial decontamination on shell eggs and its effects on the sensory characteristics. *LWT*, 142, art.ID:111067. Available at: https://doi.org/10.1016/j.lwt.2021.111067.

Liu, J., Fan, X., Zhang, Y., Zheng, H. & Jiao, J. 2020. Temperature correction to dielectric modulus and activation energy prediction of oil-immersed cellulose insulation. *IEEE Transactions on Dielectrics and Electrical Insulation*, 27(3), pp.956-963. Available at: https://doi.org/10.1109/TDEI.2019.008530.

Liu, J., Fan, X., Zheng, H., Zhang, Y., Zhang, C., Lai, B., Wang, J., Ren, G. & Zhang, E. 2019. Aging condition assessment of transformer oil-immersed cellulosic insulation based upon the average activation energy method. *Cellulose*, 26(6), pp.3891-3908. Available at: https://doi.org/10.1007/s10570-019-02331-1.

Minkner, R. & Schmid, J. 2022. *The Technology of Instrument Transformers. Current and Voltage Measurement and Insulation Systems.* Springer Fachmedien Wiesbaden. Available at: https://doi.org/10.1007/978-3-658-34863-2. ISBN: 978-3-658-34863-2.

Muangpratoom, P. & Pattanadech, N. 2018. Breakdown and partial discharge characteristics of mineral oil-based nanofluids. *IET Science, Measurement & Technology*, 12(5), pp.609-616. Available at: https://doi.org/10.1049/iet-smt.2017.0080.

Ofodu, J.C. & Abifarin, J.K. 2021. Physicochemical and dissolved gas analysis of an in-service transformer oils in Benin, Edo State, Nigeria. *Journal of Applied Sciences and Environmental Management*, in press.

Oparanti, S.O., Abdelmalik, A.A., Khaleed, A.A., Abifarin, J.K., Suleiman, M.U. & Oteikwu, V.E. 2022. Synthesis and characterization of cooling biodegradable nanofluids from non-edible oil for high voltage application. *Materials Chemistry and Physics*, 277, art.ID:125485. Available at: https://doi.org/10.1016/j.matchemphys.2021.125485.

Oparanti, S.O., Khaleed, A.A. & Abdelmalik, A.A. 2021a. Nanofluid from Palm Kernel Oil for High Voltage Insulation. *Materials Chemistry and Physics*, 259, art.ID:123961. Available at: https://doi.org/10.1016/j.matchemphys.2020.123961.

Oparanti, S.O., Khaleed, A.A. & Abdelmalik, A.A. 2021b. AC breakdown analysis of synthesized nanofluids for oil-filled transformer insulation. *The International Journal of Advanced Manufacturing Technology*, 117(5), pp.1395-1403. Available at: https://doi.org/10.1007/s00170-021-07631-0.

Oparanti, S.O., Khaleed, A.A., Abdelmalik, A.A. & Chalashkanov, N.M. 2020. Dielectric characterization of palm kernel oil ester-based insulating nanofluid. In: *2020 IEEE Conference on Electrical Insulation and Dielectric Phenomena (CEIDP)*, East Rutherford, NJ, USA, pp.211-214, October 18-30. Available at: https://doi.org/10.1109/CEIDP49254.2020.9437477.

Oyelaran, O.A., Bolaji, B.O. & Samuel, O.D. 2020. Assessment of calabash seed oil as biobased insulating fluid for power transformers. *Journal of Chemical Technology and Metallurgy*, 55(2), pp.307-313 [online]. Available at: http://repository.fuoye.edu.ng/handle/123456789/2317 [Accessed: 5 January 2022].

Peppas, G.D., Bakandritsos, A., Charalampakos, V.P., Pyrgioti, E.C., Tucek, J., Zboril, R. & Gonos, I.F. 2016a. Ultrastable Natural Ester-Based Nanofluids for High Voltage Insulation Applications. *ACS Applied Materials & Interfaces*, 8(38), pp.25202-25209. Available at: https://doi.org/10.1021/acsami.6b06084.

Peppas, G.D., Charalampakos, V.P., Pyrgioti, E.C., Danikas, M.G., Bakandritsos, A. & Gonos, I.F. 2016b. Statistical investigation of AC breakdown voltage of nanofluids compared with mineral and natural ester oil. *IET Science, Measurement & Technology*, 10(6), pp.644-652. Available at: https://doi.org/10.1049/iet-smt.2016.0031.

Rafiq, M., Lv, Y. & Li, C. 2016. A review on properties, opportunities, and challenges of transformer oil-based nanofluids. *Journal of nanomaterials*, 2016, art.ID 8371560. Available at: https://doi.org/10.1155/2016/8371560.

Sitinjak, F., Suhariadi, I. & Imsak, L. 2003. Study on the characteristics of palm oil and it's derivatives as liquid insulating materials. In: *Proceedings of the 7th International Conference on Properties and Applications of Dielectric Materials (Cat. No. 03CH37417)*, Nagoya, Japan, 2, pp.495-498, June 1-5. Available at: https://doi.org/10.1109/ICPADM.2003.1218461.

Srinivasa, D.M. & Surendra, U. 2019. Comparative study of breakdown phenomena and viscosity in liquid dielectrics. In: *2019 Innovations in Power and*

Advanced Computing Technologies (i-PACT), Vellore, India, 1, pp.1-4, March 22-23. Available at: https://doi.org/10.1109/i-PACT44901.2019.8960134.

Wang, Y. & Teng, H. 2021. A New" Intersection" Method for Multi-Objective Optimization in Material Selection. *Tehnički glasnik*, 15(4), pp.562-568. Available at: https://doi.org/10.31803/tg-20210901142449.

Yaacob, M.M. & Alsaedi, M.A. 2015. Use palm oil as alternative with insulation oil in high voltage equipment. *Physical Science International Journal*, 5(3), pp.172-178 [online] Available at: https://www.journalpsij.com/index.php/PSIJ/article/view/23629 [Accessed: 5 January 2022].

Zhang, M., Li, L., Liu, H., Jia, H., Liu, J. & Meng, F. 2021. Method for quantitative assessment of transformer oil-paper insulation non-uniform ageing parameters based on frequency domain dielectric response. *IET Science, Measurement & Technology*. Available at: https://doi.org/10.1049/smt2.12091.

Zheng, M. 2022. Application of probability-based multi-objective optimization in material engineering. *Vojnotehnički glasnik/Military Technical Courier*, 70(1), pp.1-12. Available at: https://doi.org/10.5937/vojtehg70-35366.

ПРИМЕНЕНИЕ ОПТИМИЗАЦИИ С НЕСКОЛЬКИМИ ВЫХОДАМИ, ОСНОВАННОЙ НА ВЕРОЯТНОСТИ, ДЛЯ ЖИДКИХ ТЕПЛОНОСИТЕЛЕЙ ВЫСОКОВОЛЬТНОГО ОБОРУДОВАНИЯ

Джозеф Чуквука Офоду[а], *Джонсон Кехинде* Абифарин[б]

[а] Университет Порт-Харкорта, инженерный факультет, кафедра машиностроения, г. Чоба, штат Риверс, Федеративная Республика Нигерия

[б] Университет Ахмаду Белло, инженерный факультет, кафедра машиностроения, г. Зария, Федеративная Республика Нигерия, **корреспондент**

РУБРИКА ГРНТИ: 30.17.00 Механика жидкости и газа,
47.09.00 Материалы для электроники и радиотехники
ВИД СТАТЬИ: оригинальная научная статья

Резюме:

Введение/цель: Исследователи, занимающиеся жидкостями, предназначенными для использования в технике высоких напряжений, зачастую сталкиваются с проблемами при выборе или при рекомендации соответствующей жидкости, подходящей для использования в технике высоких напряжений. Это связано с двойной функциональностью жидкостей, необходимых для высоковольтного оборудования.

Методы: В данной статье представлен и применен метод многоцелевой оптимизации, основанный на вероятности, при выборе теплоносителя для высоковольтного оборудования. В

зависимости от ожидаемых характеристик масла применялись индексы предпочтительной вероятности полезности, типа «чем больше, тем лучше» и «чем меньше, тем лучше».

Результаты: Результаты исследования показали, что наножидкость с содержанием 0.6 wt% Al_2O_3 является наиболее перспективным кандидатом для высоковольтного оборудования по сравнению с другими испытанными жидкостями. Также важно отметить, что кокосовое масло показало лучшие результаты по сравнению со стандартным маслом. В ходе исследования также выявлено, что выработанное масло ятрофы непригодно для высоковольтного оборудования.

Выводы: Рекомендуется провести предварительное исследование, необходимое для конечного использования наножидкостей с содержанием 0.6 wt% Al_2O_3, а также кокосового масла в технике высокого напряжения. Также рекомендуется улучшить характеристики масла, выработанного из растения ятрофа для использования в технике высокого напряжения.

Ключевые слова: оптимизация предпочтительной вероятности, высоковольтное оборудование, теплоносители, физико-химические свойства, диэлектрическая прочность.

ПРИМЕНА ОПТИМИЗАЦИЈЕ СА ВИШЕ ИЗЛАЗА ЗАСНОВАНЕ НА ВЕРОВАТНОЋИ ФЛУИДА ДА ПРЕНОСЕ ТОПЛОТУ У ВИСОКОНАПОНСКОЈ ОПРЕМИ

Џосеф Чуквука Офоду[а], *Џонсон Кехинде* Абифарин[б]

[а] Универзитет у Порт Харкорту, Факултет техничких наука, одсек за машинство, Чоба, Држава Риверс, Савезна Република Нигерија

[б] Универзитет Ахмаду Белло, Факултет техничких наука, одсек за машинство, Зариа, Савезна Република Нигерија, **аутор за преписку**

ОБЛАСТ: машинство, материјали
ВРСТА ЧЛАНКА: оригинални научни рад

Сажетак:

Увод/циљ: При избору одговарајућег флуида погодог за примену у високонапонској опреми наилази се на проблеме. Узрок томе је двострука функционалност флуида која се захтева за високонапонску опрему.

Методе: Овај рад уводи и примењује технику вишециљне оптимизације засноване на вероватноћи приликом селекције флуида за пренос топлоте у високонапонској опреми. Индекси корисности пожељне вероватноће типа „што више – то боље" и

типа „што мање – то боље" примењени су зависно од жељених карактеристика уља.

Резултати: Показано је да је нанофлуид са 0,6 wt% Al_2O_3 најпогоднији за високонапонску опрему у односу на остале разматране произведене флуиде. Важно је поменути да је кокосово уље показало боље перформансе у поређењу са стандардним уљем. Указано је, такође, и да произведено уље биљке Jatropha није погодно за високонапонску опрему.

Закључак: Препоручује се прелиминарна студија, неопходна за крајње коришћење нанофлуида са 0,6 wt% Al_2O_3,као и кокосовог уља за високонапонску опрему. Такође, препорука је да се побољшајукарактеристике уља биљке Jatropha ради коришћења у високонапонској опреми.

Кључне речи: оптимизација пожељне вероватноће, високонапонска опрема, флуиди за пренос топлоте, физичко-хемијска својства, диелектрична снага.

Paper received on / Дата получения работы / Датум пријема чланка: 06.01.2022.
Manuscript corrections submitted on / Дата получения исправленной версии работы / Датум достављања исправки рукописа: 10.03.2022.
Paper accepted for publishing on / Дата окончательного согласования работы / Датум коначног прихватања чланка за објављивање: 12.03.2022.

INFLUENCE OF HEAT INPUT ON THE TENSILE PROPERTIES OF AUSTENITIC-FERRITIC WELDED JOINTS

Aleksandar G. Bukvić[a], *Dalibor* P. Petrović[b], *Igor* Z. Radisavljević[c], *Saša* S. Dimitrić[d]

[a] University of Defense in Belgrade, Military Academy, Belgrade, Republic of Serbia,
e-mail: a_bukvic@yahoo.com, **corresponding author**,
ORCID iD: https://orcid.org/0000-0002-3025-8446

[b] University of Defense in Belgrade, Military Academy, Belgrade, Republic of Serbia,
e-mail: dalibor.petrovic140@gmail.com,
ORCID iD: https://orcid.org/0000-0001-6092-5695

[c] Ministry of Defense of the Republic of Serbia, Military Technical Institute, Belgrade, Republic of Serbia,
e-mail: radisavljevicigorbg@gmail.com,
ORCID iD: https://orcid.org/0000-0002-8523-0993

[d] University of Defense in Belgrade, Military Academy, Belgrade, Republic of Serbia,
e-mail: sasa.dimitric@mod.gov.rs,
ORCID iD: https://orcid.org/0000-0003-3547-7047

DOI: 10.5937/vojtehg70-36252; https://doi.org/10.5937/vojtehg70-36252

FIELD: Mechanical engineering, Mechanical materials
ARTICLE TYPE: Original scientific paper

Abstract:

Introduction/purpose: During exploitation tests of gasoline storage tanks, cracks can form in an austenitic-ferrite welded joint, which can compromise the entire tank.

Methods: In order to obtain a welded joint of satisfactory strength and durability, the paper analyzes the influence of heat input on the tensile characteristics of welded joints. In the current literature and practice, additional materials for welding the tank elements are selected according to the chemical compositions of the elements of basic materials, with the help of the Schaeffler diagram. In this paper, the characteristics of welded joints of gasoline storage tanks are examined, when the largest part of the tank is made of fine - grained microalloyed steel NIOMOL 490 K, while the roof part of the tank is made of austenitic steel. Slabs of these two materials were welded by the MIG process with additional material MIG 18/8/6, at different amounts of heat input.

Conclusion: The analysis of the results obtained by tensile testing according to SRPS EN ISO 6892-1: 2020 standard concluded that the behavior of the joint as a whole depends on the properties of each individual part of the welded joint and their mutual influence. It was also concluded that the mutual influence is better if welding is performed with a lower amount of heat input, because then a lower degree of mixing of additional material with basic materials is achieved.

Key words: austenitic-ferritic welded joint, strength, plasticity.

Introduction

Lack of storage space and obsolescence of the existing tanks for storage of petroleum products call for a rapid construction of new tanks. When designing new tanks, in addition to choosing adequate construction materials, it is necessary to perform adequate welding of the structure, so that during operation there would be no cracks that could lead to accidents with large financial losses and harmful effects on the environment (Jovičić et al, 2006).

In this paper, the characteristics of welded joints are analyzed on the example of tanks whose mantle and battom are made of microalloyed steel S500NL1, under the commercial name NIOMOL 490K, 16 mm thick. The roof covering is made of high-alloy austenitic steel X7CrNiNb18.10 according to EN 10088 (Č.4574 according to JUS C.B0.600) standard, 12 mm thick (Bukvić, 2012).

During exploitation maintenance, cracks were discovered in the welded joint of the casing and the roof covering. The X-ray reveals the cracks shown in Figure 1. Two cracks parallel to the fusion line and two cracks extending radially to the fusion line can be seen in the figure. Cracks parallel to the fusion line are found in the base materials. In welded joints of microalloyed steels, cracks usually occur in the heat affected zone (HAZ) due to structural changes caused by welding. In this case, cracks appeared in the base material, far from the zone in which structural changes occurred during welding. Crack positions indicate that in the combination of the three materials that make up the welded joint, the high-alloy austenitic steel material X7CrNiNb18.10 is weakest when the highest heat input values are entered, and that in the case of the lowest heat input, the base metal S500NL1 is the weakest link.

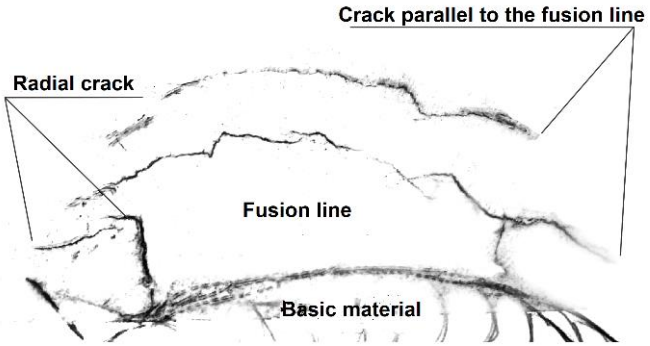

Figure 1 – X-ray of the cracked joint
Рис. 1 – Рентгеновский снимок треснувшего соединения
Слика 1 – Рендгенски снимак споја са прслинама

The metal weld structure of heterogeneous compounds can be roughly predicted using the Schaeffler diagram (Bukvić, 2012). Based on the calculated values of the Cr and Ni equivalents, the position points of the base materials and weld metals are plotted in the Schaeffler diagram shown in Figure 2.

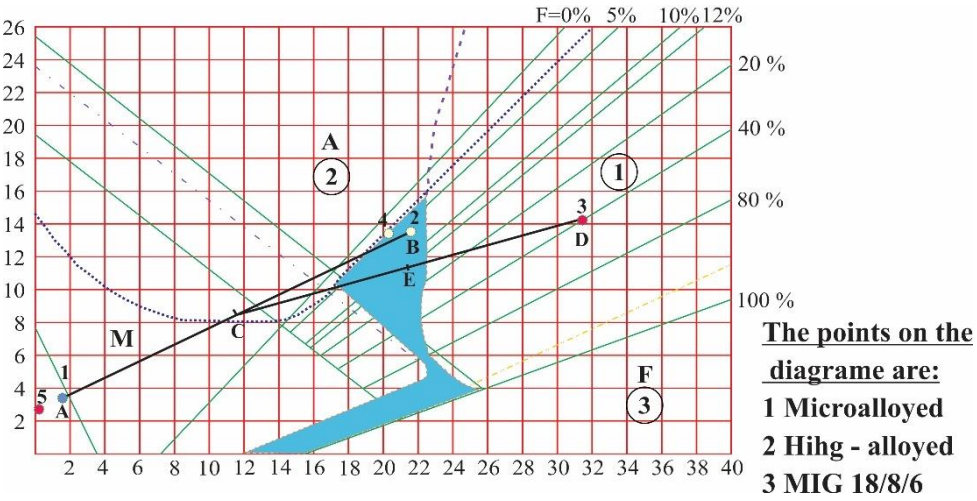

Figure 2 – Positions of the points of the basic and additional materials in the Schaeffler diagram
Рис. 2 – Положения точек основного и дополнительного материалов на диаграмме Шеффлера
Слика 2 – Положаји тачака основних и додатних материјала у Шефлеровом дијаграму

The chemical composition of the weld metal and its structure are chosen on the basis of the Schaeffler diagram so that they are in an area where there is no tendency to defects (hot cracks, martensite formation, brittleness due to grain growth and σ-phase separation). However, the chemical composition of the weld metal is not unique, but represents a series of chemical compositions created by melting the basic materials and the additional material. This is especially pronounced with multi-pass seams.

Welding technology

In order to determine the adequate welding technology which would avoid the appearance of cracks in the welded joint, samples of two welded plates were used. These two experimental plates, marked with numbers 1 and 2, were obtained by welding the basic materials from which the tank was made (microalloyed and high alloy steel). Table 1 shows the chemical compositions of the basic materials.

Table 1 – Chemical composition of the basic materials
Таблица 1 – Химический состав основных материалов
Табела 1 – Хемијски састав основних материјала

Steel	C	Si	Mn	P	S	Cr	Ni	Cu	Al	Mo	Ti	V	Nb
microalloyed	0.10	0.38	0.66	0.014	0.02	0.76	0.10	-	-	0.33	-	0.02	-
high alloy	0,04	0.35	1.73	0.031	0.004	17.9	11.6	0.18	0.061	2.16	0.38	0.079	0.016

Both plates are welded by the MIG process with additional material MIG 18/8/6, but with different amounts of heat input. The selected welding process and the additional material are identical to the connection to which the roof cover and the tank casing are connected. The chemical composition and the mechanical properties of the additional material are given in Tables 2 and 3.

Table 2 – Chemical compositions of the additional material MIG 18/8/6
Таблица 2 – Химические составы дополнительного материала MIG 18/8/6
Табела 2 – Хемијски састави додатног материјала МИГ 18/8/6

	C	Si	Mn	Cr	Ni
MIG 18/8/6	0.08	<1.0	7	18.5	9

Table 3 – Mechanical properties of the pure metal weld from the selected additional material
Таблица 3 – Механические свойства чистого металла сварного шва из выбранного дополнительного материала
Табела 3 – Механичке особине чистог метал шава од одабраног додатног материјала

	R_e, [N/mm^2]	R_m, [N/mm^2]	A_5, [%]	KV,[J]	
MIG 18/8/6	> 380	560 do 660	35	> 40 (at 20 ^{0}C)	

The additional material MIG 18/8/6 is recommended in (Jesenice Ironworks, 2005) in which a high-alloy additional material was used for welding various steels. This choice of additional material is also indicated by the data from the Schaeffler diagram, Figure 2. When choosing the additional material, it was taken into account that it has different values of yield stress and tensile strength in relation to the basic materials. A mixture of Ar gases and 2% O2 was used as a protective atmosphere during welding with the chemical composition given in Table 4.

Table 4 – Chemical composition of the gas mixtures
Таблица 4 – Химический состав газовых смесей
Табела 4 – Хемијски састав мешавина гаса

Content of components in the mixture [vol%]	
O_2	Ar
2.00	Rest

Welding is performed by the electric arc semi-automatic MIG / MAG process, bearing in mind that in recent years the use of the semi-automatic MIG / MAG welding process is increasingly common compared to other welding processes in steel structures.

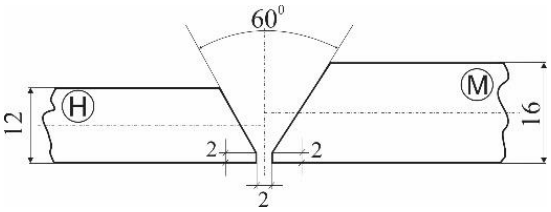

Figure 3 – Shape and dimensions of the "Y" groove
Рис. 3 – Форма и размеры канавки "Y"
Слика 3 – Облик и димензије „Y" жлеба

The MIG / MAG welding device KEMPACT 3000+ FastMig 400 was used for welding. The preheating temperature of 60 ^{0}C and the intermediate temperature of 60 ± 10 ^{0}C were adopted (Bukvić, 2012).

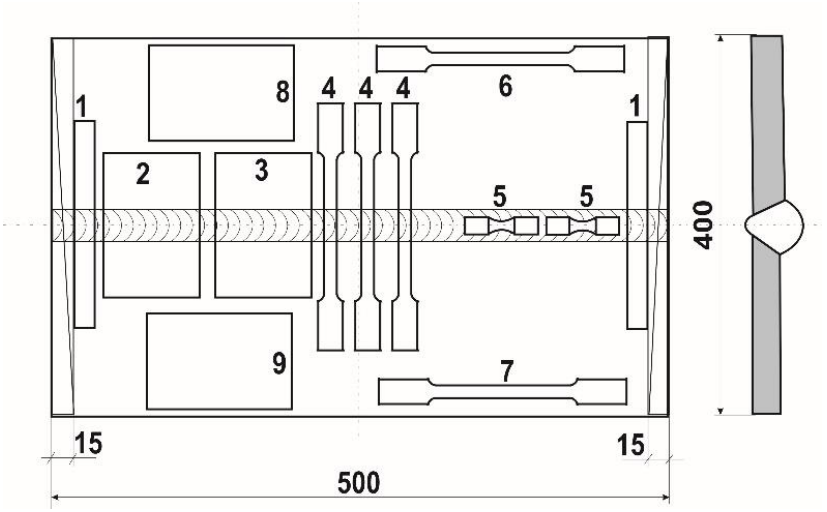

Figure 4 – Appearance of the welded plate scheme and the test tube cutting plan
Рис. 4 – Вид схемы сварной пластины и план резки эпруветки
Слика 4 – Изглед шеме заварених плоча и план исецања епрувета

The obtained welded experimental plates 1 and 2 have dimensions of 500 x 400 mm with the "Y" groove, as shown in Figure 3. Test tubes were cut from the obtained plates and the scheme of cutting tubes from the welded plates for testing the characteristics of strength, plasticity, as well as for microstructural tests and hardness tests, is shown in Figure 4.

The plates were preheated and the intermediate temperatures were maintained by heating with oxygen and acetylene. Preheating temperatures and intermediate temperatures were controlled by a contact thermometer. Figure 5 shows the layout of laying the additional material during the welding of experimental plates 1 and 2.

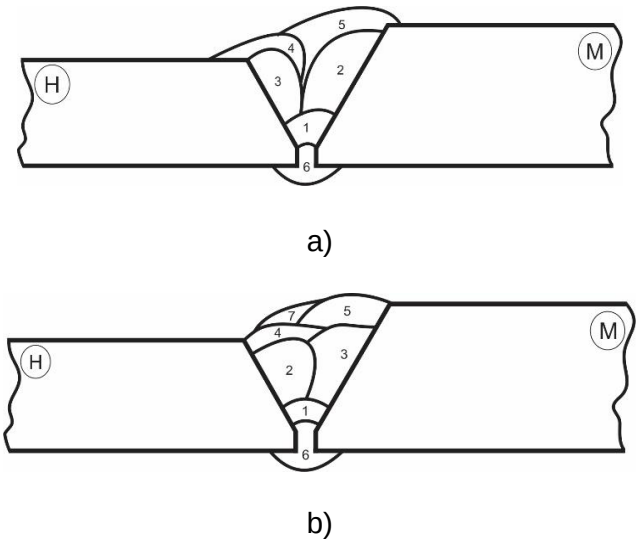

Figure 5 – Welded joint layout diagram for plates 1 and 2:
a) scheme of laying the additional material for plate 1
b) scheme of laying the additional material for plate 2
Рис. 5 – Схема расположения соединений свариваемых пластин 1 и 2:
а) схема сварного соединения пластины 1
б) схема сварного соединения пластины 2
Слика 5 – Шема завареног споја за плоче 1 и 2:
а) шема завареног споја за плочу 1,
б) шема завареног споја за плочу 2

Plate 1 was welded at an average value of the amount of heat input of 8.88 [kJ / cm], as indicated in the last column of Table 5. The upper (maximum) limit value of the amount of heat input for the selected welding process was used for welding this plate and the additional material.

Plate 2 was welded at an average heat input of 6.87 [kJ / cm] (see last column of Table 6). In plate 2, welding was performed with the lower (minimum) limit value of the amount of heat input for the selected welding procedure and the additional material.

Welding procedures are described in the literature (Bukvić, 2012) for both welded plates.

After welding, plates 1 and 2 were inspected and subjected to non-destructive testing. Radiographic irradiation with γ-rays did not reveal any defects in the joints, such as: cracks, porosity, non-penetration, sticking, edge joints and the like.

Table 5 – Passages when welding plate 1 with the amounts of heat input
Таблица 5 – Проходы при сварке пластины 1 с учетом количества подведенного тепла
Табела 5 – Пролази при заваривању плоче 1 са количинама унете топлоте

Marking of welding plates and wires	Serial number of welding	Welding		Strength electricity [A]	Voltage [V]	Amount of heat input [kJ/cm]		
		Time [min.]	Speed [cm/min]			Calculated	Real [η=0,6]	Average
Plate 1. wire 18/8/6	1 root	3.30	15.2	132	18.9	9.85	5.91	*8.88*
	2 to M	2.12	23.6	228	27.6	16.00	9.60	
	3 to H	2.33	21.5	237	28.0	18.52	11.11	
	4 to M	2.12	23.6	240	28.3	17.27	10.36	
	5 to H	2.13	23.5	235	28.3	18.06	10.84	
	6 root*	1.33	37.6	210	27.1	9.08	5.45	

* *root canal ground and re-welded (marked with 6 root)*

Table 6 – Passages when welding plate 2 with the amounts of heat input
Таблица 6 – Проходы при сварке пластины 2 с учетом количества подведенного тепла
Табела 6 – Пролази при заваривању плоче 2 са количинама унете топлоте

Marking of welding plates and wires	Serial number of welding	Welding		Strength electricity [A]	Voltage [V]	Amount of heat input [kJ/cm]		
		Time [min.]	Speed [cm/min]			Calculate	Real [η=0.6]	Average
Plate 2. wire 18/8/6	1roof	3.55	14.1	135	18.8	10.80	6.48	6.87
	2 ka M	1.73	28.9	218	27.2	12.31	7.39	
	3 ka H	1.75	28.6	230	27.6	13.32	7.99	
	4 ka H	1.37	36.5	230	27.6	10.44	6.26	
	5 ka M	1.88	26.6	220	27.3	13.55	8.13	
	6 root*	1.42	35.2	210	27.1	9.70	5.82	
	7central	1.43	35.0	215	27.2	10.03	6.02	

* *root canal ground and re-welded (marked with 6 root)*

Test results

The tensile strength test of the welded joint was performed according to SRPS EN ISO 6892-1: 2020 on smooth flat tubes with parallel sides. The test was performed on a SCHENCK – TREBEL RM 100 ripper. As the plates of both base materials were of different thicknesses (12 and 16 mm), the tubes were machined and reduced to the same thickness to a thinner plate (12mm) to obtain consistent results before the test.

For comparison, the tensile test tubes were cut from the plates of basic materials. Based on the obtained results ($F_{0,2}$, F_m), the resistance properties were calculated: the yield stress $R_{0,2}$ and the tensile strength R_m. The deformation properties were also determined: the elongation A and the contraction Z. Table 7 lists the mechanical properties of microalloyed and high alloy steel.

Table 7 – Mechanical properties of microalloyed and high alloy steel
Таблица 7 – Механические свойства микролегированной и высоколегированной стали
Табела 7 – Механичка својства микролегираног и високолегираног челика

Test tube	Yield stress $R_{0,2}$ [MPa]	Tensile strength R_m[MPa]	Elongation A [%]	Contraction Z [%]
Microalloyed	497	582	21	63
High-alloy	308	573	37	53

Figure 6 shows the σ – ε diagrams for a) microalloyed and b) high-alloy steel.

For microalloyed steel, the σ – ε diagram with a pronounced yield strength was obtained, and for high-alloy steel, the obtained diagram was without a pronounced yield strength.

Two test tubes (Figure 4, test tube number 5) were cut from both plates in the part of the metal seam for tensile characteristics tests. The results of testing the tensile properties of the metal seams for both plates are shown in Table 8.

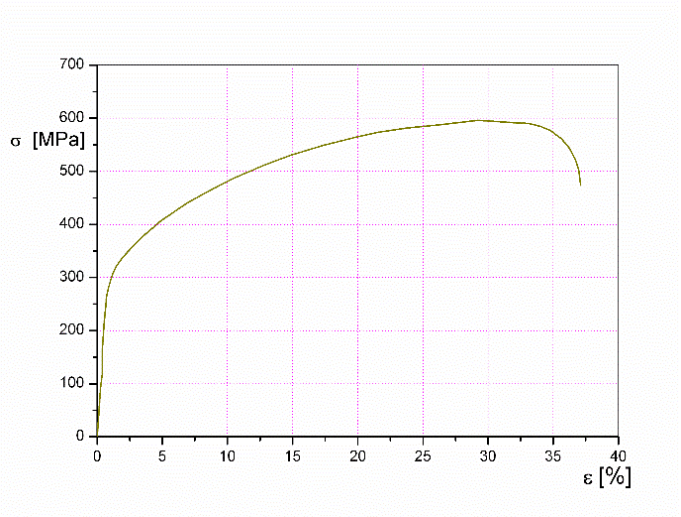

a)

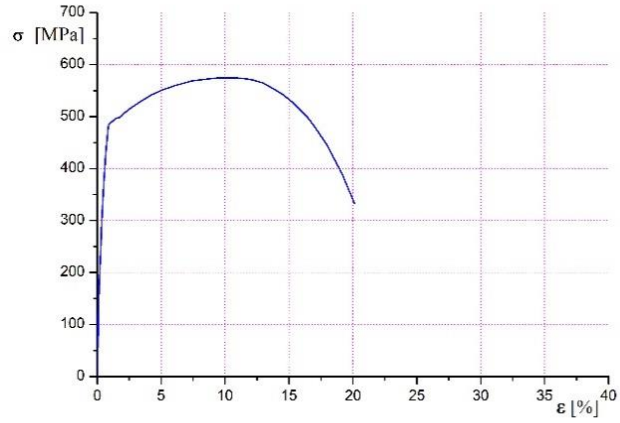

b)

Figure 6 – σ – ε diagrams for the base materials:
a) Microalloyed steel NIOMOL 490K, b) High-alloy steel X7CrNiNb18.10

Рис. 6 − Диаграммы σ – ε основных материалов:
а) Микролегированная сталь NIOMOL 490K,
б) Высоколегированная сталь X7CrNiNb18.10

Слика 6 – Дијаграми σ–ε за основне материјале:
а) микролегирани челик NIOMOL 490K,
б) високолегирани челик X7CrNiNb18.10.

Table 8 – Tensile characteristics of the metal welded tubes on the welded plates
Таблица 8 – Характеристики растяжения эпроветки металлических сварных швов на сварных пластинах
Табела 8 – Затезне карактеристике епрувета из метал шава по завареним плочама

Plate	Label on the test tube	Yield stress $R_{p0,2}$ [MPa]		Tensile strength R_m [MPa]		Elongation A [%]	
		$R_{p0,2}$	average value	R_m	average value	A	average value
1	A-2.1	473	466	678	682	43	42
	A-2.4	458		685		41	
2	A-2.2	450	443	678	693	39	39
	A-2.3	436		707		38	

As it can be seen in Table 8, the obtained yield stresses Rp0.2 and the tensile strengths Rm of the metal weld for plates 1 and 2 are similar. This is expected according to (Bukvić, 2012; Kassner, 2015), having in mind that the same basic materials and the same additional material MIG 18/8/6 were used.

After that, three tubes with the marks: 1.1, 1.2 and 1.3 were cut from plate 1, from the part of the plate where the welded joint is located (Figure 4, tubes under number 4). The test results of the joint specimens for plate 1 are given in Table 9, while the σ – ε diagram is shown in Figure 7.

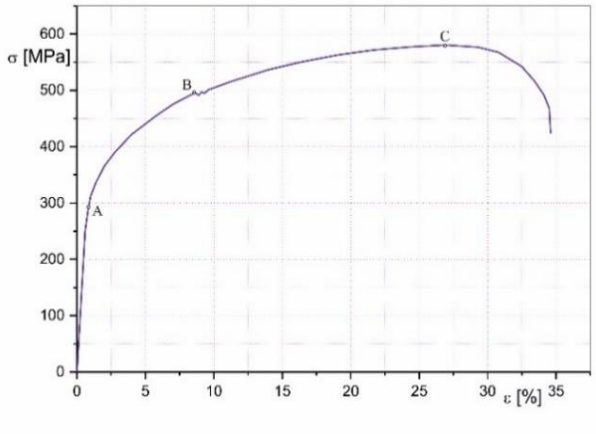

Figure 7 – Diagram σ – ε for test tube 1.1
Рис. 7 – Диаграмма σ – ε эпроветки 1.1
Слика 7 – Дијаграм σ–ε за епрувету 1.1

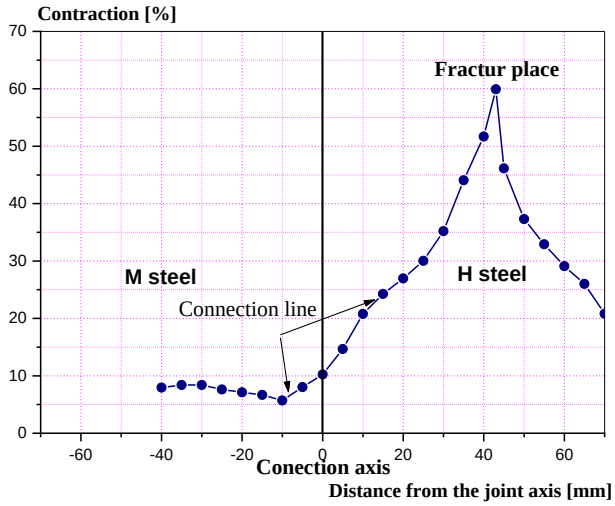

Figure 8 – Change in the contractions of the tube cross section 1.1
Рис. 8 – Изменение сужений поперечного сечения эпроветки 1.1
Слика 8 – Промена контракција попречног пресека епрувете 1.1

Figure 8 shows the change in the contraction of the cross section of test tube 1.1 along its measuring part, and Figure 9 shows the appearance of test tube 1.1 after tearing. The fracture of the test tube is accompanied by uneven deformation of the measured length.

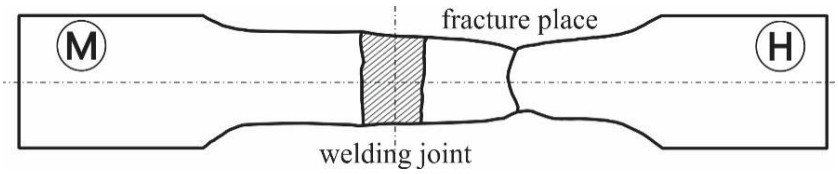

Figure 9 – Test tube 1.1 after tearing
Рис. 9 – Эпроветка 1.1 после разрыва
Слика 9 – Епрувета 1.1 након кидања

The tensile characteristics results for plate 1 for all three tested specimens are shown in Table 9. The points A, B and C are the characteristic points of the σ – ε diagram for specimen 1.1 (see Figure 7).

Table 9 – Tensile characteristics of plate joint tubes 1
Таблица 9 – Характеристики растяжения эпроветки соединения пластины 1
Табела 9 – Затезне карактеристике епрувета споја из плоче 1

Test tube number	Yield stress at the point A [MPa]		Stress at the point B [MPa]		Tensile strength at the point C [MPa]		ε [%]	
	R_A	average value	R_B	average value	R_C	average value		average value
1.1	295	308	495	497	580	573	35	34
1.2	311		495		566		35	
1.3	318		500		574		32	

The mean stress at the point A is 308 MPa, at the point B it is 497 MPa, and at the point C it is 573 MPa, as shown in Table 9. The mean percentage elongation of the tubes is 34%. The fracture occurred in high-alloy steel in all three tubes.

Table 10 compares the stresses at the characteristic points A, B and C of the σ – ε diagram for tube 1.1, according to Figure 7 and Table 9, and the mean stress values for the base materials and the value deviations.

Table 10 – Stress at the characteristic points of the σ – ε diagram for test tube 1.1
Таблица 10 – Напряжение в характерных точках диаграммы σ – ε эпроветки 1.1
Табела 10 – Напон у карактеристичним тачкама дијаграма σ–ε за епрувету 1.1

Stress at the characteristic points A. B i C		Characteristic stress values for basic materials		Deviation Δ R [MPa]	Deviation [%]
Mark	Average stress value. table 9	Mark. table 8	average value stress		
R_A	308	$R_{p0.2}$ steel H	324	16	4.9
R_B	497	$R_{p0.2}$ steel M	491	8	1.6
R_C	573	R_m steel H	595	22	3.4

Observing the changes in cross-sectional contractions along the measuring part of the test tube (Figure 8), it can be seen that the weld metal has a higher cross-sectional contraction than microalloyed steel and the HAZ towards microalloyed steel. The smallest contraction (about 6%) occurs at the fusion line of the metal weld and the microalloyed steel. Fracture occurs in high-alloy steel approximately half the measuring length of the plate 1 tube. The narrowing towards the melting line from the middle of the measuring tube is greater on the high-alloy steel side than the narrowing towards the melting line with the microalloyed steel. The

measurement showed a greater narrowing of the measuring part of the test tube on the high-alloy steel side than the measuring part of the test tube on the micro-alloy steel side.

Three tubes with the marks: 2.1, 2.2 and 2.3 were cut from plate 2, from the part of the plate in which the welded joint is located (Figure 4, tubes under number 4). The test results of the joint test tubes for plate 2 are given in Table 11, while the σ – ε diagram is shown in Figure 10.

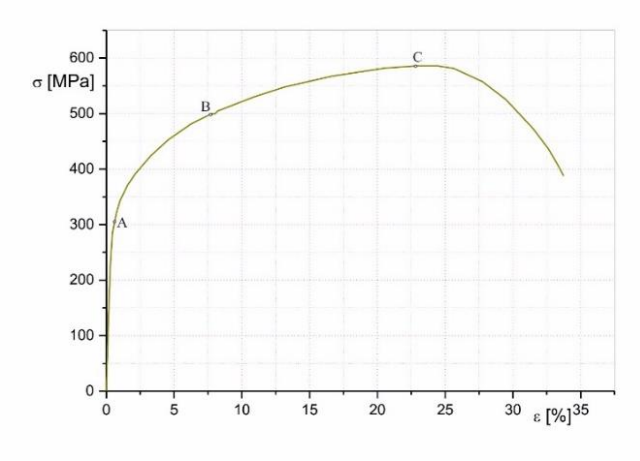

Figure 10 – Diagram σ – ε for test tube 2.1
Рис. 10 – Диаграмма σ – ε эпроветки 2.1
Слика 10 – Дијаграм σ–ε за епрувету 2.1

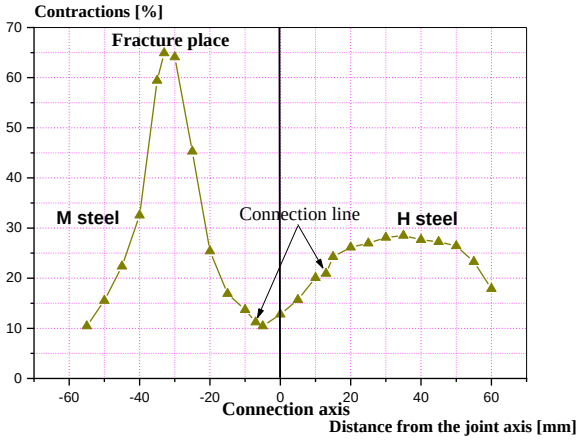

Figure 11 – Change of the contractions of the tube cross-section 2.1
Рис. 11 – Изменение сужений поперечного сечения эпроветки 2.1
Слика 11 – Промена контракција попречног пресека епрувете 2.1

Figure 11 shows the change in the contractions of the cross section of tube 2.1 along its measuring part, and Figure 12 shows the appearance of tube 2.1 after tearing. The fracture of the test tube is accompanied by uneven deformation of the measured length.

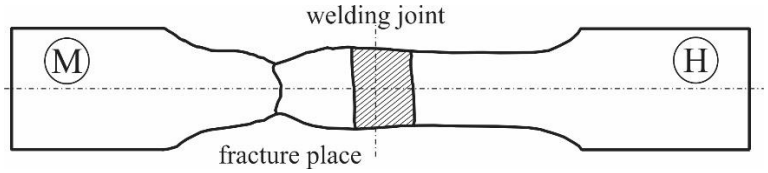

Figure 12 – Test tube 2.1 after tearing
Рис. 12 – Эпроветка 2.1 после разрыва
Слика 12 – Епрувета 2.1 након кидања

The results of the tensile characteristics of the joint for plate 2 for all three tested specimens are given in Table 11.

Table 11 – Tensile characteristics of plate joint tubes 2
Таблица 11 – Характеристики растяжения эпроветки соединения пластины 2
Табела 11 – Затезне карактеристике епрувета споја из плоче 2

Test tube number	Yield stress at the point A [MPa]		Stress at the point B [MPa]		Tensile strength at the point C [MPa]		E [%]	
	R_A	average value	R_B	average value	R_C	average value		average value
2.1	318	309	512	501	588	586	37	36
2.2	315		499		586		34	
2.3	295		493		583		36	

The average stress value at the point A is 309 MPa, at the point B is 501 MPa, and at the point C is 586 MPa, as shown in Table 11. The average value of the percentage elongation of the tubes is 36 %. Fracture occurred in microalloyed steel in all three tubes.

Table 12 compares the stresses at the characteristic points of the σ – ε diagram for tube 2.1, according to Figure 10 and Table 9, and the mean stress values for the base materials and the value deviations.

Table 12 – Stresses at the characteristic points of the σ – ε diagram for test tube 2.1
Таблица 12 – Напряжения в характерных точках диаграммы σ – ε эпроветки 2.1
Табела 12 – Напони у карактеристичним тачкама дијаграма σ–ε за епрувету 2.1

Stress at the characteristic points in Figure 10		Characteristic stress values for basic materials		Deviation Δ R [MPa]	Deviation [%]
Mark	Average stress value. Table 9	Mark. Table 8	Average stress value		
R_A	309	$R_{p0.2}$ steel H	324	15	4.6
R_B	501	$R_{p0.2}$ steel M	491	10	2.0
R_C	586	R_m steel M	583	3	0.5

The examination of the test tubes and the analysis of Figure 11 show that the smallest cross-sectional contraction (about 10%) occurs at the fusion line of the metal weld and the microalloyed steel. The fracture occurred in the microalloyed steel, approximately half of the measuring length of the tube on the side of the microalloyed steel. The narrowing towards the fusion lines with base materials is greater on the high-alloy steel side than on the fusion line with the micro-alloy steel. The total narrowing of the cross section of the measuring lengths of the base materials is greater on the side of the microalloyed steel.

Both experimental plates 1 and 2 were subjected to hardness tests of all characteristic structures located on them. The results of the hardness measurements and the microstructure tests show the usual values for the steels used (Bukvić, 2012).

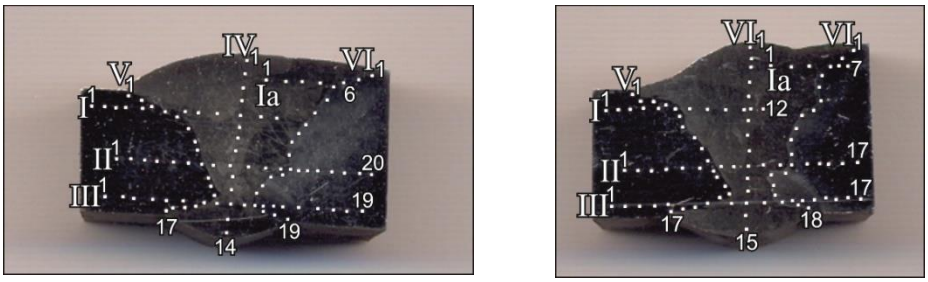

a) b)

Figure 13 – Macroscopic image of the welded plates with impressions from the hardness measurements:
a) Macroscopic image of plate 1, b) Macroscopic image of plate 2
Рис. 13 – Макроскопический снимок сварных пластин с отпечатками измерений твердости:
а) Макроскопический снимок пластины 1, б) Макроскопический снимок пластины 2
Слика 13 – Макроскопски снимак заварених плоча са отисцима од мерења тврдоће:
а) макроскопски снимак плоче 1, б) макроскопски снимак плоче 2

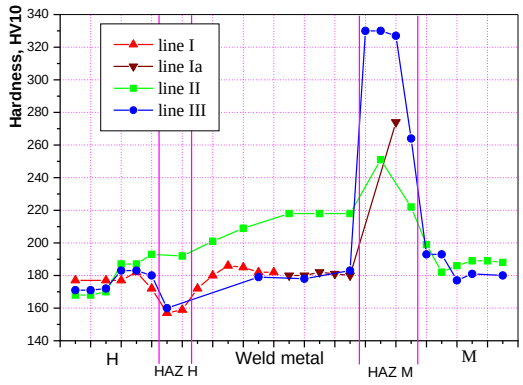

a)

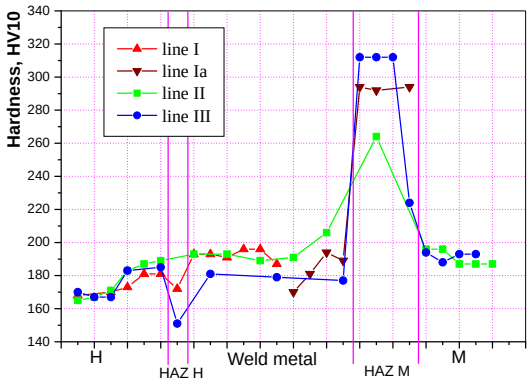

b)

Figure 14 – Graphic representations of the material hardness change in plates 1 and 2 by zones:
a) Change in hardness in plate 1
b) Change in hardness in plate 2
Рис. 14 – Графические изображения изменения твердости материала пластин 1 и 2 по зонам:
а) Изменение твердости пластины 1
б) Изменение твердости пластины 2
Слика 14 – Графички прикази промене тврдоће материјала у плочама 1 и 2 по зонама:
а) промена тврдоће у плочи 1,
б) промена тврдоће у плочи 2

According to the macroscopic image of plate 1 (Figure 13 under a), the hardness of the HAZ towards high-alloy steel (153–192 HV) does not differ significantly from the hardness of high-alloy steel (168–193 HV). As it can be seen from Figure 14 under a, the HAZ hardness values for microalloyed steel (199–333 HV) are higher than the hardness values of microalloyed steel (180–193 HV). The metal weld structure is austenitic with about 30% δ ferrite (Guo et al, 2015; Liu & Pons, 2017).

The test results of the joint from plate 2 according to the shown macroscopic image (Figure 13 under b), show that, similarly to plate 1, the values of the HAZ hardness towards high-alloy steel (151–192 HV) do not differ significantly from the hardness values of high-alloy steel (165– 189 HV). The values of the HAZ hardness towards microalloyed steel (224–333 HV) are higher than the hardness values of microalloyed steel (187–196 HV) and beinite was observed, Figure 14 under b (Guo et al, 2015; Liu & Pons, 2018).

Analysis of results

Plates 1 and 2 are welded with the maximum and minimum allowable amount of heat input. The values of the amount of heat input used in this case represent the limit values for the selected welding process and additional material. Tables 6 and 7 show that the input difference is about 30%. A lower amount of heat input would be achieved by reducing the current or by increasing the welding speed. Decreasing the current leads to the appearance of an unstable arc, and increasing the welding speed leads to poorer formation of metal seams. In both cases, unacceptable errors in the formation of metal seams (eg porosity, gluing) occur (Miletić et al, 2020; Zhang et al, 2015; Durmusoglu et al, 2015). Higher heat input would be achieved by increasing the current or reducing the welding speed. Increasing the welding current leads to the overheating of the liquid metal and poorer weld formation, and reducing the welding speed leads to a large volume of liquid metal that is difficult to control.

According to Schaeffler's diagram (Figure 2), in the welding of the used base materials (microalloyed ferritic-perlite and high-alloy austenitic steel) it is possible to use additional material MIG 18/8/6, because the result of this joint is in the safe area (Miletić et al, 2020; Zhang et al, 2015; Durmusoglu et al, 2015).

After welding, visual and radiographic control of all welded plates was performed. No errors were observed on either plate 1 or plate 2.

The results of hardness measurements on both experimental plates were obtained by the Vickers method at 10 daN. It is noticed that in plates

1 and 2 the highest values of hardness are achieved in the HAZ from microalloyed steel. In this coarse-grained zone, there was a large increase in grain, whereby the ferritic-perlite structure of microalloyed steel changed to beinitic. Microalloyed steel has higher hardness values on both welded plates than austenitic high alloy steel and its HAZ. The metal hardness values are higher than those of both base materials in all cases. The lowest values of hardness were shown by the HAZ on the part of high-alloy steel, except for plate 1, where the values are approximately the same as the values of high-alloy steel. The decrease in hardness in the HAZ of high-alloy steel was due to the increase in grain in the HAZ (Miletić et al, 2020; Sankar et al, 2021).

The obtained tensile diagrams of the metal weld tubes for plates 1 and 2 are typical for austenitic steels. When compared, the values of the tensile strength and the yield stress for additional material MIG 18/8/6 differ somewhat from the values offered by the manufacturer. The obtained values of the tensile strength Rm for additional material 18/8/6 are higher than the catalog values by 3.3 to 4.7%. The obtained percentage elongations for additional material 18/8/6 are higher by 4 to 7%. These deviations are a consequence of mixing the additional material with the basic material (Miletić et al, 2020; Zhang et al, 2015; Durmusoglu et al, 2015).

Comparing the values from Table 9 with the values of the yield stress and the tensile strength of the base materials (Table 7) and the weld metal (Table 8) for plate 1, it can be established that the point A in Figure 7 corresponds to the yield strength of high alloy steel, the point B corresponds to the yield stress of microalloyed steel and the point C corresponds to the tensile strength of high-alloy steel. This is expected according to (Sankar et al, 2021), since high-alloy steel has the lowest yield stress and plastic deformation will start in it first (point A). As the tensile force increases, the yield stress of the microalloyed steel (point B) is reached. The fracture occurred in high-alloy steel at a stress corresponding to its tensile strength (point C). The weld metal has a yield stress significantly higher than the yield stress of high-alloy, but a lower yield stress than microalloyed steel (Zhang et al, 2015; Durmusoglu et al, 2015). Therefore, the weld metal will deform before the point B is reached. As the weld metal and high-alloy steel are of similar structure, they will behave similarly when deformed, so there will be no discontinuity in the $\sigma - \varepsilon$ diagram. The results shown in Table 10 show a good agreement between the voltages in the second and fourth columns, which confirms the assumptions made.

Comparing the values from Table 11 with the values of the yield stress and the tensile strength of the base materials (Table 7) and the weld metal (Table 8) for plate 2, it can be established that the point A in Figure 10 corresponds to the yield strength of high alloy steel and the point B corresponds to the yield stress of microalloyed steel, but it is slightly pronounced in the figure, which distinguishes this diagram from the diagram obtained for plate 1 (Figure 7). The point C corresponds to the tensile strength of microalloyed steel. This sequence is possible, since high-alloy steel has the lowest yield stress and plastic deformation will first begin in it (Miletić et al, 2020; Zhang et al, 2015; Durmusoglu et al, 2015; Sankar et al, 2021) (point A). With the increase of tensile force, the high-alloy steel is strengthened and the yield stress of the micro-alloy steel is reached (point B). Fracture occurs in the microalloyed steel at a stress corresponding to its tensile strength (point C). The weld metal has a yield stress significantly higher than the yield stress of the high-alloy steel, but a slightly lower one than that of the microalloyed steel. According to the values from Tables 7 and 8, the tensile strength of the metal welds is higher than the tensile strengths of the basic materials. Therefore, the weld metal will deform before the point B is reached, as seen in Figure 11. As the weld metal and the high-alloy steel are of similar structure, they will behave similarly when deformed. Table 12 shows a good voltage matching in the second and fourth columns, which confirms the assumptions made.

Conclusions

When welding, it is recommended to use a lower amount of heat input, as this results in a lower degree of mixing the additional material with the base materials. Comparing the obtained results using austenitic additional material MIG 18/8/6 and lower heat input, we obtained a welded joint with superior mechanical characteristics, which ensures better work in all atmospheric conditions.

When cracks are found in the metal weld between the roof covering and the reservoir sheath, this joint is not the weakest point in the welded joint, because plastic deformations of the metal weld start only at stresses at which the basic materials break. The contraction of the weld metal increases with increasing the distance from its axis. The contraction at the same distance to the left and right of the axis of the weld metal is not the same and depends on the characteristics of the steel with which the weld metal is in contact.

The hardness measurements showed that, in all cases, the highest values were found in the HAZ towards the microalloyed base material, and the lowest values were in the HAZ towards the high alloyed base material.

References

Bukvić, A. 2012. *Research of the influence of additional materials on the behavior of ferritic austenitic welded joints*. Ph.D. thesis. Belgrade: University of Belgrade - Faculty of Mechanical Engineering (in Serbian).

Durmusoglu, Ş., Türker, M. & Tosun, M. 2015. Effect of welding parameters on the mechanical properties of GMA-welded HY-80 steels. *Materials Testing*, 57(10), pp.866-871. Available at: https://doi.org/10.3139/120.110797.

Guo, Y., Collins, D.M., Tarleton, E., Hofmann, F., Tischler, J., Liu, W., Xu, R., Wilkinson, A.J. & Britton, T.B. 2015. Measurements of stress fields near a grain boundary: Exploring blocked arrays of dislocations in 3D. *Acta Materialia*, 96, pp.229-236. Available at: https://doi.org/10.1016/j.actamat.2015.05.041.

-Jesenice Ironworks. 2005. *Additional welding materials, catalog*. Jesenice Ironworks.

Jovičić, R., Ažman, S., Popović, O. & Prokić–Cvetković, R. 2006. Prednosti primene čelika NIOMOL 490 K pri izradi skladišnih rezervoara za naftne derivate. *Energija*, 7(3-4), pp.66-69 (in Serbian).

Kassner, M.E. 2015. *Fundamentals of Creep in Metals and Alloys, 3rd Edition*. Elsevier & Butterworth-Heinemann. ISBN: 9780080994277.

Liu, D. & Pons, D.J. 2017. Physical-mechanism exploration of the low-cycle unified creep-fatigue formulation. *Metals*, 7(9), art.ID:379. Available at: https://doi.org/10.3390/met7090379.

Liu, D. & Pons, D.J. 2018. Crack Propagation Mechanisms for Creep Fatique: A Consolidated Explatation of Fundamental Beaviours from Inititation to Failure. *Metals*, 8(8), art.ID:623. Available at: https://doi.org/10.3390/met8080623.

Miletić, I., Ilić, A., Nikolić, R.R., Ulewicz, R. Ivanović, L . & Sczygiol, N. 2020. Analysis of Selected Properties of Welded Joints of the HSLA Steels. *Materials*, 13(6), art.ID:1301. Available at: https://doi.org/10.3390/ma13061301.

Sankar, N., Malarvizhi, S. & Balasubramanian, V. 2021. Mechanical properties and microstructural characteristics of rotating arc-gas metal arc welded carbon steel joints. *Journal of the Mechanical Behavior of Materials*, 30(1), pp.49-58. Available at: https://doi.org/10.1515/jmbm-2021-0006.

Zhang, X-Z., Zhao, M-S., Chiew, S-P., Lee, C-K. & Fung, T-C. 2015. Influence of welding on the strength of high performance steels. In: *7th Asia Pacific Young Researchers and Graduates Symposium (YRGS 2015),* Kuala Lumpur, Malaysia, August 20-21 [online]. Available at: https://hdl.handle.net/10356/80558 [Accessed: 1 Feabruary 2022].

ТЕРМИЧЕСКОЕ ВОЗДЕЙСТВИЕ НА ФИЗИКО-МЕХАНИЧЕСКИЕ СВОЙСТВА АУСТЕНИТНО-ФЕРРИТНЫХ СВАРНЫХ ШВОВ

Александар Г. Буквич[а], **корресподент**, *Далибор* П. Петрович[а], *Игор* З. Радисавлевич[б], *Саша* С. Димитрич[а]

[а] Университет обороны в г. Белград, Военная академия, г. Белград, Республика Сербия

[б] Министерство обороны Республики Сербия, Военно-технический институт, г. Белград, Республика Сербия

РУБРИКА ГРНТИ: 81.35.39 Сварные металлоконструкции, 81.35.13 Технология и оборудование сварочного производства

ВИД СТАТЬИ: оригинальная научная статья

Резюме:

Введение/цель: Во время эксплуатационных испытаний резервуаров для хранения бензина в сварном аустенитно-ферритном соединении могут образоваться трещины, что может испортить весь резервуар.

Методы: С целью достижения удовлетворительной прочности и долговечности сварного соединения в данной статье анализируется воздействие подведенного тепла на растяжение сварных соединений. В существующей литературе и на практике дополнительные материалы для сварки элементов резервуара подбираются в соответствии с химическим составом элементов основных материалов с помощью диаграммы Шеффлера. В данной статье описаны характеристики сварных соединений резервуаров для хранения бензина, большая часть которых изготовлена из мелкозернистой микролегированной стали NIOMOL 490 K, а часть крышки резервуара изготовлена из аустенитной стали. Сварка плит, изготовленнных из этих двух материалов, производится методом MIG с дополнительным материалом MIG 18/8/6 при разном количестве подведенного тепла.

Выводы: На основании результатов, полученных при испытании на растяжение в соответствии со стандартом SRPS EN ISO 6892-1:2020, сделан вывод, что поведение соединения в целом зависит от свойств каждой отдельной части сварного соединения и их взаимодействия. Также был сделан вывод, что взаимодействие будет лучше, если сварка выполняется с меньшим количеством подведенного тепла, поскольку в таком случае дополнительные материалы в меньшей степени смешиваются с основными материалами.

Ключевые слова: ферритно-аустенитный сварной шов, твердость, пластичность.

УТИЦАЈ УНЕТЕ ТОПЛОТЕ НА ЗАТЕЗНЕ КАРАКТЕРИСТИКЕ АУСТЕНИТНО-ФЕРИТНИХ ЗАВАРЕНИХ СПОЈЕВА

Александар Г. Буквић[а], **аутор за преписку**, *Далибор* П. Петровић[а], *Игор* З. Радисављевић[б], *Саша* С. Димитрић[а]

[а] Универзитет одбране у Београду, Војна академија, Београд, Република Србија

[б] Министарство одбране Републике Србије, Војнотехнички институт, Београд, Република Србија

ОБЛАСТ: машинство, машински материјали
ВРСТА ЧЛАНКА: оригинални научни рад

Сажетак:

Увод/циљ: Током експлоатацијских испитивања резервоара за складиштење бензина, у аустенитно-феритном завареном споју могу настати прслине што може компромитовати цео резервоар.

Методе: Ради постизања завареног споја задовољавајуће чврстоће и трајности, у раду је анализиран утицај уноса топлоте на затезне карактеристике заварених спојева. У досадашњој пракси додатни материјали за заваривање елемената резервоара бирају се према хемијском саставу елемената основних материјала, а уз помоћ Шефлеровог дијаграма. У овом раду испитиване су карактеристике заварених спојева резервоара за складиштење бензина. Највећи део резервоара израђен је од ситнозрног микролегираног челика NIOMOL 490 K, док је кровни део резервоара израђен од аустенитног челика. Плоче од ова два материјала заварене су MIG поступком са додатним материјалом MIG 18/8/6, при различитим количинама унете топлоте.

Закључак: Анализом резултата добијених испитивањем на затезање, према стандарду SRPS EN ISO 6892-1:2020, закључено је да понашање споја као целине зависи од особина сваког појединачног дела завареног споја и од њиховог међусобног утицаја. Такође, закључено је да је међусобни утицај ефикаснији уколико се заваривање врши нижом количином топлоте, јер се тада остварује мањи степен мешања додатног материјала са основним материјалима.

Кључне речи: аустенитно-феритни заварени спој, чврстоћа, пластичност.

Paper received on / Дата получения работы / Датум пријема чланка: 03.02.2022.
Manuscript corrections submitted on / Дата получения исправленной версии работы / Датум достављања исправки рукописа: 17.03.2022.
Paper accepted for publishing on / Дата окончательного согласования работы / Датум коначног прихватања чланка за објављивање: 19.03.2022.

DETERMINATION OF AN EFFICIENT POWER EQUIPMENT OIL THROUGH A MULTI-CRITERIA DECISION MAKING ANALYSIS

Johnson Kehinde Abifarin[a], *Joseph Chukwuka* Ofodu[b]

[a] Ahmadu Bello University, Faculty of Engineering,
Department of Mechanical Engineering,
Zaria, Federal Republic of Nigeria,
e-mail: jkabifarin@abu.edu.ng, abifarinjohnsonk@yahoo.com,
corresponding author,
ORCID iD: https://orcid.org/0000-0003-4930-9132

[b] University of Port Harcourt, Faculty of Engineering,
Department of Mechanical Engineering,
Choba, Rivers State, Federal Republic of Nigeria,
e-mail: rofnelenergy@yahoo.com,
ORCID iD: https://orcid.org/0000-0001-8311-7332

DOI: 10.5937/vojtehg70-36024; https://doi.org/10.5937/vojtehg70-36024

FIELD: Mechanical engineering, Materials
ARTICLE TYPE: Original scientific paper

Abstract:

Introduction/purpose: Several studies in the area of the development of nanofluids for power equipment have left a gap unfilled as to how to determine the best oil among the produced oils for power equipment application. Therefore, this study presents a multi-criterial decision making analysis to determine the best oil for power equipment.

Methods: The Grey relational analysis (GRA) and the Probability based multi-objective optimization techniques were employed as the multi-criterial decision making analytical tools for the optimization. Dielectric strength, dielectric loss, viscosity, and flash point were analyzed as multiple performance characteristics of different oils, after which different oil candidates were ranked based on their performance.

Results: Interestingly, the GRA and the Probability based multi-objective optimization techniques revealed that Jatropha oil + Neem nanofluid is the best oil candidate for power equipment and it is better than conventional mineral oil. The Probability based multi-objective optimization technique places Jatropha nanofluid over mineral oil, but not for the GRA technique. Also, mineral oil and ordinary Jatropha nanofluids are at a competitive level. Meaning, if Jatropha nanofluid is further worked on, it can beat mineral oil.

Conclusion: The two techniques substantially established that when Jatropha oil is mixed with Neem oil together with nanoparticles, there will

be better power equipment performance compared to mineral oil. It can be recommended that a further analysis should be conducted in the area of direct application of Jatropha + Neem nanofluid for power equipment to understand the overall behavior of power equipment compared to the conventional mineral oil.

Keywords: nanofluids, power equipment, grey relational analysis, probability optimization, vegetable oil, dielectric property, insulating property.

Introduction

Oil is filled in power equipment to serve as electrical insulation and for cooling. It ensures that there is heat transfer from power equipment and equally block arcing and corona discharge within the equipment system. In addition, it suggests the quality of the service lifespan of the equipment (Shafi et al, 2018; Oparanti et al, 2022). Since the beginning of the 20th century, mineral oil has been conventional oil for power equipment application because of its lifelong tendency, low cost, low viscosity, etc. (Fofana, 2013). Even though mineral oil exhibits the above mentioned advantages, it is disadvantaged due to its high fire risk and its non-biodegradable nature. Apart from its non-biodegradable nature, its leakage is detrimental to the environmental and toxic to living organisms (Tambuwal et al, 2022). These tradeoffs have motivated several researchers to dwell on the production of an alternative oil to mineral oil for power equipment from biodegradable sources, such as vegetables. Vegetable oil has been proven to be environmentally friendly, but generally exhibits high dielectric loss and poor viscosity (Abdelmalik, 2015; Rajab et al, 2011; Oparanti et al, 2020). Reports have shown that nanoparticles can be used to improve some insulating and electrical properties of oils for better performance (Mansour et al, 2012; Oparanti et al, 2021a, 2021b). Despite the improvement of vegetable oil as an alternative for mineral oil, there is a challenge in the selection and recommendation of optimal synthesis conditions for better performance in power equipment. Hence there is a need to research on the determination of optimal conditions in the production of nanofluids for better performance. This study applied two different multi-objective optimization techniques (the Grey relational analysis and the Probability based multi-objective optimization technique) to determine the best performing nanofluids for power equipment.

The Grey relational analysis (GRA) is usually applied when there is a need to optimize multiple performance properties, in addition to some uncertainties associated with the problem (Abifarin, 2021; Abifarin et al, 2022a, 2022b, 2022c; Abifarin et al, 2021; Avodi et al, 2021; Javed et al,

2019, 2020; Mahmoudi et al, 2019). The GRA was applied to address the uncertainties and complexities encountered in the choice of nanofluids with the best performance characteristics. Researchers have applied this optimization technique in different applications. Abifarin (2021) employed the GRA to assist Taguchi optimization in the fabrication of biomedical hydroxyapatite. Javed & Liu (2019) employed the bidirectional absolute GRA model for uncertainty systems, specifically in project management. Tosun (2006) employed the GRA to optimize drilling conditions for multiple performance characteristics. Tzeng et al. (2009) optimized turning operations using Taguchi assisted by the GRA. Abifarin & Ofodu (2022) modeled and employed the GRA for multiple performance properties of chemical additives and engine parameters for high efficient diesel engines. Kung & Wen (2007) applied the GRA and the grey decision maker to determine the relationship between company attributes and its financial performance using some venture capital enterprises in Taiwan as a case study. Hence, the GRA has been extensively proven to be effective as a multi-objective optimization technique. Furthermore, the Probability based multi-objective optimization technique has been recently developed to optimize more than one performance characteristics of conditions, process, systems, or products. Zheng et al. (2021) newly introduced the probability optimization technique in the selection of engineering materials based on some more than one essential attributes. Zheng (2022) selected some data relevant to material engineering and employed the technique to select material with better performance characteristics. Zheng et al. (2021) and Zheng (2022) were able to establish that Probability based optimization technique does not have any additional contributing factors which normally alter the accuracy of an optimization analysis as compared to some other existing ones. Ofodu & Abifarin (2022) applied the technique to optimize for high voltage thermofluids. The two optimization techniques were chosen because of their simplicity and proven accuracy in optimization analyses. This assertion has been proven in some past research studies a few ones of which have been discussed above. The two optimization techniques were also chosen to run the same problem for validation and comparative study.

Having highlighted the state of the art, this study employed two different optimization techniques to determine the best efficient power equipment oil. The two techniques, namely, the GRA and the Probability based multi-objective optimization technique were the numerical analysis chosen because of their simplicity and also to validate optimal predictions. The data analyzed was employed from the study of Tambuwal et al. (2022).

Data curation

The data used was obtained from the study of Tambuwal et al. (2022). The authors only investigated and reported the results without analyzing multiple performance characteristics, hence it was difficult to determine the oil sample with the best performance for power equipment. Table 1 presents the employed dataset in this study. The oil properties essential for power equipment are presented in the Table, i.e. breakdown strength, dielectric loss, viscosity, and flash point. These multiple properties were analyzed using two different multi-objective optimization techniques to determine the best performance oil sample for power equipment.

Table 1 – Insulating and electrical properties of different oil samples
Таблица 1 – Изоляционные и электрические свойства различных образцов масел
Табела 1 – Изолациона и електрична својства различитих узорака уља

Samples	Breakdown strength (kV mm^{-1})	Dielectric loss	Viscosity (mPas)	Flash point (^oC)
Mineral oil	36.8	0.00225	9.82	140
Jatropha oil	28.7	0.0551	11.07	245
Neem oil	15.1	0.0244	11.1	242
Jatropha + neem oil	15.8	0.02365	11.41	238
Neem nanofluid	18.5	0.002151	10.01	256
Jatropha nanofluid	25.7	0.00208	9.93	248
Jatropha + neem nanofluid	35.6	0.001862	9.874	261

Multi-criteria decision making analysis

Grey relational analysis (GRA)

The GRA was employed on four performance characteristics. The step by step methods in the GRA analysis are as shown below:

The Grey relational analysis was conducted on the experimental data presented in Table 1. The data was first normalized using grey relational generation. The breakdown strength and the flash point were normalized using the higher-the-better normalization condition, as given in Equation 1. The higher-the-better normalization was applied because higher breakdown strength shows a higher dielectric property which is needed for power equipment, while a high flash point is needed for higher insulating properties and reduced fire outbreak. Next, dielectric loss and viscosity

were normalized using the smaller-the-better normalization condition, as shown in Equation 2. The smaller-the-better normalization condition was chosen because as small as possible is required from the properties for better dielectric and insulation behavior of the oil. The normalized data sequence is presented in Table 2:

$$x_i(k) = \frac{y_i(k) - \min y_i(k)}{max\ y_i(k) - \min y_i(k)} \quad (1)$$

$$x_i(k) = \frac{\max y_i(k) - y_i(k)}{max\ y_i(k) - \min y_i(k)} \quad (2)$$

$x_i(k)$ is the data being preprocessed for the i^{th} experiment, and $y_i(k)$ is the initial sequence of the mean of the responses**.**

Table 2 – Normalized Insulating and electrical properties
Таблица 2 – Нормализованные изоляционные и электрические свойства
Табела 2 – Нормализована изолациона и електрична својства

Samples	$x_i(k)$ of Breakdown strength	$x_i(k)$ of Dielectric loss	$x_i(k)$ of Viscosity	$x_i(k)$ of Flash point
Mineral oil	1	0.99271	1	0
Jatropha oil	0.62673	0	0.21384	0.86777
Neem oil	0	0.57666	0.19497	0.84298
Jatropha + neem oil	0.03226	0.59074	0	0.80992
Neem nanofluid	0.15668	0.99457	0.8805	0.95868
Jatropha nanofluid	0.48848	0.99591	0.93082	0.89256
Jatropha + neem nanofluid	0.9447	1	0.96604	1

A comparison was made with an ideal sequence, $x_0(k)$ (k= 1, 2,…,7) for the four performance characteristics. The deviation sequence (Equation 3) was subsequently calculated to enable the determination of the grey relational coefficient (GRC). The grey relational generation and the deviation sequence of the four experimental data are shown in Table 4. The deviation data sequence is shown in Table 3:

$$\Delta_{oi}(k) = \|x_o(k) - x_i(k)\| \quad (3)$$

where $\Delta_{oi}(k)$, x_o *(k)*, and x_i *(k)* are the deviation, the reference sequence, and the normalized data, respectively.

Table 3 – Deviation sequence of the insulating and electrical properties
Таблица 3 – Ряд отклонений изоляционных и электрических свойств
Табела 3 – Девијациони низ изолационих и електричних својстава

Samples	$\Delta_{oi}(k)$ of Breakdown strength	$\Delta_{oi}(k)$ of Dielectric loss	$\Delta_{oi}(k)$ of Viscosity	$\Delta_{oi}(k)$ of Flash point
Mineral oil	0	0.00729	0	1
Jatropha oil	0.37327	1	0.78616	0.13223
Neem oil	1	0.42334	0.80503	0.15702
Jatropha + neem oil	0.96774	0.40926	1	0.19008
Neem nanofluid	0.84332	0.00543	0.1195	0.04132
Jatropha nanofluid	0.51152	0.00409	0.06918	0.10744
Jatropha + neem nanofluid	0.0553	0	0.03396	0

The GRC values were computed using Equation 4. The GRC values show the relationship between the expected and obtained experimental data.

$$\xi_i(k) = \frac{\Delta_{min} + \zeta\Delta_{max}}{\Delta_{oi}(k) + \zeta\Delta_{max}} \quad (4)$$

where $\xi_i(k)$ is the GRC value of the individual experimental data, computed as a function of Δ_{min} and Δ_{max}, the minimum and the maximum deviations of each experimental data. ζ is the distinguishing coefficient of 0.5, and it is usually assigned to each response.

Lastly, the grey relational grade (GRG) was calculated using Equation 5. The GRG, i.e., the converted singular response gives the overall multiple performance characteristics for the four experimental data. The GRC, the GRG, and the ranking are presented in Table 4:

$$\gamma_i = \frac{1}{n}\sum_{i=1}^{n} \xi_i(k) \quad (5)$$

γ_i is the GRG value obtained for the ith experiment and *n* is the number of performance characteristics.

Table 4 – GRC, the GRG and the ranking of oil types
Таблица 4 – Серый реляционный коэффициент (GRC), серый реляционный градиент (GRG) и ранжирование видов масел
Табела 4 – Сиви релациони коефицијент (СРК), сиви релациони градијент (СРГ) и рангирање типова уља

Samples	$\xi_i(k)$ of Breakdown strength	$\xi_i(k)$ of Dielectric loss	$\xi_i(k)$ of Viscosity	$\xi_i(k)$ of Flash point	GRG	Rank
Mineral oil	1	0.98563	1	0.33333	0.82974	2
Jatropha oil	0.57256	0.33333	0.38875	0.79085	0.52137	5
Neem oil	0.33333	0.54151	0.38313	0.76101	0.50475	6
Jatropha + neem oil	0.34066	0.5499	0.33333	0.72455	0.48711	7
Neem nanofluid	0.37221	0.98926	0.80711	0.92366	0.77306	4
Jatropha nanofluid	0.49431	0.99188	0.87845	0.82313	0.79694	3
Jatropha + neem nanofluid	0.90041	1	0.9364	1	0.9592	1

Probability based analysis

The Probability based multi-objective optimization analysis is based on the beneficial and unbeneficial utility index method.

The beneficial utility index method is applied to a characteristic desired to be as high as possible. The index characteristic indicator contributes positively to a partial preferable probability linearly. The breakdown strength and the flash point were run with the beneficial utility index method since the as high as possible condition is required for the properties. Equation 6 was used to compute the partial positive probability index (*Pij*), while Equation 7 was used to compute the normalized factor (α_j) of the jth utility index of the performance characteristic indicator.

$$Pij = \alpha_{ij} X_{ij},\ i = 1, 2,...,n;\ j = 1, 2,..m \quad (6)$$

$$\alpha_j = 1/(\mathrm{n}\overline{X}_J) \quad (7)$$

where X_{ij} *is the* j^{th} beneficial utility index of the characteristic performance indicator of the i^{th} number of sample, n is the total number of samples considered in the study, while m is the total number of the utility indices of each sample involved, and X_j is the value of the arithmetic mean of the utility index of the sample characteristic performance indicator. The partial positive utility indexes for the breakdown strength and the flash point are shown in Table 5.

The unbeneficial utility index method is applied to a characteristic desired to be as small as possible. The index characteristic indicator contributes negatively to a partial preferable probability. Equation 8 was used to compute the partial negative probability index (*Pij*), while Equation 9 was used to compute its normalized factor (β_j) of the j[th] utility index of the performance characteristic indicator. and X_i is an arbitrary utility index of the characteristic performance indicator of the i^{th} sampling number. The utility indexes for dielectric loss and viscosity are also shown in Table 5.

$$Pij = \beta_{ij}(X_{jmax} + X_{jmin} - X_i),\ i = 1, 2,...,n;\ j = 1, 2,..m \quad (8)$$

$$\beta_{ij} = 1/[n(X_{j\min} + X_{j\max}) - nX_j] \quad (9)$$

Furthermore, the total preferable probability of the analysis was computed using the product of the individual partial preferable probability of a corresponding candidate oil type. Afterwards, the ranking was done to show the candidate sample with the best performance characteristics. Please check Table 5 for proper highlights.

Table 5 – Partial and total probability utility index of oil types
Таблица 5 – Частичный и общий вероятностный индекс полезности типов нефти
Табела 5 – Индекс корисности делимичне и укупне вероватноће типова уља

Samples	*Pij* of Breakdown strength	*Pij* of Dielectric loss	*Pij* of Viscosity	*Pij* of Flash point	Pt*10E4	Pt*10E4	P Rank
Mineral oil	0.20887	0.19048	0.15134	0.08589	5.17133	5.17133	3
Jatropha oil	0.16289	0.00648	0.13476	0.1503	0.21388	0.21388	5
Neem oil	0.0857	0.11336	0.13436	0.14846	1.93808	1.93808	7
Jatropha + Neem oil	0.08968	0.11597	0.13025	0.14601	1.9779	1.9779	6
Neem nanofluid	0.105	0.19082	0.14882	0.15705	4.68307	4.68307	4
Jatropha nanofluid	0.14587	0.19107	0.14988	0.15215	6.35553	6.35553	2
Jatropha + Neem nanofluid	0.20205	0.19183	0.15063	0.16012	9.34816	9.34816	1

Discussion of results

The GRA was successfully applied to determine the best performance oil type in this study. Table 4 shows the ranking of the oil types. The results obtained show that a mixture of Jatropha oil and neem oil when nanoparticle is added is the best oil for power equipment, as it is ranked number one, followed by mineral oil. It is interesting to emphasize that the

GRA revealed that vegetable nanofluid is better than mineral oil, which is the second best oil type for power equipment application. This shows that vegetable oil, specifically a mixture of Jatropha and Neem sourced oil when nanoparticle is added, stands a good chance to replace mineral oil in power equipment application.

The Probability based multi-objective optimization technique was also successfully employed as shown in Table 5. The results obtained also revealed that a mixture of Jatropha oil and neem oil when nanoparticle is added is ranked as the best oil for power equipment, followed by Jatropha oil, then mineral oil. This technique further validates the choice of the best candidate oil for power equipment. To a higher level of confidence, the Jatropha oil + Neem nanofluid can better serve in power equipment.

Conclusion

Essentially, the Probability based multi-objective optimization technique places Jatropha nanolfuid over mineral oil, while it is the other way round for the GRA technique. It can be deduced from these findings that mineral oil and ordinary Jatropha nanofluids are at a competitive level. When Jatropha nanofluid is further worked on, it can be better than mineral oil. This claim is backed up by the results presented in the two techniques, i.e. when Jatropha oil is mixed with Neem oil together with nanoparticles, there will be better power equipment performance compared to the performance of the power equipment using mineral oil. In this study, recommendation is made that a further analysis should be conducted in the area of direct application of Jatropha + Neem nanofluid in power equipment to see the overall behavior of power equipment as compared to that of the conventional mineral oil.

References

Abdelmalik, A.A. 2015. Analysis of thermally aged insulation paper in a natural ester-based dielectric fluid. *IEEE Transactions on Dielectrics and Electrical Insulation*, 22(5), pp.2408-2414. Available at: https://doi.org/10.1109/TDEI.2014.004824.

Abifarin, J.K. 2021. Taguchi grey relational analysis on the mechanical properties of natural hydroxyapatite: effect of sintering parameters. *The International Journal of Advanced Manufacturing Technology*, 117, pp.49-57. Available at: https://doi.org/10.1007/s00170-021-07288-9.

Abifarin, J.K., Fidelis, F.B., Abdulrahim, M.Y., Oyedeji, E.O., Nkwuo, T. & Prakash, C. 2022a. Response Surface Grey Relational Analysis On The Manufacturing of High Grade Biomedical Ti-13Zr-13Nb. *The International Journal*

of Advanced Manufacturing Technology, under review. Available at: https://doi.org/10.21203/rs.3.rs-1225030/v1.

Abifarin, J.K., Obada, D.O., Dauda, E.T. & Oyedeji, E.O. 2021. Taguchi Grey Relational Optimization of the Multi-mechanical Characteristics of Kaolin Reinforced Hydroxyapatite: Effect of Fabrication Parameters. *International Journal of Grey Systems*, 1(2), pp.20-32. Available at: https://doi.org/10.52812/ijgs.30.

Abifarin, J.K. & Ofodu, J.C. 2022. Modeling and Grey Relational Multi-response Optimization of Chemical Additives and Engine Parameters on Performance Efficiency of Diesel Engine. *International Journal of Grey Systems,* in press. Available at: https://doi.org/10.52812/ijgs.33.

Abifarin, J.K., Prakash, C. & Singh, S. 2022b. Optimization and significance of fabrication parameters on the mechanical properties of 3D printed chitosan/PLA scaffold. *Materials Today: Proceedings*, 50(5), pp. 2018-2025. Available at: https://doi.org/10.1016/j.matpr.2021.09.386.

Abifarin, J.K., Suleiman, M.U., Abifarin, E.A., Fidelis, F.B., Oyelakin, O.K., Jacob, D.I. & Abdulrahim, M.Y. 2022c. Fabrication of mechanically enhanced hydroxyapatite scaffold with the assistance of numerical analysis. *The International Journal of Advanced Manufacturing Technology*, 118, pp.3331-3344. Available at: https://doi.org/10.1007/s00170-021-08184-y

Awodi, E., Ishiaku, U.S., Yakubu, M.K. & Abifarin, J.K. 2021. Experimentally Predicted Optimum Processing Parameters Assisted by Numerical Analysis on the Multi-physicomechanical Characteristics of Coir Fiber Reinforced Recycled High Density Polyethylene Composites. *Research Square*, posted. Available at: https://doi.org/10.21203/rs.3.rs-591200/v1.

Fofana, I. 2013. 50 years in the development of insulating liquids. *IEEE Electrical Insulation Magazine*, 29(5), pp.13-25. Available at: https://doi.org/10.1109/MEI.2013.6585853.

Javed, S.A. & Liu, S. 2019. Bidirectional Absolute GRA/GIA Model for Uncertain Systems: Application in Project Management. *IEEE Access*, *7*, pp.60885-60896. Available at: https://doi.org/10.1109/ACCESS.2019.2904632.

Javed, S.A., Liu, S., Mahmoudi, A. & Nawaz, M. 2019. Patients' satisfaction and public and private sectors' health care service quality in Pakistan: Application of grey decision analysis approaches. *The International journal of Health Planning and Management*, 34(1), pp.e168-e182. Available at: https://doi.org/10.1002/hpm.2629.

Javed, S.A., Zhu, B. & Liu, S. 2020. Forecast of biofuel production and consumption in top CO_2 emitting countries using a novel grey model. *Journal of Cleaner Production*, 276(art.ID:123997). Available at: https://doi.org/10.1016/j.jclepro.2020.123997.

Kung, C.Y. & Wen, K.L. 2007. Applying grey relational analysis and grey decision-making to evaluate the relationship between company attributes and its financial performance—a case study of venture capital enterprises in Taiwan. *Decision support systems*, 43(3), pp.842-852. Available at: https://doi.org/10.1016/j.dss.2006.12.012.

Mahmoudi, A., Liu, S., Javed, S.A. & Abbasi, M. 2019. A novel method for solving linear programming with grey parameters. *Journal of Intelligent & Fuzzy Systems*, 36(1), pp.161-172. Available at: https://doi.org/10.3233/JIFS-181071.

Mansour, D.E.A., Atiya, E.G., Khattab, R.M. & Azmy, A.M. 2012. Effect of titania nanoparticles on the dielectric properties of transformer oil-based nanofluids. In: *2012 annual report conference on electrical insulation and dielectric phenomena*, Montreal, QC, Canada, pp.295-298, October 14-17. Available at: https://doi.org/10.1109/CEIDP.2012.6378779.

Ofodu, J.C. & Abifarin, J.K. 2022. Employment of probability - based multi-response optimization in high voltage thermofluids. *Vojnotehnički glasnik/Military Technical Courier*, 70(2), pp.393-408. Available at: https://doi.org/10.5937/vojtehg70-35764.

Oparanti, S.O., Abdelmalik, A.A., Khaleed, A.A., Abifarin, J.K., Suleiman, M.U. & Oteikwu, V.E. 2022. Synthesis and characterization of cooling biodegradable nanofluids from non-edible oil for high voltage application. *Materials Chemistry and Physics*, 277(art.ID:125485). Available at: https://doi.org/10.1016/j.matchemphys.2021.125485.

Oparanti, S.O., Khaleed, A.A., & Abdelmalik, A.A. 2021a. Nanofluid from Palm Kernel Oil for High Voltage Insulation. *Materials Chemistry and Physics*, 259(art.ID:123961). Available at: https://doi.org/10.1016/j.matchemphys.2020.123961.

Oparanti, S.O., Khaleed, A.A. & Abdelmalik, A.A. 2021b. AC breakdown analysis of synthesized nanofluids for oil-filled transformer insulation. *The International Journal of Advanced Manufacturing Technology*, 117(5), pp.1395-1403. Available at: https://doi.org/10.1007/s00170-021-07631-0.

Oparanti, S.O., Khaleed, A.A., Abdelmalik, A.A. & Chalashkanov, N.M. 2020. Dielectric characterization of palm kernel oil ester-based insulating nanofluid. In: *2020 IEEE Conference on Electrical Insulation and Dielectric Phenomena (CEIDP),* East Rutherford, NJ, USA, pp.211-214, October 18-30. Available at: https://doi.org/10.1109/CEIDP49254.2020.9437477.

Rajab, A., Sulaeman, A., Sudirham, S. & Suwarno. 2011. A Comparison of Dielectric Properties of Palm Oil with Mineral and Synthetic Types Insulating Liquid under Temperature Variation. *ITB Journal of Engineering Science*, 43(3), pp.191-208. Available at: https://doi.org/10.5614/itbj.eng.sci.2011.43.3.3.

Shafi, W.K., Raina, A. & Ul Haq, M.I. 2018. Friction and wear characteristics of vegetable oils using nanoparticles for sustainable lubrication. *Tribology - Materials, Surfaces & Interfaces*, 12(1), pp.27-43. Available at: https://doi.org/10.1080/17515831.2018.1435343.

Tambuwal, F.R., Oparanti, S.O., Abdulkadir, I., Sadiq, U. & Abdelmalik, A.A. 2022. Investigative study on the AC and DC breakdown voltage of nanofluid from Jatropha–Neem oil mixture for use in oil-filled power equipment. *The International Journal of Advanced Manufacturing Technology*, pp.1-9. Available at: https://doi.org/10.1007/s00170-021-08447-8.

Tosun, N. 2006. Determination of optimum parameters for multi-performance characteristics in drilling by using grey relational analysis. *The International*

Journal of Advanced Manufacturing Technology, 28(5), pp.450-455. Available at: https://doi.org/10.1007/s00170-004-2386-y.

Tzeng, C-J., Lin, Y-H., Yang, Y-K. & Jeng, M-C. 2009. Optimization of turning operations with multiple performance characteristics using the Taguchi method and Grey relational analysis. *Journal of Materials Processing Technology*, 209(6), pp.2753-2759. Available at: https://doi.org/10.1016/j.jmatprotec.2008.06.046.

Zheng, M. 2022. Application of probability-based multi-objective optimization in material engineering. *Vojnotehnički glasnik/Military Technical Courier,* 70(1), pp.1-12. Available at: https://doi.org/10.5937/vojtehg70-35366.

Zheng, M., Wang, Y. & Teng, H. 2021. A New" Intersection" Method for Multi-Objective Optimization in Material Selection. *Tehnički glasnik*, 15(4), pp.562-568. Available at: https://doi.org/10.31803/tg-20210901142449.

ОПРЕДЕЛЕНИЕ ЭФФЕКТИВНОСТИ МАСЛА ДЛЯ ЭНЕРГЕТИЧЕСКОГО ОБОРУДОВАНИЯ С ИСПОЛЬЗОВАНИЕМ МНОГОКРИТЕРИАЛЬНОГО АНАЛИЗА ПРИНЯТИЯ РЕШЕНИЙ

Джонсон Кехинде Абифарин[а], *Джозеф Чуквука* Офоду[б]

[а] Университет Ахмаду Белло, инженерный факультет, кафедра машиностроения, г. Зария, Федеративная Республика Нигерия, **корреспондент**

[б] Университет Порт-Харкорта, инженерный факультет, кафедра машиностроения, г. Чоба, штат Риверс, Федеративная Республика Нигерия

РУБРИКА ГРНТИ: 30.17.00 Механика жидкости и газа,
47.09.00 Материалы для электроники и радиотехники
ВИД СТАТЬИ: оригинальная научная статья

Резюме:

Введение/цель: Поскольку несколько исследований в области разработки наножидкостей для энергетического оборудования не смогли определить лучшего кандидата среди масел для силовых установок, данное исследование посвящается анализу многокритериального принятия решений по определению масла − лучшего кандидата для энергетического оборудования.

Методы: Серый реляционный анализ и основанные на вероятности методы многокритериальной оптимизации были использованы для оптимизации. Диэлектрическая прочность, диэлектрические потери, вязкость и температура вспышки были проанализированы в качестве эксплуатационных характеристик различных масел, после чего различные масла-кандидаты были ранжированы в соответствии со своими характеристиками.

Результаты: Интересно, что серый реляционный анализ и многокритериальная оптимизация, основанная на вероятности

определили, что комбинация масел ятрофы + наножидкости нима является лучшим кандидатом для энергетического оборудования и, что она лучше, чем обычное минеральное масло. Метод многокритериальной оптимизации, основанный на вероятности отдает предпочтение наножидкости ятрофы по отношению к минеральному маслу, однако метод серого реляционного анализа не дал подобных результатов. Кроме того, минеральное масло и обычные наножидкости ятрофы находятся на одинаковом уровне конкурентноспособности, следовательно, наножидкость ятрофы может превзойти минеральное масло, если ее доработать.

Выводы: Два метода показали, что при смешивании растительного масла ятрофы с маслом нима и наночастицами достигается лучшая производительность энергетического оборудования, чем при использовании минерального масла. Считаем целесообразным провести дальнейшие анализы в области непосредственного применения ятрофы и наножидкостей нима в энергетическм оборудованим, с целью лучшего понимания общего поведения силовых установок и сравнения с ситуациями, когда используется обычное минеральное масло.

Ключевые слова: наножидкости, энергетическое оборудование, серый реляционный анализ, вероятностная оптимизация, растительное масло, диэлектрические свойства, изоляционные свойства.

ОДРЕЂИВАЊЕ ЕФИКАСНОГ УЉА ЗА ЕНЕРГЕТСКУ ОПРЕМУ КОРИШЋЕЊЕМ АНАЛИЗЕ ВИШЕКРИТЕРИЈУМСКОГ ОДЛУЧИВАЊА

Џонсон Кехинде Абифарин[а], *Џосеф Чуквука* Офоду[б]

[б] Универзитет Ахмаду Бело, Факултет техничких наука, одсек за машинство, Зариа, Савезна Република Нигерија, **аутор за преписку**

[б] Универзитет у Порт Харкорту, Факултет техничких наука, одсек за машинство, Чоба, Држава Риверс, Савезна Република Нигерија

ОБЛАСТ: машинство, материјали
ВРСТА ЧЛАНКА: оригинални научни рад

Сажетак:

Увод/циљ: Неколико студија из области развоја нанофлуида за енергетску опрему пропустило је да утврди које уље је најбоље међу уљима произведеним за примену у погонској опреми. Зато ова студија представља анализу вишекритеријумског одлучивања за одређивање најбољег уља погодног за енергетску опрему.

Abifarin, J.K. et al, Determination of an efficient power equipment oil through a multi-criteria decision making analysis, pp.433-446

Методе: Сива релациона анализа и техника вишекритеријумске оптимизације заснована на вероватноћи коришћене су за оптимизацију. Анализирани си диелектрична снага, диелектрични губитак, вискозност и тачка паљења, као карактеристике вишеструког учинка различитих уља, након чега су различита уља рангирана на основу својих перформанси.

Резултати: Занимљиво је да су сива релациона анализа и вишекритеријумска оптимизација заснована на вероватноћи утврдиле да је комбинација уља биљке јатропа и ним нанофлуида најбоља за енергетску опрему, као и да је боља од конвенционалног минералног уља. Техника вишекритеријумске оптимизације заснована на вероватноћи рангира јатропа нанофлуид испред минералног уља, али не и техника сиве релационе анализе. Такође, минерано уље и обични јатропа нанофлуиди су на компетитивном нивоу, што значи да јатропа нанофлуид може да буде ефикаснији од минералног уља ако се поради на њему.

Закључак: Две технике су утврдиле да се постижу боље перформансе енергетске опреме када се уље биљке јатропа помеша са ним уљем и нано честицама него када се користи минерално уље. Било би препоручљиво да се даље анализе врше у области директне примене јатропа и ним нанофлуида за енергетску опрему ради бољег разумевања функционисања погонске опреме и поређења са случајевима када се користи конвенционално минерално уље.

Кључне речи: нанофлуиди, енергетска опрема, сива релациона анализа, оптимизација вероватноће, биљно уље, диелектрично својство, изолационо својство.

Paper received on / Дата получения работы / Датум пријема чланка: 23.01.2022.
Manuscript corrections submitted on / Дата получения исправленной версии работы / Датум достављања исправки рукописа: 12.03.2022.
Paper accepted for publishing on / Дата окончательного согласования работы / Датум коначног прихватања чланка за објављивање: 14.03.2022.

ПРЕГЛЕДНИ РАДОВИ
ОБЗОРНЫЕ СТАТЬИ
REVIEW PAPERS

SADDLE POINT APPROXIMATION TO HIGHER ORDER

Nicola Fabiano[a], *Nikola* Mirkov[b]

[a] University of Belgrade, "Vinča" Institute of Nuclear Sciences - National Institute of the Republic of Serbia, Belgrade, Republic of Serbia,
e-mail: nicola.fabiano@gmail.com,
ORCID iD: https://orcid.org/0000-0003-1645-2071

[b] University of Belgrade, "Vinča" Institute of Nuclear Sciences - National Institute of the Republic of Serbia, Belgrade, Republic of Serbia,
e-mail: nmirkov@vin.bg.ac.rs,
ORCID iD: https://orcid.org/0000-0002-3057-9784

DOI: 10.5937/vojtehg70-33507;https://doi.org/10.5937/vojtehg70-33507

FIELD: Mathematics
ARTICLE TYPE: Review paper

Abstract:

Introduction/purpose: Saddle point approximation has been considered in the paper

Methods: The saddle point method is used in several different fields of mathematics and physics. Several terms of the expansion for the factorial function have been explicitely computed.

Results: The integrals estimated in this way have values close to the exact one.

Conclusions: Higher order corrections are not negligible even when requiring moderate levels of precision.

Keywords: saddle point approximation, Stirling's formula, Quantum Field Theory.

Saddle Point method

The saddle point method is an extension of the original method of Laplace (Laplace, 1986) for approximating the value of an integral of the

form

$$\int_a^b \exp[\lambda f(x)]dx \ , \tag{1}$$

where $f(x)$ is at least twice differentiable, λ is a large number and the extrema of the integral could also be infinite. Assuming that x_0 is the global maximum of the function $f(x)$, Laplace observed that the ratio

$$\frac{\exp[\lambda f(x_0)]}{\exp[\lambda f(x)]} = \exp[\lambda(f(x_0) - f(x))] \tag{2}$$

would increase exponentially with λ, while the ratio

$$\frac{\lambda f(x_0)}{\lambda f(x)} = \frac{f(x_0)}{f(x)} \tag{3}$$

is independent of λ. Therefore, he concluded that the main contribution to the integral (1) comes only from the values of x in the neighborhood of x_0, and the latter could be easily calculated.

Our aim is to compute the integral

$$I(\hbar) = \int_{-\infty}^{+\infty} \exp\left[\frac{if(z)}{\hbar}\right] dz. \tag{4}$$

Following the notation of (Parisi, 1988), we expand the so–called saddle point approximation first proposed by Daniels (Daniels, 1954) (also known as the steepest descend method) beyond first order approximation obtaining several terms of approximation, which is the main scope of this paper. As usual, one expands about the maximum $df/dz = 0$ obtaining a Gaussian integral for $I(\hbar)$, e.g. as in the Stirling's formula for $n!$. This suffices for many applications, as the Gaussian falls down quite quickly so further corrections are usually not necessary, unless a precision better than the percent order is required as it will be seen.

We want to compute eq. (4) beyond the first order in $\hbar$. From here onward, $\hbar$ plays a role of a generic small expansion parameter beyond its physical meaning. In order to achieve this goal, we expand $f(z)$ around the critical point z_0 such that $df(z_0)/dz = 0$:

$$f(z) = f(z_0) + \frac{1}{2}f^{(2)}(z_0)(z-z_0)^2 + \frac{1}{6}f^{(3)}(z_0)(z-z_0)^3 + \frac{1}{24}f^{(4)}(z_0)(z-z_0)^4 + \mathcal{O}((z-z_0)^5) \tag{5}$$

The trick is to separate the exponential in two parts: the Gaussian and the remnant. The latter is expanded again in Taylor's series, i.e. we write:

$$\exp\left[\frac{if(z)}{\hbar}\right] = \exp\left[\frac{i(f(z_0)+\frac{1}{2}f^{(2)}(z_0)(z-z_0)^2)}{\hbar}\right]$$
$$\times \exp\left[\frac{i}{\hbar}\left(\frac{1}{6}f^{(3)}(z_0)(z-z_0)^3+\frac{1}{24}f^{(4)}(z_0)(z-z_0)^4+\mathcal{O}((z-z_0)^5)\right)\right] \quad (6)$$

that is, a Gaussian times some other function that will be eventually expanded in Taylor's series. We could rewrite eq. (6) as

$$\exp\left[\frac{if(z)}{\hbar}\right] = \exp\left[\frac{i(f(z_0)+\frac{1}{2}f^{(2)}(z_0)(z-z_0)^2)}{\hbar}\right] \times \exp\left[\frac{ig(z)}{\hbar}\right] \quad (7)$$

where at least formally $g(z)$ is the remainder from the third order of the expansion of $f(z)$:

$$g(z) = \sum_{n=3}^{+\infty} \frac{f^{(n)}(z_0)}{n!}(z-z_0)^n \quad (8)$$

Of course Taylor's expansion of eq. (8) is not the one of $f(z)$ given in eq. (5) due to the exponential function. Great care has to be applied in order to pick the right power of $\hbar$. For instance, to second order in $\hbar$ we have:

$$\exp\left[\frac{ig(z)}{\hbar}\right] = \exp\left[\frac{ig(z_0)}{\hbar}\right] \times \left[1+\frac{i}{\hbar}g'(z_0)(z-z_0)\right]$$
$$+\exp\left[\frac{ig(z_0)}{\hbar}\right] \times \left[\frac{1}{2\hbar^2}\left(i\hbar g''(z_0)-g'(z_0)^2\right)(z-z_0)^2\right] \quad (9)$$

and powers of $\hbar$ are mixed as it can be seen. We obtain

$$\exp\left[\frac{ig(z)}{\hbar}\right] = \sum_{n=0}^{+\infty} \frac{\phi^{(n)}(z_0)}{n!}(z-z_0)^n \quad (10)$$

for $\phi(z) = \exp(ig(z)/\hbar)$. Plugging it back in eqs (7) and (4), we obtain

$$I(\hbar) = \exp\left[\frac{if(z_0)}{\hbar}\right]\int_{-\infty}^{+\infty} \exp\left[\frac{if^{(2)}(z_0)(z-z_0)^2)}{2\hbar}\right] \times \sum_{n=0}^{+\infty} \frac{\phi^{(n)}(z_0)}{n!}(z-z_0)^n dz \quad (11)$$

Pulling the sum out of the integral shows clearly that only even powers survive because of the Gaussian integral.

Calling I_0 the Gaussian integral

$$I_0(\hbar) = \exp\left[\frac{if(z_0)}{\hbar}\right]\int_{-\infty}^{+\infty}\exp\left[\frac{if^{(2)}(z_0)(z-z_0)^2)}{2\hbar}\right]dz \tag{12}$$

that has the value

$$I_0(\hbar) = \exp\left[\frac{if(z_0)}{\hbar}\right]\left[\frac{2\pi i\hbar}{f^{(2)}(z_0)}\right]^{1/2} \tag{13}$$

compared to eq. (4) gives the result to first order in $\hbar$

$$I(\hbar) = I_0(\hbar)(1+\mathcal{O}(\hbar)) \tag{14}$$

With a notation where $f^{(n)}$ is the n-th derivative of $f(z)$ computed in z_0, the $\mathcal{O}(\hbar^2)$ correction to $I(\hbar)$ is given by:

$$I_2(\hbar) = \frac{5\,(f^{(3)})^2 - 3\,f^{(2)}\,f^{(4)}}{24\,(f^{(2)})^3} \tag{15}$$

while the $\mathcal{O}(\hbar^3)$ correction reads

$$I_3(\hbar) = \frac{-24\,(f^{(2)})^3\,f^{(6)} + (f^{(2)})^2\,\left(168\,f^{(3)}\,f^{(5)} + 105\,(f^{(4)})^2\right)}{1152\,(f^{(2)})^6} - \frac{630\,f^{(2)}\,(f^{(3)})^2\,f^{(4)} + 385\,(f^{(3)})^4}{1152\,(f^{(2)})^6}. \tag{16}$$

That is

$$I(\hbar) = I_0(\hbar)\left[1 + (i\hbar)I_2(\hbar) + (i\hbar)^2 I_3(\hbar) + \mathcal{O}(\hbar^3)\right]. \tag{17}$$

More terms of the expansion have been calculated and terms up to $\mathcal{O}(\hbar^7)$ are shown in the Appendix .

This kind of approximation is often used in physics, in statistical mechanics when counting the configurations by means of Stirling's formula (see later). The WKB approximation can be thought of as a saddle point approximation (Wentzel, 1926; Kramers, 1926; Brillouin, 1926). Starting from the work of Dirac (Dirac, 1933), Feynman devised the method of the path integral and with a saddle point approximation derived the Schrödinger equation (Feynman, 1965).

In the quantum field theory, for example, it is used to evaluate path integral perturbatively in order to compute the effective action for a given

model (Ramond, 1989). Consider for instance the action S of a bosonic field φ:

$$S[\varphi] = \int \frac{1}{2}(\partial\varphi)^2 + \frac{m}{2}\varphi^2 + V(\varphi)\, d^4x. \tag{18}$$

One could then apply the procedure of eq. (11), expanding the path integral in the Euclidean space around the classical field φ_0 which is extremal for the action (18), i.e.

$$\left.\frac{\delta S[\varphi]}{\delta\varphi}\right|_{\varphi=\varphi_0} = 0 \tag{19}$$

and performing the Gaussian integral yields the standard result:

$$\Gamma[\varphi] = S[\varphi_0] + \frac{\hbar}{2}\mathsf{Tr}\left[\log(-\partial^2 + m^2 + V''(\varphi_0))\right] + \mathcal{O}(\hbar^2). \tag{20}$$

Including more terms in the expression beyond the leading order of eq. (13) shows that the resulting analytic approximation retains its validity over the whole integration range, not just towards the point z_0.

An Example: Stirling's approximation

The expression given in eq. (17) has been verified with Stirling's formula (Stirling, 1764) for the Gamma function, given by

$$\Gamma(z+1) = \int_0^{+\infty} t^z \exp(-t)dt = \int_0^{+\infty} \exp(-t + z\log(t))dt \tag{21}$$

which is equal to $n!$ when z is an integer n. With the position $\hbar = -i$ and $f(t) = t - z\log(t)$ using the formulæ starting from expansion of eq. (17) and considering the terms given in eqs. (23)–(26), we obtain the fifth order for $z \to +\infty$:

$$\Gamma(z+1) = \sqrt{2\pi z}\left(\frac{z}{e}\right)^z \left[1 + \frac{1}{12z} + \frac{1}{288z^2} - \frac{139}{51840z^3} - \frac{571}{2488320z^4} + \mathcal{O}\left(\frac{1}{z^5}\right)\right]. \tag{22}$$

After the publication of the book of de Moivre (Moivre, 1730) where he developed an approximation to $\binom{n}{n/2}/2^n$ while developing general procedures for probability, Stirling found his asymptotic series (22) for

Fabiano, N. et al, Saddle point approximation to higher order, pp.447–460

$\log n!$ improving de Moivre's result and introducing the "Stirling's constant" $(\log 2\pi)/2$. After this result, de Moivre used a different method to compute the asymptotic series to $\log n!$ obtaining a similar expansion (Moivre, 1730, 1756).

Notice that Stirling's asymptotic expansion[1] of eq. (22) is not a convergent series (Whittaker & Watson, 1927; Erdelyi, 1956), that is, at the fixed z the accuracy improves when adding more terms, up to a point where it actually gets worse while increasing the approximation order.

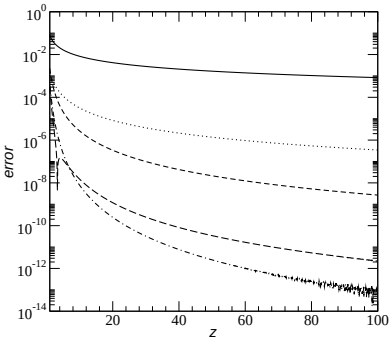

Figure 1 – Relative error for Stirling's approximation of $\Gamma(z)$ as a function of z. The various decreasing curves are in the increasing approximation order, from 1 to 5 terms.
Рис. 1 − Относительная погрешность по приближению Стирлинга $\Gamma(z)$ как функции z. Различные убывающие кривые расположены в порядке возрастания аппроксимации, от 1 до 5 членов.
Слика 1 – Релативна грешка за Стирлингову апроксимацију $\Gamma(z)$ као функције од z. Различите падајуће криве дате су по растућем реду апроксимација, од 1 до 5 термина.

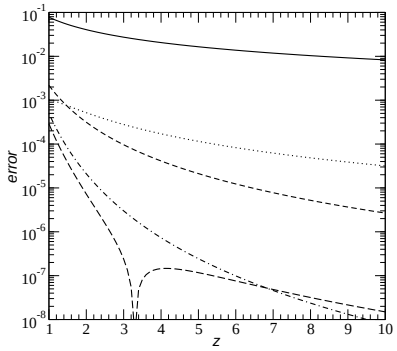

Figure 2 – The same plot as Fig. (1) for a positive z range less than 10. This enhancement shows the crossing of the accuracy for various approximation orders.
Рис. 2 − Тот же график, что и на рис. (1) для положительного значения z менее 10. Это увеличение показывает пересечение точности в аппроксимации различных порядков.
Слика 2 – Исти график као на слици (1) за позитивну вредност z мању од 10. Ово увећање показује укрштање тачности за апроксимације различитог реда.

[1]Contrary to popular belief, an asymptotic expansion is not necessarily a divergent series (Erdelyi, 1956).

In Fig. (1), we have shown the relative error of the first 5 terms approximating $\Gamma(z)$ as the functions of z. As it could be seen, the increasing order shows better accuracy for the values of z larger than about 10, as one could expect from the structure of eq. (22).

One could readily notice that the first order approximation is not enough if requiring a better accuracy than one at the percentage level. From Fig. (2), it is also clear than for a small z a great level of accuracy could only be met by retaining several orders of approximation.

In Table 1, we show some values of $n!$ for small values of n and compare the results of different approximation orders. It readily appears that, even to achieve the precision of a pocket calculator, we have to retain several terms of eq. (17), and in particular for those n one has to consider at least the one shown in eq. (25), much more complicated than the simple expression usually cited of eq. (13).

n	$n!$	$\mathcal{O}(\hbar)$	$\mathcal{O}(\hbar^2)$	$\mathcal{O}(\hbar^3)$	$\mathcal{O}(\hbar^4)$
9	362880	359536.9	362865.9	362881.3	362880.0
10	3628800	3598695.6	3628684.7	3628809.7	3628800.0
11	39916800	39615625.1	39915743.4	39916880.2	39916800.4
12	479001600	475687486.5	478990871.8	479002341.9	479001603.7

Table 1 – The value of $n!$ for different orders of approximation
Таблица 1 − Значение $n!$ для аппроксимации различного порядка
Табела 1 − Вредност $n!$ за апроксимације различитог реда

Conclusions

We have shown in some detail the procedure of computing the integrals via the saddle point method, also known as the steepest descent method, which finds its application in several branches ranging from theoretical physics to computational methods. We have explicitly computed many terms of this asymptotic expansions furnishing analytical results, and applied its results to a well-known integral, estimating the error. We have also shown that, in order to obtain a certain degree of precision, the usual Gaussian term is not enough and a better approximation should be pursued.

Appendix

Here f_n refers to the n-th derivative of f taken at the point z_0.

Second order $\mathcal{O}(\hbar^2)$:

$$\frac{5\,f_3^2}{24\,f_2^3} - \frac{f_4}{8\,f_2^2} \tag{23}$$

Third order $\mathcal{O}(\hbar^3)$:

$$-\frac{f_6}{48\,f_2^3} + \frac{56\,f_3\,f_5 + 35\,f_4^2}{384\,f_2^4} - \frac{35\,f_3^2\,f_4}{64\,f_2^5} + \frac{385\,f_3^4}{1152\,f_2^6} \tag{24}$$

Fourth order $\mathcal{O}(\hbar^4)$:

$$\begin{aligned} &-\frac{f_8}{384\,f_2^4} - \frac{-20\,f_3\,f_7 - 35\,f_4\,f_6 - 21\,f_5^2}{640\,f_2^5} + \frac{-616\,f_3^2\,f_6 - 1848\,f_3\,f_4\,f_5}{3072\,f_2^6} \\ &-\frac{385\,f_4^3}{3072\,f_2^6} - \frac{-8008\,f_3^3\,f_5 - 15015\,f_3^2\,f_4^2}{9216\,f_2^7} - \frac{25025\,f_3^4\,f_4}{9216\,f_2^8} + \frac{85085\,f_3^6}{82944\,f_2^9} \end{aligned} \tag{25}$$

Fifth order $\mathcal{O}(\hbar^5)$:

$$\begin{aligned} &-\frac{f_{10}}{3840\,f_2^5} + \frac{220\,f_3\,f_9 + 495\,f_4\,f_8 + 792\,f_5\,f_7 + 462\,f_6^2}{46080\,f_2^6} \\ &+\frac{-1430\,f_3^2\,f_8 - 5720\,f_3\,f_4\,f_7 - \left(8008\,f_3\,f_5 + 5005\,f_4^2\right)\,f_6 - 6006\,f_4\,f_5^2}{30720\,f_2^7} \\ &+\frac{91520\,f_3^3\,f_7 + 480480\,f_3^2\,f_4\,f_6 + 288288\,f_3^2\,f_5^2 + 720720\,f_3\,f_4^2\,f_5 + 75075\,f_4^4}{294912\,f_2^8} \\ &+\frac{-340340\,f_3^4\,f_6 - 2042040\,f_3^3\,f_4\,f_5 - 1276275\,f_3^2\,f_4^3}{221184\,f_2^9} \\ &+\frac{2586584\,f_3^5\,f_5 + 8083075\,f_3^4\,f_4^2}{442368\,f_2^{10}} - \frac{11316305\,f_3^6\,f_4}{663552\,f_2^{11}} + \frac{37182145\,f_3^8}{7962624\,f_2^{12}} \end{aligned} \tag{26}$$

Sixth order $\mathcal{O}(\hbar^6)$:

$$\begin{aligned} &-\frac{f_{12}}{46080\,f_2^6} - \frac{-364\,f_3\,f_{11} - 1001\,f_4\,f_{10} - 2002\,f_5\,f_9 - 3003\,f_6\,f_8 - 1716\,f_7^2}{645120\,f_2^7} \\ &+\frac{-5720\,f_3^2\,f_{10} - 28600\,f_3\,f_4\,f_9 - \left(51480\,f_3\,f_5 + 32175\,f_4^2\right)\,f_8}{737280\,f_2^8} \end{aligned}$$

$$
\begin{aligned}
&- \frac{(68640\, f_3\, f_6 + 102960\, f_4\, f_5)\, f_7 - 60060\, f_4\, f_6^2 - 72072\, f_5^2\, f_6}{737280\, f_2^8} \\
&- \frac{-486200\, f_3^3\, f_9 - 3281850\, f_3^2\, f_4\, f_8 - \left(5250960\, f_3^2\, f_5 + 6563700\, f_3\, f_4^2\right) f_7}{6635520\, f_2^9} \\
&- \frac{3063060\, f_3^2\, f_6^2 - \left(18378360\, f_3\, f_4\, f_5 + 3828825\, f_4^3\right) f_6 - 3675672\, f_3\, f_5^3}{6635520\, f_2^9} \\
&- \frac{6891885\, f_4^2\, f_5^2}{6635520\, f_2^9} \\
&+ \frac{-3695120\, f_3^4\, f_8 - 29560960\, f_3^3\, f_4\, f_7 - \left(41385344\, f_3^3\, f_5 + 77597520\, f_3^2\, f_4^2\right) f_6}{7077888\, f_2^{10}} \\
&- \frac{93117024\, f_3^2\, f_4\, f_5^2 - 77597520\, f_3\, f_4^3\, f_5 - 4849845\, f_4^5}{7077888\, f_2^{10}} \\
&- \frac{-20692672\, f_3^5\, f_7 - 181060880\, f_3^4\, f_4\, f_6 - 108636528\, f_3^4\, f_5^2}{7077888\, f_2^{11}} \\
&- \frac{543182640\, f_3^3\, f_4^2\, f_5}{7077888\, f_2^{11}} \\
&- \frac{169744575\, f_3^2\, f_4^4}{7077888\, f_2^{11}} + \frac{-416440024\, f_3^6\, f_6 - 3747960216\, f_3^5\, f_4\, f_5}{31850496\, f_2^{12}} \\
&- \frac{3904125225\, f_3^4\, f_4^3}{31850496\, f_2^{12}} \\
&- \frac{-1487285800\, f_3^7\, f_5 - 6506875375\, f_3^6\, f_4^2}{31850496\, f_2^{13}} - \frac{929553625\, f_3^8\, f_4}{7077888\, f_2^{14}} + \frac{5391411025\, f_3^{10}}{191102976\, f_2^{15}}
\end{aligned}
\tag{27}
$$

Seventh order $\mathcal{O}(\hbar^7)$:

$$
\begin{aligned}
&- \frac{f_{14}}{645120\, f_2^7} + \frac{560\, f_3\, f_{13} + 1820\, f_4\, f_{12} + 4368\, f_5\, f_{11} + 8008\, f_6\, f_{10}}{10321920\, f_2^8} \\
&+ \frac{11440\, f_7\, f_9 + 6435\, f_8^2}{10321920\, f_2^8} \\
&+ \frac{-30940\, f_3^2\, f_{12} - 185640\, f_3\, f_4\, f_{11} - \left(408408\, f_3\, f_5 + 255255\, f_4^2\right) f_{10}}{30965760\, f_2^9} \\
&- \frac{(680680\, f_3\, f_6 + 1021020\, f_4\, f_5)\, f_9}{30965760\, f_2^9}
\end{aligned}
$$

Fabiano, N. et al, Saddle point approximation to higher order, pp.447–460

$$
\begin{aligned}
&- \frac{\left(875160\, f_3\, f_7 + 1531530\, f_4\, f_6 + 918918\, f_5^2\right)\, f_8}{30965760\, f_2^9} \\
&- \frac{875160\, f_4\, f_7^2 - 2450448\, f_5\, f_6\, f_7 - 476476\, f_6^3}{30965760\, f_2^9} \\
&+ \frac{23514400\, f_3^3\, f_{11} + 193993800\, f_3^2\, f_4\, f_{10}}{1857945600\, f_2^{10}} \\
&+ \frac{\left(387987600\, f_3^2\, f_5 + 484984500\, f_3\, f_4^2\right)\, f_9}{1857945600\, f_2^{10}} \\
&+ \frac{\left(581981400\, f_3^2\, f_6 + 1745944200\, f_3\, f_4\, f_5 + 363738375\, f_4^3\right)\, f_8}{1857945600\, f_2^{10}} \\
&+ \frac{332560800\, f_3^2\, f_7^2}{1857945600\, f_2^{10}} \\
&+ \frac{\left(2327925600\, f_3\, f_4\, f_6 + 1396755360\, f_3\, f_5^2 + 1745944200\, f_4^2\, f_5\right)\, f_7}{1857945600\, f_2^{10}} \\
&+ \frac{\left(1629547920\, f_3\, f_5 + 1018467450\, f_4^2\right)\, f_6^2 + 2444321880\, f_4\, f_5^2\, f_6}{1857945600\, f_2^{10}} \\
&+ \frac{244432188\, f_5^4}{1857945600\, f_2^{10}} \\
&+ \frac{-25865840\, f_3^4\, f_{10} - 258658400\, f_3^3\, f_4\, f_9}{212336640\, f_2^{11}} \\
&- \frac{\left(465585120\, f_3^3\, f_5 + 872972100\, f_3^2\, f_4^2\right)\, f_8}{212336640\, f_2^{11}} \\
&- \frac{\left(620780160\, f_3^3\, f_6 + 2793510720\, f_3^2\, f_4\, f_5 + 1163962800\, f_3\, f_4^3\right)\, f_7}{212336640\, f_2^{11}} \\
&- \frac{1629547920\, f_3^2\, f_4\, f_6^2}{212336640\, f_2^{11}} \\
&- \frac{\left(1955457504\, f_3^2\, f_5^2 + 4888643760\, f_3\, f_4^2\, f_5 + 509233725\, f_4^4\right)\, f_6}{212336640\, f_2^{11}} \\
&- \frac{1955457504\, f_3\, f_4\, f_5^3 - 1222160940\, f_4^3\, f_5^2}{212336640\, f_2^{11}} \\
&+ \frac{4759314560\, f_3^5\, f_9 + 53542288800\, f_3^4\, f_4\, f_8}{5096079360\, f_2^{12}}
\end{aligned}
$$

$$+\frac{\left(85667662080\,f_3^4\,f_5+214169155200\,f_3^3\,f_4^2\right)\,f_7}{5096079360\,f_2^{12}}$$
$$+\frac{49972802880\,f_3^4\,f_6^2+\left(599673634560\,f_3^3\,f_4\,f_5+374796021600\,f_3^2\,f_4^3\right)\,f_6}{5096079360\,f_2^{12}}$$
$$+\frac{119934726912\,f_3^3\,f_5^3+674632838880\,f_3^2\,f_4^2\,f_5^2+281097016200\,f_3\,f_4^4\,f_5}{5096079360\,f_2^{12}}$$
$$+\frac{11712375675\,f_4^6}{5096079360\,f_2^{12}}$$
$$+\frac{-2974571600\,f_3^6\,f_8-35694859200\,f_3^5\,f_4\,f_7}{509607936\,f_2^{13}}$$
$$-\frac{\left(49972802880\,f_3^5\,f_5+156165009000\,f_3^4\,f_4^2\right)\,f_6}{509607936\,f_2^{13}}$$
$$-\frac{187398010800\,f_3^4\,f_4\,f_5^2-312330018000\,f_3^3\,f_4^3\,f_5-58561878375\,f_3^2\,f_4^5}{509607936\,f_2^{13}}$$
$$+\frac{3399510400\,f_3^7\,f_7+41644002400\,f_3^6\,f_4\,f_6+24986401440\,f_3^6\,f_5^2}{113246208\,f_2^{14}}$$
$$+\frac{187398010800\,f_3^5\,f_4^2\,f_5}{113246208\,f_2^{14}}$$
$$+\frac{97603130625\,f_3^4\,f_4^4}{113246208\,f_2^{14}}+\frac{-10782822050\,f_3^8\,f_6-129393864600\,f_3^7\,f_4\,f_5}{84934656\,f_2^{15}}$$
$$-\frac{188699385875\,f_3^6\,f_4^3}{84934656\,f_2^{15}}$$
$$+\frac{1337069934200\,f_3^9\,f_5+7521018379875\,f_3^8\,f_4^2}{3057647616\,f_2^{16}}$$
$$-\frac{1838471159525\,f_3^{10}\,f_4}{1528823808\,f_2^{17}}+\frac{5849680962125\,f_3^{12}}{27518828544\,f_2^{18}} \quad (28)$$

References

Brillouin, L. 1926. La mécanique ondulatoire de Schrödinger: une méthode générale de resolution par approximations successives. *Comptes Rendus de l'Académie des Sciences*, 183, pp.24–26.

Daniels, H.E. 1954. Saddlepoint Approximations in Statistics. *The Annals of Mathematical Statistics*, 25(4), pp.631-650 [online]. Available at: http://www.jstor.org/stable/2236650 [Accessed: 15 January 2022].

Dirac, P.A.M. 1933. The Lagrangian in Quantum Mechanics. *Physikalische Zeitschrift der Sowjetunion*, 3(1), pp.64–72.

Erdelyi, A. 1956. *Asymptotic expansions*. New York: Dover Publications, Inc.

Feynman, R.P. 1965. Nobel Lecture. The Development of the Space-Time View of Quantum Electrodynamics. *The Nobel Prize*, December 11 [online]. Available at: https://www.nobelprize.org/prizes/physics/1965/feynman/lecture/ [Accessed: 15 January 2022].

Kramers, H.A. 1926. Wellenmechanik und halbzahlige Quantisierung. *Zeitschrift für Physik*, 39(10-11), pp.828–840. Available at: https://doi.org/10.1007/BF01451751.

Laplace, P.S. 1986. Memoir on the Probability of the Causes of Events. *Statistical Science*, 1(3), pp.364-378 [online]. Available at: http://www.jstor.org/stable/2245476 [Accessed: 15 January 2022].

Moivre, A. de. 1730. *Miscellanea analytica de seriebus et quadraturis*. London: J. Tonson & J. Watts

Moivre, A. de. 1756. *The Doctrine of Chances: Or, a Method of Calculating the Probabilities of Events in Play, the third edition*. London: A. Millar.

Parisi, G. 1988. *Statistical field theory*. Boston, MA, USA: Addison-Wesley Pub. Co. ISBN-13: 978-0201059854.

Ramond, P. 1989. *Field theory: A modern primer (Frontiers in physics)*. Boston, MA, USA: Addison-Wesley Pub. Co. ISBN-13: 978-0201157727.

Stirling, J. 1764. *Methodus differentialis: sive tractatus de summatione et interpolatione serierum infinitarum*. London: Prostat apud J. Whiston & B. White.

Wentzel, G. 1926. Eine Verallgemeinerung der Quantenbedingungen für die Zwecke der Wellenmechanik. *Zeitschrift für Physik*, 38(6-7), pp.518–529. Available at: https://doi.org/10.1007/BF01397171.

Whittaker, E.T. & Watson, G.N. 1927. *A Course of Modern Analysis, 4th edition*. Cambridge University Press. ISBN-13: 978-0521091893.

ПРИБЛИЖЕНИЕ СЕДЛОВОЙ ТОЧКИ К ВЫСШЕМУ ПОРЯДКУ

Никола Фабиано, **корреспондент**, *Никола* Мирков

Белградский университет, Институт ядерных исследований «Винча» − Институт государственного значения для Республики Сербия, г. Белград, Республика Сербия

РУБРИКА ГРНТИ: 27.27.15 Функции одного комплексного переменного,
27.35.57 Математические модели квантовой физики,
27.35.59 Методы теории возмущений
ВИД СТАТЬИ: обзорная статья

Резюме:

Введение / цель: В данной статье рассмотрено приближение седловой точки.

Методы: Метод седловой точки используется в нескольких различных областях математики и физики. В статье наглядно вычисляются несколько членов расширения для факторной функции.

Результаты: Интегралы, вычисленные таким образом, имеют значения близкие к точному.

Выводы: Поправками высшего порядка не следует пренебрегать, даже в тех случаях, когда требуются умеренные уровни точности.

Ключевые слова: приближение перевала, формула Стирлинга, квантовая теория поля.

АПРОКСИМАЦИЈА СЕДЛАСТЕ ТАЧКЕ ВИШЕГ РЕДА

Никола Фабиано, **аутор за преписку**, *Никола* Мирков

Универзитет у Београду, Институт за нуклеарне науке „Винча” - Институт од националног значаја за Републику Србију, Београд, Република Србија

ОБЛАСТ: математика
ВРСТА ЧЛАНКА: прегледни рад

Сажетак:

Увод/циљ: У овом раду разматра се апроксимација седласте тачке.

Методе: Метода седласте тачке користи се у неколико различитих области математике и физике. Израчунава се експлицитно неколико чланова проширења за факторску функцију.

Fabiano, N. et al, Saddle point approximation to higher order, pp.447–460

Резултати: Овако процењени интеграли имају приближно тачне вредности.

Закључак: Корекције вишег реда нису занемариве чак ни када се захтева умерени ниво прецизности.

Кључне речи: апроксимација седласте тачке, Стирлингова формула, квантна теорија поља.

Paper received on / Дата получения работы / Датум пријема чланка: 11.08.2021.
Manuscript corrections submitted on / Дата получения исправленной версии работы / Датум достављања исправки рукописа: 19.03.2022.
Paper accepted for publishing on / Дата окончательного согласования работы / Датум коначног прихватања чланка за објављивање: 20.03.2022.

THE PHASE STABILITY OF NANOSECOND GUNN OSCILLATORS

Vasily Y. Kozhevnikov[a], *Andrey* V. Kozyrev[b], *Vladimir* Y. Konev[c], *Aleksey* I. Klimov[d]

[a] Institute of High Current Electronics, Laboratory of Theoretical Physics, Tomsk, Russian Federation, e-mail: Vasily.Y.Kozhevnikov@ieee.org, **corresponding author**, ORCID iD: https://orcid.org/0000-0001-7499-0578

[b] Institute of High Current Electronics, Laboratory of Theoretical Physics, Tomsk, Russian Federation, e-mail: kozyrev@to.hcei.tsc.ru, ORCID iD: https://orcid.org/0000-0002-7078-7991

[c] Institute of High Current Electronics, Laboratory of Nonlinear Electrodynamic Systems, Tomsk, Russian Federation, e-mail: konev@lnes.hcei.tsc.ru, ORCID iD: https://orcid.org/0000-0001-8728-6491

[d] Institute of High Current Electronics, Physical Electronics Department, Tomsk, Russian Federation, e-mail: klimov@lfe.hcei.tsc.ru, ORCID iD: https://orcid.org/0000-0003-0953-1644

DOI: 10.5937/vojtehg70-36094; https://doi.org/10.5937/vojtehg70-36094

FIELD: Microwave Electronics
ARTICLE TYPE: Review paper

Summary:

Introduction/purpose: Detailed theoretical and experimental studies have been carried out in order to investigate the problem of a phase stability in electrodynamically uncoupled Gunn oscillators.

Methods: The influence of modulating pulse instabilities has been investigated by means of computer simulation in the framework of a nonlinear one-dimensional theoretical model of the GaAs Gunn diode semiconductor active region. Experimental observations were also conducted including microwave measurements and antenna far-field estimation. They confirm the main theoretical results and extend the key work conclusions.

Results: It was shown that the initial phase of the microwave oscillation out of the Gunn oscillator is independent of internal noises of the semiconductor structure and can be fixed only by the modulating voltage pulse.

ACKNOWLEDGMENT: The authors thank Dr. Herbert Krömer (Nobel Prize winner, IEEE Fellow) and Valery S. Syuvatkin for their help and fruitful discussion on the problem of phase synchronization phenomenon. Also, the authors express their sincere gratitude to doctors and nurses around the world who fight against COVID-19 infection, not sparing their health and lives for the benefit of all mankind.

Conclusion: Gunn-diodes based microwave oscillators were stabilized using the leading edge of the voltage pulse from the modulating power supply. These results open up serious prospects for designing antenna phased arrays based on Gunn oscillators without mutual feedback (electrodynamically independent).

Key words: microwave circuits, space-charge-limited devices, Gunn effect devices.

Introduction

The problem of phase synchronization in microwave oscillators has been of interest for decades (Schamiloglu, 2012). Creation of coherent high-frequency radiation sources offers great opportunities for the development of modern microwave technology. It allows to carry out the coherent spatial summation of radiated power and to provide the coherent signal accumulation mode in the near- and far-field radar systems. In turn, this can significantly increase the capabilities of receiving and transmitting devices (e.g. noise-to-signal ratio). The use of coherent microwave pulse oscillators will significantly improve the location range resolution. Furthermore, these capabilities allow developing active phased arrays modules.

The analysis of the excitation of microwave oscillations conventionally assumes the decisive role of noise in phase setting, resulting in randomness of the phase (Holliday, 1970). The phase stabilization of microwave oscillators is generally attained by using injection locking and phase locking providing strong electrodynamic feedback between oscillators (Pikovsky et al, 2010). The possibility of obtaining coherent oscillations from electrodynamically independent Gunn oscillators remained undiscovered for a long time. However, one more way has been discovered - to use a modulating voltage pulse (Vvedensky et al, 1975; Vvedensky et al, 1985). Vvedensky with co-authors explain the observed phase stabilization effect by a current spike which arises in the resonator of a Gunn oscillator and sets the initial phase (“shock” excitation). It has been emphasized that a reliable phase stabilization requires a rather short modulating pulse rise time (of about the oscillation period).

Based on the hypothetical possibility of synchronizing an oscillator without feedback, in our later experimental papers dealing with two electrodynamically independent nanosecond X-band Gunn oscillators producing ~ 30 W of microwave power (Gubanov et al, 2010; Konev et al, 2011), we observed phase stabilization and synchronization when the oscillators were excited from a common modulator with the modulating pulse rise time much longer than the oscillation period. The minimum

standard deviation of the phase difference between the oscillator signals was ~ 2 ps at a modulating pulse rise time of 6.5 ns (Konev et al, 2013).

These observations have been explained by means of a computer simulation and additional experiments. The results obtained suggest that the phase stabilization of a Gunn oscillator by a modulating voltage pulse, $U_{GD}(t)$, is governed by the intrinsic properties of the Gunn diode semiconductor. Specifically, the microwave oscillation phase is stabilized, once the semiconductor starts operating in a mode of negative differential resistance and a first high-field domain appears. This corresponds to a threshold voltage $U_{GD} = U_{th}$ reached at some point of the modulating pulse leading edge. The discovered effect was rather unexpected for us because we failed to find similar interpretation in the previous investigations.

This paper presents an extended review of the theoretical and experimental results regarding the phase stabilization of an uncoupled (independent) Gunn-diode based oscillator. The results convincingly suggest the possibility of the initial phase fixation in electrodynamically uncoupled X-band Gunn oscillators. This phase fixation is carried out only by a modulating voltage pulse applied to the oscillator.

Theoretical results

The initial experimental work led us to the idea that widely used electrotechnical computational methods (for example, the technique of replacing a semiconductor Gunn diode with an equivalent RCL circuit) are not sufficiently informative for studying the phase stability of a device. So we proposed theoretical studying of electronic processes in Gunn diodes to be based on a numerical simulation of the active layer of the Gunn diode semiconductor crystal in a non-stationary model. All proposed simulations have been carried out using the nonlinear local field model (McCumber & Chynoweth, 1966; Kroemer, 1966). The semiconductor structure of the Gunn diode is considered to be a GaAs one-dimensional crystal with two ohmic contacts at the opposite faces. Its microscopic structure in calculations is given by simplified quasihomogeneous doping profile containing localized inhomogeneity, the so-called "notch" (Figure 1).

In most computations, the quasihomogeneous semiconductor was assumed to have a donor concentration of 10^{15} cm^{-3}. The semiconductor layer diameter and length were 300 μm and 12.5 μm, respectively. A high field domain was formed due to the existence of a 0.6 μm long region of lower donor concentration ($0.9 \cdot 10^{15}$ cm^{-3}) located 0.6 μm away from the cathode ("notch" region). To describe the relation between the electron velocity and the electric field strength, a well-known approximation

(McCumber & Chynoweth, 1966) was used with the electron mobility taken equal to 8000 $cm^2/(V \cdot s)$ and the saturation drift velocity of carriers at high field (4000 V/cm) equal to 10^7 cm/s. The diffusion coefficient was taken constant and equal to 200 cm^2/s.

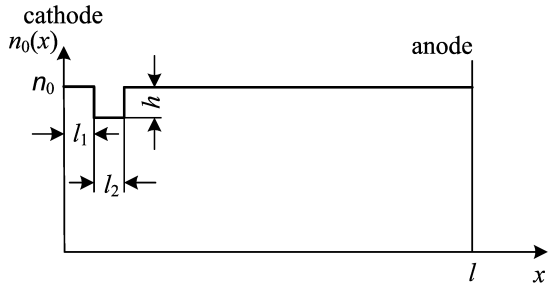

Figure 1 – Simplified active layer quasihomogeneous doping profile $n_0(x)$ of the Gunn diode semiconductor
Рисунок 1 – Упрощенный профиль квазиоднородного легирования активного слоя $n_0(x)$ полупроводника с диодом Ганна
Слика 1 – Поједностављени профил квазихомогене легуре активног слоја $n_0(x)$ полупроводника са Гановом диодом

Two important cases of connecting Gunn diodes were considered. In the first case, a simulation was performed for the simplest Gunn oscillator circuit consisting of a Gunn diode, a modulator, and a current-limiting resistor (R = 1 Ω) connected in series (Kozhevnikov et al, 2013).

In the other case, the Gunn oscillator equivalent circuit (with parameters R_1 = 1 Ω, L_1 = 0.5 nH, C_1 = 0.5 pF, L_2 = 1.2 nH, C_2 = 1.2 pF, R_2 = 0.5 Ω, L_3 = 0.5 nH) contained a resonator (Figure 2) to take into account the effect of the electric field on the processes occurring in the semiconductor layer (Konev et al, 2013). The units of this circuit and its parameters were specified to match the design of the oscillator used in our experiments (Gubanov et al, 2011) and so that sinusoidal microwave oscillations with a carrier frequency of 10 GHz were excited at the load R_2 simulating the output waveguide. The voltage pulse generated by the modulator had a trapezoidal shape and its instability was simulated by variations in the rise time t_e and the amplitude U_0. These variations produced phase deviations in the microwave pulse. For instance, for the circuit with resistive load, the variation Δt_e = ± 0.05 ns about an average value of 1 ns gave a current phase deviation Δt_{ph} equal to ± 0.016 ns (Figure 3*a*). For the circuit with a resonator under the same conditions, the Δt_{ph} was ± 0.022 ns (Figure 3*b*).

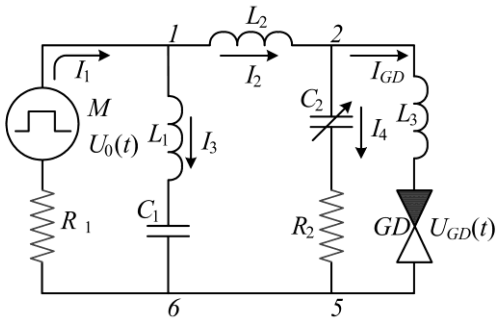

Figure 2 – Equivalent circuit simulating a Gunn oscillator in a resonator
Рисунок 2 – Эквивалентная схема, моделирующая генератор Ганна в резонаторе
Слика 2 – Еквивалентно коло које симулира Ганов осцилатор у резонатору

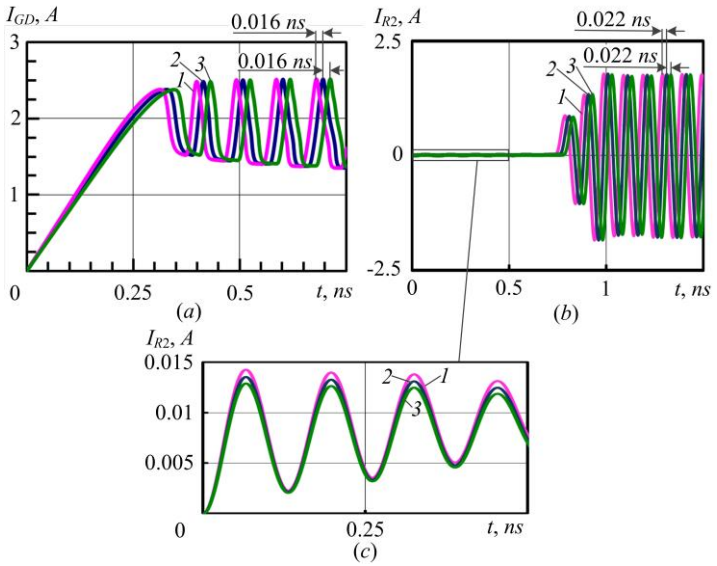

Figure 3 – Time dependences of the Gunn diode current at voltage pulse rise times t_e of 0.95 (1), 1 (2), and 1.05 ns (3) for the single-layer structure (a) in the circuit with resistive load and (b) at the load R_2 in the equivalent circuit, U_0 = 20 V.
Рисунок 3 – Профили тока диода Ганна в контуре с резистивной нагрузкой (а) и на нагрузке R_2 в эквивалентной схеме резонатора на рисунке 3 (б):
t_e = 0.95 (*1*), 1 (*2*), and 1.05 ns (*3*); U_0 = 20 V.
Слика 3 – Напонски профили Ганове диоде у колу резистивног оптерећења (а) и на оптерећењу R_2 у еквивалентном колу резонатора на слици 3 (б):
t_e = 0.95 (*1*), 1 (*2*), and 1.05 ns (*3*); U_0 = 20 V.

The simulation has also shown that Δt_{ph} did not increase on increasing

t_e at a fixed U_0 and $\Delta t_e \neq 0$, whereas an increase in t_e at a fixed $\Delta t_e = 0$ and $\Delta U_0 \neq 0$ gave an increase in Δt_{ph}. This means that the modulating pulse amplitude noise is the main reason of the oscillator phase instability increase caused by the pulse leading edge rise.

For the circuit with a resonator, the effect of phase stabilization was observed in the background of "shock" excitation in the oscillatory circuit, as demonstrated in Figure 3*c.* As it was shown (Konev et al, 2013), the only microwave oscillations appeared due to "shock" excitation observed both in the simulation and in the experiment could be considered as some appreciable "noise". The calculations show that in all studied cases, the oscillation amplitude of the Gunn diode current is about 1 A even in the first period when U_{GD} exceeds U_{th}, and this amplitude is noticeably higher than the above mentioned "noise" amplitude (Figure 3*b*). As a result, the observed phase deviation is defined by the instability of the modulating pulse rise time and amplitude, and the Gunn diode itself provides a stable phase during the excitation of the oscillatory process.

Experimental results

The experimental work was aimed to investigate the possibility of creating synchronized Gunn diodes oscillators. It includes several series of experiments. Most of experimental setups were carried out on nanosecond Gunn oscillators with one and two series-connected 3A762-type Gunn diodes. The use of two diodes implied, along with phase measurements, a study of the possibility for power enhancement. The oscillators were tuned to a carrier frequency of 10 GHz.

The first group of experiments have been conducted in order to measure the phase delay standard deviation with respect to the modulator pulse rise time (in Figure 4). The measurements were performed with a LeCroy WaveMaster 830Zi oscilloscope. The "delay" function was used to measure the standard deviations σ_{t1} and σ_{t2} of phase delay with respect to a certain time point during the modulating pulse rise $U_{DG}(t)$ for one and two series-connected Gunn diodes, respectively. The measuring channel for the modulating pulse had a working bandwidth of 1 GHz and each of those for the microwave signal had a working bandwidth of 13 GHz. The oscilloscope trigger voltage was ~ 500 mV.

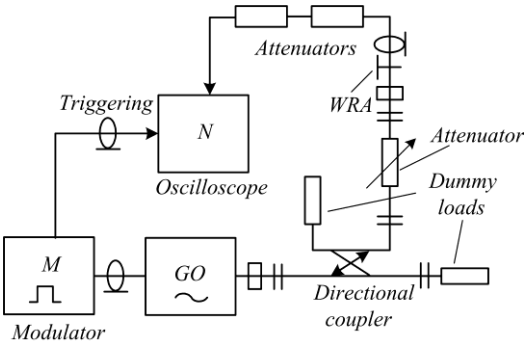

Figure 4 – Measuring circuit for the standard deviation of phase delay
Рисунок 4 – Схема измерения стандартного отклонения фазовой задержки
Слика 4 – Мерно коло за стандардну девијацију фазног кашњења

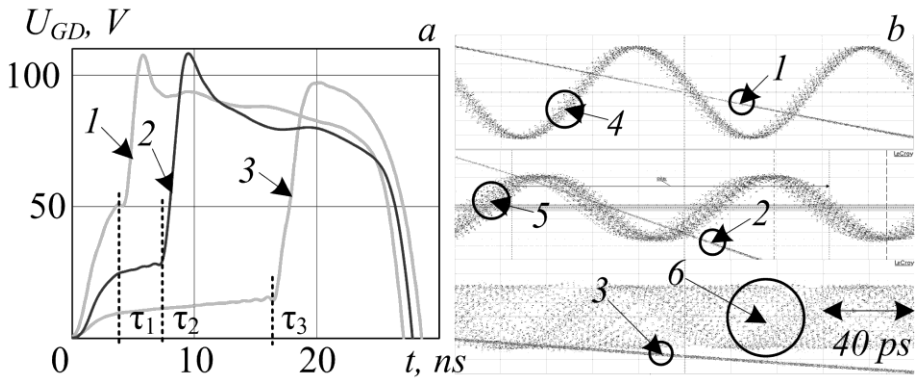

Figure 5 – (a) Oscillograms of the modulating pulse and (b) set of 2500 superimposed oscillograms of the modulating pulse and the microwave signal at different voltage rise times.
Рисунок 5 – (a) Осциллограммы модулирующего импульса и (b) набор из 2500 наложенных осциллограмм модулирующего импульса и СВЧ-сигнала при различном времени нарастания напряжения
Слика 5 – (a) Осцилограми модулационог импулса и (b) сет од 2500 суперпонираних осцилограма модулационог импулса и микроталасног сигнала у различитим временским интервалима пораста напона

The minimum standard deviations were σ_{t1} = 2.1 ps and σ_{t2} = 0.8 ps after excluding the oscilloscope jitter. The peak power with one and two diodes was ~ 30 and ~ 60 W, respectively. The much lower value of σ_{t2} compared with σ_{t1} suggests that the semiconductor structure has a stabilizing effect on the microwave oscillation phase.

In the experiments, we studied the influence of the voltage pulse rise time (rate of voltage rise dU_{GD}/dt) on σ_{t1}. For this purpose, chip inductors

L of 8.2 and 82 nH were connected in series with a Gunn diode between the modulator and the oscillator resonance chamber. Figure 5a and Figure 5b show the waveforms of the voltage pulse (1–3) and the microwave signal (4–6) for L = 0 nH (traces 1, 4), L = 8.2 nH (traces 2, 5), and L = 82 nH (traces 3, 6).

In the first case, the minimum standard deviation σ_{t1} was 2.1 ps; in the second case, it was 14.5 ps; and in the third case, the phase becomes unstable. The voltage rise times shown in Figure 5a are as follows: τ_1 = 4 ns, τ_2 = 7.2 ns, τ_3 = 16.4 ns. This dependence of σ_{t1} on the voltage rise time is explained by the fact that the phase deviation Δt_{ph} increases with increasing t_e due to some instability of the voltage pulse amplitude, as found in the simulation.

In the second experiment (Figure 6), we studied the phase synchronization of two oscillators with a peak power of 30 W which were connected in parallel and excited concurrently by a common modulator via strip lines of a geometric length of 120 cm (insulator – fiber glass laminate). This excluded the oscillators coupling via the modulator. Measurements were performed by a special procedure (Konev et al, 2011).

The modulating pulse rise time was 6.4 ns. Figure 7 shows the synchronized oscillograms of microwave signals 1 and 2 for these two oscillators. The oscillograms demonstrate that the microwave oscillation arising on time interval 4 due to the transition of the Gunn diode semiconductor structures to the mode of negative differential resistance is independent of the oscillations appeared within time interval 3 due to the “shock” excitation of the oscillatory circuit. It is seen that signal 2 (green) displays some phase failure.

Nevertheless, after several periods, signal phases 1 and 2 are aligned. On alternately switching off one of the Gunn oscillators, the oscillograms remained unchanged. Thus, a crosstalk-induced synchronization was excluded. The oscillations remained cophased during the whole microwave pulse with a full width at a half maximum of 16 ns.

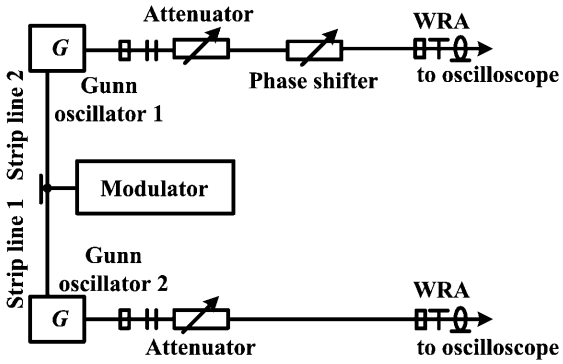

Figure 6 – Experimental measuring circuit for the syncronization of two independent Gunn oscillators
Рисунок 6 – Экспериментальная измерительная схема синхронизации двух независимых генераторов Ганна
Слика 6 – Експериментално мерно коло за синхронизацију два независна Ганова осцилатора

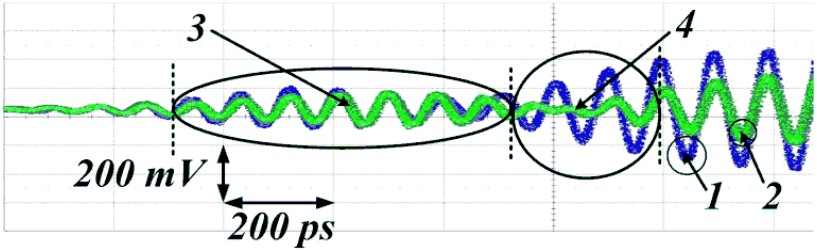

Figure 7 – Set of 2500 superimposed oscillograms of two Gunn oscillators
Рисунок 7 – Набор из 2500 наложенных осциллограмм двух осцилляторов Ганна
Слика 7 – Сет од 2500 суперпониpаних осцилограма два Ганова осцилатора

As the measured deviation value was 2.1 ps, so it fits the phase stability criterion for the development of antenna active phased arrays. It was also established that the serial connection of two identical Gunn diodes led to a significant reduction of the standard deviation value as compared to the same value for a single diode. Both of these favorable factors prompted another experimental study of the antenna system wave field (Kozhevnikov et al, 2015). Its visual scheme is shown in Figure 8. The antenna system consists of two synchronized nanosecond X-band Gunn oscillators GO_1 and GO_2 connected to rectangular horns 8 via attenuators 2 and a phase shifter 3. The Gunn oscillators were fed from a single voltage source 1 through strip lines. The horn antennas 8 were arranged in parallel to each other at a distance a = 14 cm between them.

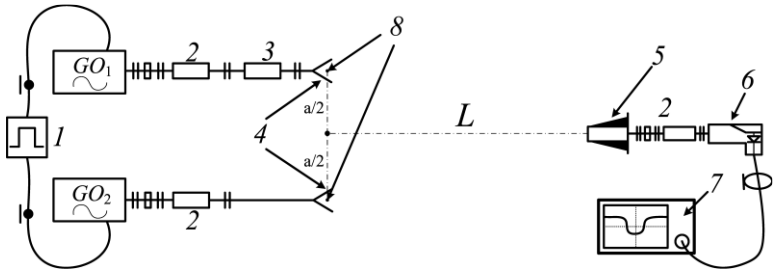

Figure 8 – Experimental setup of a wave field measurement of an antenna system
Рисунок 8 – Экспериментальная установка измерения волнового поля антенной системы
Слика 8 – Експериментална инсталација мерења таласног поља антенског система

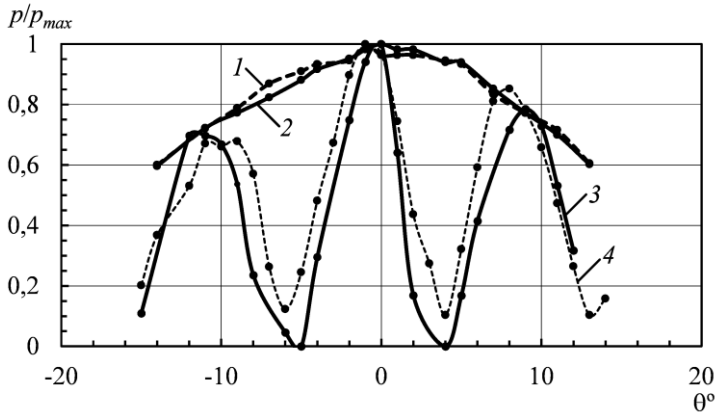

Figure 9 – Far-field measurement results: 1, 2 *– radiation pattern of each horn excited by an independent Gunn oscillator;* 3 *– microwave oscillations superposition of two horn antennas powered by a single standard oscillator with 500 us pulse duration;* 4 *– microwave oscillations superposition of two synchronized nanosecond Gunn oscillators*
Рисунок 9 – Результаты измерений в дальней зоне: 1, 2 – диаграммы направленности каждого рупора, возбуждаемые независимым генератором Ганна; 3 – суперпозиция СВЧ колебаний двух рупорных антенн с питанием от одного эталонного генератора с длительностью импульса 500 мкс; 4 – суперпозиция СВЧ колебаний двух синхронизированных наносекундных генераторов Ганна
Слика 9 – Резултати мерења у далеком пољу: 1, 2 – дијаграм зрачења сваког рога антене, побуђене независним Гановим осцилатором; 3 – суперпозиција микроталасних осцилација две рог антене са напајањем од једног стандардног осцилатора са трајањем импулса од 500 μс ; 4 – суперпозиција микроталасних осцилација двају синхронизованих наносекундних Ганових осцилатора

The receiving antenna 5 was connected to the waveguide

semiconductor detector 6 through an adjustable attenuator 2. The detected signal was recorded with the Tektronix-5401 real-time oscilloscope 7 with 1 GHz operating band. The coherent summation of the wave field patterns from two horn antennas powered by a single standard oscillator with a 500 us pulse duration, and powered by two synchronized nanosecond Gunn oscillators is shown in Figure 9.

Conclusions

The studies show that the microwave oscillation phase in the Gunn oscillators is stabilized in an instant when the Gunn diode semiconductor structure passes to the mode of negative differential resistance. In the experiments, we did not find the influence of noises that can perceptibly affect the phase. Appreciable oscillations were only those arising due to the pulse excitation of the oscillator resonance system. Once the threshold voltage is reached and the first high field domain is formed, the current amplitude through the Gunn diode structure increases in a time of about the oscillation period, reaching a near-stationary value which is much higher than the noise and “shock” excitation values. Thus, the oscillation phase of the Gunn oscillators with a microwave power of several tens of watt (e.g., those based on 3A762 diodes), can be stable even at much longer modulating pulse rise time compared to the microwave oscillation period.

The discovered effect and the phase instability measurements results suggest prerequisites for the development of phased arrays. It requires a simple phase synchronization mechanism with only the voltage pulse of common modulator or several synchronized modulators that produce a repeatable modulating pulse without strict limitations on its rise time.

References

Gubanov, V.P., Klimov, A.I., Koval’chuk, O.B., Konev, V.Yu. & Rostov V.V. 2010. An X-band nanosecond gunn oscillator. *Instruments and Experimental Techniques*, 53(5), pp.710-713. Available at: https://doi.org/10.1134/s0020441210050167.

Holliday, H.R. 1970. The effect of operating parameters and oscillator characteristics upon the phase angle between a locked X-band Gunn oscillator and its locking signal. *IEEE Transactions on Electron Devices*, 17(7), pp.527-533. Available at: https://doi.org/10.1109/t-ed.1970.17025.

Konev, V.Y., Gubanov, V.P., Klimov, A.I., Koval’chuk, O.B., Rostov, V.V., Sharypov, K.A. & Yalandin, M.I. 2011. Phase locking of nanosecond Gunn-effect oscillators. *Instruments and Experimental Techniques*, 54(6), pp.781-784. Available at: https://doi.org/10.1134/s0020441211050216.

Konev, V.Y., Klimov, A.I., Koval'chuk, O.B., Gubanov, V.P., Kozhevnikov, V.Yu., Kozyrev, A.V. & Torkhov, N.A. 2013. The effect of phase stabilization of microwave oscillations in nanosecond Gunn oscillators. *Technical Physics Letters*, 39(11), pp.957-959. Available at: https://doi.org/10.1134/s1063785013110072.

Kozhevnikov, V.Y., Konev, V.Y. & Klimov, A.I. 2015. Coherent radiation summation of two X-band nanosecond Gunn oscillators synchronized by a modulating pulse. In: *23rd Telecommunications Forum Telfor (TELFOR)*, Belgrade, Serbia, November 24-26. Available at: https://doi.org/10.1109/telfor.2015.7377524.

Kozhevnikov, V.Y., Konev, V.Yu., Klimov, A.I., Gubanov, V.P., Kovalchuk, O.B. & Kozyrev, A.V. 2013. Phase stabilization effect in nanosecond microwave Gunn oscillators. In: *21st Telecommunications Forum Telfor (TELFOR)*, Belgrade, Serbia, November 26-28. Available at: https://doi.org/10.1109/telfor.2013.6716324.

Kroemer, H. 1966. Nonlinear space-charge domain dynamics in a semiconductor with negative differential mobility. *IEEE Transactions on Electron Devices*, ED-13(1), pp.27-40. Available at: https://doi.org/10.1109/t-ed.1966.15631.

McCumber, D.E. & Chynoweth, A.G. 1966. Theory of negative-conductance amplification and of Gunn instabilities in "two-valley" semiconductors. *IEEE Transactions on Electron Devices*, ED-13(1), pp.4-21. Available at: https://doi.org/10.1109/t-ed.1966.15629.

Pikovsky, A., Rosenblum, M. & Kurths, J. 2010. Preface. In: *Synchronization: A Universal Concept in Nonlinear Sciences (Cambridge Nonlinear Science Series)*, pp.Xvii-Xx. Cambridge: Cambridge University Press. Available at: https://doi.org/10.1017/cbo9780511755743.001.

Schamiloglu, E. 2012. Recent trends in high power microwave source research: Multispectral and phase coherent solutions. In: *2012 Asia-Pacific Symposium on Electromagnetic Compatibility*, Singapore, pp.357-360, May 21-24. Available at: https://doi.org/10.1109/apemc.2012.6237975.

Vvedensky, V., Andrianov, A. & Ermilov, E. 1975. Coherent nanosecond radio pulse oscillator. *Pribory i tekhnika eksperimenta*, 1, pp.114-115.

Vvedensky, V., Suvatkin, V. & Khrustalev, A. 1985. Investigation of microwave oscillation phase stabilization in pulsed Gunn oscillators. *Radiotekhnika i elektronika*, 30(10), pp.2063-2064.

ФАЗОВАЯ УСТОЙЧИВОСТЬ НАНОСЕКУНДНЫХ ГЕНЕРАТОРОВ ГАННА

Василий Ю. Кожевников[а], **корреспондент**, *Андрей В.* Козырев[а], *Владимир Ю.* Конев[б], *Алексей И.* Климов[в]

Институт сильноточной электроники, г. Томск, Российская Федерация

[а] Лаборатория теоретической физики

[б] Лаборатория нелинейных электродинамических систем

[в] Отдел физической электроники

РУБРИКА ГРНТИ: 47.45.99 Прочие элементы СВЧ-техники
47.05.05 Теория радиотехнических цепей
ВИД СТАТЬИ: обзорная статья

Резюме:

Введение/цель: Подробные теоретические и экспериментальные исследования были проведены для изучения проблемы фазовой устойчивости в электродинамически развязанных генераторах Ганна.

Методы: С помощью компьютерного моделирования в рамках нелинейной одномерной теоретической модели активной области полупроводникового GaAs-диода Ганна исследовано влияние нестабильностей модулирующего импульса. Также были проведены экспериментальные наблюдения, включая микроволновые измерения и оценку дальнего поля антенны, которые подтвердили ключевые теоретические результаты и расширили основные выводы работы.

Результаты: Показано, что начальная фаза СВЧ колебаний вне генератора Ганна не зависит от внутренних шумов полупроводниковой структуры и может фиксироваться только импульсом модулирующего напряжения.

Выводы: Генераторы СВЧ на диодах Ганна стабилизировались по переднему фронту импульса напряжения от модулирующего источника питания. Эти результаты открывают серьезные перспективы для создания антенных фазированных решеток на основе генераторов Ганна без взаимной обратной связи (электродинамически независимых).

Ключевые слова: СВЧ-схемы, устройства с ограничением объемного заряда, устройства на эффекте Ганна.

ФАЗНА СТАБИЛНОСТ НАНОСЕКУНДНИХ ГАНОВИХ ОСЦИЛАТОРА

Василиј J. Кожевников[а], **аутор за преписку**, *Андреј* В. Козирев[а], *Владимир* J. Конев[б], *Алексеј И.* Климов[в]

Институт за високострујну електронику, Томск, Руска Федерација

[а] Лабораторија за теоријску физику

[б] Лабораторија за нелинеарне електродинамичке системе

[в] Одсек за физичку електронику

ОБЛАСТ: микроталасна електроника
ВРСТА ЧЛАНКА: прегледни рад

Сажетак:

Увод/циљ: Спроведена су детаљна теоријска и експериментална истраживања ради испитивања проблема фазне стабилности у електродинамички раздвојеним Гановим осцилаторима.

Методе: Коришћењем рачунарске симулације у оквиру нелинеарног једнодимензионалног теоријског модела активне зоне GaAs полупроводничке Ганове диоде проучен је утицај нестабилности модулационог сигнала. Такође, извршена су експериментална испитивања, укључујући микроталасна мерења и процену далеког поља антене, која су потврдила кључне теоријске резултате и проширила основне закључке рада.

Резултати: Доказано је да почетна фаза микроталасних осцилација ван Гановог генератора не зависи од унутрашњег шума полупроводничке структуре и да се може детектовати само модулационим сигналом напона.

Закључци: Микроталасни генератори са Гановим диодама стабилизовани су на предњој ивици напонског импулса из модулационог напајања. Ови резултати потврђују да постоје озбиљни изгледи за стварање антенских фазних решетака на бази Ганових генератора без међусобне повратне спреге (електродинамички независне).

Кључне речи: микроталасна кола, уређаји са ограниченим пуњењем, уређаји са Гановим ефектом.

Paper received on / Дата получения работы / Датум пријема чланка: 26.01.2022.
Manuscript corrections submitted on / Дата получения исправленной версии работы / Датум достављања исправки рукописа: 16.03.2022.
Paper accepted for publishing on / Дата окончательного согласования работы / Датум коначног прихватања чланка за објављивање: 18.03.2022.

LOGISTICS SUPPORT OF THE SERBIAN ARMED FORCES (SUPPLY AND MAINTENANCE THROUGH PUBLIC PROCUREMENT)

Milan D. Ilić

Serbian Arned Forces, Land Army, 69. logistic battalion,
Niš, Republic of Serbia,
e-mail: lanemts83@hotmail.com,
ORCID iD: https://orcid.org/0000-0001-5915-1303

DOI: 10.5937/vojtehg70-35171; https://doi.org/10.5937/vojtehg70-35171

FIELD: Logistics
ARTICLE TYPE: Review paper

Abstract:

Introduction/purpose: The work is based on the Rule of the Technical Service, the Law on Public Procurement, as well as on the experience gained in performing the duties of the Chief of Logistics in the Logistics Battalion of the Armed Forces. It contains the concept of Logistics Support and presents a part of the supply and maintenance system through Public Procurement in the Logistics Battalion of the Armed Forces.

Methods: The theoretical system of supply and maintenance is very complex and consists of a number of elements, organizational units, as well as certain principles. During the implementation, it is necessary to take into account all the principles and adhere to the rules and instructions. Also important was the help of colleagues from the Armed Forces and other state institutions who are in relevant positions and are important for logistics support.

Results: The final result of the work is a presentation of some activities performed by the logistics body in the battalion with a review of procurement under account 4252. In the final part of the paper, the emphasis is placed on the instructions which regulate and define the division of procurement in more detail, as well as on the implementation according to expenditure account 4252 on "ongoing maintenance and repair of equipment".

Conclusion: During the preparation of the paper, the biggest difficulty was the change of various rules and laws. Some rules and literature were written in the 1970s, and are still in force. A proposal for further tendencies would be to define new rules and organizations based on the experience of the countries in the region where the system has taken root.

Key words: logistics support, public procurement, supply, maintenance, ongoing maintenance.

Introduction

The paper is based on the Rule of the Technical Service, the Law on Public Procurement, as well as on the experience gained in performing the duties of the Chief of Logistics in the Logistics Battalion of the Armed Forces.

The paper discusses logistics support in general and the implementation of procurement at the battalion level.

In the final part, the emphasis is placed on the instructions which regulate and define the division of procurement in more detail, as well as on the implementation according to expenditure account 4252 i.e. "ongoing maintenance and repair of equipment".

The concept of logistics

The origin of the term logistics is related to the Greek word "logistikos", which means the skill of counting with numbers, and later with algebraic symbolism. Athenian officials who calculated state needs were called logisticians. According to other sources, this term is related to the French word "la logistique" which means lodger, predecessor.

In the military sense, this word was first used in the ninth century by Leo VI the Wise, the Byzantine emperor, who divided the art of war into strategy, logistics and tactics, and under logistics he understood activities related to the preparation of military campaigns (supply as well as assessment of enemies and land).

Much later, the French, and later the Russian general, the Swiss Antonie Henri Jominie (1779-1869), more specifically defined the concept of logistics and extended it to other general staff affairs. Many people associate this word with the word logic, because logistics deals with the logical integration of different activities.

It can be said that logistics today represents a qualitatively new approach to solving problems. It is a powerful scientific discipline in development for which the subject, theory, methods and language are not yet precisely defined, but which integrates numerous theoretical and practical achievements from several fields related to technical and organizational systems.

Logistics (as a science and function) has significant applications in both military and civilian systems, and therefore specific types of logistics are being developed such as: national logistics, civilian logistics, military logistics, industrial logistics, integrated logistics support and the like.

We are certainly primarily interested in military logistics. However, military logistics (although it is considered relatively independently) is

also part of national logistics, and, through it, part of international logistics. For its successful functioning, it is necessary to incorporate integrated logistics i.e. integrated logistics support (with significant influence and to be discussed later) directly related to armaments (weapons systems) and other technical materiel (systems) and military equipment as a link between the military and the country's economy.

Admiral Eccles gave simple definitions of logistics (Eklz, 1968), which, given the technical and technological development and current international relations, may require a better interpretation, which we can, in fact, understand well.

- International logistics is the process of planning and providing goods, facilities and services to support the military and the civilian economy at the international level.
- National logistics is the process of planning and providing goods and services to support national military forces and their operations, the national and civilian economy and its international obligations and requirements.
- Civil logistics is a process of planning and providing goods and services to support the civil economy.
- Military logistics is the process of planning and providing goods and services to support military forces.

National and military logistics are interesting for us in clarifying the importance and need for the introduction of logistics and logistics support in the Serbian Army. Therefore, they could be defined (although not fully in line with the requirements of scientific definition) as follows (Nikolić, 2000).

- National logistics aims to provide optimal logistics support to the national economy and national defense as a single system, provided that the internal and external requirements of such a system are met.
- Military logistics aims to provide logistics support to national defense, i.e. to its military forces and their operations (i.e. actions) in peace and war.

Logistics support

Logistics support (LS) in peace is organized and performed to support combat training, create favorable conditions for life and work as well as to prepare for timely transition from peacetime to war organization and maintenance of the necessary combat readiness. Both in war and in peace, the LS system is continuous.

The principles of LS (Pantelić, 1986) represent the attitudes that guide the preparation and implementation of logistics support functions in the implementation of missions and tasks. These are the starting points in the construction of the system, and they are derived from the scientific knowledge of the legality of armed combat and the valid doctrinal statements on the use of the Army.

By analyzing the conditions for planning and implementing LS, we can see the existence of general and special principles in LS.

The general principles of LS are: continuity, timeliness, completeness, elasticity, economy, and flexibility.

Continuity implies constant realization of LS in all conditions. It is achieved by establishing a favorable organization, allocating material reserves and service resources by synchronizing the work of commands, staffs, administrations, bodies and units and logistic support institutions, which ensure continuity in logistics support.

In order to achieve continuity of LS, it is necessary to improve and train all elements of the logistics support system for work in war and in the most unfavorable conditions.

Timeliness means delivering assets to users and providing services to users when needed. For example, if an artillery unit is supplied with ammunition for fire preparation much in advance, the unit's movement, if required, will be more difficult. If ammunition is delivered after fire preparation is completed, it is clear that the unit could not have completed its task to the fullest, and the responsibility lies with the bodies that did not provide timely delivery.

Completeness means the completeness of the delivered material resources, meeting the needs of the units with all the necessary resources and providing all the necessary services. For example, if fuzes are not delivered with artillery shells, the unit cannot perform its task. Or, if the unit does not receive all kinds of necessary material resources or if technical material resources are not renewed, the execution of the task may be called into question.

Flexibility means the ability of the LS system to adapt its organization and work to the conditions and changes of a particular situation. The flexibility of the system ensures the functioning of the LS system in all forms of armed actions and in the entire territory of combat operations.

Economy means performing tasks with the least expenditure of resources and labor. Although the military is a non-productive organization, it is still important, given the value of the material flowing through the LS system, to ensure rationality and economy in the system.

Economy is achieved by taking complex measures, with special attention must be paid to the orderliness and timeliness of preparations.

The special principles of LS are derived from the principles of the national war skills. They change in accordance with changes in the objective conditions and legality of armed combat. Therefore, they must be creatively applied, new ones found, theoretically shaped and tested in practice.

The special principles of LS are the following principles: unity of logistics support system, centralized management of logistics support, territorial organization of logistics support, universality of logistics support units, automation in LS, and LS as required.

The unity of the LS system implies that the LS system is unique to the defense system as a whole, with a division of responsibilities. It fits into a single system of providing material conditions by the state, with full reliance on the potential of the territory as a whole.

Territoriality of the LS organization implies the territorial organization of the logistics support system. In that sense, adequate territorial LS and institutions are formed, and they present executive bodies for LS on their territories. They perform LS of all units and institutions that rely on them in accordance with the reliance scheme and of all units that perform their tasks in that territory.

The universality of LS units is reflected in the organizational and formative ability of LS units to perform complete LS of all units and institutions that rely on them. Rapid changes in the situation and different conditions for conducting combat operations will affect the formation of temporary formations and frequent changes in subordination of units. That is why the logistic units - institutions are organized in such a way as to provide quick subordination, maneuvering of reserves and monitoring of combat schedules.

The functions of logistics support are realized through technical, quartermaster, medical, veterinary, traffic, and construction support (Conić, 2008).

Technical support

Technical support is an organized and mutually harmonized set of activities, actions and procedures of commands (administrative units) and units (institutions) of the army which, in cooperation with the competent state bodies, ensure the supply and maintenance of TMR. Timely and uninterrupted TS creates the necessary material and technical conditions for living, working and performing combat activities.

It is realized through bases that are qualified for TS of all units-institutions in the territory they cover (SSNO, 1979).

Technical support includes:
- supply of technical material resources, and
- maintenance of technical material resources.

Concept of supply

Supply of material resources is the basic function of logistics support. It is a planned and organized activity of commands, administrations, units and institutions as professional bearers which ensures timely and uninterrupted provision of LS resources with timely and uninterrupted provision of units and institutions with material resources (MR) necessary for life, work, training, construction - maintaining combat readiness, that is, in order to create the necessary material and technical conditions for armed combat (Maksić et al, 2005).

Supply can be:

- indirect (through the line of administrative bodies) - when the flows of documents are realized according to the basic supply scheme: from the highest to the lowest bodies, and
- direct (through the line of executive bodies) - when the units and institutions address the executive supply bodies: units and warehouses.

Supply is realized when appropriate conditions are met, i.e. when in a process or system there is a need for a certain type of assets and such assets can be provided from appropriate sources of supply. Sources of supply must be able to provide necessary assets in required quantities. It should be taken into account that, in order to realize the needs in a given time, different supply elements are engaged and that there is a constant exchange of information about the needs of users and possibilities of realization of supplies.

Supply processes

Supply processes are:
- planning,
- procurement,
- fulfillment, and
- managing and handling.

Planning includes planning activities of administrative bodies about the fulfillment with MR, material formation, sets, criteria, norms and

spending of MR, as well as other normative acts. It is done through long-term and medium-term development plans. Various data from studies and analyzes are used in making the plans.

Procurement is the process by which procurement and technical authorities implement equipment plans, as well as task and funding plans. It is done on the basis of approved plans of tasks and financing for the current year.

The order fulfillment is the process of realization of plans for equipping units and institutions with assets with the aim of forming the initial fulfillment of war reserve (WR) and peacetime supplies at all levels of supply and their maintenance at the prescribed level. Data from records, equipment plans, and various orders are the basis for planning the fulfillment of MR.

Managing and handling include the processes of receiving and sending MR, as well as storing, renewing, categorizing and distributing them. Material resources distributed to units and institutions are managed by commanders and handled by operators.

Concept of maintenance

Maintenance is an activity which ensures the required degree of correctness and reliability of TMR by the planned use of available maintenance capacities and the application of prescribed measures and procedures (Škola nacionalne odbrane, 2005).

The basic principles on which maintenance is based are:

- Centralized management - resulting from the commanding system in the Army of Serbia. Based on this principle, commands and administrations make unique plans, organize and manage the maintenance of TMR.
- Territoriality in the organization of maintenance - it is reflected in the support of units and institutions and the planned and prepared capacities of the territory.
- Autonomy in maintenance – it is expressed by qualified staff and material equipment of ships, units and institutions for the execution of all activities in the maintenance of TMR within their competence.
- Unique technology – it provides identical access to an appropriate type of maintenance at each command and executive level and allows continuous maintenance of TMR.
- Timeliness in maintenance – it is achieved by timely implementation of measures, procedures and actions to keep TMR in good condition for as long as possible.

- Rationality – it is reflected in the long-term preservation of the correctness of TMR and proper handling of human and material resources.

Elements of the maintenance system

The elements of the maintenance system are:

- personnel (officers, non-commissioned officers, military officers and employees, contract soldiers, conscripts), who exist in administrative and executive bodies;
- technical material resources (reserves and stocks of OS, equipment, etc.);
- the space in which the elements of the maintenance system are developed;
- maintenance plans;
- maintenance documents; and
- military professional literature in the field of maintenance.

The organization and implementation of maintenance is carried out by administrative and executive bodies.

Administrative bodies plan and organize the implementation of maintenance, adopt regulations governing the work of services, monitor development and propose the most favorable organizational and formation solutions, plan education, training and advanced training of personnel and keep the prescribed documentation and records.

Executive bodies are institutions and units of LS that perform and directly conduct maintenance for units and institutions that are under their jurisdiction.

Executive bodies consist of units and institutions. They are responsible for the immediate professional realization of maintenance tasks.

Maintenance units are part of LS units. These are organizational and formation teams intended for the realization of certain tasks within the prescribed types of maintenance of TMR.

Depending on the purpose, type of maintenance they perform, the scope and types of tasks in the field of maintenance of technical material resources and the command level they support, maintenance units are organized as:

- maintenance companies;
- maintenance platoons; and
- maintenance squads.

Within maintenance units, or independently, specialized maintenance units are formed based on TMR groups: weapons, motor vehicles, military communications, electronics and electric power means.

Supply and maintenance through public procurement in the logistics battalion of the Land Army

In the brigades of the Land Army, the bearer of logistics affairs is the logistics battalion on which organic and extra-organic formations rely for various account expenditures.

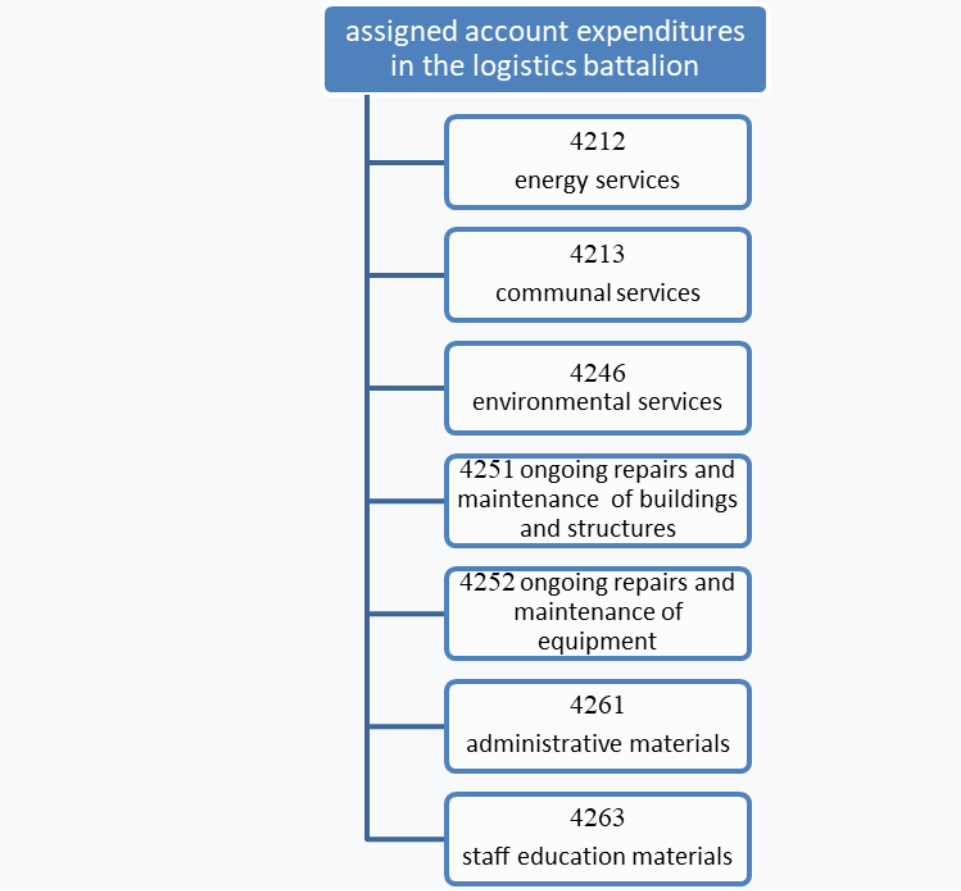

Figure 1 – Assigned account expenditures in logistics battalions
Рис. 1 – Расходы по затратным счетам тылового обеспечения в батальоне
Слика 1 – Додељени контни расходи у логистичким батаљонима

Regarding the realization of supply and current maintenance through public procurement, procurement according to expenditure account 4252, i.e. "ongoing maintenance and repair of equipment", is realized by the Logistics Group S-4 Battalion Command by initiating Public Procurement in accordance with the Law on Public Procurement and Rulebook on Material and Financial Operations.

Public procurement procedures

Pursuant to the general provisions of the Law on Public Procurement Article 51 (Službeni glasnik Republike Srbije, 91/2019), public procurement procedures are:

1) open procedure;
2) restrictive procedure;
3) competitive procedure with negotiation;
4) competitive dialogue;
5) negotiation procedure with a public invitation;
6) innovation partnership; and
7) negotiation procedure without a public invitation.

At the battalion level, based on expenditure account 4252 ("ongoing maintenance and repair of equipment"), an open procedure (by concluding Framework Agreements) is usually conducted as well as a procedure under Article 27 of the Law on Public Procurement to which the Law does not apply.

Procurement carried out by logistics authorities in logistics battalions based on expenditure account 4252 is divided into three parts:

- Consolidated Procurement (procurement applicable through Framework Agreements);
- Procurement in the field of defense and security; and
- Procurement to which the law does not apply.

Within the stated account expenditure, there are different purchases of "services" and "goods". Procurement is considered initiated at the moment when the "Decision on initiating procurement" is made, and not by introducing the request into the records of the user unit.

Consolidated procurement

As a rule, the contracting authority awards the contract in an open or restrictive procedure, and may also perform it in other public procurement procedures if the conditions prescribed by this Law are met, except for the negotiation procedure with a public invitation. As a rule, the

contracting authority awards the contract in an open procedure, restrictive procedure, negotiation procedure with a public invitation or competitive dialogue, and may also perform in other public procurement procedures if the conditions prescribed by this Law are met, except in competitive negotiating procedures.

The minimum deadline for submitting bids in an open procedure is:

1) 35 days from the day of sending the announcement of the public invitation, for public procurement whose estimated value is equal to or greater than the amount of European thresholds;

2) 25 days from the day of sending the announcement of the public invitation, for public procurement whose estimated value is less than the amount of European thresholds;

3) 15 days from the day of sending the announcement of the public invitation, for the procurement of works whose estimated value is lower than 30,000,000 dinars; and

4) ten days from the day of sending the announcement of the public invitation, for the procurement of goods and services whose estimated value is lower than 10,000,000 dinars

Procurement through Framework Agreements is divided into procurement related to services or goods. Battalion commands rarely enter into Framework Agreements which, during their validity, carry out the procurement of goods and services by concluding contracts or issuing purchase orders.

The framework agreement is in principle concluded by the Logistics Directorate J-4 with a validity period of 2 to 3 years, depending on whether it is concluded with 1 or more bidders.

The Law on Public Procurement does not follow the current Rulebook on material and financial operations, according to which the valid rule is that if the value of the procurement exceeds 500,000.00 dinars without VAT, a contract is signed for it, otherwise an order form is issued. The Law on Public Procurement has a higher "threshold of the amount" of issuing a purchase order and it is 5,000,000.00 dinars.

Procurement in the field of defense and security

Procurements in the field of defense and security were conducted on the basis of Article 20 of the Law on Public Procurement (Special Exceptions in the Field of Defense and Security), paragraph 6) concluded

by the Republic of Serbia with state, regional or local self-government bodies of other countries.

(1) procurement of military equipment or security-sensitive equipment;

(2) works and services directly related to such equipment; or

(3) works and services exclusively for military purposes or security-sensitive works and security-sensitive services.

Bidders who apply and who enter the selection procedure for signing the Framework Agreement pass the security check and the validity of the Framework Agreement is for 5 years.

The procurement is announced by the Tactical Holder of a certain asset, and is carried out by the end user in the Air Force (logistics battalions).

Procurement to which the law does not apply:

Procurement in the sense of the Law on Public Procurement to which the law does not apply is defined on the basis of Article 27 of the LPP.

The provisions of this law do not apply to:

1) procurement of goods, services and conducting design competitions, the estimated value of which is less than 1,000,000 dinars, and procurement of works whose estimated value is less than 3,000,000 dinars;

2) procurement of goods, services and conducting design competitions, the estimated value of which is less than 15,000,000 dinars, for the needs of diplomatic missions, diplomatic and consular missions and performing other activities of the Republic of Serbia abroad, as well as procurement of works for those needs the estimated value is less than 650,000,000 dinars;

3) procurement of social and other special services referred to in Article 75 of this Law, the estimated value of which is less than 15,000,000 dinars when the procurement is conducted by a public procuring entity, or less than 20,000,000 dinars when the procurement is conducted by a sectoral procuring entity.

In the case referred to in paragraph 1 of this Article, the principles of this Law are applied in a manner that is appropriate to the circumstances of the specific procurement.

When the procurement from this article is performed, the contracting authority is obliged to prevent the existence of conflicts of interest, to

ensure competition and that the agreed price is not higher than the comparable market price.

The public procurement procedure is conducted by a public procurement officer, i.e. a person employed in public procurement, unless the complexity of the subject of public procurement does not require the participation of other experts. In the procurement procedure, the procuring entity invites at least 3 persons who perform the activity that is the subject of public procurement and who, according to the information, are able to perform the procurement, submit bids and at the same time perform the invitation to submit bids on the public procurement portal and its website.

In practice, each SA unit of the operational level has a certain account and certain funds by groups of PS, which is available at certain time intervals. A commission is established to act in accordance with Articles 31 and 39 of the Law on Public Procurement (Službeni vojni list 29/2014).

Before each procurement of goods, regardless of the type of procurement, it is necessary to send a request to CLoB as the carrier of logistics at the level of the Serbian Army, whether the required spare part is in stock. After receiving a negative answer, the unit that sent the request initiates the procurement in accordance with the Laws and regulations.

Conclusion

This paper covers the concept of Logistics Support and presents a part of the supply and maintenance system through public procurement in the Logistics Battalion of the Armed Forces.

The theoretical system of supply and maintenance is very complex and consists of a number of elements, organizational units, as well as certain principles.

During the implementation, it is necessary to take into account all the principles and adhere to the rules and instructions.

References

Conić, N. 2008. *Mornaričkotehničko i tehničko obezbeđenje, zabeleške sa predavanja*. Beograd: Vojna akademija (in Serbian).

Eklz, E.H. 1968. *Logistika u nacionalnoj odbrani*. Beograd: Vojnoizdavački zavod (in Serbian).

Maksić, R., Andrejić, M.& Nikolić, N. 2005. *Taktika tehničke službe*. Beograd: Ministarstvo odbrane, Sektor za ljudske resurse, Uprava za školstvo (in Serbian).

Nikolić, M. 2000. *Nacionalna logistika, predavanja u ŠNO*. Beograd: Škola nacionalne odbrane (in Serbian).

Pantelić, B. 1986. *Snabdevanje tehničkim materijalnim sredstvima*. Zagreb: Visoke Vojne Škole KoV JNA (in Serbian).

-Službeni glasnik Republike Srbije. 91/2019. *Zakon o Javnim nabavkama*. Beograd: JP „Službeni glasnik“ (in Serbian).

-Službeni vojni list. 29/2014. *Pravilnik o Materijalnom poslovanju.* Beograd: Ministarstvo odbrane Republike Srbije (in Serbian).

-SSNO. 1979. *Pravilo Tehničke službe*. Beograd: SSNO, TehničkaUprava (in Serbian).

-Škola nacionalne odbrane. 2005. *Organizacija održavanja TMS, skripta*. Beograd: Škola nacionalne odbrane (in Serbian).

МАТЕРИАЛЬНО-ТЕХНИЧЕСКОЕ ОБЕСПЕЧЕНИЕ ВООРУЖЕННЫХ СИЛ (СНАБЖЕНИЕ И ТЕХНИЧЕСКОЕ ОБСЛУЖИВАНИЕ С ПОМОЩЬЮ ГОСУДАРСТВЕННЫХ ЗАКУПОК)

Милан Д. Илич

Вооружённые силы Республики Сербия, Сухопутные войска,
69-й тыловой батальон, г. Ниш, Республика Сербия

РУБРИКА ГРНТИ: 81.88.00 Материально-техническое снабжение. Логистика;
81.88.75 Экономика, организация, управление, планирование и прогнозирование в материальнотехническом снабжении

ВИД СТАТЬИ: обзорная статья

Резюме:

Введение/цель: Данная статья основана на Регламенте о технической службе, Законе о государственных закупках, а также на опыте, полученном при исполнении обязанностей начальника тылового обеспечения при батальоне логистики Вооруженных сил Республики Сербия. В работе приведены положения о материально-техническом обеспечении в целом и снабжении на уровне батальона.

Методы: Теоретическая система снабжения и обслуживания представляет собой сложную структуру и состоит из ряда элементов, организационных единиц, а также определенных принципов. При ее воплощении в жизнь необходимо учитывать все принципы и придерживаться правил и инструкций. Немаловажной оказалась и помощь коллег - представителей

Вооруженных сил и других государственных учреждений, занимающих важные для тылового обеспечения должности.

Результаты: Конечным итогом статьи является представление части работы, выполненной отделом материально-технического обеспечения батальона, с обзором закупок по счету 4252. В заключительной части статьи акцентируется внимание на инструкциях, дополнительно регламентирующих и определяющих разделение закупок и выполнение отчета по расходам 4252 «текущий ремонт и техническое обслуживание оборудования».

Выводы: Самой большой трудностью в написании статьи оказались изменения различных правил и законов. Несмотря на то, что некоторые правила и литература были написаны в 1970-х годах прошлого века они все еще в силе. В данной связи предложено применение современных тенденций в определении новых правил и организации, основанных на опыте соседних стран, где эта система укоренилась и успешно действует.

Ключевые слова: материально-техническое обеспечение, государственные закупки, снабжение, техническое обслуживание, текущее техническое обслуживание.

ЛОГИСТИЧКА ПОДРШКА ВОЈСКЕ СРБИЈЕ (СНАБДЕВАЊЕ И ОДРЖАВАЊЕ ПУТЕМ ЈАВНИХ НАБАВКИ)

Милан Д. Илић

Војска Србије, Копнена војска, 69. логистички батаљон,
Ниш, Република Србија

ОБЛАСТ: логистика
ВРСТА ЧЛАНКА: прегледни рад

Сажетак:

Увод/циљ: Рад је заснован на Правилу техничке службе, Закону о јавним набавкама, као и на искуствима начелника логистике у логистичком батаљону КоВ-а стеченим на обављању дужности.. Наведене су одредбе о логистичкој подршци уопште и спровођењу набавки на нивоу батаљона.

Методе: Теоријски систем снабдевања и одржавања је веома сложен; састоји се од низа елемената, организацијских целина, као и од одређених начела. При реализацији је потребно узети у обзир сва начела и придржавати се правила и упутстава. Такође, значајна је и помоћ колега из ВС и других државних институција, који се налазе на одговарајућим позицијама, а битни су за логистичку подршку.

Ilić, M., Logistics support of the Serbian Armed Forces (supply and maintenance through public procurement), pp.475-490

Резултати: Крајњи резултат рада јесте приказ дела послова које обавља орган логистике у батаљону са освртом на набавке по конту 4252. Тежиште завршног дела рада је на инструкцијама којима се ближе регулише и дефинише подела набавки, као и спровођење по контном расходу 4252 – „текуће поправке и одржавање опреме".

Закључак: Приликом израде рада највећу потешкоћу представљала су разна правила и закони. Наиме, поједина правила писана су седамдесетих година прошлог века, и још увек су на снази. Стога би било потребно да се дефинишу нова правила и организације, по угледу на земље у окружењу у којима је тај систем заживео.

Кључне речи: логистичка подршка, јавне набавке, снабдевање, одржавање, текуће одржавање.

Paper received on / Дата получения работы / Датум пријема чланка: 01.12.2021.
Manuscript corrections submitted on / Дата получения исправленной версии работы / Датум достављања исправки рукописа: 18.03.2022.
Paper accepted for publishing on / Дата окончательного согласования работы / Датум коначног прихватања чланка за објављивање: 19.03.2022.

Руска војска добија прве модернизоване самоходне хаубице 203 мм 2S7M Malka[1]

Према наводима компаније *Uralvagonzavod,* прва серија модернизованих самоходних хаубица 2S7M *Malka* предата је руском Министарству одбране.

Модернизована самоходна хаубица 2S7M Malka утоварена за испоруку руској војсци

Тренутно нема информација о броју хаубица испоручених војсци; само је наведено да се ради о првој тури самоходних хаубица 2S7M *Malka* које су ремонтоване и модернизоване. Модернизација је обављена у компанији *Uraltransmash*, а односила се назамену мењача, дистрибуционих механизама, погонских јединица, осматрачких уређаја и система вођења, комуникационе опреме и радио-станице. Систем АБХ заштите такође је модернизован. Поред тога, омогућено је гађање мета употребом беспилотних летелица.

Током априла 2020. године, компанија *Uralvagonzavod* најавила је завршетак дубинске модернизације првог примерка самоходне хаубице

[1] Defense News December 2021 Global Security army industry 07 December 2021

2S7M *Malka* и спремност за серијску модернизацију целе флоте самоходних хаубица. Наводно је тада Министарство одбране закључило и одговарајући уговор са том компанијом.

Самоходна хаубица 2S7M *Malka* може испаљивати различите врсте муниције из свог топа 2A44 од 203 мм. Сам топ тежи 14,6 тона, а муниција се састоји од различитих врста граната, укључујући активно-реактивне гранате, као и оне са нуклеарном бојевом главом. Ова хаубица великог калибра првенствено је развијена за тактички нуклеарни удар. Прва модификација хаубице 2S7 *Pion* је у оперативној употреби од 1975, а модернизована верзија 2S7M од 1986. године.

Маса самоходне хаубице у оперативној употреби износила је 46,5 тона, а радио-опрема R-173 била је стандардна. Хаубица је носила четири гранате, друге четири превозило је возило у пратњи, и била је спремна за борбену употребу у року од 7 минута. Брзина спремности хаубице за дејство омогућавала је испаљивање једне до две гранате пре премештања на други ватрени положај. Посаду чини 14 чланова од којих седморица седе на задњем делу хаубице, док се остатак вози у пратећем возилу или оклопном транспортеру.

Хаубица 2S7 има посебно развијену шасију, а заснована је на шасији тенка Т-80 и спада у највеће шасије међу руским оклопним возилима. Шасија је необичног облика, јер је кабина за посаду смештена скроз напред и служи као контратег у односу на топ. Иза кабине налази се мотор.

Мотор има велики део делова са тенкова Т-72 и Т-80. Покреће га дизел мотор, а V-46-1 развија 750 КС. Возило је опремљено и помоћним агрегатом који развија 24 КС и напаја све системе када се угаси главни погон.

Године 2020. развијена је нова генерација граната за верзију *Malka*.

Самоходна хаубица 2S7 Malka 203 мм на приказу наоружања 2018. године

Историјат самоходне хаубице 2S7 Malka

Технички захтеви за хаубицу први пут су изнети у марту 1970. године, па су прве самоходне хаубице *Pion* 2S7 почеле да стижу у артиљеријске јединице током друге половине седамдесетих година. Ова хаубица нема куполу, а топ се налази на задњем делу возила. Муниција је подразумевала високоексплозивне пројектиле и пројектиле потпомогнуте ракетним моторима. Високоексплозивне гранате, ознаке *ZVOF43* и *ZVOF42,* теже 110 кг и садрже 17,8 кг експлозива. Максимални домет је 37,5 км, а брзина гранате у лету износи 960 м/с . Реактивни пројектил *ZVOFZ5* тежи 103 кг и садржи 13,8 кг експлозива. Гранате ознаке *ZVOF15* и *ZVOF16* садрже касетну муницију чији једомет 47,5 км. Топ, такође, испаљује и противбетонске, нуклеарне и хемијске гранате. Током 16 година произведено је око 500 самоходних хаубица 2S7 у различитим модификацијама.

Самоходна хаубица *Pion* 2S7 опремљена је механичким осматрачким уређајем D-726, панорамским уређајем PG-1M, колиматором K-1 и нишанским уређајем OP-4M који се користи за непосредно гађање циљева. Осим пешадијског наоружања посаде, самоходна хаубица у свом арсеналу поседује и преносни противавионски систем 9K32 „*Strela-2*", као и ручни ракетни бацач *RPG-7*.

Године 1983. хаубица 2S7 је модернизована под ознаком 2S7M *Malka*. Војни часопис *Military Balance* објавио је 2018. године да је руска артиљерија опремљена са 60 оваквих хаубица.

Ова верзија опремљена је јачим мотором, који осим дизел горива може користити керозин и бензин, а повећан је и број граната за употребу на самом возилу (8). Такође, повећана је каденца ватре на 2,5 до 3 гранате у минути, а постоји и нови систем за управљање ватром. Поред тога, самоходна хаубица је опремљена уређајем за примање и одашиљање информација који аутоматски припрема прву серију података за гађање, водећи рачуна о временским условима.

Совјетска војска није никада употребила самоходну хаубицу *Pion* у неком оружаном сукобу. Хаубице су се углавном налазиле у наоружању руских трупа у Источној Немачкој, а након повлачења из ове земље, све хаубице типа *Pion* и *Malka* враћене су у Русију. Упркос својој моћи, ова самоходна хаубица је коришћена искључиво на војним вежбама. Током 2008. године, употребила ју је грузијска војска за време ратних сукоба у Јужној Осетији али без значајнијих резултата. Руска војска је у том сукобу толико брзо напредовала да су грузијске оружане снаге напустиле целу батерију од шест возила. Једну самоходну хаубицу запленила је руска војска, док су друге уништене. Неки извештаји говоре да је украјинска војска употребила самоходне хаубице 2S7 током сукоба на југоистоку Украјине, али те информације није могуће проверити.

Током модернизације замењени су мотор и мењач који су у првобитним верзијама произведени у Украјини. Тежиште је било на опреми

за примање и процесуирање података, модерним комуникационим системима који омогућују рад хаубице, као што је тактички линк.

Овај оружани систем се до сада одликовао ниском прецизношћу погађања малих циљева. Модерни начини означавања мете и вођење пројектила у потпуности решава овај проблем. Русија већ има значајна искуства на овом пољу након употребе беспилотних летелица у откривању непријатељских ватрених положаја и контрабатирању.

Malka ће бити укључена у аутоматски командни и контролни систем, па ће бити у могућности да погађа циљеве које ће проналазити сателити, беспилотне летелице, авиони и извиђачке трупе специјалних снага које ће дејствовати унутар непријатељеве територије.

Модернизована *Malka* ће постати земаљски снајпер. Њене гранате су знатно јефтиније од крстарећих ракета или чак и обичних авио-бомби, као што су KAB-500, а имају велику убојиту моћ. Поред тога, чињеница је да постоји огроман број граната за ове хаубице које су на располагању још од хладног рата.

Драган М. Вучковић (*Dragan* M. Vučković),
e-mail: draganvuckovic64@gmail.com,
ORCID iD: https://orcid.org/0000-0003-1620-5601

Амерички систем *Javelin* против руских тенкова[2]

FGM-148 Javelin

Амерички противтенковски ракетни систем представља врло скуп део војне опреме; ракета обично кошта више од циља који елиминише.

Ипак, инфрацрвено вођена ракета *Javelin* борбено је доказана у ратовима у Ираку, Авганистану и Сирији и у стању је да уништи сваки тенк,

[2] The National Interest, December 3, 2021

јер их углавном погађа са горње стране куполе, тамо где је оклоп најтањи. Систем се одликује великом покретљивошћу захваљујући својој малој маси и може се употребити у условима када се очекује напад великог броја тенкова, што је сценарио који су Американци очекивали током операције „Пустињски штит" када је само америчка лака пешадија бранила Саудијску Арабију. Сличну ситуацију Американци очекују и на Балтику.

Командна лансирна јединица (*Command Launch Unit—CLU*) система *Javelin* опремљена је софистицираним инфрацрвеним сензором са више начина осматрања, укључујући оптичко увеличање од четири пута, четвороструко увећану слику на термалном сензору и 12 пута увећање приликом нишањења. Трагач у самој ракети омогућава чак до 9 пута повећану термалну слику, па сам CLU може служити и као осматрачка справа пешадије. Термална камера на систему *Javelin* мора бити добро хлађена ради несметаног функционисања, што теоретски траје до 30 секунди, али може трајати и дуже, што се и показало током дејстава у Ираку. Систем је опремљен и сигурносним уређајима ради превенције случајних опаљења.

Систем има масу до 25 кг (најтежа је сама ракета) и много је лакши од жично вођеног противтенковског система *TOW* и других сличних противтенковских ракетних система.

Након што стрелац лоцира мету, закључава инфрацрвени трагач на њу и повлачи окидач, а ракета *Javelin* се лансира из *CLU* без употребе ракетног мотора, такозваним „хладним лансирањем". У овом случају непријатељ не уочава димни и ватрени траг лансирања ракете, па тиме ни ватрени положај противтенковског система. Такође, могуће је и лансирање ракете из затвореног простора (на пример из зграде).

Након тога, ракета *Javelin* више не захтева никакву интервенцију оператера, јер се ради о ракети система „испали и заборави". Посада система *Javelin* може се склонити са положаја у заклон уместо да и даље прати лет ракете до циља као што је то случај са системом полуаутоматског вођења код жичновођеног система *TOW* или ласерски вођеног система *AT-14 Kornet*.

Након лансирања ракета *Javelin* лети хоризонтално пар секунди пре него што се упали ракетни мотор, а ракета се попне 150 метара увис.

На овај начин ракета удара у горњи део оклопног возила који је увек много слабије оклопљен од чеоног или бочног дела. Кумулативна бојева глава 127 мм пробија еквивалент од 600 до 800 мм ваљаног панцирног челика, што није импресивно имајући у виду могућности пробијања других противтенковских ракета (и до 1200 мм ваљаног панцирног челика), али је и то више него довољно за пробијање танког слоја оклопа на врху куполе, наравно ако се не узму у обзир други одбрамбени механизми.

Један од уобичајених система заштите на тенковима је и експлозивно-реактивни оклоп (ERO), односно слој експлозивних плоча које изазивају прерану детонацију бојеве главе.

Међутим, због таквих одлика експлозивно-реактивног оклопа, ракета *Javelin* има тандем бојеву главу која пробија први слој ERO-a, а затим и детонира на основном оклопу.

Систем *Javelin* може бити употребљен и у начину директног напада на циљеве који су превише близу за напад са врха или су заклоњени као што су бункери или улази у пећине. Овај начин напада може се применити и за напад на нисколетеће хеликоптере.

Један од главних недостатака система јесте радијус дејства који износи само 2,5 км. Иако је то довољно за већину борбених ситуација, старији модели противтенковских ракета, као што су *TOW* или *Kornet,* имају домет и преко 5 км.

Русија је потпуно свесна могућности система *Javelin,* па њени најновији тенкови поседују одређене противмере. Тако руски тенкови, као што су *Relikt* и *Mechanit,* имају дупли слој ERO-a који су пројектовани за сузбијање тандем кумулативних бојевих глава. Активни системи заштите *Shtora* и новији *Afganit* користе мултиспектралне гранате и мамце који имају за циљ сакривање тенка од инфрацрвених трагача или њихово одвраћање ка другим топлотним изворима.

Међутим, најновији инфрацрвени сензори имају могућност разликовања одраза мамаца од оригиналног циља. С друге стране, активни системи заштите типа *hard-kill,*чији је циљ обарање надолазећих пројектила, морају имати способност обарања ракета које долазе са горње, вертикалне, стране тенка, што нови руски систем *Afganit* на тенку Т-14, чије се лансирне цеви налазе под хоризонталним углом испод куполе, изгледа не постиже.

Да ли ERO типа *Relikt* и инфрацрвене мере заштите *soft-kill* могу онемогућити напад ракета типа *Javelin* моћи ће се сазнати тек у оружаном сукобу.

Да ли је заиста ефикасан?

Систем *Javelin* је пројектован седамдесетих и осамдесетих година, у време када су се амерички војни планери прибојавали напада великог броја совјетских тенкова, јер су тада Американци имали у употреби само систем *M47 Dragon* који није важио за поуздан.

Систем *Javelin* је на крају ушао у оперативну употребу током 1996. године, након што је хладни рат завршен и први пут је борбено употребљен 2003. године током инвазије на Ирак.

У том тренутку, САД нису могле да пребаце своје трупе у северни Ирак копненим путем, тако да су употребиле специјалне снаге и падобранце који су се борили заједно са курдским борцима. Током битке у пролазу Дебека, у северном делу Ирака, неколико десетина америчких специјалаца, у садејству са већим број курдских Пешмерга, напали су и уништили ирачку механизовану формацију са преко стотину војника. Америчке снаге су имале четири система *Javelin*. Испалили су 19 ракета, од којих је 17 погодило циљеве: два тенка Т-55, осам оклопних

транспортера пешадије типа *MT-LB* и неколико камиона. Сви погоци ракета *Javelin* извршени су са даљине од 2.200 м и даље, док је једна ракета, наводно, погодила циљ који се налазио чак на 4.200 м.

Ракете *Javelin* уништиле су још неколико тенкова током рата у Ираку, укључујући и тенкове типа *Type 69* и *Lion of Babylon T-72,* од којих ниједан није спадао у модерне тенкове. Када је завршена конвенционална фаза рата, системи *Javelin* бивали су употребљени у прецизном гађању као, на пример, на непријатељева митраљеска гнезда, тимове са бестрзајним топовима, као и на наоружане пикапове.

Проблем је у томе што је вредност уништених циљева била много мања од цене једне ракете која је била процењена на 80 000 долара. Стога су Американци били принуђени да штеде ове ракете у Авганистану.

С друге стране, како су САД потрошиле десетине или стотине хиљада долара на скупе ловце бомбардере са скупим паметним ракетама, употреба система *Javelin,* као тешког снајперског оружја, и није тако апсурдна. Мања је колатерална штета приликом детонације ракете *Javelin* него при детонацији велике вођене ласерске бомбе или батеријског дејства хаубица, а, наравно, мањи је и трошак.

Ипак, све то треба примити са резервом, јер иако је систем *Javelin* једини ракетни систем за напад на горњи део оклопних возила, он није испробан против модерних тенкова, што није случај са ракетама *TOW* или *Kornet*.

Будућност система Javelin

Од увођења у оперативну употребу, систем *Javelin* је прошао кроз неколико модернизација.

С обзиром на то да је првенствено коришћен за напад на „меке" циљеве и структуре, развијена је нова верзија бојеве главе са парчадним дејством, под ознаком *FGM-148F*. Наводно је ова верзија бојеве главе такође ефикасна против тенкова и није скупља у односу на претходне бојеве главе.

Развија се и лакша верзија командне лансирне јединице. Нови лансирни систем требало би да има за 70 посто мању масу и нову модернизовану електронику, нови ласерски усмеривач, камеру у боји високе резолуције и инфрацрвене сензоре већег домета и резолуције.

Скоро је тестирана и нова верзија система са продуженим дометом која може гађати циљеве на даљинама до 4,5 км, што би приближило овај систем даљинама гађања противтенковске ракете *TOW* чији је максимални домет до 5 км.

Системи *Javelin* се постављају и на возила. Америчка војска је одлучила да ће пола своје флоте оклопних возила *Stryker* опремити поменутим ракетама (друга половина флоте биће наоружана топовима од 30 мм).

Овакав потез следи и Русија која ће опремити своју флоту оклопних возила *Bumerang, Kurganets* и*T-15 Armata* ракетним системима *Kornet*.

Систем J*avelin* је флексибилнији од старијег система *TOW,* јер се лансирно возило може одмах склонити у заклон након испаљења ракете.

Интересантно питање је шта ће се десити са ракетом *TOW* која спада у основно противтенковско наоружање. Нова ракета *TOW-2B Aero* има могућност напада са врха кинетичком бојевом главом са бежичним системом навођења, што значи да оператор не мора више бити статичан него се може и кретати приликом навођења пројектила на циљ.

Иако је ракета *TOW* изгубила своју предност у радијусу дејства, она је оптички вођена, а цена једне ракете износи око 59 000 долара.

Сједињене Државе су продале системе *Javelin* земљама чланицама НАТО-а, укључујући Француску и Велику Британију, својим савезницима на Средњем истоку, као што су Саудијска Арабија и Уједињени Арапски Емирати, и Азијско-пацифичким земљама, као што су Аустралија, Индонезија и Тајван. Систем је продат и Естонији и Литванији.

Када је Русија пружила војну помоћ сепаратистима у Украјини, САД су одлучиле да Украјини, у оквиру директне војне помоћи, продају *Javelin,* мада у том случају јача могућност ескалирања конфликта између Русије и САД.

У сваком случају, ракете *Javelin* остају и даље један од моћнијих земаљских противоклопних система.

Драган М. Вучковић (*Dragan* M. Vučković),
e-mail: draganvuckovic64@gmail.com,
ORCID iD: https://orcid.org/0000-0003-1620-5601

Руски беспилотни пресретач[3]

Русија тестира беспилотну летелицу *Orion* у улози „пресретача дронова", користећи нову верзију постојеће вођене ракете за обарање других беспилотних летелица на Криму. Руско Министарство одбране тврди да експеримент доказује да беспилотна летелица *Orion,* која је у класи америчке БПЛ *Predato*r, може нападати друге БПЛ.

Недавно је руско Министарство одбране објавило видео-снимак на којем се види БПЛ *Orion,* односно *Inokhodets,* како лансира нову ваздушну верзију руске противтенковске вођене ракете 9М113 *Kornet* против БПЛ хеликоптерског типа која је служила као мета. Напад је почео када су се обе БПЛ налазиле на удаљености од око 90 км, а ракета је лансирана на мету са удаљености од око 4 км.

Основна верзија противтенковске вођене ракете *Kornet* наводи се ласерским путем, али је потребно да се ручно наводи на циљ. Ваздушна верзија ракете има и инфрацрвено и телевизијско вођење, али још није познато на који начин оператор БПЛ налази мету. Руски медији наводе да се иста ракета може користити и са БПЛ типа *Forpost* и *Altius*.

[3] The War Zone, December 20, 2021

Беспилотна летелица Orion

Лансер за ракету Kh-BPLA на БПЛ Orion

Orion је обично опремљен куполом на којој се налазе електро-оптичка опрема са камерама, као и ласерски обележивач којим се ракете наводе на копнене циљеве. На основу приказаног видео-снимка претпоставља се да

оператор БПЛ користи сензоре летелице за захватање циља и лансирање ракете.

На снимку се јасно види траг кумулативног млаза пре удара у летелицу

Ракета носи ознаку Kh-BPLA и више пута је лансирана са јуришног хеликоптера Ka-52M. Наводи се да је максимални домет ракете око 9 км, а очекује се уништавање нисколетећих, спорих летећих циљева, као и оклопних возила. Противваздухопловна верзија противтенковске ракете *Kornet* већ је постојала под ознаком 9M133FM-3 и развијена је ради одбране копнених трупа и возила од БПЛ, хеликоптера и других нисколетећих претњи, тако да се претпоставља да је овај модел ракете сада модификован за ваздушно лансирање.

Изгледа да је Русија разматрала употребу још једне противтенковске ракете у исту сврху – *Vikhr-M* која је једном тестирана тако што је лансирана са јуришног авиона Su-25 и оборила беспилотни бомбардер Tu-16. Али, ова идеја остала је на нивоу експеримента, па ракета *Vikhr* није постала део наоружања јуришника Su-25.

Хеликоптерску БПЛ која је употребљена у тесту произвела је компанија CSTS Dinamika. Она има улогу мете и врло је слична аустријској БПЛ *Schiebel S-100 Camcopter*, али још увек није објављена њена ознака.

Руски званичници су изјавиле да *Orion* може обарати турске БПЛ типа *Bayraktar TB2* и друге БПЛ. Иначе, турске БПЛ овог типа су драстично измениле начин ратовања у Сирији, Либији и у рату између Азербејџана и Јерменије. Такође, поседује је и Украјина, а претпоставља се да је Русија дошла у посед најмање једне БПЛ типа *Bayraktar TB2*.

Хеликоптерска БПЛ која је употребљена као мета

Тестирање обављено на Криму носи и поруку Украјини да се не поуздаје превише у своје БПЛ, али поручује и купцима да постоји БПЛ која се може супротставити турским барјактарима.

Иначе, БПЛ *Orion* је већ борбено употребљавана у Сирији где је користила ракете за гађање копнених циљева.

До сада се програм *Orion* суочавао са извесним проблемима, укључујући и одбијање руског Министарства одбране због непостизања тражених техничких карактеристика. Најмање једна од летелица се срушила, јер и даље постоје проблеми са погонским агрегатом.

Израел је користио своје јуришне хеликоптере типа АН-64 за обарање непријатељских БПЛ, такође користећи противтенковску ракету *Hellfire*.

Међутим, до данас је било само неколико случајева сукобљавања БПЛ и ваздушних платформи са ракетама ваздух-ваздух.

Америчко ратно ваздухопловство започело је рад у овом правцу још од 2003. године, када је наоружало БПЛ *MQ-1* ракетама ваздух-ваздух *Stinger* ради заштите од ирачких ловаца. Од тада је Америчко ратно ваздухопловство користило своју БПЛ *MQ-9 Reaper* за лансирање ракета ваздух-ваздух AIM-9X *Sidewinder* против маневришуће мете у тесту новембра 2017. године.

Иран је у међувремену употребио своју БПЛ *Karrar* као „пресретачку" за уништавање ваздушних мета за време вежби. Иако се на снимцима види како *Karrar* лансира ракету *Azarakhsh*, нема доказа да је нека ракета и уништила мету.

С друге стране, развој на пољу БПЛ у противваздухопловним задацима напредује. Америчко ратно ваздухопловство ради на програму *LongShot*, у оквиру којег се развија БПЛ са својим ракетама ваздух-ваздух, које се лансирају из авиона.

Овакав развој указује на то колико озбиљно Русија приступа наоружавању својих БПЛ убојним средствима за борбу против циљева у ваздушном простору и на копну. Након заостатка за САД, Кином и другим државама у развоју модерних БПЛ, Русија је развила БПЛ *Orion* и *Okhotnik*.

Драган М. Вучковић (*Dragan* M. Vučković),
e-mail: draganvuckovic64@gmail.com,
ORCID iD: https://orcid.org/0000-0003-1620-5601

Развој радара у служби праћења хиперсоничних претњи[4]

Нови пројекти повећавају могућност налажења решења за праћење хиперсоничних ракета и оружја.

Хиперсонична технологија омогућава достизање брзина преко 5 маха и убрзано се развија. Руске ваздушно-космичке снаге увеле су у наоружање хиперсонично оружје као што је нуклеарна ракета ваздух-земља Kh47M2 која достиже брзину од 10 маха.

Ракета ваздух-земља Kh47M2

Кина развија планирајуће возило *DF-ZF,* Руска компанија NPO *Mashinostroyeniya* ради на ракети земља-земља 3M22 *Zircon,* а и Америка се ангажује на том пољу.

Хиперсоничне ракете представљају велики изазов пројектантима радара због своје маневарабилости, великих брзина и радарске површине. Док софтвер који контролише стандардне копнене и поморске радаре ради на завидним брзинама, брзина хиперсоничног оружја може изазвати велике

[4] Jane's Defence International, May 2020

проблеме. На пример, уколико је радару потребно две секунде да детектује и започне праћење ракете *Kh-47M2*, она би за то време прешла већ 7 км.

Ситуација се додатно компликује уколико радар мора открити и пратити оружје и пресрести га. Поморски борбени системи менаџмента породице *Aegis,* на пример, захтевају време од неколико секунди од момента када је надолазећа претња откривена до активирања система пресретања. Тако долази до проблема уколико је потребно послати прецизне локација које су потребне за навођење ракете земља-ваздух или ваздух-ваздух на мету при таквој брзини. Наводи се да хиперсоничне претње могу бити толико брзе да могу избећи време доплерског праћења у одређеним случајевима.

Време радарске детекције, као услов прецизне детекције и праћења хиперсоничних претњи, ограничено је дометом радарског откривања. На пример, поморски осматрачки радари *Type-997 Artisan* који се налазе на британским носачима авиона класе *Queen Elizabeth* имају домет од 200 км, али хиперсонична противбродска ракета већи део свог лета проводи на врло малим висинама изнад мора ради избегавања детекције радара.

Према томе, неопходно је да морнарица више користи своје протоколе за дељење радарске слике по системима америчке морнарице, као што је *US Navy's Cooperative Engagement Capability,* односно систем француске морнарице, као што је *French Navy's Veille Coopérative Navale (Cooperative Naval Surveillance*), за праћење хиперсоничних претњи од радара који су најближи месту лансирања и циљу проналажења потенцијалних мета у домету лансиране ракете. Дејство оваквих система могло би се појачати обавештајним подацима са осматрачких сателита који могу открити топлотни траг хиперсоничног пројектила ван домета радара и, на тај начин, додати нове елементе локације радарима за праћење циља.

Поред тога, док хиперсонична ракета лети у атмосфери, загревање температуре ваздуха преко молекуларне дисоцијације и јонизације формира облак плазме који се састоји од јона, електрона и неутралних атома, односно молекула (познат као фреквенција плазме). Овај облак може абсорбовати електромагнетске таласе које емитује радар. Иначе, руска хиперсонична ракета је и пројектована тако да искористи облак плазме ради прикривања свог радарског одраза.

Америчка војска је развила радар са активним електронским скенирањем *Lower Tier and Missile Defence Sensor (LTAMDS)* за који се тврди да може пратити хиперсоничне циљеве. Поморски осматрачки радар *AN/SPY-6,* којим су опремљени амерички бродови, наводно такође може пратити хиперсоничне претње.

Представници компаније *Raytheon* су изјавили да је могуће добити побољшану слику употребом интегрисаних зрака мањих дистрибутивних сензора, као када би се, на пример, један објекат обасјао са више лампи у мраку. На тај начин остварили би се боље перформансе употребом више сензора који заједно посматрају један циљ, па би се повећао и ниво преживљавања система.

Компанија *Saab* извештава да њихов поморски радар *Sea Giraffe* сада укључује опцију за хиперсоничну детекцију која је посебно оптимизирана за *Sea Giraffe 4A Fixed Face*, што је фиксна мрежна конфигурација која припада радарским системима *AESA* у S таласу. Компаније *Thales, Leonardo,* као и други произвођачи, такође раде на развијању радара који би успешно пратили хиперсоничне пројектиле.

Може се закључити да је могуће развити нови радарски систем који би откривао и пратио хиперсонична оружја, а такође је могуће модификовати постојеће радарске системе у ту сврху. Повећавање понављања пулсне фреквенције један је од корака које треба преузети, а добра вест јесте да већина модерних радара дигитално обрађују сигнал, а софтвер је лакше преправити него хардвер.

Драган М. Вучковић (*Dragan* M. Vučković),
e-mail: draganvuckovic64@gmail.com,
ORCID iD: https://orcid.org/0000-0003-1620-5601

ПОЗИВ И УПУТСТВО АУТОРИМА
ПРИГЛАШЕНИЕ И ИНСТРУКЦИЯ ДЛЯ АВТОРОВ РАБОТ
CALL FOR PAPERS AND INSTRUCTIONS FOR AUTHORS

ПОЗИВ И УПУТСТВО АУТОРИМА О НАЧИНУ ПРИПРЕМЕ ЧЛАНКА

Упутство ауторима о начину припреме чланка за објављивање у Војнотехничком гласнику урађено је на основу Правилника о категоризацији и рангирању научних часописа Министарства просвете, науке и технолошког развоја Републике Србије ("Службени гласник РС", број 159/20). Примена овог Правилника првенствено служи унапређењу квалитета домаћих часописа и њиховог потпунијег укључивања у међународни систем размене научних информација.

Војнотехнички гласник / Vojnotehnički glasnik / Military Technical Courier (втг.мо.упр.срб, www.vtg.mod.gov.rs, ISSN 0042-8469 – штампано издање, e-ISSN 2217-4753 – online, UDC 623+355/359, DOI: 10.5937/VojnotehnickiGlasnik; https://doi.org/10.5937/VojnotehnickiGlasnik), јесте рецензирани међународни научни часопис.

Власници часописа су Министарство одбране Републике Србије и Војска Србије. Издавач и финансијер часописа је Универзитет одбране у Београду (Војна академија).

Програмска оријентација часописа заснива се на годишњој категоризацији часописа, коју врши надлежно државно министарство у одређеним областима, као и на његовом индексирању у међународним индексним базама.

Часопис обухвата научне, односно стручне области у оквиру образовно-научног поља **природно-математичких наука**, као и у оквиру образовно-научног поља **техничко-технолошких наука**, а нарочито области **одбрамбених наука и технологија**. Објављује теоријска и практична достигнућа која доприносе усавршавању свих припадника српске, регионалне и међународне академске заједнице, а посебно припадника војски и министарстава одбране. Публикује радове са уравнотеженим извештавањем о аналитичким, експерименталним и примењеним истраживањима, као и нумеричким симулацијама, обухватајући различите дисциплине. Објављени материјали су високог квалитета и релевантности, написани на начин који их чини доступним широкој читалачкој публици. Сви радови који извештавају о оригиналним теоријским и/или практично оријентисаним истраживањима или проширеним верзијама већ објављених радова са конференција су добродошли. Радови за објављивање одабиру се двоструко слепим поступком рецензије како би се осигурала оригиналност, релевантност и читљивост. Притом циљ није само да се квалитет објављених радова одржи високим већ и да се обезбеди правовремени, темељни и уравнотежени поступак рецензије.

Уређивачка политика Војнотехничког гласника заснива се на препорукама Одбора за етичност у издаваштву (COPE Core Practices), као и на најбољим прихваћеним праксама у научном издаваштву. Војнотехнички гласник је члан COPE (Committee on Publication Ethics) од 2. маја 2018. године.

Министарство просвете, науке и технолошког развоја Републике Србије утврдило је дана 23. 12. 2021. године категоризацију Војнотехничког гласника, за 2021. годину:

– на листи часописа за рачунарске науке:
категорија истакнути национални часопис **(М52)**,

– на листи часописа за електронику, телекомуникације и информационе технологије:
категорија истакнути национални часопис **(М52)**,
– на листи часописа за машинство:
категорија врхунски часопис националног значаја **(М51)**,
– на листи часописа за материјале и хемијске технологије:
категорија врхунски часопис националног значаја **(М51)**.

Усвојене листе домаћих часописа за 2021. годину могу се видети на сајту Војнотехничког гласника, страница *Категоризација часописа*.

Детаљније информације могу се пронаћи и на сајту Министарства просвете, науке и технолошког развоја Републике Србије.

Подаци о категоризацији могу се пратити и на сајту КОБСОН-а (Конзорцијум библиотека Србије за обједињену набавку).

Категоризација часописа извршена је према Правилнику о категоризацији и рангирању научних часописа Министарства просвете, науке и технолошког развоја Републике Србије ("Службени гласник РС", број 159/20).

Часопис се прати у контексту Српског цитатног индекса – СЦИндекс (база података домаћих научних часописа) и Руског индекса научног цитирања (РИНЦ). Подвргнут је сталном вредновању (мониторингу) у зависности од утицајности (импакта) у самим базама и, посредно, у међународним (Clarivate Analytics) цитатним индексима. Детаљи о индексирању могу се видети на сајту Војнотехничког гласника, страница *Индексирање часописа*.

Војнотехнички гласник омогућава и примењује Creative Commons (CC BY) одредбе о ауторским правима. Детаљи о ауторским правима могу се видети на сајту часописа, страница *Ауторска права и политика самоархивирања*.

Радови се предају путем онлајн система за електронско уређивање АСИСТЕНТ, који је развио Центар за евалуацију у образовању и науци (ЦЕОН).

Приступ и регистрација за сервис врше се на сајту www.vtg.mod.gov.rs, преко странице *АСИСТЕНТ* или *СЦИНДЕКС*, односно директно на линку aseestant.ceon.rs/index.php/vtg.

Детаљно упутство о регистрацији и пријави за сервис налази се на сајту www.vtg.mod.gov.rs, страница *Упутство за АСИСТЕНТ*.

Потребно је да се сви аутори који подносе рукопис за објављивање у Војнотехничком гласнику региструју у регистар ORCID (Open Researcher and Contributor ID), према упутству на страници сајта *Регистрација за добијање ORCID идентификационе шифре*.

Војнотехнички гласник објављује чланке на енглеском језику (arial, величина слова 11 pt, проред Single).

Поступак припреме, писања и уређивања чланка треба да буде у сагласности са *Изјавом о етичком поступању* (http://www.vtg.mod.gov.rs/izjava-o-etickom-postupanju.html).

Чланак треба да садржи сажетак са кључним речима, увод (мотивацију за рад), разраду (адекватан преглед репрезентативности рада у његовој области, јасну изјаву о новини у представљеном истраживању, одговарајућу теоријску позадину, један или више примера за демонстрирање и дискусију о представљеним идејама), закључак и литературу (без нумерације наслова и поднаслова). Обим чланка треба да буде до једног ауторског табака (16 страница формата А4 са проредом Single), а највише 24 странице.

Чланак треба да буде написан на обрасцу за писање чланка, који се у електронској форми може преузети са сајта на страници *Образац за писање чланка*.

Наслов

Наслов треба да одражава тему чланка. У интересу је часописа и аутора да се користе речи прикладне за индексирање и претраживање. Ако таквих речи нема у наслову, пожељно је да се придода и поднаслов.

Текући наслов

Текући наслов се исписује са стране сваке странице чланка ради лакше идентификације, посебно копија чланака у електронском облику. Садржи презиме и иницијал имена аутора (ако аутора има више, преостали се означавају са „et al.“ или „и др.“), наслове рада и часописа и колацију (година, волумен, свеска, почетна и завршна страница). Наслови часописа и чланка могу се дати у скраћеном облику.

Име аутора

Наводи се пуно име и презиме (свих) аутора. Веома је пожељно да се наведу и средња слова аутора. Имена и презимена домаћих аутора увек се исписују у оригиналном облику (са српским дијакритичким знаковима), независно од језика на којем је написан рад.

Назив установе аутора (афилијација)

Наводи се пун (званични) назив и седиште установе у којој је аутор запослен, а евентуално и назив установе у којој је аутор обавио истраживање. У сложеним организацијама наводи се укупна хијерархија (нпр. Универзитет одбране у Београду, Војна академија, Катедра природно-математичких наука). Бар једна организација у хијерархији мора бити правно лице. Ако аутора има више, а неки потичу из исте установе, мора се, посебним ознакама или на други начин, назначити из које од наведених установа потиче сваки од наведених аутора. Афилијација се исписује непосредно након имена аутора. Функција и звање аутора се не наводе.

Контакт подаци

Адреса или е-адреса свих аутора даје се поред имена и презимена аутора.

Категорија (тип) чланка

Категоризација чланака обавеза је уредништва и од посебне је важности. Категорију чланка могу предлагати рецензенти и чланови уредништва, односно уредници рубрика, али одговорност за категоризацију сноси искључиво главни уредник.

Чланци у *Војнотехничком гласнику* класификују се на научне и стручне чланке.

Научни чланак је:

– оригиналан научни рад (рад у којем се износе претходно необјављени резултати сопствених истраживања научним методом);

– прегледни рад (рад који садржи оригиналан, детаљан и критички приказ истраживачког проблема или подручја у којем је аутор остварио одређени допринос, видљив на основу аутоцитата);

– кратко или претходно саопштење (оригинални научни рад пуног формата, али мањег обима или прелиминарног карактера);

– научна критика, односно полемика (расправа на одређену научну тему, заснована искључиво на научној аргументацији) и осврти.

Изузетно, у неким областима, научни рад у часопису може имати облик монографске студије, као и критичког издања научне грађе (историјско-архивске, лексикографске, библиографске, прегледа података и сл.), дотад непознате или недовољно приступачне за научна истраживања.

Радови класификовани као научни морају имати бар две позитивне рецензије.

Ако се у часопису објављују и прилози ваннаучног карактера, научни чланци треба да буду груписани и јасно издвојени у првом делу свеске.

Стручни чланак је:

– стручни рад (прилог у којем се нуде искуства корисна за унапређење професионалне праксе, али која нису нужно заснована на научном методу);

– информативни прилог (уводник, коментар и сл.);

– приказ (књиге, рачунарског програма, случаја, научног догађаја, и сл).

Пожељно је да обим кратких саопштења буде 4 до 7 страница, научних чланака и студија случаја 10 до 14 страница, док прегледни радови могу бити и дужи. Број страница није строго ограничен и, уз одговарајуће образложење, пријављени чланци такође могу бити дужи или краћи.

Ако су радови који су претходно објављени на конференцији проширени, уредници ће проверити да ли је додато довољно новог материјала који испуњава стандарде часописа и квалификује поднесак за поступак рецензије. Додати материјал не сме бити претходно објављен. Нови резултати нису нужно потребни, али су пожељни. Међутим, поднесак треба да садржи проширене кључне идеје, примере, разраде, итд., који су претходно били садржани у поднеску са конференције.

Језик рада

Језик рада треба да буде енглески.

Текст мора бити језички и стилски дотеран, систематизован, без скраћеница (осим стандардних). Све физичке величине морају бити изражене у Међународном систему мерних јединица – SI. Редослед образаца (формула) означава се редним бројевима, са десне стране у округлим заградама.

Сажетак

Сажетак јесте кратак информативан приказ садржаја чланка који читаоцу омогућава да брзо и тачно оцени његову релевантност. У интересу је уредништава и аутора да сажетак садржи термине који се често користе за индексирање и претрагу чланака. Саставни делови сажетка су увод/циљ истраживања, методи, резултати и закључак. Сажетак треба да има од 100 до 250 речи и треба да се налази између заглавља (наслов, имена аутора и др.) и кључних речи, након којих следи текст чланка.

Кључне речи

Кључне речи су термини или фразе које адекватно представљају садржај чланка за потребе индексирања и претраживања. Треба их додељивати ослањајући се на неки међународни извор (попис, речник или тезаурус) који је најшире прихваћен или унутар дате научне области. За нпр. науку уопште, то је листа кључних речи Web of Science. Број кључних речи не може бити већи од 10, а у

интересу је уредништва и аутора да учесталост њихове употребе буде што већа. У чланку се пишу непосредно након сажетка.

Систем АСИСТЕНТ у ту сврху користи специјалну алатку KWASS: аутоматско екстраховање кључних речи из дисциплинарних тезауруса/речника по избору и рутине за њихов одабир, тј. прихватање односно одбацивање од стране аутора и/или уредника.

Датум прихватања чланка

Датум када је уредништво примило чланак, датум када је уредништво коначно прихватило чланак за објављивање, као и датуми када су у међувремену достављене евентуалне исправке рукописа наводе се хронолошким редоследом, на сталном месту, по правилу на крају чланка.

Захвалница

Назив и број пројекта, односно назив програма у оквиру којег је чланак настао, као и назив институције која је финансирала пројекат или програм, наводи се у посебној напомени на сталном месту, по правилу при дну прве стране чланка.

Претходне верзије рада

Ако је чланак у претходној верзији био изложен на скупу у виду усменог саопштења (под истим или сличним насловом), податак о томе треба да буде наведен у посебној напомени, по правилу при дну прве стране чланка. Рад који је већ објављен у неком часопису не може се објавити у Војнотехничком гласнику (прештампати), ни под сличним насловом и измењеном облику.

Табеларни и графички прикази

Пожељно је да наслови свих приказа, а по могућству и текстуални садржај, буду дати двојезично, на језику рада и на енглеском језику.

Табеле се пишу на исти начин као и текст, а означавају се редним бројевима са горње стране. Фотографије и цртежи треба да буду јасни, прегледни и погодни за репродукцију. Цртеже треба радити у програму word или corel. Фотографије и цртеже треба поставити на жељено место у тексту.

За слике и графиконе не сме се користити снимак са екрана рачунара програма за прикупљање података. У самом тексту чланка препоручује се употреба слика и графикона непосредно из програма за анализу података (као што су Excel, Matlab, Origin, SigmaPlot и други).

Навођење (цитирање) у тексту

Начин позивања на изворе у оквиру чланка мора бити једнообразан.

Војнотехнички гласник за референцирање (цитирање и навођење литературе) примењује Харвардски систем референци, односно Харвардски приручник за стил (Harvard Referencing System, Harvard Style Manual). У самом тексту, у обичним заградама, на месту на којем се врши позивање, односно цитирање литературе набројане на крају чланка, обавезно у обичној загради написати презиме цитираног аутора, годину издања публикације из које цитирате и, евентуално, број страница. Нпр. (Petrović, 2012, pp.10–12).

Детаљно упутство о начину цитирања, са примерима, дато је на страници сајта *Упутство за Харвардски приручник за стил*. Потребно је да се позивање на литературу у тексту уради у складу са поменутим упутством.

Систем АСИСТЕНТ у сврху контроле навођења (цитирања) у тексту користи специјалну алатку CiteMatcher: откривање изостављених цитата у тексту рада и у попису референци.

Напомене (фусноте)

Напомене се дају при дну стране на којој се налази текст на који се односе. Могу садржати мање важне детаље, допунска објашњења, назнаке о коришћеним изворима (на пример, научној грађи, приручницима), али не могу бити замена за цитирану литературу.

Листа референци (литература)

Цитирана литература обухвата, по правилу, библиографске изворе (чланке, монографије и сл.) и даје се искључиво у засебном одељку чланка, у виду листе референци. Референце се не преводе на језик рада и набрајају се у посебном одељку на крају чланка.

Војнотехнички гласник, као начин исписа литературе, примењује Харвардски систем референци, односно Харвардски приручник за стил (Harvard Referencing System, Harvard Style Manual).

Литература се обавезно пише на латиничном писму и набраја по абецедном редоследу, наводећи најпре презимена аутора, без нумерације.

Детаљно упутство о начину пописа референци, са примерима, дато је на страници сајта *Упутство за Харвардски приручник за стил*. Потребно је да се попис литературе на крају чланка уради у складу са поменутим упутством.

Нестандардно, непотпуно или недоследно навођење литературе у системима вредновања часописа сматра се довољним разлогом за оспоравање научног статуса часописа.

Систем АСИСТЕНТ у сврху контроле правилног исписа листе референци користи специјалну алатку RefFormatter: контрола обликовања референци у складу са Харвардским приручником за стил.

Изјава о ауторству

Поред чланка доставља се *Изјава о ауторству* у којој аутори наводе свој појединачни допринос у изради чланка. Такође, у тој изјави потврђују да су чланак урадили у складу са *Позивом и упутством ауторима* и *Изјавом о етичком поступању часописа*.

Сви радови подлежу стручној рецензији.

Списак рецензената Војнотехничког гласника може се видети на страници сајта *Списак рецензената*. Процес рецензирања објашњен је на страници сајта *Рецензентски поступак*.

Уредништво

Адреса редакције:
Војнотехнички гласник
Вељка Лукића Курјака 33
11042 Београд
e-mail: vojnotehnicki.glasnik@mod.gov.rs.
тел: војни 40-260 (011/3603-260), 066/8700-123

ПРИГЛАШЕНИЕ И ИНСТРУКЦИЯ ДЛЯ АВТОРОВ О ПОРЯДКЕ ПОДГОТОВКИ СТАТЬИ

Инструкция для авторов о порядке подготовки статьи к опубликованию в журнале «Военно-технический вестник» разработана согласно Регламенту о категоризации и ранжировании научных журналов Министерства образования, науки и технологического развития Республики Сербия («Службени гласник РС», № 159/20). Применение этого Регламента способствует повышению качества отечественных журналов и их более полному вовлечению в международную систему обмена научной информацией.

Военно-технический вестник (**Vojnotehnički glasnik / Military Technical Courier**), втг.мо.упр.срб, www.vtg.mod.gov.rs/index-ru.html, ISSN 0042-8469 – печатное издание, e-ISSN 2217-4753 – online, UDK 623+355/359, DOI: 10.5937/VojnotehnickiGlasnik; https://doi.org/10.5937/VojnotehnickiGlasnik, является рецензируемым международным научным журналом.

Собственники журнала: Министерство обороны и Вооруженые силы Республики Србия.

Издатель журнала: Университет обороны в г. Белград (Военная академия).

Программная ориентация журнала основана на ежегодной категоризации журнала, которая производится соответствующим отраслевым министерством, в зависимости от области исследований, а также на его индексировании в международных наукометрических базах данных.

Журнал охватывает научные и профессиональные сферы в рамках учебно-научной области **естественно-математических наук**, а также в рамках учебно-научной области **технико-технологических наук**, особенно в области **оборонных наук и технологии**. В журнале публикуются теоретические и практические достижения, которые способствуют повышению квалификации представителей сербского, регионального и международного академического сообщества, особенно служащих Министерств Обороны и Вооружённых сил. В журнале публикуются статьи со соответствующими обзорами об аналитических, экспериментальных и прикладных исследованиях, а также о численном моделировании, охватывая различные дисциплины. Публикуемые материалы отличаются высоким качеством и актуальностью. Они написаны научным, но понятным и доступным для широкого круга читателей языком. Приветствуются все статьи, сообщающие об оригинальных теоретических и/или практических исследованиях и/или расширенные версии ранее опубликованных статей, представленных на конференциях. Статьи для публикации отбираются путем двойного слепого рецензирования, которое гарантирует оригинальность, актуальность и удобочитаемость. Цель состоит не только в поддержании высокого качества публикуемых статей, но и в обеспечении своевременного, тщательного и соответствующего процесса рецензирования.

Редакционная политика журнала «Военно-технический вестник» основана на рекомендациях Комитета по этике научных публикаций (COPE Core Practices), а также на лучшей практике в научно-издательской деятельности. «Военно-технический вестник» является членом COPE со 2 мая 2018 года.

Министерством образования, науки и технологического развития Республики Сербия утверждена 23 декабря 2021 г. категоризация журнала «Военно-технический вестник» за 2021 год:

– Область компьютерные науки:
высококачественный национальный журнал **(M52)**,

– **Область электроники, телекоммуникаций и информационных технологий:** высококачественный национальный журнал **(M52)**,
– **Область машиностроения:** ведущий журнал государственного значения **(M51)**,
– **Область материалов и химической технологии:** ведущий журнал государственного значения **(M51)**.

С информацией относительно категоризации за 2021 год можно ознакомиться на странице сайта «Военно-технического вестника» *Категоризация Вестника*.

Более подробную информацию можно найти на сайте Министерства образования, науки и технологического развития Республики Сербия.

С информацией о категоризации можно ознакомиться и на сайте КОБСОН (Консорциум библиотек Республики Сербия по вопросам объединения закупок).

Категоризация Вестника проведена согласно Регламенту о категоризации и ранжировании научных журналов Министерства образования, науки и технологического развития Республики Сербия («Службени гласник РС», № 159/20)

Журнал соответствует стандартам Сербского индекса научного цитирования (СЦИндекс/SCIndeks) – наукометрической базы данных научных журналов Республики Сербия, а также Российского индекса научного цитирования (РИНЦ). Журнал постоянно подвергается мониторингу и оценивается количественными наукометрическими показателями, отражающими его научную ценность, в т.ч. опосредованно в международных индексах цитирования (Clarivate Analytics).

С информацией об индексировании можно ознакомиться на странице сайта журнала *Индексирование Вестника*.

«Военно-технический вестник» обеспечивает читателям возможность открытого доступа, в соответствии с положениями об авторских правах, утверждёнными Creative Commons (CC BY). С инструкцией об авторских правах можно ознакомиться на странице *Авторские права и политика самоархивирования*, перейдя по ссылке http://www.vtg.mod.gov.rs/index-ru.html.

Рукописи статей направляются в редакцию журнала с использованием online системы ASSISTANT, запущенной Центром поддержи развития образования и науки (ЦПРОН).

Регистрация в системе и оформление прав доступа выполняется по адресу http://www.vtg.mod.gov.rs/index-ru.html, через страницу *ASSISTANT* или *СЦИНДЕКС* (aseestant.ceon.rs/index.php/vtg).

С инструкцией по регистрации и правам доступа можно ознакомиться по адресу http://www.vtg.mod.gov.rs/index-ru.html, на странице *Инструкция по ASSISTANT*.

Все авторы, предоставляющие свои рукописи для публикации в редакцию журнала «Военно-технический вестник» должны пройти предварительную регистрацию в реестре ORCID (Open Researcher and Contributor ID). Эта процедура осуществляется в соответствии с инструкцией, размещенной на странице сайта *Регистрация в реестре ORCID для присвоения идентификационного кода*.

«Военно-технический вестник» публикует статьи на английском языке (Arial, шрифт 11 pt, пробел Single).

Процесс подготовки, написания и редактирования статьи должен осуществляться в соответствии с принципами *Этического кодекса* (http://www.vtg.mod.gov.rs/etichyeskiy-kodyeks.html).

Статья должна содержать резюме с ключевыми словами, введение (цель исследования), основную часть (соответствующий обзор представительного исследования в данной области, четкое изложение научной новизны в представленном исследовании, соответствующую теоретическую основу, один или несколько примеров для демонстрирования и обсуждения представленных тезисов), заключение и список литературы (без нумерации заголовков и подзаголовков). Объем статьи не должен превышать один авторский лист (16 страниц формата А4 с одинарным интервалом, максимум до 24 страниц, включая ссылки и приложения).

Статья должна быть набрана на компьютере с использованием специально подготовленного редакцией макета, который можно скачать на странице сайта *Правила и образец составления статьи*.

Заголовок

Заголовок должен отражать тему статьи. В интересах журнала и автора необходимо использовать слова и словосочетания, удобные для индексации и поиска. Если такие слова не содержатся в заголовке, то желательно их добавить в подзаголовок.

Текущий заголовок

Текущий заголовок пишется в титуле каждой страницы статьи с целью упрощения процесса идентификации, в первую очередь копий статьей в электронном виде. Заголовок содержит в себе фамилию и инициал имени автора (в случае если авторов несколько, остальные обозначаются с «et al.» или «и др.»), название работы и журнала (год, том, выпуск, начальная и заключительная страница). Заголовок статьи и название журнала могут быть приведены в сокращенном виде.

ФИО автора

Приводятся полная фамилия и полное имя (всех) авторов. Желательно, чтобы были указаны инициалы отчеств авторов. Фамилия и имя авторов из Республики Сербия всегда пишутся в оригинальном виде (с сербскими диакритическими знаками), независимо от языка, на котором написана работа.

Наименование учреждения автора (аффилиация)

Приводится полное (официальное) наименование и местонахождение учреждения, в котором работает автор, а также наименование учреждения, в котором автор провёл исследование. В случае организаций со сложной структурой приводится их иерархическая соподчинённость (напр. Военная академия, кафедра военных электронных систем, г. Белград). По крайней мере, одна из организаций в иерархии должна иметь статус юридического лица. В случае если указано несколько авторов, и если некоторые из них работают в одном учреждении, нужно отдельными обозначениями или каким-либо другим способом указать в каком из приведённых учреждений работает каждый из авторов. Аффилиация пишется непосредственно после ФИО автора. Должность и специальность по диплому не указываются.

Контактные данные

Электронный адрес автора указываются рядом с его именем на первой страницы статьи.

Категория (тип) статьи

Категоризация статьей является обязанностью редакции и имеет особое значение. Категорию статьи могут предлагать рецензенты и члены редакции, т.е. редакторы рубрик, но ответственность за категоризацию несет исключительно главный редактор. Статьи в журнале распределяются по следующим категориям:

Научные статьи:

– оригинальная научная статья (работа, в которой приводятся ранее неопубликованные результаты собственных исследований, полученных научным методом);

– обзорная статья (работа, содержащая оригинальный, детальный и критический обзор исследуемой проблемы или области, в который автор внёс определённый вклад, видимый на основе автоцитат);

– краткое сообщение (оригинальная научная работа полного формата, но меньшего объёма или имеющая предварительный характер);

– научная критическая статья (дискуссия-полемика на определённую научную тему, основанная исключительно на научной аргументации) и научный комментарий.

Однако, в некоторых областях знаний научная работа в журнале может иметь форму монографического исследования, а также критического обсуждения научного материала (историко-архивного, лексикографического, библиографического, обзора данных и т.п.) – до сих пор неизвестного или недостаточно доступного для научных исследований. Работы, классифицированные в качестве научных, должны иметь, по меньшей мере, две положительные рецензии.

В случае если в журнале объявляются и приложения, не имеющие научный характер, научные статьи должны быть сгруппированы и четко выделены в первой части номера.

Профессиональные статьи:

– профессиональная работа (приложения, в которых предлагаются опыты, полезные для совершенствования профессиональной практики, но которые не должны в обязательном порядке быть обоснованы на научном методе);

– информативное приложение (передовая статья, комментарий и т.п.);

– обзор (книги, компьютерной программы, случая, научного события и т.п.).

Объем кратких сообщений составляет 4-7 страниц, исследовательские статьи и тематические исследования с проблемно-ситуационным анализом − 10-14 страниц, однако объем обзорных статей может быть больше. Ограничения по количеству страниц не являются строгими, следовательно при соответствующем обосновании предоставленные работы могут быть длиннее или короче. В случае подачи расширенных версий ранее опубликованных докладов, представленных на конференции, редакция проверит было ли добавлено достаточно новых материалов для того, чтобы статья соответствовала стандартам журнала и условиям рецензирования. Добавленный материал должен быть новым, неопубликованным ранее. Новые результаты приветствуются, но не являются обязательным условием; однако ключевые тезисы, примеры, разработки и пр. должны быть более подробно представлены в статье по сравнению с первичным докладом на конфереции.

Язык работы

Статья должна быть написана на английском языке.

Текст должен быть в лингвистическом и стилистическом смысле упорядочен, систематизирован, без сокращений (за исключением стандартных). Все физические величины должны соответствовать Международной системе единиц измерения – СИ. Очередность формул обозначается порядковыми номерами, проставляемыми с правой стороны в круглых скобках.

Резюме

Резюме является кратким информативным обзором содержания статьи, обеспечивающим читателю быстроту и точность оценки её релевантности. В интересах редакции и авторов, чтобы резюме содержало термины, часто используемые для индексирования и поиска статьей. Составными частями резюме являются введение/цель исследования, методы, результаты и выводы. В резюме должно быть от 100 до 250 слов, и оно должно находится между титулами (заголовок, ФИО авторов и др.) и ключевыми словами, за которыми следует текст статьи.

Ключевые слова

Ключевыми словами являются термины или фразы, адекватно представляющие содержание статьи, необходимые для индексирования и поиска. Ключевые слова необходимо выбирать, опираясь при этом на какой-либо международный источник (регистр, словарь, тезаурус), наиболее используемый внутри данной научной области. Число ключевых слов не может превышать 10. В интересах редакции и авторов, чтобы частота их встречи в статье была как можно большей. В статье они пишутся непосредственно после резюме.

Программа ASSISTANT предоставляет возможность использования сервиса KWASS, автоматически фиксирующего ключевые слова из источников/словарей по выбору автора/редактора.

Дата получения статьи

Дата, когда редакция получила статью; дата, когда редакция окончательно приняла статью к публикации; а также дата, когда были предоставлены необходимые исправления рукописи, приводятся в хронологическом порядке, как правило, в конце статьи.

Выражение благодарности

Наименование и номер проекта, т.е. название программы благодаря которой статья возникла, совместно с наименованием учреждения, которое финансировало проект или программу, приводятся в отдельном примечании, как правило, внизу первой страницы статьи.

Предыдущие версии работы

В случае если статья в предыдущей версии была изложена устно (под одинаковым или похожим названием, например, в виде доклада на научной конференции), сведения об этом должны быть указаны в отдельном примечании, как правило, внизу первой страницы статьи. Работа, которая уже была опубликована в каком-либо из журналов, не может быть напечатана в «Военно-техническом вестнике» ни под похожим названием, ни в изменённом виде.

Нумерация и название таблиц и графиков

Желательно, чтобы нумерация и название таблиц и графиков были исполнены на двух языках (на языке оригинала и на английском). Таблицы подписываются таким же способом как и текст и обозначаются порядковым номером с верхней стороны. Фотографии и рисунки должны быть понятны, наглядны и удобны для репродукции. Рисунки необходимо делать в программах Word или Corel. Фотографии и рисунки надо поставить на желаемое место в тексте. Для создания изображений и графиков использование функции снимка с экрана (скриншота) не допускается. В самом тексте статьи рекомендуется применение изображений и графиков, обработанных такими компьютерными программами, как: Excel, Matlab, Origin, SigmaPlot и др.

Ссылки (цитирование) в тексте

Оформление ссылок на источники в рамках статьи должно быть однообразным. «Военно-технический вестник» для оформления ссылок, цитат и списка использованной литературы применяет Гарвардскую систему (Harvard Referencing System, Harvard Style Manual). В тексте в скобках приводится фамилия цитируемого автора (или фамилия первого автора, если авторов несколько), год издания и по необходимости номер страницы. Например: (Petrović, 2010, pp.10-20). Рекомендации о способе цитирования размещены на странице сайта *Инструкция по использованию Гарвардского стиля*. При оформлении ссылок, цитат и списка использованной литературы необходимо придерживаться установленных норм. Программа ASSISTANT предоставляет при цитировании возможность использования сервиса CiteMatcher, фиксирующего пропущенные цитаты в работе и в списке литературы.

Примечания (сноски)

Примечания (сноски) к тексту указываются внизу страницы, к которой они относятся. Примечания могут содержать менее важные детали, дополнительные объяснения, указания об использованных источниках (напр. научном материале, справочниках), но не могут быть заменой процедуры цитирования литературы.

Литература (референции)

Цитированной литературой охватываются, как правило, такие библиографические источники как статьи, монографии и т.п. Вся используемая литература в виде референций размещается в отдельном разделе статьи.

Названия литературных источников не переводятся на язык работы.

«Военно-технический вестник» для оформления списка использованной литературы применяет Гарвардскую систему (Harvard Style Manual). В списке литературы источники указываются в алфавитном порядке фамилий авторов или редакторов. Рекомендации о способе цитирования размещены на странице сайта *Инструкция по использованию Гарвардского стиля*. При оформлении списка использованной литературы необходимо придерживаться установленных норм.

При оформлении списка литературы программа ASSISTANT предоставляет возможность использования сервиса RefFormatter, осуществляющего контроль оформления списка литературы в соответствии со стандартами Гарвардского стиля.

Нестандартное, неполное и непоследовательное приведение литературы в системах оценки журнала считается достаточной причиной для оспаривания научного статуса журнала.

Авторское заявление

Авторское заявление предоставляется вместе со статьей, в нем авторы заявляют о своем личном вкладе в написание статьи. В заявлении авторы подтверждают, что статья написана в соответствии с *Приглашением и инструкциями для авторов*, а также с *Кодексом профессиональной этики журнала*.

Все рукописи статей подлежат профессиональному рецензированию.

Список рецензентов журнала «Военно-технический вестник» размещён на странице сайта *Список рецензентов*. Процесс рецензирования описан в разделе *Правила рецензирования*.

Редакция

Почтовый адрес редакции:
«Војнотехнички гласник»
ул. Велька Лукича Куряка 33
11042 Белград, Республика Сербия
e-mail: vojnotehnicki.glasnik@mod.gov.rs.
тел: +381 11 3603 260, +381 66 8700 123

CALL FOR PAPERS AND ARTICLE FORMATTING INSTRUCTIONS

The instructions to authors about the article preparation for publication in the Military Technical Courier are based on the Regulations on categorization and ranking of scientific journals of the Ministry of Education, Science and Technological Development of the Republic of Serbia (Official Gazette of the Republic of Serbia, No 159/20). This Regulations aims at improving the quality of national journals and raising the level of their compliance with the international system of scientific information exchange.

The Military Technical Courier / Vojnotehnički glasnik (www.vtg.mod.gov.rs/index-e.html, втг.мо.упр.срб, ISSN 0042-8469 – print issue, e-ISSN 2217-4753 – online, UDC 623+355/359, DOI: 10.5937/VojnotehnickiGlasnik; https://doi.org/10.5937/VojnotehnickiGlasnik), is an international peer-reviewed scientific journal.

The owners of the journal are the Ministry of Defence of the Republic of Serbia and the Serbian Armed Forces. The publisher and financier of the Military Technical Courier is the University of Defence in Belgrade (Military Academy).

The program of the journal is based on the annual classification of journals performed by a relevant Ministry as well as on its indexing in international indexing databases.

The journal covers scientific and professional fields within the educational-scientific field of **Natural-Mathematical Sciences**, as well as within the educational-scientific field of **Technical-Technological Sciences**, and especially the field of **defense sciences and technologies**. It publishes theoretical and practical achievements leading to professional development of all members of Serbian, regional and international academic communities as well as members of the military and ministries of defence in particular. It publishes papers with balanced coverage of analytical, experimental, and applied research as well as numerical simulations from various disciplines. The material published is of high quality and relevance, written in a manner that makes it accessible to a wider readership. The journal welcomes papers reporting original theoretical and/or practice-oriented research as well as extended versions of already published conference papers. Manuscripts for publication are selected through a double-blind peer-review process to validate their originality, relevance, and readability. This being so, the objective is not only to keep the quality of published papers high but also to provide a timely, thorough, and balanced review process.

The editorial policy of the Military Technical Courier is based on the COPE Core Practices and the journal articles are consistent with accepted best practices in their subject areas. As of 2 May 2018, the Military Technical Courier is a member of COPE (Committee on Publication Ethics).

The Ministry of Education, Science and Technological Development of the Republic of Serbia classified the Military Technical Courier for the year 2021, on December 23, 2021

- **on the list of periodicals for computer sciences,**
  category: quality national journal **(M52)**,
- **on the list of periodicals for electronics, telecommunications and IT,**
  category: quality national journal **(M52)**,
- **on the list of periodicals for mechanical engineering,**
  category: reputed national journal **(M51)**,
- **on the list of periodicals for materials and chemical technology,**
  category: reputed national journal **(M51)**.

The approved lists of national periodicals for the year 2021 can be viewed on the website of the Military Technical Courier, page *Journal categorization*.

More detailed information can be found on the website of the Ministry of Education, Science and Technological Development of the Republic of Serbia.

The information on the categorization can be also found on the website of KOBSON (Consortium of Libraries of Serbia for Unified Acquisition).

The periodical is categorized in compliance with the Regulations on categorization and ranking of scientific journals of the Ministry of Education, Science and Technological Development of the Republic of Serbia (Official Gazette of the Republic of Serbia, No 159/20). More detailed information can be found on the website of the Ministry of Education, Science and Technological Development.

The journal is in the Serbian Citation Index – SCIndex (data base of national scientific journals), in the Russian Index of Science Citation/Российский индекс научного цитирования (RINC/РИНЦ) and is constantly monitored depending on the impact within the bases themselves and indirectly in the international (e.g. Clarivate Analytics) citation indexes. More detailed information can be viewed on the website of the Military Technical Courier, page *Journal indexing*.

Military Technical Courier enables open access and applies the Creative Commons Attribution (CC BY) licence provisions on copyright. The copyright details can be found on the *Copyright notice and Self-archiving policy* page of the journal's website.

Manuscripts are submitted online, through the electronic editing system ASSISTANT, developed by the Center for Evaluation in Education and Science – CEON.

The access and the registration are through the Military Technical Courier site http://www.vtg.mod.gov.rs/index-e.html, on the page *ASSISTANT* or the page *SCINDEKS* or directly through the link (aseestant.ceon.rs/index.php/vtg).

The detailed instructions about the registration for the service are on the website http://www.vtg.mod.gov.rs/index-e.html, on the page *Instructions for ASSISTANT*.

All authors submitting a manuscript for publishing in the Military Technical Courier should register for an ORCID ID following the instructions on the web page *Registration for an ORCID identifier*.

The Military Technical Courier publishes articles in English, using Arial and a font size of 11pt with Single Spacing.

The procedures of article preparation, writing and editing should be in accordance with the *Publication ethics statement* (http://www.vtg.mod.gov.rs/publication-ethics-statement.html).

The article should contain an abstract with keywords, introduction (motivation for the work), body (adequate overview of the representative work in the field, a clear statement of the novelty in the presented research, suitable theoretical background, one or more examples to demonstrate and discuss the presented ideas), conclusion, and references (without heading and subheading enumeration). The article length should not normally exceed 16 pages of the A4 paper format with single spacing, up to a maximum of 24 pages with references and supplementary material included.

The article should be formatted following the instructions in the Article Form which can be downloaded from website page *Article form*.

Title

The title should be informative. It is in both Journal's and author's best interest to use terms suitable for indexing and word search. If there are no such terms in the title, the author is strongly advised to add a subtitle.

Letterhead title

The letterhead title is given at a top of each page for easier identification of article copies in an electronic form in particular. It contains the author's surname and first name initial (for multiple authors add "et al"), article title, journal title and collation (year, volume, issue, first and last page). The journal and article titles can be given in a shortened form.

Author's name

Full name(s) of author(s) should be used. It is advisable to give the middle initial. Names are given in their original form (with diacritic signs if in Serbian).

Author's affiliation

The full official name and seat of the author's affiliation is given, possibly with the name of the institution where the research was carried out. For organizations with complex structures, give the whole hierarchy (for example, University of Defence in Belgrade, Military Academy, Department for Military Electronic Systems). At least one organization in the hierarchy must be a legal entity. When some of multiple authors have the same affiliation, it must be clearly stated, by special signs or in other way, which department exactly they are affiliated with. The affiliation follows the author's name. The function and title are not given.

Contact details

The postal addresses or the e-mail addresses of the authors are given in the first page.

Type of articles

Classification of articles is a duty of the editorial staff and is of special importance. Referees and the members of the editorial staff, or section editors, can propose a category, but the editor-in-chief has the sole responsibility for their classification.

Journal articles are classified as follows:
Scientific articles:

– Original scientific papers (giving the previously unpublished results of the author's own research based on scientific methods);

– Review papers (giving an original, detailed and critical view of a research problem or an area to which the author has made a contribution demonstrated by self-citation);

– Short communications or Preliminary communications (original scientific full papers but shorter or of a preliminary character);

– Scientific commentaries or discussions (discussions on a particular scientific topic, based exclusively on scientific argumentation) and opinion pieces.

Exceptionally, in particular areas, a scientific paper in the Journal can be in a form of a monograph or a critical edition of scientific data (historical, archival, lexicographic, bibliographic, data survey, etc.) which were unknown or hardly accessible for scientific research.

Papers classified as scientific must have at least two positive reviews.

If the journal contains non-scientific contributions as well, the section with scientific papers should be clearly denoted in the first part of the Journal.

Professional articles:

– Professional papers (contributions offering experience useful for improvement of professional practice but not necessarily based on scientific methods);

– Informative contributions (editorial, commentary, etc.);

– Reviews (of a book, software, case study, scientific event, etc.)

Short communications are usually 4-7 pages long, research articles and case studies 10-14 pages, while reviews can be longer. Page number limits are not strict and, with appropriate reasoning, submitted manuscripts can also be longer or shorter. If extended versions of previously published conference papers are submitted, Editors will check if sufficient new material has been added to meet the journal standards and to qualify such manuscripts for the review process. The added material must not have been previously published. New results are desired but not necessarily required; however, submissions should contain expansions of key ideas, examples, elaborations, etc. of conference papers.

Language

The language of the article should be in English.

The grammar and style of the article should be of good quality. The systematized text should be without abbreviations (except standard ones). All measurements must be in SI units. The sequence of formulae is denoted in Arabic numerals in parentheses on the right-hand side.

Abstract and summary

An abstract is a concise informative presentation of the article content for fast and accurate evaluation of its relevance. It contains the terms often used for indexing and article search. A 100- to 250-word abstract has the following parts: introduction/purpose of the research, methods, results and conclusion.

Keywords

Keywords are terms or phrases showing adequately the article content for indexing and search purposes. They should be allocated heaving in mind widely accepted international sources (index, dictionary or thesaurus), such as the Web of Science keyword list for science in general. The higher their usage frequency is, the better. Up to 10 keywords immediately follow the abstract and the summary, in respective languages.

For this purpose, the ASSISTANT system uses a special tool KWASS for the automatic extraction of key words from disciplinary thesauruses/dictionaries by choice and the routine for their selection, i.e. acceptance or rejection by author and/or editor.

Article acceptance date

The date of the reception of the article, the dates of submitted corrections in the manuscript (optional) and the date when the Editorial Board accepted the article for publication are all given in a chronological order at the end of the article.

Acknowledgements

The name and the number of the project or programme within which the article was realised is given in a separate note at the bottom of the first page together with the name of the institution which financially supported the project or programme.

Article preliminary version

If an article preliminary version has appeared previously at a meeting in a form of an oral presentation (under the same or similar title), this should be stated in a separate note at the bottom of the first page. An article published previously cannot be published in the *Military Technical Courier* even under a similar title or in a changed form.

Tables and illustrations

All the captions should be in the original language as well as in English, together with the texts in illustrations if possible. Tables are typed in the same style as the text and are denoted by Arabic numerals at the top. Photographs and drawings, placed appropriately in the text, should be clear, precise and suitable for reproduction. Drawings should be created in Word or Corel.

For figures and graphs, proper data plot is recommended i.e. using a data analysis program such as Excel, Matlab, Origin, SigmaPlot, etc. It is not recommended to use a screen capture of a data acquisition program as a figure or a graph.

Citation in the text

Citation in the text must be uniform. The Military Technical Courier applies the Harvard Referencing System given in the Harvard Style Manual. When citing sources within your paper, i.e. for in-text references of the works listed at the end of the paper, place the year of publication of the work in parentheses and optionally the number of the page(s) after the author's name, e.g. (Petrovic, 2012, pp.10-12). A detailed guide on citing, with examples, can be found on Military Technical Courier website on the page *Instructions for Harvard Style Manual*. In-text citations should follow its guidelines.

For checking in-text citations, the ASSISTANT system uses a special tool CiteMatcher to find out quotes left out within papers and in reference lists.

Footnotes

Footnotes are given at the bottom of the page with the text they refer to. They can contain less relevant details, additional explanations or used sources (e.g. scientific material, manuals). They cannot replace the cited literature.

Reference list (Literature)

The cited literature encompasses bibliographic sources such as articles and monographs and is given in a separate section in a form of a reference list.

References are not translated to the language of the article.

In compiling the reference list and bibliography, the Military Technical Courier applies the Harvard System – Harvard Style Manual. All bibliography items should be listed alphabetically by author's name, without numeration. A detailed guide for listing references, with examples, can be found on Military Technical Courier website on the page *Instructions for Harvard Style Manual*. Reference lists at the end of papers should follow its guidelines.

In journal evaluation systems, non-standard, insufficient or inconsequent citation is considered to be a sufficient cause for denying the scientific status to a journal.

Authorship Statement

The Authorship statement, submitted together with the paper, states authors' individual contributions to the creation of the paper. In this statement, the authors also confirm that they followed the guidelines given in *the Call for papers* and the *Publication ethics and malpractice statement of the journal*.

All articles are peer reviewed.

The list of referees of the Military Technical Courier can be viewed at website page *List of referees*. The article review process is described on the *Peer Review Process* page of the website.

Editorial Team

Address of the Editorial Office:
Vojnotehnički glasnik / Military Technical Courier
Veljka Lukića Kurjaka 33
11042 Belgrade, Republic of Serbia
e-mail: vojnotehnicki.glasnik@mod.gov.rs.
tel.: +381 11 3603 260, +381 66 8700 123

Ликовно-графички уредник
Марија Марић, e-mail: marija.maric@mod.gov.rs

Лектор
Добрила Милетић, e-mail: miletic.dobrila@gmail.com

Превод на енглески
Јасна Вишњић, e-mail: jasnavisnjic@yahoo.com

Превод на руски
Др *Карина* Авагјан, e-mail: karinka2576@mail.ru

CIP – Каталогизација у публикацији
Народна библиотека Србије, Београд

623+355/359

ВОЈНОТЕХНИЧКИ гласник : научни часопис Министарства одбране и Војске Србије = Военно-технический вестник : научный журнал Министерства обороны и Вооружённых сил Республики Сербия = Military Technical Courier : scientific Journal of the Ministry of Defence and the Serbian Armed Forces / главни и одговорни уредник Драган Памучар. - Год. 1, бр. 1 (1. јан. 1953)- . - Београд : Универзитет одбране у Београду, Војна академија, 1953- (Београд : Војна штампарија). - 23 cm

Тромесечно. - Текст на срп., рус. и енгл. језику. - Друго издање на другом медијуму: Vojnotehnički glasnik (Online) = ISSN 2217-4753
ISSN 0042-8469 = Војнотехнички гласник
COBISS.SR-ID 4423938

Цена: 600,00 динара

Тираж: 100 примерака

На основу мишљења Министарства за науку, технологију и развој Републике Србије, број 413-00-1201/2001-01 од 12. 9. 2001. године, часопис „Војнотехнички гласник“ је публикација од посебног интереса за науку.

УДК: Народна библиотека Србије, Београд

Адреса редакције: Војнотехнички гласник,
Вељка Лукића Курјака 33, 11042 Београд

http://www.vtg.mod.gov.rs
http://aseestant.ceon.rs/index.php/vtg/issue/current
http://scindeks.nb.rs/journaldetails.aspx?issn=0042-8469
http://elibrary.ru/title_about.asp?id=53280
https://doaj.org/toc/2217-4753

Војнотехнички гласник је лиценциран код EBSCO Publishing-a.
Комплетан текст *Војнотехничког гласника* доступан је у базама података EBSCO Publishing-a.

e-mail: vojnotehnicki.glasnik@mod.gov.rs

Претплата на штампано издање: e-mail: vojnotehnicki.glasnik@mod.gov.rs; тел. 066/87-00-123.

Часопис излази тромесечно.

Први штампани број *Војнотехничког гласника* објављен је 1. 1. 1953. године.

Прво електронско издање *Војнотехничког гласника* на Интернету објављено је 1. 1. 2011. године.

Штампа: Војна штампарија – Београд, Ресавска 40б, e-mail: vojna.stamparija@mod.gov.rs

Художественный редактор
Мария Марич, e-mail: marija.maric@mod.gov.rs

Корректор
Добрила Милетич, e-mail: miletic.dobrila@gmail.com

Перевод на английский язык
Ясна Вишнич, e-mail: jasnavisnjic@yahoo.com

Перевод на русский язык
Д.филол.н. *Карина* Кареновна Авагян, e-mail: karinka2576@mail.ru

CIP – Каталогизация в публикации
Национальная библиотека Сербии, г. Белград

623+355/359

ВОЈНОТЕХНИЧКИ гласник : научни часопис Министарства одбране
и Војске Србије = Военно-технический вестник : научный журнал
Министерства обороны и Вооружённых сил Республики Сербия =
Military Technical Courier : scientific Journal of the Ministry of Defence and the Serbian
Armed Forces / главни и одговорни уредник Драган Памучар. -
Год. 1, бр. 1 (1. јан. 1953)- . - Београд : Универзитет одбране у Београду,
Војна академија, 1953- (Београд : Војна штампарија). - 23 cm

Тромесечно. - Текст на срп., рус. и енгл. језику. - Друго издање
на другом медијуму: Vojnotehnički glasnik (Online) = ISSN 2217-4753
ISSN 0042-8469 = Војнотехнички гласник
COBISS.SR-ID 4423938

Цена: 600,00 динаров

Тираж: 100 экземпляров

На основании решения Министерства науки и технологий Республики Сербия,
№ 413-00-1201/2001-01 от 12. 9. 2001 года, журнал «Военно-технический вестник»
объявлен изданием, имеющим особое значение для науки.

УДК: Национальная библиотека Сербии, г. Белград

Адрес редакции: Војнотехнички гласник,
Ул. Велька Лукича Куряка 33, 11042 Белград, Республика Сербия

http://www.vtg.mod.gov.rs
http://aseestant.ceon.rs/index.php/vtg/issue/current
http://scindeks.nb.rs/journaldetails.aspx?issn=0042-8469
http://elibrary.ru/title_about.asp?id=53280
https://doaj.org/toc/2217-4753

«Военно-технический вестник» включен в систему EBSCO. Полный текст журнала
«Военно-технический вестник» можно найти в базах данных EBSCO Publishing.

e-mail: vojnotehnicki.glasnik@mod.gov.rs

Подписка на печатную версию журнала: e-mail: vojnotehnicki.glasnik@mod.gov.rs;
тел. +381 66 87 00 123.

Журнал выпускается ежеквартально.

Первый номер журнала «Военно-технический вестник» выпущен 1.1.1953 года.

Первая электронная версия журнала размещена на интернет странице 1.1.2011 года.

Типография: Војна штампарија – Белград, Ресавска 40б, e-mail: vojna.stamparija@mod.gov.rs

Graphic design editor
Marija Marić, e-mail: marija.maric@mod.gov.rs

Proofreader
Dobrila Miletić, e-mail: miletic.dobrila@gmail.com

English translation and polishing
Jasna Višnjić, e-mail: jasnavisnjic@yahoo.com

Russian translation and polishing
Dr. *Karina* Avagyan, e-mail: karinka2576@mail.ru

CIP – Catalogisation in the publication
National Library of Serbia, Belgrade

623+355/359

ВОЈНОТЕХНИЧКИ гласник : научни часопис Министарства одбране и Војске Србије = Военно-технический вестник : научный журнал Министерства обороны и Вооружённых сил Республики Сербия = Military Technical Courier : scientific Journal of the Ministry of Defence and the Serbian Armed Forces / главни и одговорни уредник Драган Памучар. - Год. 1, бр. 1 (1. јан. 1953)- . - Београд : Универзитет одбране у Београду, Војна академија, 1953- (Београд : Војна штампарија). - 23 cm

Тромесечно. - Текст на срп., рус. и енгл. језику. - Друго издање на другом медијуму: Vojnotehnički glasnik (Online) = ISSN 2217-4753
ISSN 0042-8469 = Војнотехнички гласник
COBISS.SR-ID 4423938

Price: 600.00 RSD

Printed in 100 copies

According to the Opinion of the Ministry of Science and Technological Development No 413-00-1201/2001-01 of 12th September 2001, the *Military Technical Courier* is a publication of special interest for science.

UDC: National Library of Serbia, Belgrade

Address: Vojnotehnički glasnik/Military Technical Courier,
Veljka Lukića Kurjaka 33, 11042 Belgrade, Republic of Serbia

http://www.vtg.mod.gov.rs/index-e.html
http://aseestant.ceon.rs/index.php/vtg/issue/current
http://scindeks.nb.rs/journaldetails.aspx?issn=0042-8469
http://elibrary.ru/title_about.asp?id=53280
https://doaj.org/toc/2217-4753

Military Technical Courier has entered into an electronic licensing relationship with EBSCO Publishing. The full text of *Military Technical Courier* can be found on EBSCO Publishing's databases.

e-mail: vojnotehnicki.glasnik@mod.gov.rs

Subscription to print edition: e-mail: vojnotehnicki.glasnik@mod.gov.rs; Tel. +381 66 87 00 123.

The journal is published quarterly.

The first printed issue of the *Military Technical Courier* appeared on 1st January 1953.
The first electronic edition of the *Military Technical Courier* on the Internet appeared on 1st January 2011.

Printed by Vojna štamparija – Belgrade, Resavska 40b, e-mail: vojna.stamparija@mod.gov.rs


ОД 1953.
ВТГ
ГОДИНА


OD 1953.
VTG
GODINA


С 1953 г.
ВТБ
ЛЕТ


SINCE 1953
MTG
YEARS